

NEDO-30730
DRF B31-00106
Class I
September 1984

PILGRIM NUCLEAR POWER STATION
RECIRCULATION NOZZLE REPAIR PROGRAM
AND HYDROGEN WATER CHEMISTRY
MATERIALS QUALIFICATION

Approved: _____

E. Kiss
In
E. Kiss, Manager
Plant Technology

Approved: _____

J. D. Heidl
for
R. L. Gridley, Manager
Fuel and Services Licensing

NUCLEAR ENERGY BUSINESS OPERATIONS • GENERAL ELECTRIC COMPANY
SAN JOSE, CALIFORNIA 95125

GENERAL  ELECTRIC

8411160182 841109
PDR ADOCK 05000293
Q PDR

DISCLAIMER OF RESPONSIBILITY

This document was prepared by or for the General Electric Company. Neither the General Electric Company nor any of the contributors to this document:

- A. Makes any warranty or representation, express or implied, with respect to the accuracy, completeness, or usefulness of the information contained in this document, or that the use of any information disclosed in this document may not infringe privately owned rights; or*
- B. Assumes any responsibility for liability or damage of any kind which may result from the use of any information disclosed in this document.*

CONTENTS

	<u>Page</u>
1. INTRODUCTION	1-1
2. SUMMARY	2-1
2.1 Recirculation Safe-End to Nozzle Weld Cracking and Repair	2-1
2.2 Recirculation Inlet Thermal Sleeve Indications	2-1
3. RECIRCULATION SAFE-END TO NOZZLE WELD CRACKING AND REPAIR	3-1
3.1 Metallurgical Evaluation of Pilgrim Recirculation Nozzle Weld Butter Cracking	3-1
3.1.1 Introduction	3-1
3.1.2 Non-Destructive Examination Results	3-4
3.1.3 Boat Sample Metallurgical Examination	3-5
3.1.4 Summary	3-8
3.2 Residual Stress Analysis and Structural Integrity Evaluation	3-21
3.2.1 Introduction	3-21
3.2.2 Residual Stress Analysis	3-21
3.2.3 Explanation of Observed Cracking	3-23
3.2.4 Effect of Final Weld on Stresses Due to Half-Bead Repair	3-24
3.2.5 Structural Integrity	3-25
3.2.6 Summary	3-28
3.3 Recirculation Nozzle and Safe-End Fabrication History	3-40
3.3.1 Introduction	3-40
3.3.2 Initial Safe-End Installation	3-40
3.3.3 Furnace Sensitized Safe-End Removal	3-41
3.3.4 Replacement Safe-End Fabrication	3-42
3.3.5 Field Installation	3-42
3.3.6 Repairs or Other Special Findings	3-42
3.3.7 Summary	3-43
3.4 Weld Butter Repair Program	3-53
3.4.1 Introduction	3-53
3.4.2 Safe-End Replacement Program	3-53
3.4.3 Repair Approach	3-54
3.4.4 Conventional and Low Penetration Repair Welding	3-55
3.4.5 Half-Bead Weld Repair	3-56
3.4.6 Application of Half-Bead Repair	3-66
3.4.7 Additional Half-Bead Repair Requirements	3-67
3.4.8 Local Post-Weld Heat Treatment Repair	3-68
3.4.9 Summary	3-69
3.5 Qualification of Hydrogen Water Chemistry	3-85
3.5.1 Introduction	3-85
3.5.2 Research Objectives and Principal Findings	3-86
3.5.3 In-Reactor H ₂ WC Test Results	3-96
3.5.4 Summary	3-101
3.6 Behavior of Ni-Cr-Fe Alloys in Hydrogen Water Chemistry	3-127
3.6.1 Introduction	3-127
3.6.2 Background on the Physical and Corrosion Properties of Alloy 600 and its Weld Metal - Alloy 182	3-127

CONTENTS (Continued)

	<u>Page</u>
3.6.3 Evaluation of Baseline Behavior of Alloy 600 and Alloy 182 in Oxygenated High Temperature Water at GE San Jose	3-128
3.6.4 Crack Growth Behavior in Oxygenated Environment	3-129
3.6.5 Crack Growth Rates in Hydrogen Water Chemistry Environments	3-131
3.6.6 Summary	3-132
3.7 Nozzle to Safe-End Dissimilar Weld Inspection Program	3-141
3.7.1 Introduction	3-141
3.7.2 UT Technique Development Approach	3-141
4. THERMAL SLEEVE INDICATIONS	4-1
4.1 Non-Destructive Examination Results	4-4
4.2 Residual Stress Analysis of the Thermal Sleeve Fillet Weld	4-6
4.2.1 Thermal Analysis	4-6
4.2.2 Stress Analysis	4-7
4.3 Structural Integrity of the Thermal Sleeve	4-15
4.3.1 Applied Loading	4-15
4.3.2 Allowable Flaw Parameters Assuming Four Separate Indications	4-16
4.3.3 Allowable Flaw Parameters Assuming One Continuous Indication	4-17
4.3.4 Structural Significance of the Observed Cracking	4-18
4.4 Crack Growth Assessment	4-23
4.5 Justification for Operation with Cracked Thermal Sleeves	4-24
4.5.1 Pressure Boundary Integrity	4-24
4.5.2 Thermal Sleeve Structural Integrity	4-24
4.5.3 Thermal Sleeve Leakage	4-24
4.5.4 Postulated Thermal Sleeve Separation	4-25
4.5.5 Summary	4-25
5. REFERENCES	5-1

APPENDICES

A. COMBUSTION ENGINEERING DETAIL WELD PROCEDURE WC-21466-345-0	A-1
B. COMBUSTION ENGINEERING DRAWING E-232-345	B-1
C. COMBUSTION ENGINEERING DETAIL WELD PROCEDURE WK-21466-345-1	C-1
D. COMBUSTION ENGINEERING DRAWING E-232-369	D-1
E. COMBUSTION ENGINEERING DETAIL WELD PROCEDURE WA-21466-369-1	E-1
F. COMBUSTION ENGINEERING DETAIL WELD PROCEDURE WB-21466-369-1	F-1

CONTENTS (Continued)

	<u>Page</u>
G. SPECIFICATION M&P 5.5.5.5(a)	G-1
H. WELDING PROCEDURE SPECIFICATION P12-P8-AT-Ag (F43), Revision 1	H-1
I. HALF-BEAD HARDNESS TESTING RESULTS	I-1
J. THERMAL SLEEVE PT AND RT CRACKING MAPS	J-1

TABLES

<u>Table</u>	<u>Title</u>	<u>Page</u>
3.1-1	Summary of NDE Results on Nozzle to Safe-End Weld Examinations	3-9
3.3-1	Alloy 182 Heat Numbers for Pilgrim	3-45
3.3-2	Alloy 82 and 182 Heat Numbers for Pilgrim	3-46
3.4-1	Half-Bead Welding Parameters	3-71
3.4-2	Half-Bead Repair Qualification-Mechanical Test Results	3-72
3.4-3	Chemistry of Low Alloy Steels Used in Half-Bead Repair Program	3-73
3.4-4	Parameters for Bead on Plate Test for As-Welded HAZ Hardness	3-74
3.4-5	Equivalent Hardness Conversions	3-74a
3.5-1	Test Matrix for Hydrogen Water Chemistry Pipe Tests	3-103
3.5-2	Exposures and Results of H ₂ WC Pipe Tests	3-104
3.5-3	SCC Crack Growth Test Results in H ₂ WC	3-106
3.5-4	SCC Crack Growth Test in 200 ppb Oxygen Water	3-106
3.5-5	Fatigue Crack Growth Test Results	3-107
3.5-6	CERT Results for Materials Tested in High Purity Water at 274°C (525°F)	3-108
3.5-7	CERT Test Results in H ₂ WC	3-109
3.5-8	SET Results in 0.01N Na ₂ SO ₄ at 274°C (525°F)	3-110
3.5-9	Results of Dresden-2 and Laboratory H ₂ WC CERT Tests	3-111
3.5-10	Mid-Cycle ISI Results from Dresden-2	3-112
3.6-1	Summary of Composition and Mechanical Properties	3-133
3.6-2	Crack Growth Rates in 0.2 ppm O ₂ , High Temperature Water	3-134
3.6-3	Crack Growth Rates in Hydrogen Water Chemistry Environments	3-135
3.7-1	Mockups for UT Technique Development Program	3-143
4.1-1	Thermal Sleeve NDE	4-5

LIST OF ILLUSTRATIONS

<u>Figure</u>	<u>Title</u>	<u>Page</u>
3.0-1	Existing Pilgrim Recirc Inlet Nozzle - 12-inch	3-2
3.0-2	Complex Metallurgical Condition of Safe-End to Nozzle Attachment	3-3
3.1-1	28-Inch Recirculation Outlet Nozzle-to-Safe-End Weld N1-B	3-10
3.1-2	Boat Sample Locations	3-11
3.1-3	Intergranular Cracking in Alloy 182 Butter (Boat Sample 1)	3-12
3.1-4	Cracking Near Weld Interface, Boat Sample No. 2, 125X Magnification	3-13
3.1-5	Short Circumferential Branch of an Intergranular Crack at Alloy 182/304SS Safe-End Interface (Boat Sample 2)	3-14
3.1-6	Axial Interdendritic Cracking in Alloy 182 Butter Adjacent to Weld Root on Safe-End Side (Boat Sample 3)	3-15
3.1-7	High Magnification View of Interdendritic Crack No. 1 of 33X Composite - Alloy 182 Butter (Boat Sample 3)	3-16
3.1-8	Interdendritic Cracking in Alloy 183 (Boat Sample 3, Crack No. 2)	3-17
3.1-9	High Magnification View of Interdendritic Crack No. 3 of 33X Composite - Alloy 182 Butter (Boat Sample 3)	3-18
3.1-10	Crack Arrest in Alloy 82 Weld Root (Boat Sample 3)	3-19
3.1-11	Scanning Electron Micrograph of Axial Crack in Boat Sample No. 3	3-20
3.2-1	Pilgrim Recirculation Outlet Nozzle Finite Element Model	3-29
3.2-2	Nuggett Area Modelling	3-30
3.2-3	Nuggett Area Heating Temperature History	3-30
3.2-4	Isotherms at 3 Seconds	3-31
3.2-5	Isotherms at 6 Seconds	3-32
3.2-6	Isotherms at 9 Seconds	3-33

ILLUSTRATIONS (Continued)

<u>Figure</u>	<u>Title</u>	<u>Page</u>
3.2-7	Isotherms During Cooldown	3-34
3.2-8	Pilgrim Recirculation Outlet Nozzle Residual Stress Analysis	3-35
3.2-9	Throughwall Residual Stress	3-36
3.2-10	Region of Yielding	3-37
3.2-11	Effective Strain Versus Load Step (Time)	3-38
3.2-12	Critical Flaw Size Assuming LEFM	3-39
3.3-1	Shop Fabrication Procedure for Original Furnace Sensitized Safe-End	3-47
3.3-2	Shop Fabrication: Machine Safe-End Prior to Installation in Vessel Shell Course	3-48
3.3-3	Shop Fabrication After Nozzle Installed in Vessel	3-49
3.3-4	Shop Fabrication - Cut Off Safe-End and Re-Prep for Field Weld	3-50
3.3-5	Shop Fabrication of Replacement Safe-End	3-51
3.3-6	Field Weld Technique for Safe-End Installation	3-52
3.4-1	Safe-End Removal and Weld Preparation Technique	3-75
3.4-2	Configuration for Nozzles Where Field Weld and Original Safe-End Weld are Acceptable to Retain Desired Butter Thickness	3-76
3.4-3	Configuration for Nozzles Where Unacceptable Indications in Field Weld Require Removal by Machining, Resulting in a Reduced Butter Thickness	3-76
3.4-4	Effect of Bead Overlap on Half-Bead Tempering Process	3-77
3.4-5	Half-Bead Weld Procedure Qualification Sample	3-78
3.4-6	Weld Groove Design for Half-Bead Qualification	3-79
3.4-7	Half-Bead Welding Procedure for Horizontal Weld Grooves	3-80
3.4-8	Half-Bead Welding Procedure for Vertical Weld Grooves	3-81
3.4-9	Locations for Half-Bead HAZ Microhardness Traverses	3-82

ILLUSTRATIONS (Continued)

<u>Figure</u>	<u>Title</u>	<u>Page</u>
3.4-10	Half-Bead Repair Technique for Short Horizontal Repair Cavity	3-83
3.4-11	Half-Bead Repair Technique for Longer Horizontal Repair Cavity	3-84
3.5-1	Pipe Test Specimen Fabrication Drawing	3-113
3.5-2	Pipe Test Specimen Loading Stand	3-114
3.5-3	Loading Waveform Used for Hydrogen Water Chemistry Pipe Tests	3-115
3.5-4	Typical WOL or Compact Tension Specimen for Crack Growth Rate Study	3-115
3.5-5a	Stress Corrosion Test Loading History	3-116
3.5-5b	Slow Cyclic Loading Waveform Detail	3-116
3.5-5c	Constant Load Detail	3-116
3.5-6	Cyclic Loading Waveform	3-117
3.5-7	Comparison of Cyclic Crack Growth Data (0.74 cph, R = 0.6) in H ₂ WC versus Nominal Environment for Furnace Sensitized Stainless Steel	3-118
3.5-8	Comparison of Cyclic Crack Growth Data (0.74 cph, R = 0.6) in H ₂ WC versus Nominal Environment for Carbon and Low Alloy Steel	3-119
3.5-9	Comparison of Cyclic Crack Growth Data (7.5 cph, R = 0.6) in H ₂ WC versus Nominal Environment for Furnace Sensitized Stainless Steel	3-120
3.5-10	Comparison of Cyclic Crack Growth Data (7.5 cph, R = 0.6) in H ₂ WC versus Nominal Environment for Carbon and Low Alloy Steel	3-121
3.5-11	Relationship Between Dissolved Oxygen and Potential to IGSCC of Welded Type 304 Stainless Steel	3-122
3.5-12	The Effect of Dissolved Oxygen on the Corrosion Potential of Type 304 Stainless Steel in High Purity Water at 274°C (525°F)	3-123
3.5-13	Example of ECP Memory Effect During H ₂ WC	3-124
3.5-14	IGSCC Behavior of Sensitized Stainless Steel in Dresden-2 Tests	3-125

ILLUSTRATIONS (Continued)

<u>Figure</u>	<u>Title</u>	<u>Page</u>
3.5-15	Dresden-2 H ₂ WC Crack Growth Test - Furnace Sensitized Type 304 SS	3-126
3.6-1	Stress Dependency of Materials in 288°C, 8 ppm Oxygenated Water	3-136
3.6-2	Pipe Test Results, 0.2 ppm O ₂ , 288°C	3-137
3.6-3	WOL Specimen for Crack Growth Rate Study	3-138
3.6-4	Schematic of Test Vessel VI, Multispecimen Environmental Test Facility	3-139
3.6-5	High Pressure/Temperature Environmental Test Loop	3-140
4.0-1	Cross-section of Pilgrim Recirculation Inlet Thermal Sleeve/ Nozzle at Alignment Pad Locations	4-2
4.0-2	Thermal Sleeve Pad Configuration and Welding Distortion	4-3
4.2-1	Nuggett Area Modelling	4-9
4.2-2	Nuggett Area Heating Temperature History	4-9
4.2-3	Isotherms at Time = 5 Seconds	4-10
4.2-4	Isotherms at Time = 9 Seconds	4-10
4.2-5	Isotherms at Time = 12 Seconds	4-10
4.2-6	Isotherms at Time = 25 Seconds	4-11
4.2-7	Isotherms at Time = 70 Seconds	4-11
4.2-8	Isotherms at Time = 192 Seconds	4-11
4.2-9	Pilgrim Recirculation Inlet Nozzle Element Mesh	4-12
4.2-10	Calculated Residual Stress Due to End Weld	4-13
4.2-11	Calculated Through-Wall Residual Stress Due to End Weld Outer Sleeve	4-14
4.3-1	Crack Configuration for Four Separate Indications	4-19
4.3-2	Allowable Flaw Sizes for Pilgrim Recirculation Inlet Thermal Sleeve (Four Separate Indications)	4-20
4.3-3	Crack Configuration for One Continuous Indication	4-21
4.3-4	Allowable Flaw Sizes for Pilgrim Recirculation Inlet Thermal Sleeve (One Continuous Indication)	4-22

1. INTRODUCTION

Boston Edison Company (BECo) has elected to replace existing drywell piping made from Type 304 stainless steel material with Type 316 nuclear grade (NG) material at the Pilgrim Nuclear Power Station. The 316 NG piping provides significantly improved resistance to intergranular stress corrosion cracking (IGSCC) in a BWR environment.

In May 1984, during recirculation safe-end replacement, dye penetrant tests (PT) identified axial crack-like indications in the Alloy-182 weld metal associated with the recirculation stainless steel safe-end to low alloy reactor pressure vessel nozzle welds. In addition, subsequent non-destructive examination (NDE) showed intermittent PT cracking indications on 7 of 8 recirculation inlet nozzle thermal sleeve pad and fillet weld heat-affected zones. One indication was found by radiography in each of the two thermal sleeves not examined by PT.

On June 15, 1984, BECo and the General Electric Company (GE) briefed NRC management and staff on the repair plan for the nozzle to safe-end welds. The repair plan employs a half-bead repair technique for weld butter thicknesses less than 1/8". A hydrogen water chemistry program will be developed during 1985 to further mitigate IGSCC in the Alloy 182 material, in addition to other reactor materials.

At BECo's request, GE advised the NRC on July 16, 1984 of the results of the thermal sleeve examination. Since the indications found on the thermal sleeves are quite limited in extent, current plans are to leave the thermal sleeves in place and suppress further cracking through the development of hydrogen water chemistry.

This report expands upon the information presented at the July 15, 1984 NRC meeting. Additionally, justification for continued operation with cracked recirculation inlet nozzle thermal sleeves is provided.

2. SUMMARY

2.1 RECIRCULATION SAFE-END TO NOZZLE WELD CRACKING AND REPAIR

Liquid penetrant indications were observed in the Alloy-182 weld metal of 3 out of the 10 recirculation inlet nozzles to safe-end welds and 1 out of the 2 outlet nozzle to safe-end welds. The indications were axially oriented with depths ranging up to 70% wall thickness and lengths up to 0.5 inches. Metallographic examination of boat samples taken from the outlet nozzle weld region confirmed that crack initiation was caused by intergranular stress corrosion cracking (IGSCC). A detailed review of the fabrication history did not identify any correlation with the observed cracking.

A residual stress analysis of the nozzle to safe-end weld indicates that predominantly axial cracking is expected due to internal pressure and high weld residual hoop stresses. In addition, a crack growth analysis concludes that structural integrity is maintained and sufficient leak-before-break margins exist. Consequently, cracking in Alloy-182 weld metal does not pose any safety concerns and can be mitigated with an orderly remedial program.

A qualified half-bead repair technique was utilized on three recirculation inlet nozzles and a Local Post Weld Heat Treatment was performed on one recirculation outlet nozzle. Also, as part of the repair program, Boston Edison Company (BECO) has committed to the development of hydrogen water chemistry (H_2WC). Laboratory tests have confirmed that the hydrogen water chemistry environment will suppress IGSCC in the Alloy-182 weld metal, in addition to other reactor materials.

2.2 RECIRCULATION INLET THERMAL SLEEVE INDICATIONS

Non-destructive examinations (both dye-penetrant and radiographic) identified linear indications in 9 out of the 10 recirculation inlet nozzle thermal sleeves. These indications were limited in extent (typically between 0.25-in. and 1.0 in. in length) and were located on the O.D. of the outer thermal

sleeve in areas associated with the pad weld buildup heat affected zones. A residual stress analysis shows that the observed cracking correlated well with the location of the high tensile residual stress and weld sensitization.

Boston Edison Company has elected not to repair the thermal sleeves during the pipe replacement outage. A crack growth analysis confirms that the required Code safety margins are maintained during the next 18 months of operation. As stated above, BECo will develop H₂WC, which when implemented, will arrest crack initiation and propagation.

There are no safety concerns associated with continued full power operation of Pilgrim Nuclear Power Station with the currently cracked thermal sleeves both prior to and subsequent to H₂WC implementation.

3. RECIRCULATION SAFE-END TO NOZZLE WELD CRACKING AND REPAIR

Recirculation inlet and outlet nozzle safe-ends provide a geometric and material transition from the reactor pressure vessel low alloy steel nozzle to the austenitic recirculation system piping. The principle function of the safe-end is to avoid field attachment welding of connecting piping to a material which would require local post weld heat treatment.

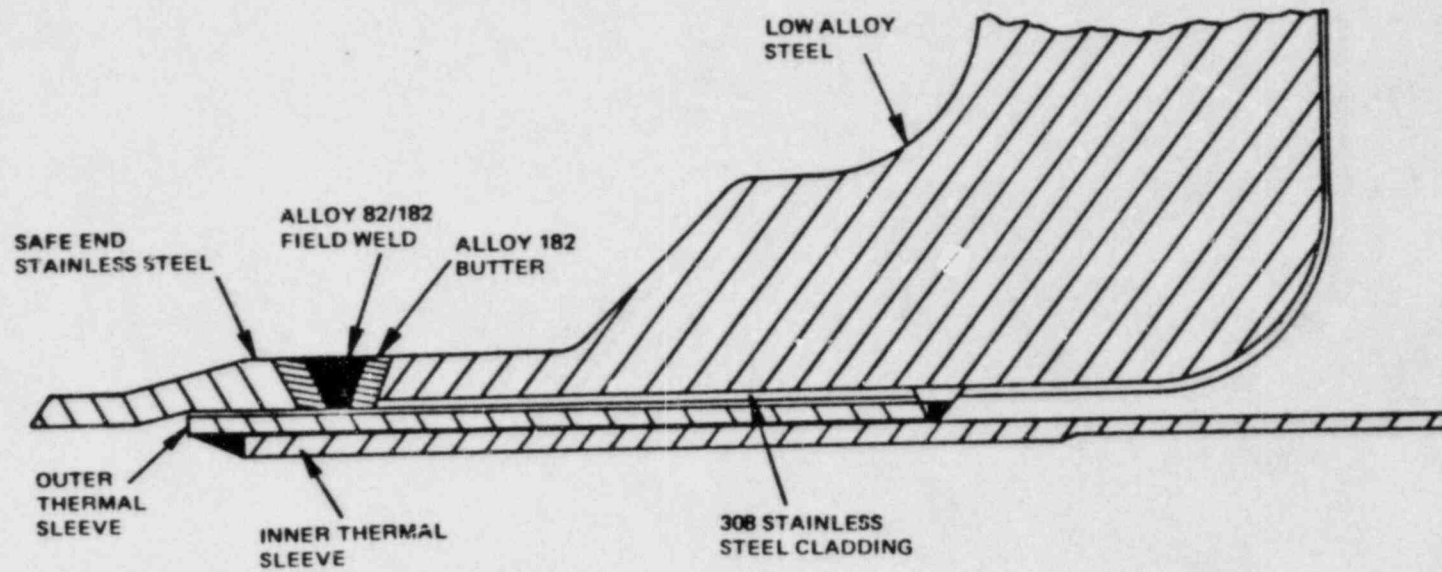
An axial cross section of the 12-inch recirculation inlet nozzle is shown in Figure 3.0-1. (The configuration of the 28-inch outlet nozzles is identical except that the thermal sleeve is absent.) The complex metallurgical condition of the safe-end to nozzle attachment is illustrated in Figure 3.0-2. The nozzle consists of low alloy steel, the safe-end of Type 304 stainless steel, and both have Alloy 182 weld buildup (butter) on the welded face. The weld metal is Alloy 182 except for the root pass and the next two weld passes consisting of Alloy 82 which were applied by the Gas Tungsten Arc process. The I.D. of the low alloy steel nozzle has been clad with Type 308 stainless steel.

The following subsections review the metallurgical evaluation of the recirculation weld metal cracking, the residual stress analysis, the structural integrity margins and the fabrication history of the existing safe-ends. In addition, the details of the weld butter repair plan are discussed. Technical bases supporting long-term mitigation of intergranular stress corrosion cracking in the Alloy 182 weld metal through the implementation of hydrogen water chemistry and development plans for improved ultrasonic inspection techniques are also provided.

3.1 METALLURGICAL EVALUATION OF PILGRIM RECIRCULATION NOZZLE WELD BUTTER CRACKING

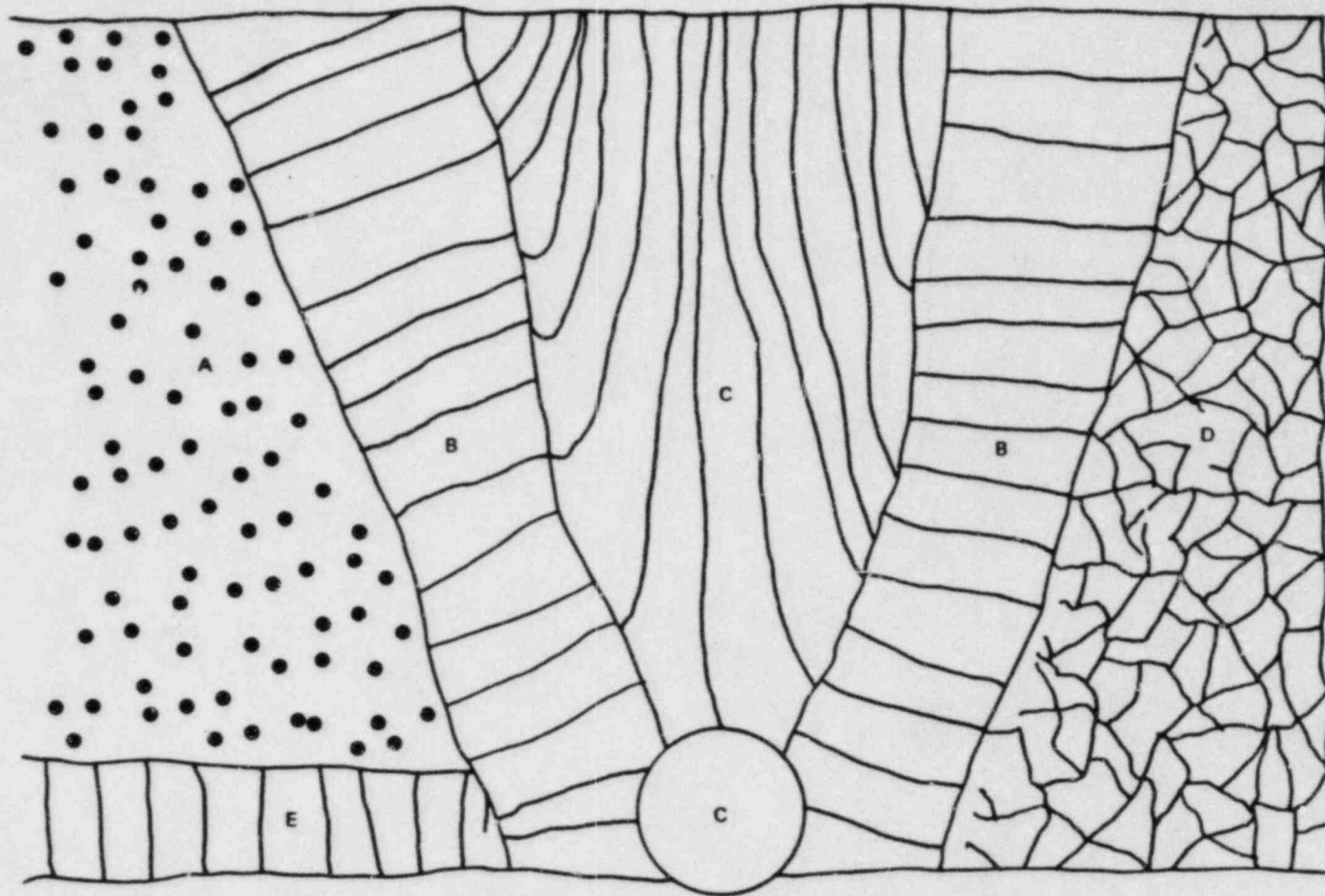
3.1.1 Introduction

In May, 1984 liquid penetrant (PT) examination of the machined face of a 12-inch recirculation inlet nozzle revealed radial crack indications in the Alloy 182 weld butter. Subsequent PT examination of the remaining inlet



NOTE: 28-INCH RECIRCULATION OUTLETS HAVE NO THERMAL SLEEVES

Figure 3.0-1. Existing Pilgrim Recirc Inlet Nozzle - 12 inch



- A) LOW ALLOY STEEL NOZZLE
- B) ALLOY 182 WELD BUTTER
- C) ALLOY 182 OR ALLOY 82 WELD METAL
- D) STAINLESS STEEL 304 SAFE-END
- E) STAINLESS STEEL CLADDING

Figure 3.0-2. Complex Metallurgical Condition of Safe-End to Nozzle Attachment

nozzles revealed two additional nozzles with crack indications in the weld butter to a depth of approximately 70% of the wall thickness. An I.D. surface examination of the 28-inch recirculation outlet nozzles revealed multiple axial cracks in one of two nozzles. The cracks were confined to the 182 weld butter on both the safe-end and nozzle side of the weld except for slight crack extension into the stainless steel safe-end base material in a few instances. No cracking was found in the low alloy steel nozzle base material or in the Alloy 82 weld root pass of the field weld.

To determine the nature of the cracking, a total of four boat samples were taken from recirculation outlet nozzle N1-B, three of which were examined at the General Electric Company Vallejos Nuclear Center. In this subsection the non-destructive examination results and the boat sample metallurgical examination will be reviewed.

3.1.2 Non-Destructive Examination Results

In order to fully assess the extent of cracking in the recirculation system nozzles, an array of non-destructive examinations was performed. Liquid penetrant (PT) examination was performed on the I.D. surface of the outlet nozzles, the accessible areas of the inlet nozzles, the machined (weld butter) faces of inlet nozzles, and the thermal sleeves (where accessible). Radiographic examination (RT) was used to confirm the PT results and to evaluate the thermal sleeve cracking (see Section 4.1). Ultrasonic examination (UT) was performed to examine the nozzle base material and I.D. cladding for extension of axial cracks from the weld metal and to look for circumferential cracking in the weld butter. The nozzle-to-safe-end examination results are presented in Table 3.1-1.

Indications characteristic of stress corrosion cracking were discovered in three of the ten inlet nozzle to safe-end welds and in one of the two outlet nozzle to safe-end welds.

3.1.3 Boat Sample Metallurgical Examination

A total of four boat samples were removed from 28-inch recirculation outlet nozzle N1-B. Three of the samples were examined by General Electric at the Vallecitos Nuclear Center. A fourth sample was given to the NRC for an independent analysis. Sketches of the recirculation nozzle showing the locations of the boat samples are given in Figures 3.1-1 and 3.1-2. A description of the boat samples is given below:

<u>Sample</u>	<u>Location</u>	<u>Comments</u>
1	180°	Axial crack in 182 butter on safe-end side of weld; crack extension into safe-end.
2	30°	Short circumferential crack near butter/safe-end interface.
3	185°	Two axial cracks in 182 butter (safe-end side); one subsurface crack which apparently initiated on the nozzle side butter.
4 (NRC Sample)	195°	Two axial cracks in butter on safe-end side of weld.

Boat Sample No. 1

As shown in Figure 3.1-1, boat sample No. 1 was removed from near the 180° azimuth (0° is nozzle top dead center) and was oriented at a slight angle with respect to the weld. This sample contains part of an axial crack in the Alloy 182 weld butter and includes the crack extension into the Type 304 stainless steel safe-end. It was mounted on its upper surface (I.D. surface of nozzle) in order to examine the nature of the cracking in both the 182 butter and the safe-end. Photomicrographs of this plane of examination are shown in Figure 3.1-3. The crack is interdendritic in the 182 weld metal and intergranular in the safe-end. Judging from the appearance of other axial cracks in the N1-B weld butter, which did not propagate into the safe-end, it would be reasonable to conclude that this particular crack initiated in the Alloy 182 weld butter rather than the safe-end.

Upon closer examination of the Figure 3.1-3 photos, one can see a change in structure in the Alloy 182 weld butter. This is considered normal for Alloy 182 weld metal. The material closest to the weld interface has retained its original solidification structure - a dendritic structure. Further from the interface, the weld metal has recrystallized due to heat input from subsequent weld passes. Distinct grain boundaries, rather than dendrite boundaries, can be seen. In the recrystallized area the crack is intergranular. In the non-recrystallized area it is interdendritic.

Boat Sample No. 2

This sample contains a short circumferential crack near the butter/safe-end interface, at approximately the 30° azimuth, with an axial branch into the Alloy 182 weld butter. The sample was divided into three portions - two for metallography and one for scanning electron microscopy (SEM). Planes parallel and perpendicular to the nozzle I.D. were examined by metallography. The plane normal to the nozzle I.D. (parallel to the axis of the nozzle) is shown in Figure 3.1-4. At this location, the circumferential crack follows the weld interface near the I.D. surface with short intergranular penetrations into the

Alloy 182 weld butter and the safe-end. Towards the bottom of the boat sample, the crack is primarily in the safe-end. The surface plane is shown in Figure 3.1-5. Again, it is seen that the cracking is along the weld interface or in the safe-end.

It should be noted that the cracking at this location is not typical of the other cracks found in the N1-B nozzle. Cracking would not be expected in the stainless steel safe-end (since the safe-ends were solution heat treated following weld buttering) unless it first initiated somewhere else. At this particular location, it appears that the circumferential crack is a branch of an axial crack which initiated in the weld butter.

Boat Sample No. 3

The third boat sample was removed near the 185° azimuth. As shown in Figure 3.1-2, two axial cracks were found at this location in the butter material on the safe-end side of the weld. This sample was cut from the weld metal interface to include a portion of the Alloy 82 root pass. After the sample was removed, an axially oriented subsurface crack was discovered between the other two cracks in the weld butter. This is also shown in Figure 3.1-2. Since the tip of this crack was not open to the surface anywhere on the safe-end side of the weld, it would appear that this is the extension of an axial crack found in the butter on the nozzle side of the weld. This crack must have initiated in the nozzle side butter and "tunneled" under the Alloy 82 root pass toward the safe-end.

Following visual examination, this sample was mounted on its front face so that each of the three axial cracks could be examined. These are shown at low magnification in Figure 3.1-6 and at higher magnification in Figures 3.1-7 through 3.1-9. Consistent with the findings from the first two samples, these cracks are interdendritic (or intergranular in the portions of the weld butter that have recrystallized).

In order to examine the behavior of the subsurface crack in the vicinity of the Alloy 82 weld root pass, the sample was removed from its mount and separated at the location of the subsurface crack. One was submitted for SEM examination and the other was re-mounted on its fracture face.

A photomicrograph from this second metallographic mount is shown in Figure 3.1-10. Branches of the subsurface crack are seen to have extended up to the weld interface and into the dilution zone of the root pass, but not beyond. This behavior is consistent with General Electric's understanding of Alloy 82 and 182 weld metal. Laboratory data has shown that Alloy 182 has a greater susceptibility to IGSCC in a high temperature water environment than Alloy 82.

A scanning electron micrograph of the Alloy 182 portion of the fracture surface is presented in Figure 3.1-11. The surface is characteristic of interdendritic stress corrosion cracking in a high temperature water environment.

3.1.4 Summary

A total of four boat samples were removed from 28-inch outlet nozzle N1-B, three of which were examined at the General Electric Company Vallecitos Nuclear Center. It was found that the cracking in the Alloy 182 weld butter was due to interdendritic (intergranular) stress corrosion cracking. Since the majority of the cracking was confined to the Alloy 182 material, it is apparent that they initiated in the Alloy 182.

Table 3.1-1

SUMMARY OF NDE RESULTS ON NOZZLE TO SAFE-END WELD EXAMINATIONS

<u>Nozzle</u>	<u>PT for Cracks</u>	<u>UT for Circumferential Cracks</u>	<u>UT for Axial Cracks</u> ¹	<u>Comments</u>
N1-A	OK	NA	NA	OK
N1-B	33 Axial 1 Short Circ Branch of Axial	NA	OK	RT Confirmed
N2-A	OK	OK	OK	OK
N2-B	12 Axial	OK	OK	RT Confirmed
N2-C	OK	OK	OK	OK
N2-D	OK	OK	NA	OK
N2-E	OK	OK	NA	OK
N2-F	13 Axial	OK	5 Axial ²	RT Confirmed
N2-G	OK	OK	NA	OK
N2-H	OK	OK	NA	OK
N2-J	5 Axial	OK	Not Performed	RT Confirmed
N2-K	OK	OK	NA	OK

¹ UT for axial cracks in nozzle base material or clad.

² Subsequent grinding and etching confirmed that cracking did not extend into the low alloy steel.

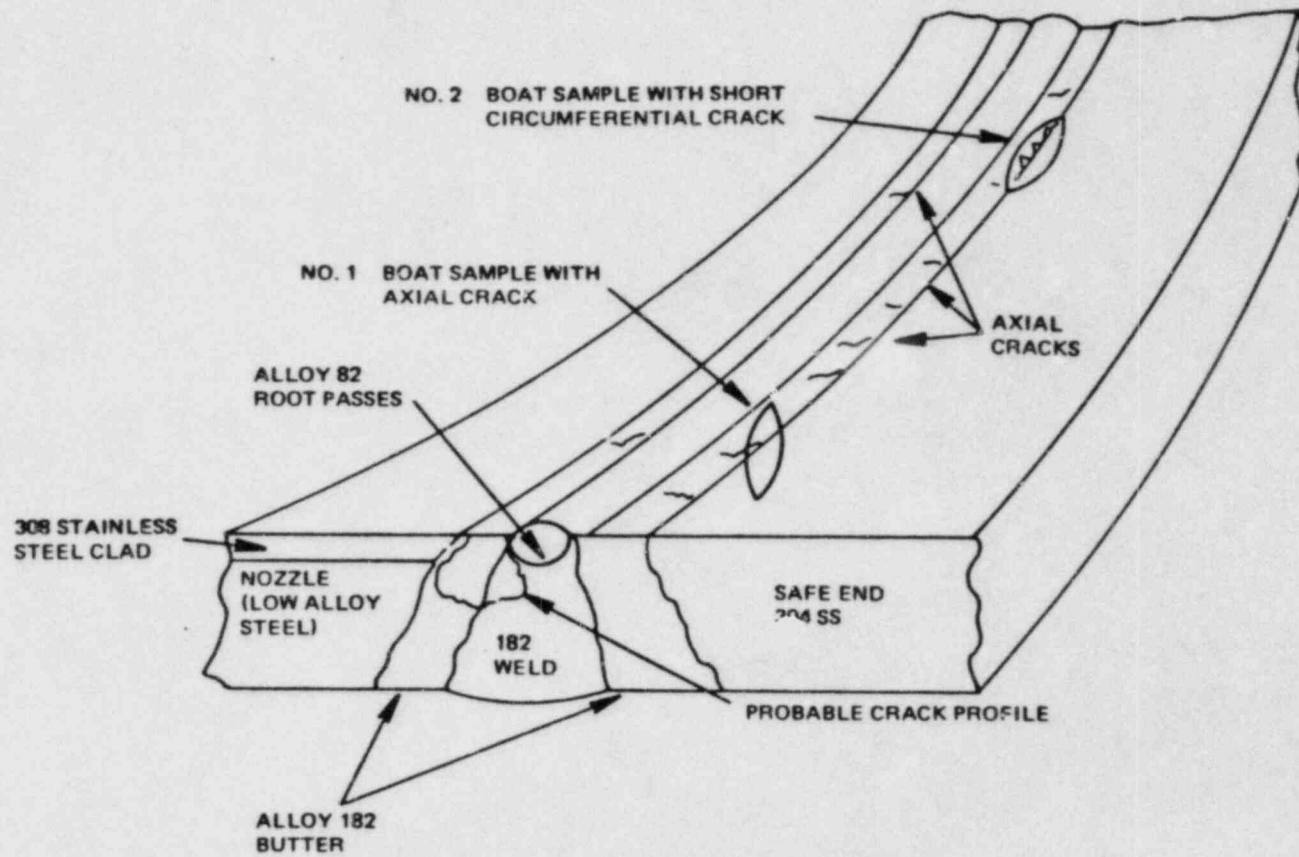


Figure 3.1-1. 28-Inch Recirculation Outlet Nozzle-to-Safe-End Weld N1-B

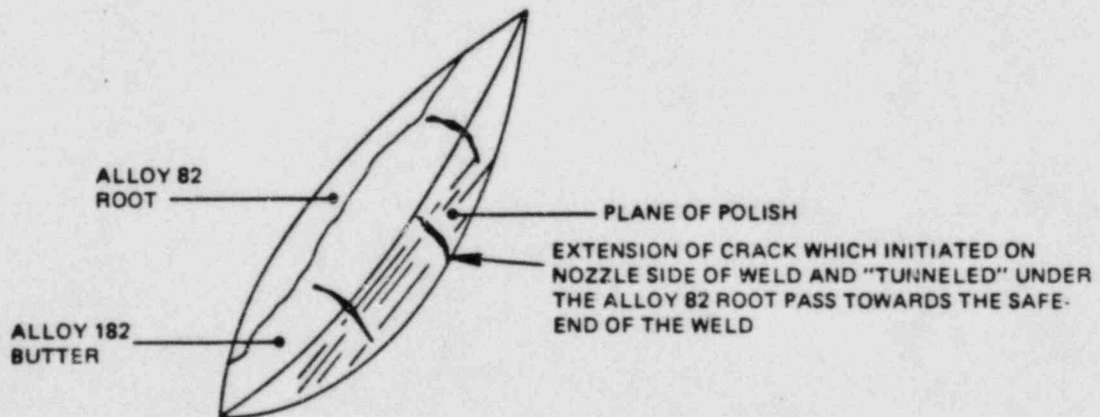
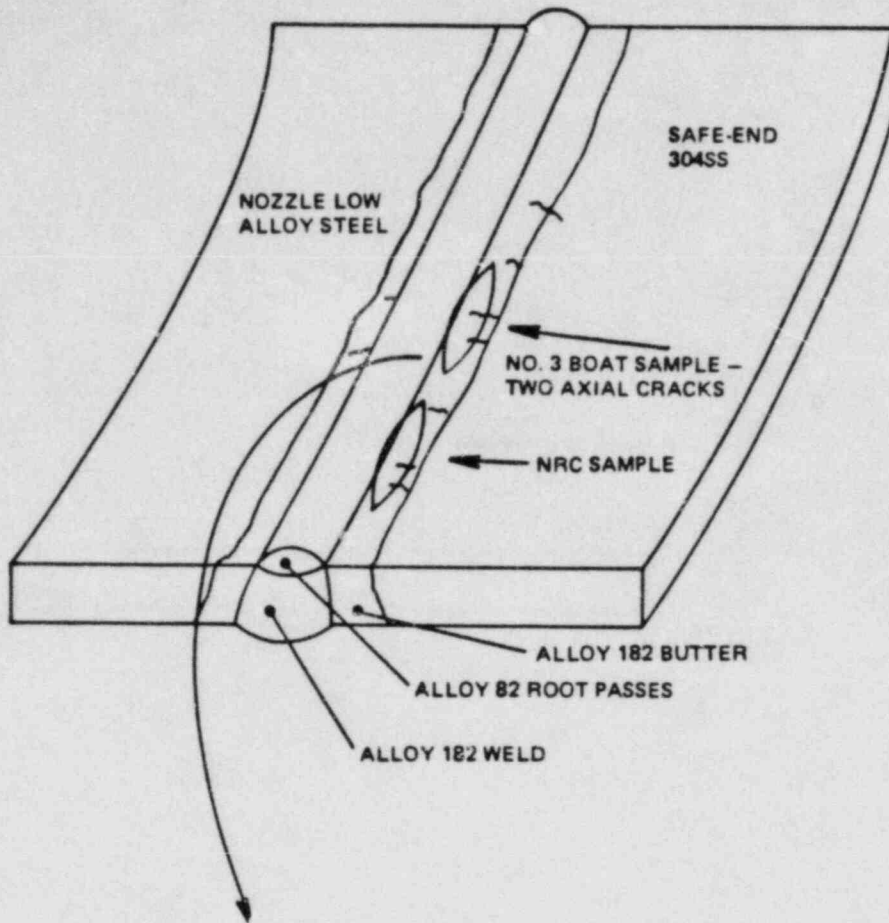


Figure 3.1-2. Boat Sample Locations

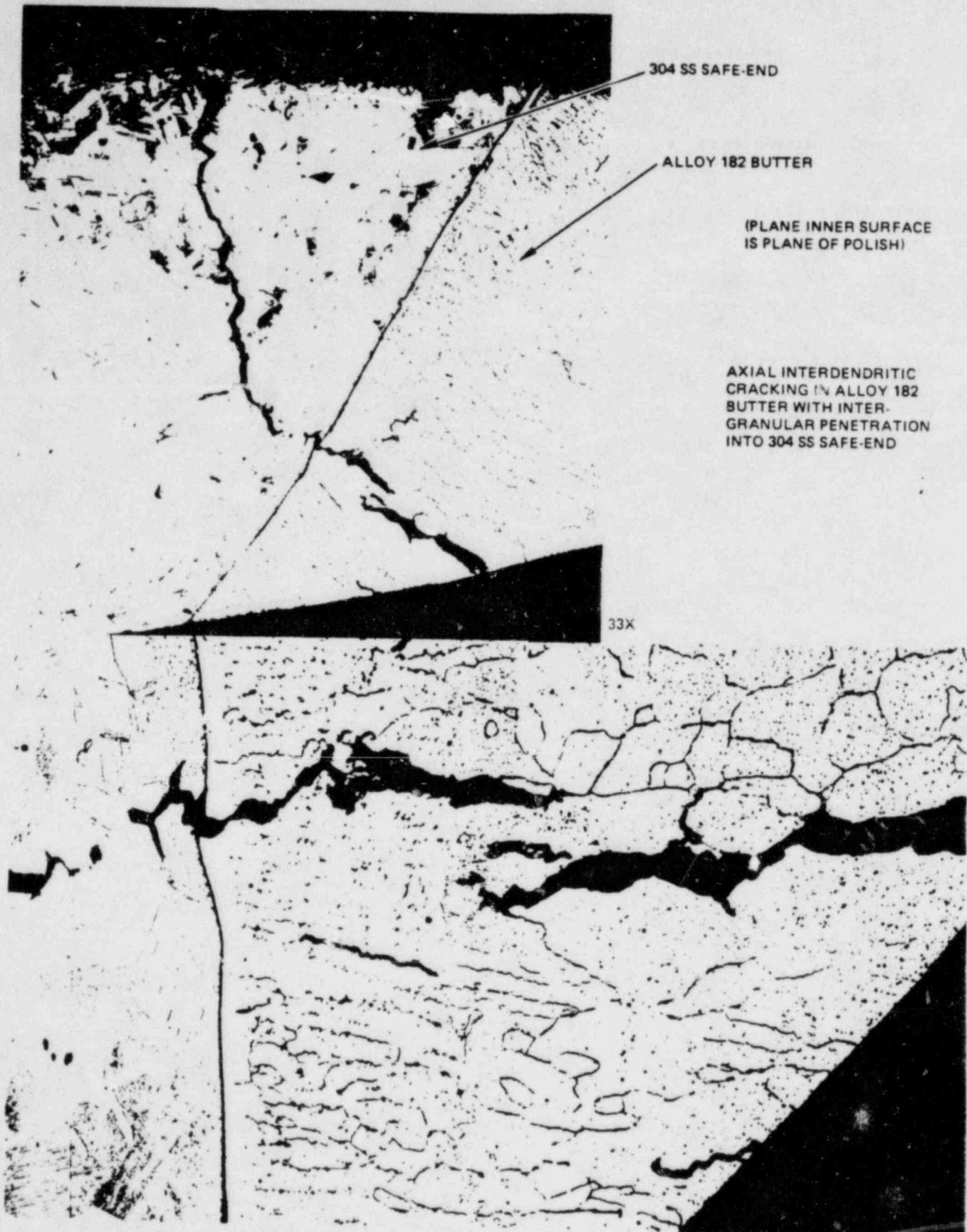


Figure 3.1-3. Intergranular Cracking in Alloy 182 Butter (Boat Sample 1)

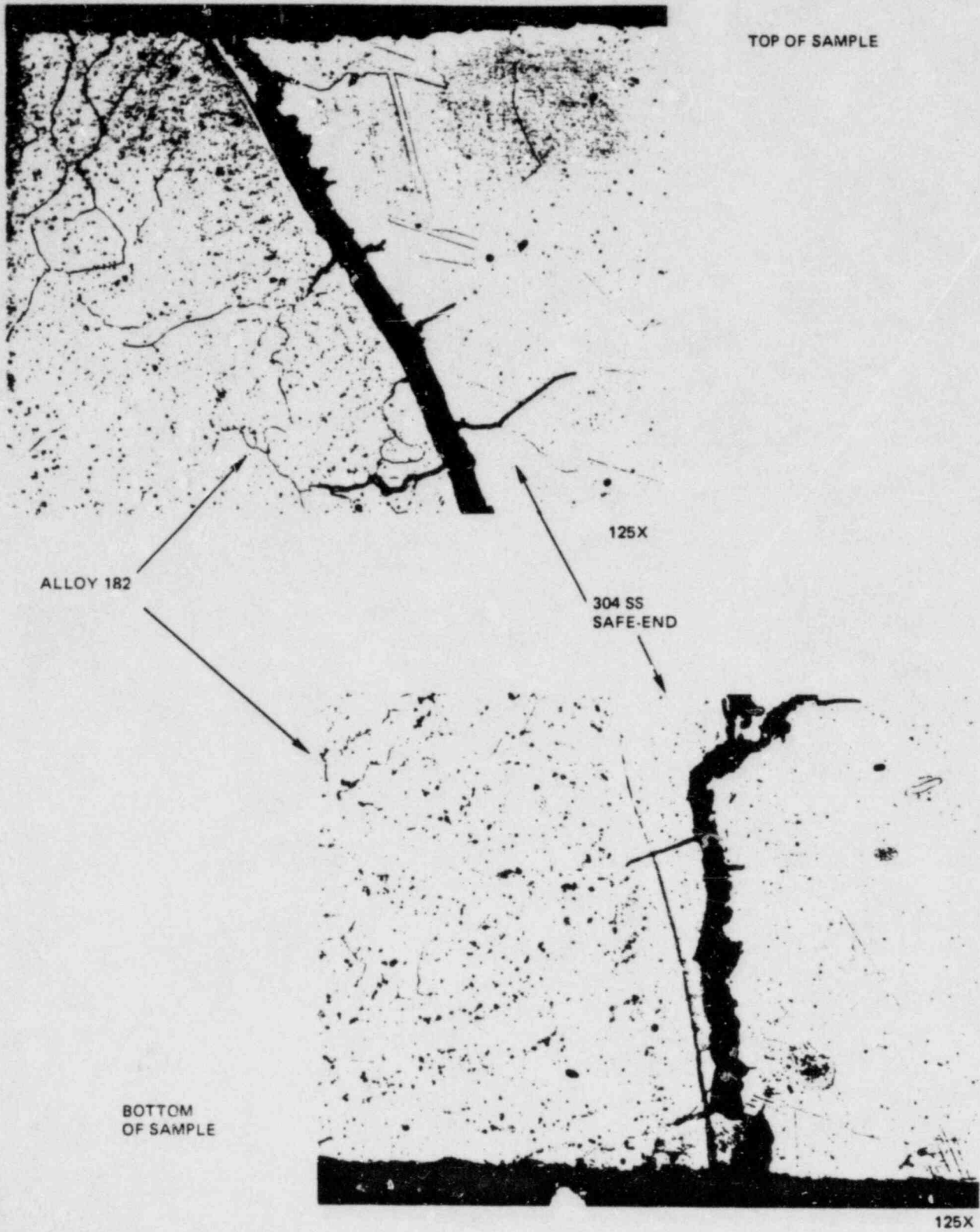
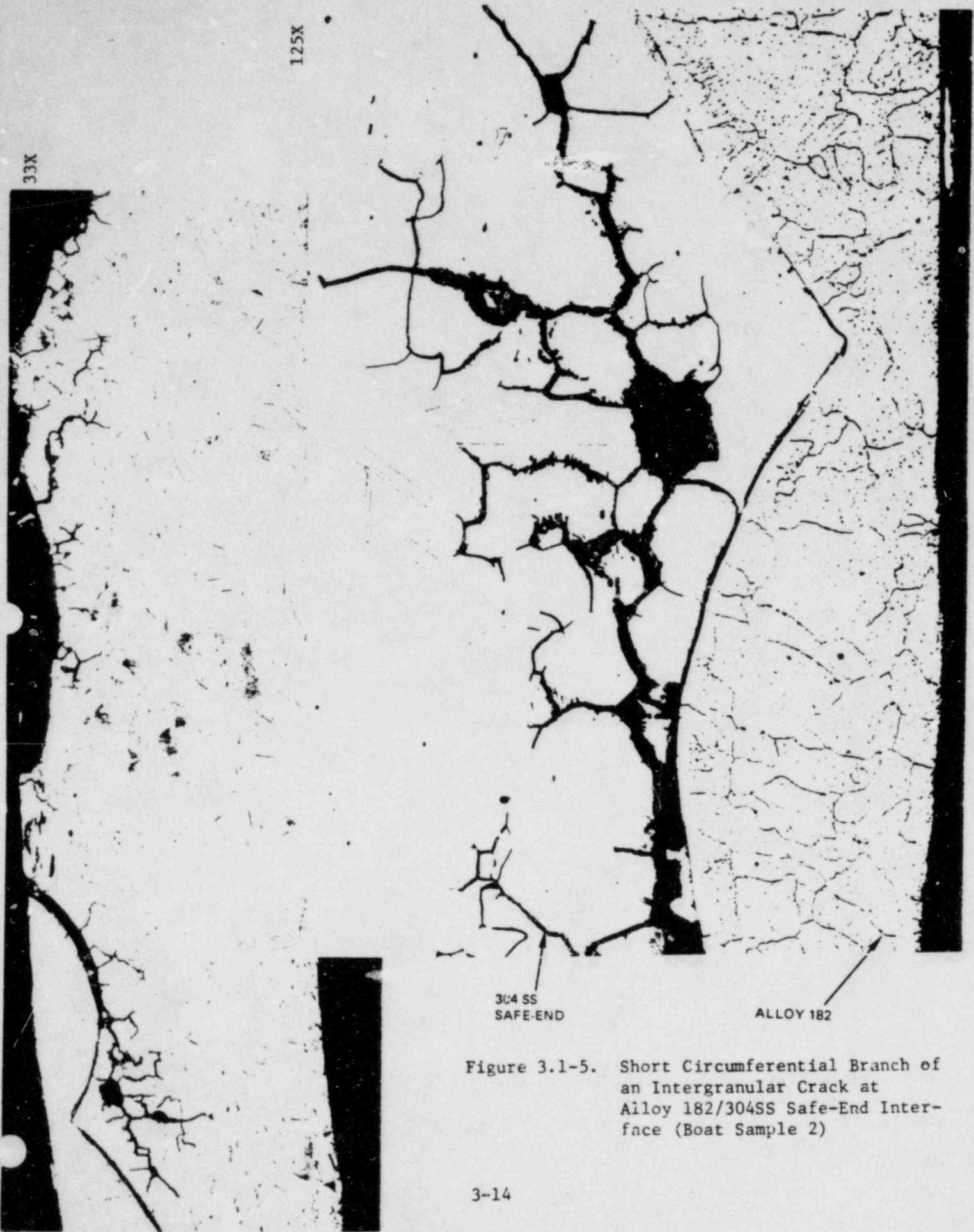


Figure 3.1-4. Cracking Near Weld Interface, Boat Sample No. 2, 125X Magnification

125X

33X

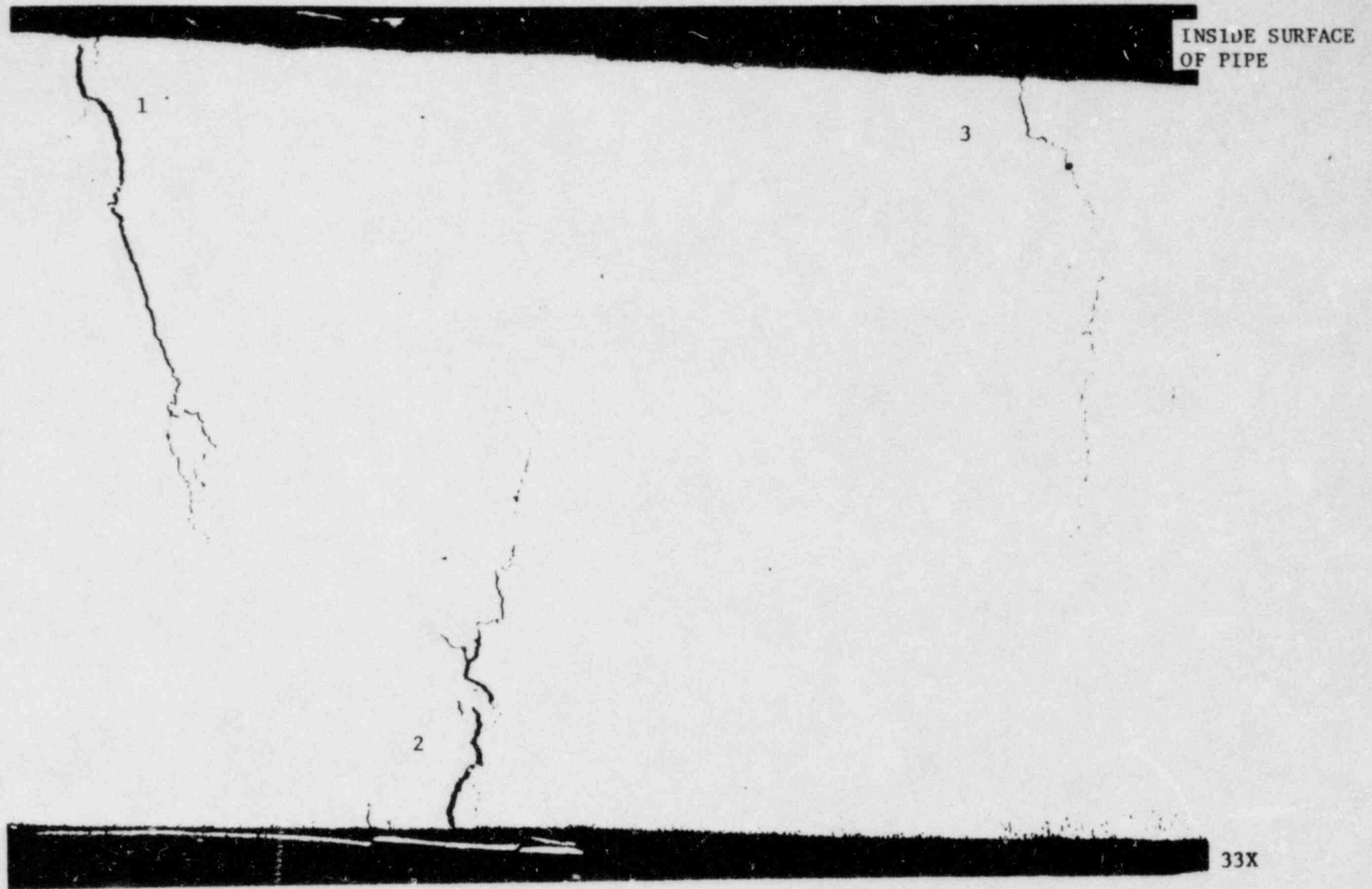


304 SS
SAFE-END

ALLOY 182

Figure 3.1-5. Short Circumferential Branch of an Intergranular Crack at Alloy 182/304SS Safe-End Interface (Boat Sample 2)

3-15



NEDO-30730

Figure 3.1-6. Axial Interdendritic Cracking in Alloy 182 Butter Adjacent to Weld Root on Safe-End Side (Boat Sample 3) (Crack in center of photo initiated in Alloy 182 butter on nozzle side of the weld).

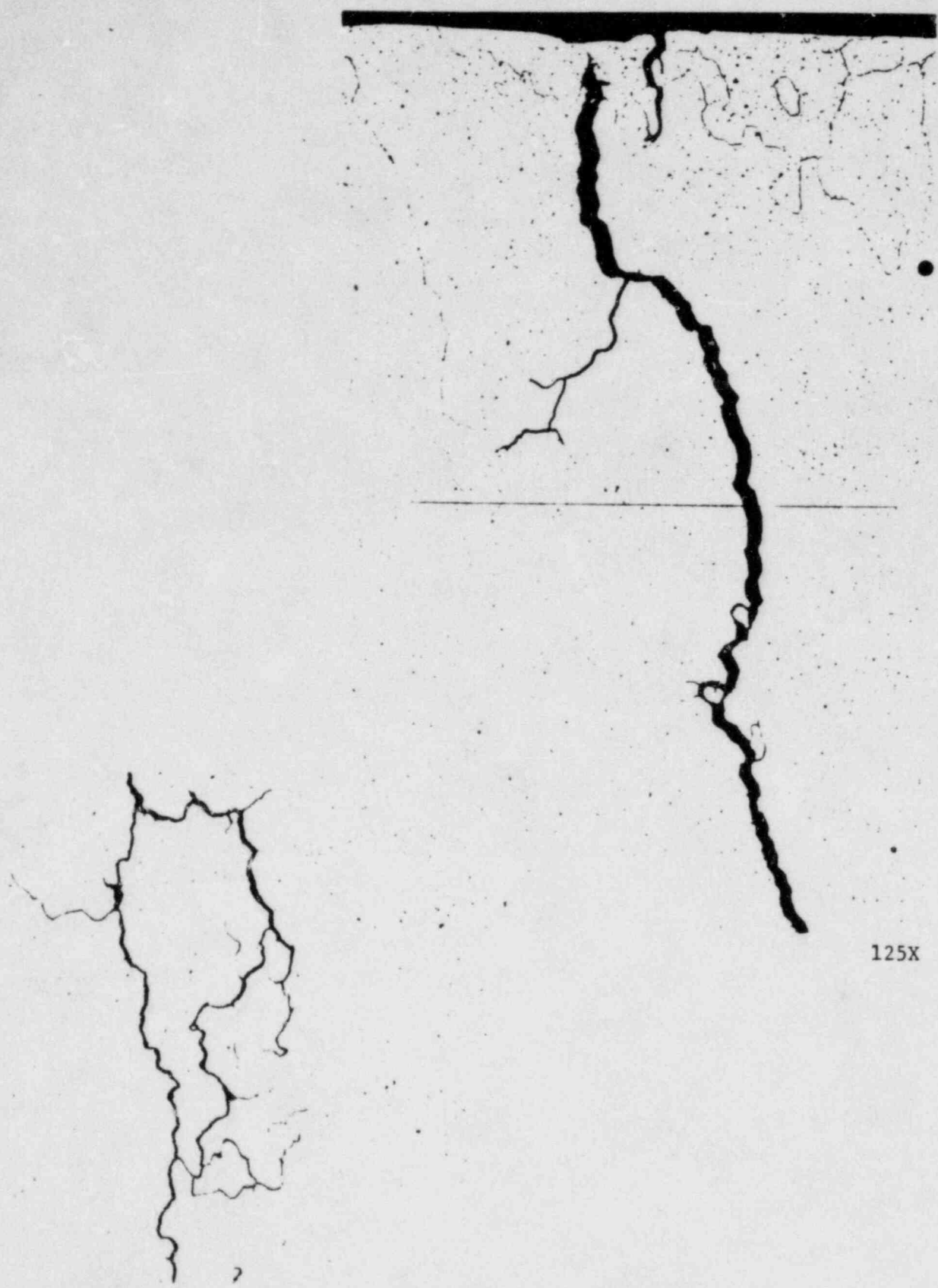


Figure 3.1-7. High Magnification View of Interdendritic Crack No. 1 of 33X Composite - Alloy 182 Butter (Boat Sample 3)

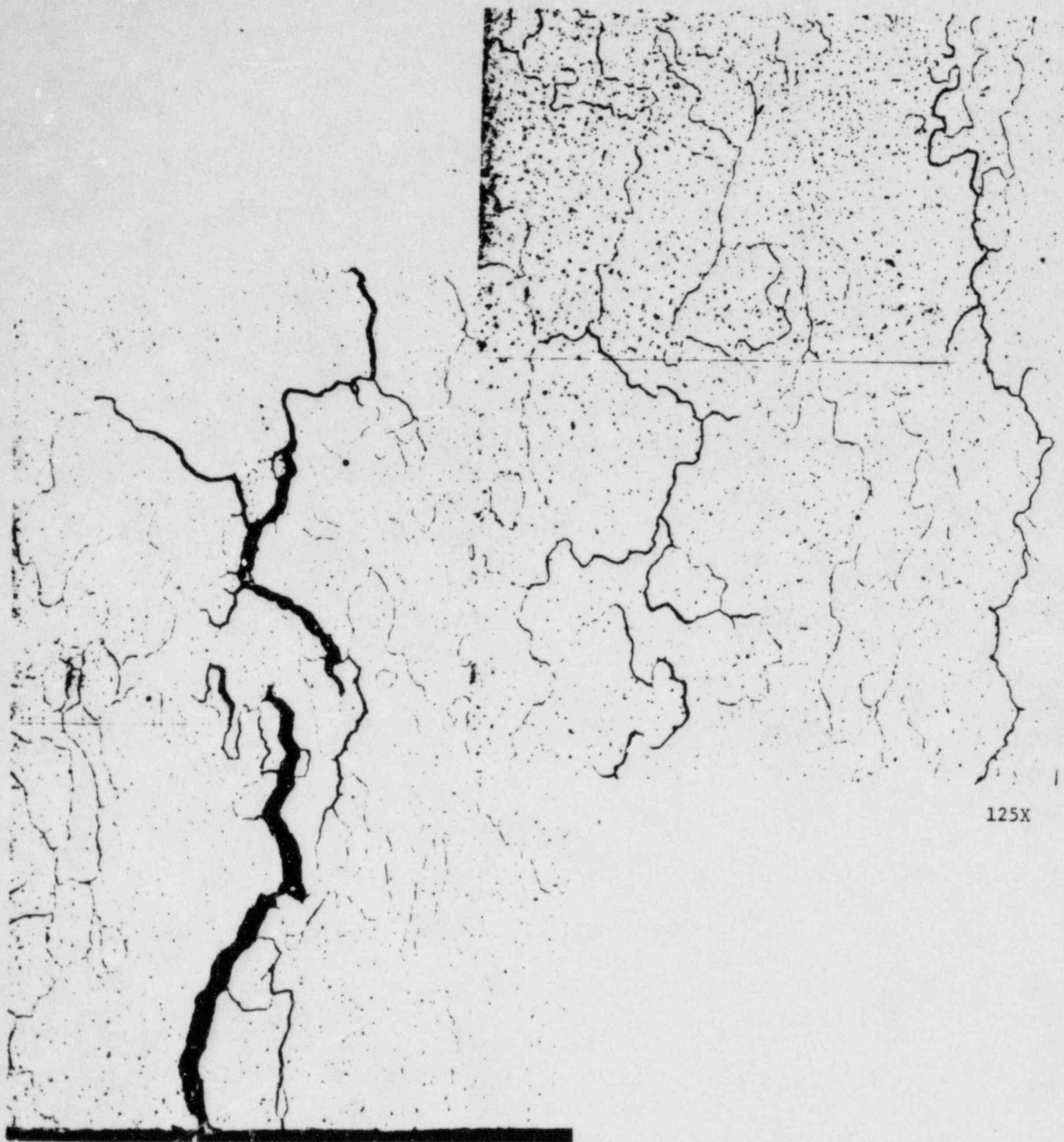
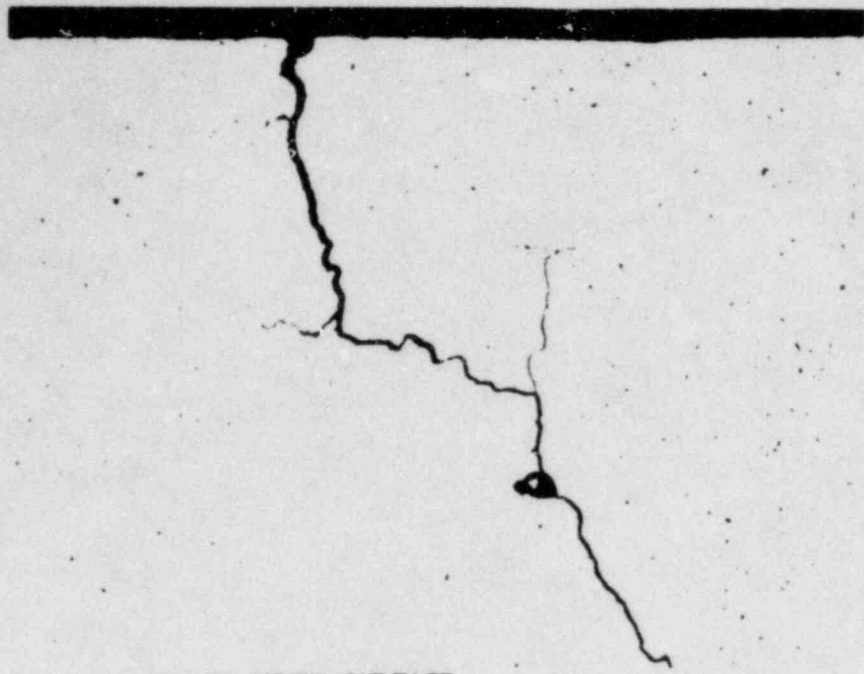


Figure 3.1-8. Interdentritic Cracking in Alloy 182 (Boat Sample 3, Crack No. 2)



CRACK INNER SURFACE

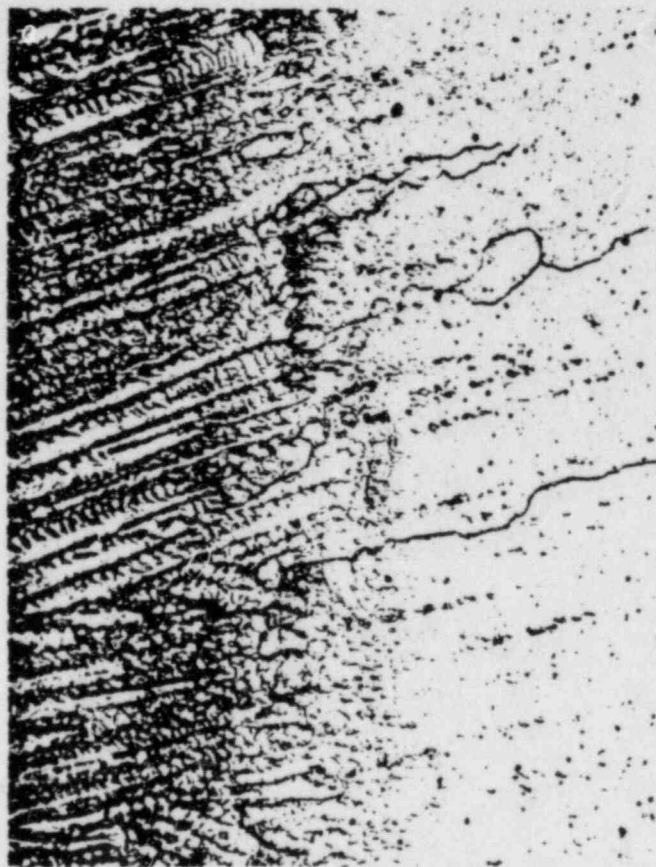
125X



CRACK TIP

Figure 3.1-9. High Magnification View of Interdendritic Crack No. 3 of 33X Composite - Alloy 182 Butter (Boat Sample 3)

ALLOY 82
ROOT PASS



ALLOY 182
BUTTER

250X

Figure 3.1-10. Crack Arrest in Alloy 82 Weld Root (Boat Sample 3)



Figure 3.1-11. Scanning Electron Micrograph of Axial Crack in Boat Sample No. 3

3.2 RESIDUAL STRESS ANALYSIS AND STRUCTURAL INTEGRITY EVALUATION

3.2.1 Introduction

In this section the results of the residual stress analysis of the recirculation nozzle/safe-end weld joint are discussed. The results show that the residual stress is a major contributor to the observed cracking. In addition, the plastic yielding at the final weld overwhelms the stresses resulting from half-bead repair. Thus, the half-bead repair is not a controlling factor in the stress state after completion of the weld. Finally, the effect of the observed cracks on the structural integrity of the weld joint is evaluated. It is concluded that short axial cracks of the type seen in service do not pose any safety concerns.

3.2.2 Residual Stress Analysis

The analysis to determine weld residual stress consisted of three main parts:

- (1) Finite element modelling
- (2) Thermal analysis
- (3) Residual stress analysis

Each part of the analysis is described in the following subsections.

3.2.2.1 Finite Element Modelling

The finite element analysis was performed using the ANSYS computer program.¹ The axisymmetric finite element model used in the thermal stress analysis is shown in Figure 3.2-1. Also shown in Figure 3.2-1 is the stainless steel piping material, low alloy nozzle material, and Alloy 82 and 182 weld material. Different material properties were assigned to the three sets

of elements. The model was made up of axisymmetric quadrilateral isoparametric elements for both the thermal and stress analysis. The length of the model on both sides of the weld was chosen to be in excess of three attenuation lengths ($3\sqrt{Rt}$) to eliminate end effects.

3.2.2.2 Thermal Analysis

The temperature distribution throughout the welding was first determined by performing a thermal analysis. The temperature-time history from the thermal analysis was input to a stress analysis model to determine the resulting stress. Temperature-dependent properties were used and a transient thermal analysis was performed to determine the temperatures during welding.

The predicted residual stress distribution from welding is dependent on a good representation of the transient temperature behavior of the pipe during welding. The Nugget Area Heating (NAH) method was used in the thermal analysis of the welded pipe. The NAH method simulates the welding process by heating all nodes which lie within the finite element model molten area to the melting temperature of Alloy 182. The temperature of the molten area is held at the melting temperature for a period of time. At the end of the hold time, the nodal temperature boundary conditions are released and the pipe cools back to ambient temperature. Figures 3.2-2 and 3.2-3 show the simulation of the welding process. Heat transfer coefficients were assigned to the inside and outside surface to simulate natural convection and radiation to the surroundings.

Figures 3.2-4 through 3.2-7 show the results of the thermal analysis. Isotherms at various times throughout the transient are shown in the figures. The effect of material discontinuity can be seen by the higher heat flow rate in the low alloy steel as compared to the stainless steel.

3.2.2.3 Stress Analysis

Plastic analysis was performed based on the von Mises yield criteria and the Prandtl-Reuss equations. Subsequent yielding was evaluated using a kinematic hardening model and a bilinear temperature dependent stress-strain curve.

The stress analysis used the temperature-time history from the thermal analysis to determine the residual stress. Sufficiently small time steps between the temperature distributions were chosen for the stress analysis. This assures numerical convergence as well as a proper description of the cyclic thermal loading.

Figure 3.2-8 shows the residual hoop and axial stress on the inside surface of the pipe. Also shown on the same figure are the interfaces between the three materials present. The results show that the hoop stress is approximately 20 ksi greater than the axial stress in the area of cracking. The axial cracking in the Pilgrim nozzle confirms that residual hoop stress was a major contributing factor.

Figure 3.2-9 shows the through wall hoop and axial residual stress at the cracked cross-section. The residual hoop stress remains highly tensile throughout the pipe section. The residual axial stress decreases rapidly and becomes compressive at approximately 30% of pipe wall depth.

3.2.3 Explanation of Observed Cracking

The main sources of stress in the region of the weld between the safe-end and the nozzle are from pressure and welding. For the recirculation outlet nozzle safe-end (pressure = 1050 psi, thickness = 1.5 in. and outside diameter = 29.3 in.), the hoop stress under internal pressure is 10 ksi. In addition, the hoop residual stress in the weld region varies from 50 to 70 ksi. The combination of high hoop stress due to pressure and weld residual stress is sufficient to explain the observed axial cracking. The axial residual stress

in the weld region is lower than the corresponding hoop stress. More significantly, the axial pressure stress (which is a primary stress and is therefore more significant from the IGSCC viewpoint) is 5 ksi, half of the hoop stress. Therefore, compared to the hoop stress, the overall axial stress is significantly lower and circumferential cracking is less likely to occur.

The predominant axial cracking can be further explained based on the through-wall stress distribution shown in Figure 3.2-9. The hoop residual stress is uniform through the thickness and promotes crack growth, whereas the axial stress is a bending stress and is less severe for crack growth.

3.2.4 Effect of Final Weld on Stresses Due to Half-Bead Repair

The purpose of this section is to determine if the residual stress due to half-bead repair increases the overall stress after completion of the final weld. Any increase in the overall stress can be assessed by examining the extent of yielding in the Alloy 182 weld butter region. If, during the final weld, the plastic yielding is sufficient to overwhelm the previous stress history, then the final stress state will be independent of the stresses resulting from half-bead repair.

Figure 3.2-10 shows the region of yielding from the finite element analysis results. Elements which experienced yielding during the welding process are shown with a solid dot in Figure 3.2-10. It is seen that there is extensive through-wall yielding on both sides of the final safe-end to nozzle weld. Figure 3.2-11 also shows the effect of strain as a function of load steps (or time) during welding and subsequent cooling. It is seen that the strain at the centroid of the ID surface element is in excess of 1%. A strain in excess of 1% is high enough to assure that the half-bead repair stresses are eliminated.

Previous analytical and experimental studies on Induction Heating Stress Improvement (IHSI)² and Last Pass Heat Sink Welding (LPHSW)³ have shown that plastic yielding 'wipes out' the prior residual stress as well as the previous

stress-strain history. Based on this, it can be concluded that the final stresses in the safe-end/nozzle weld and surrounding material are essentially the same as that in a weld without half-bead repair.

3.2.5 Structural Integrity

In this section an evaluation is performed to determine the structural integrity of the recirculation safe-end/nozzle weld joint.

3.2.5.1 Critical Crack Size for Longitudinal Cracks

Analysis was performed to determine critical crack sizes for both the recirculation inlet and outlet nozzle weld region. A through-wall crack was conservatively assumed and evaluations were performed assuming both linear elastic fracture mechanics (LEFM) and limit load failure mechanisms. Details of the analysis are outlined here.

The dimensions of the recirculation inlet nozzle are given below:

Outside Diameter (OD): 13.37 in.

Inside Diameter (ID): 11.50 in.

Mean Radius (R): 6.22 in.

Thickness (t): 0.94 in.

Pressure Stress: $\frac{PD}{2t} = 7.47 \text{ ksi}$

All other stress (e.g., residual stress) are insignificant, especially when long cracks which extend beyond the weld region are considered.

The stress intensity factor for a through-wall crack in a cylindrical shell is given by

$$k = \sigma \sqrt{\pi a} \cdot Y(\lambda) \quad (3.2-1)$$

where

$$Y = (1 + 1.25 \lambda^2)^{1/2} \quad \text{for } 0 \leq \lambda \leq 1$$
$$= (0.5 + 0.9 \lambda) \quad \text{for } 1 \leq \lambda \leq 5$$

and

$$\lambda = \sqrt{\frac{a}{Rt}}$$

where σ is the applied stress and $2a$ is the crack length. Figure 3.2-12 shows the applied stress intensity factor as a function of crack length. The temperature of the low alloy steel nozzle is sufficiently high to assure a material toughness of at least 200 ksi $\sqrt{\text{in}}$.

Figure 3.2-12 shows that the critical crack length for a through-wall crack is approximately 22 inches for the recirculation inlet nozzle.

For a limit load failure mechanism the hoop stress at critical conditions is given by

$$\sigma_h = \sigma_f / M \quad (3.2-2)$$

where

σ_f = flow stress

= average of yield and ultimate strength

$$= \frac{42.6 + 80}{2} = 61.3 \text{ ksi}$$

and

$$M = (1 + 1.61 \lambda^2)^{1/2} \quad (3.2-3)$$

Substituting $\sigma_h = 7.47$ ksi in Equation 3.2-3, the corresponding value of λ is 6.42 and the critical crack length is 31 inches.

Using the lesser of the calculated values for the two failure mechanisms the critical crack length for a through-wall crack in the 12-inch recirculation inlet nozzle is 22 inches. The corresponding critical crack length for the stainless steel safe-end is higher.

The recirculation outlet nozzle dimensions and hoop stress are:

Outside Diameter (OD):	29.31 in.
Inside Diameter (ID):	26.06 in.
Mean Radius (R):	13.84 in.
Hoop Stress:	9.47 ksi

Figure 3.2-12 also shows the applied stress intensity factor as a function of through-wall crack length. It is seen that the critical crack length is in excess of 27 inches for the recirculation outlet nozzle.

The value of λ corresponding to a failure at a hoop stress of 9.47 ksi was 5.02. This is equivalent to a crack length of 47 inches.

Selecting the lower of the LEFM and limit load calculations, the critical crack length for the 28-inch recirculation outlet nozzle is determined to be 27 inches. As before, the corresponding value for the stainless steel safe-end is higher.

The actual cracking in the Alloy 182 weld butter has been predominately axially oriented with length of approximately 1/2 inch. Even if the observed cracking were through-wall, this length is short relative to the critical crack sizes calculated for a through-wall crack in either the low alloy steel nozzle or the stainless steel safe-end. If the observed cracks propagate to be through-wall, the leakage would be detected before the lengths become significant. Consequently, the inherent leak-before-break margin associated with the IGSCC phenomenon is maintained.

3.2.6 Summary

Based on the above analysis, the following conclusions can be made:

- (1) The predominantly axial cracking is expected due to high weld residual hoop stress.
- (2) Plastic yielding produced by the safe-end/nozzle weld is sufficient to overwhelm the previous stress history produced by the half-bead repair.
- (3) Structural integrity of the safe-end/nozzle weld joint is maintained.

Therefore, the cracking in the Alloy 182 weld butter does not pose any safety concerns and can be mitigated with an orderly remedial program.

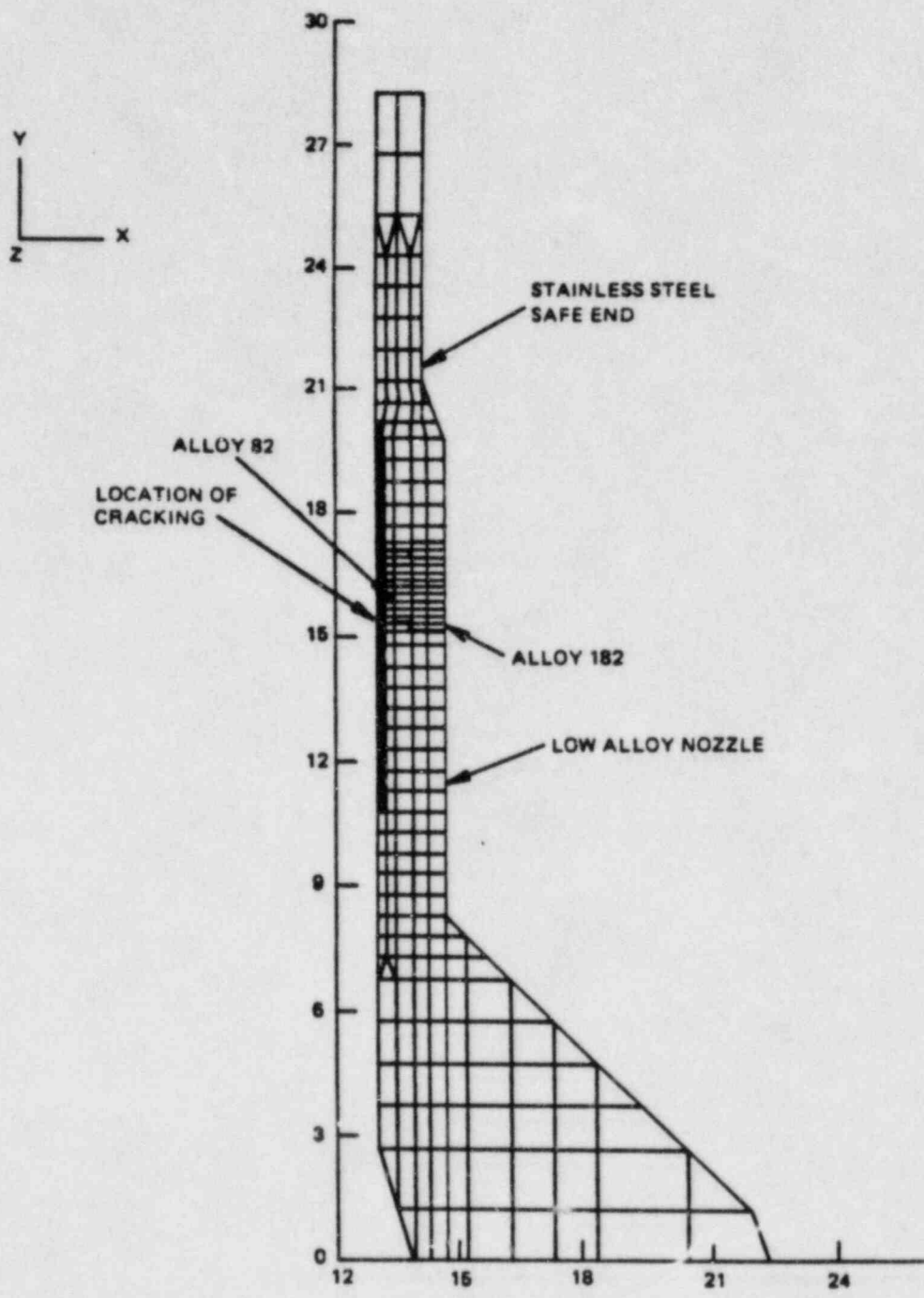


Figure 3.2-1. Pilgrim Recirculation Outlet Nozzle Finite Element Model

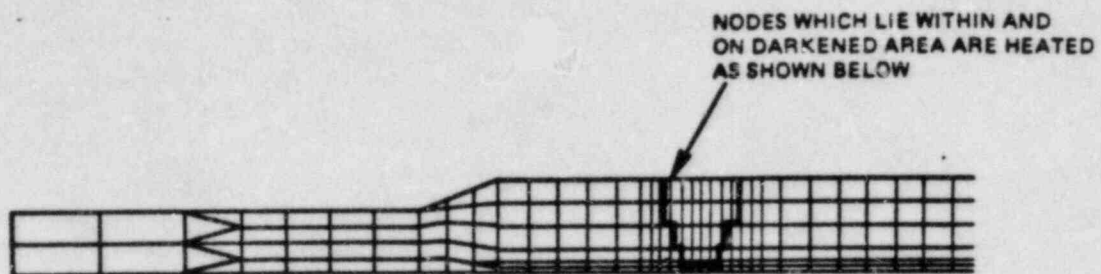


Figure 3.2-2. Nuggett Area Modelling

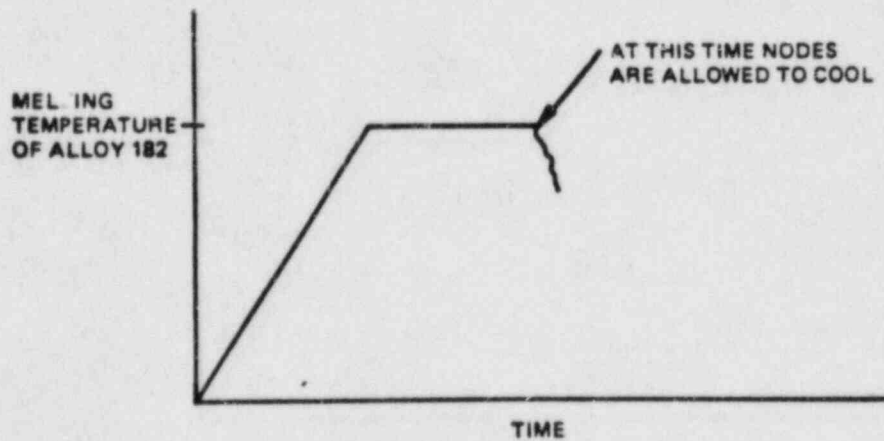


Figure 3.2-3. Nuggett Area Heating Temperature History

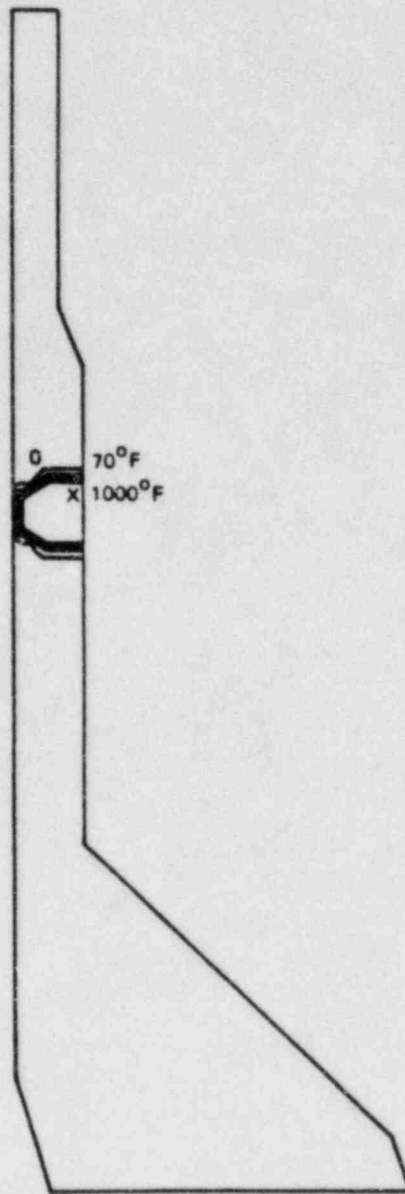


Figure 3.2-4. Isotherms at 3 Seconds

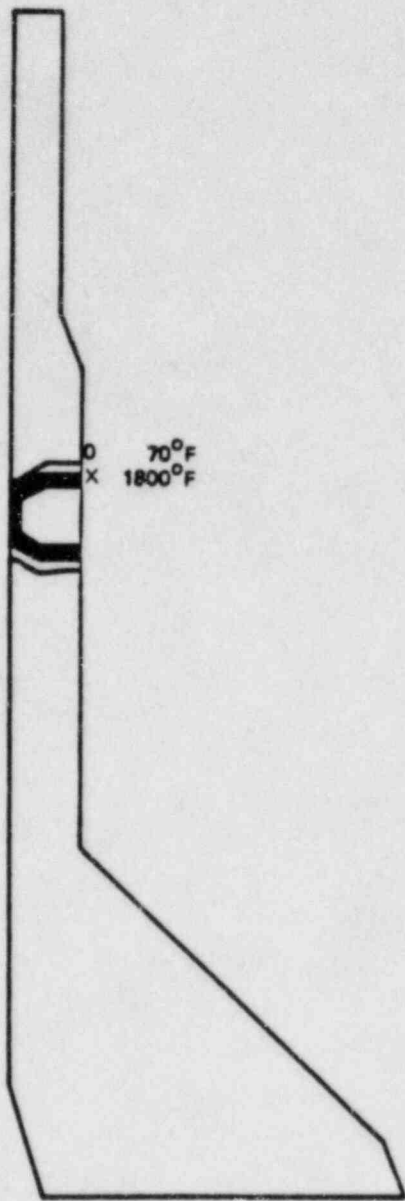


Figure 3.2-5. Isotherms at 6 Seconds

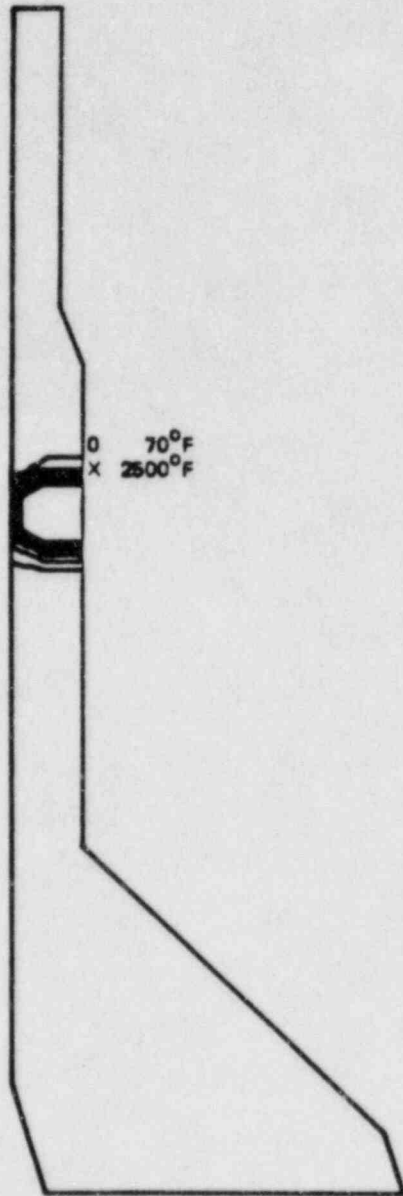


Figure 3.2-6. Isotherms at 9 Seconds

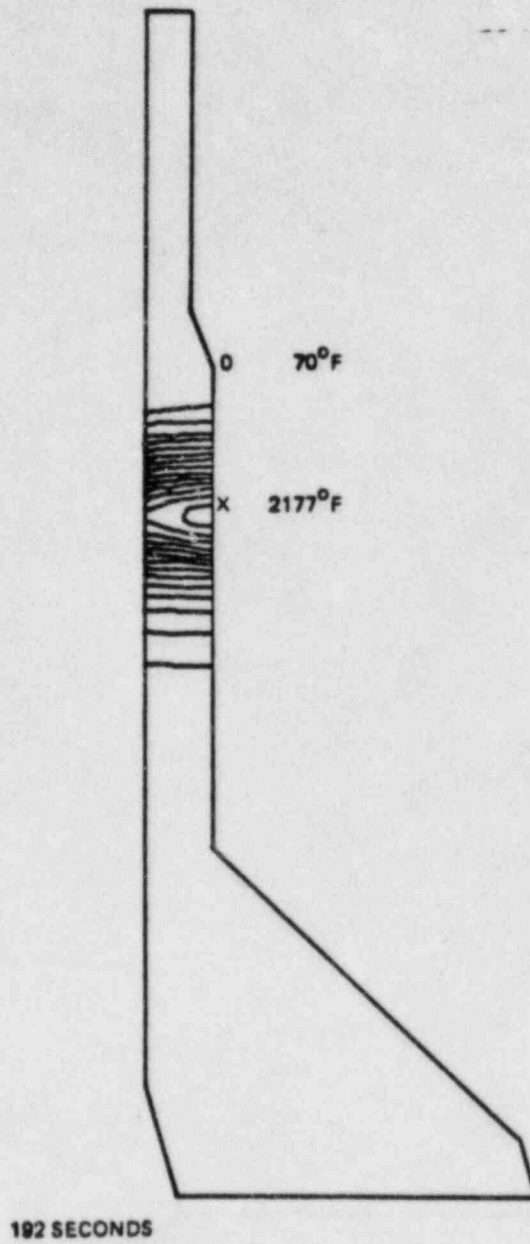


Figure 3.2-7. Isotherms During Cooldown

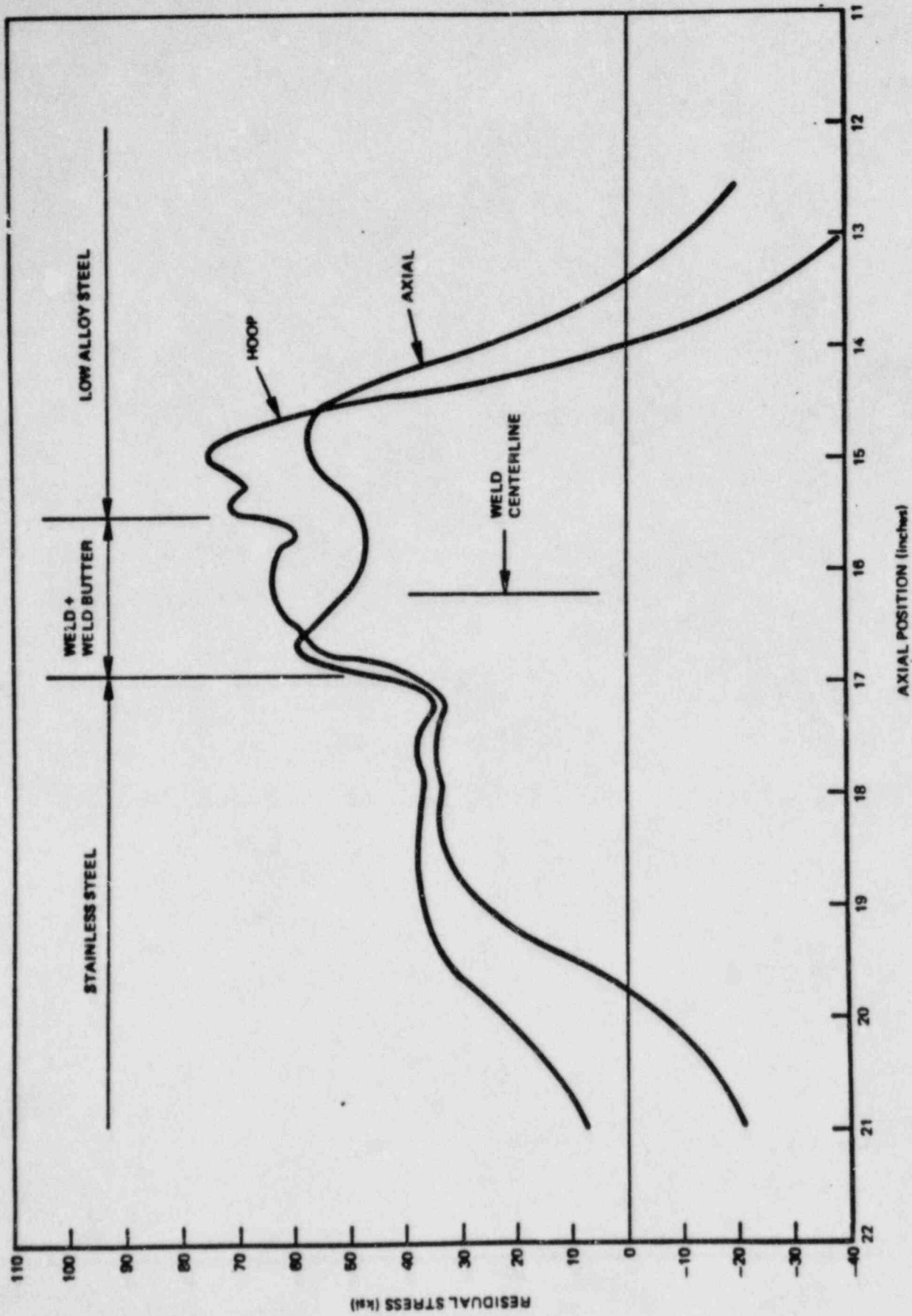


Figure 3.2-8. Pilgrim Recirculation Outlet Nozzle Residual Stress Analysis

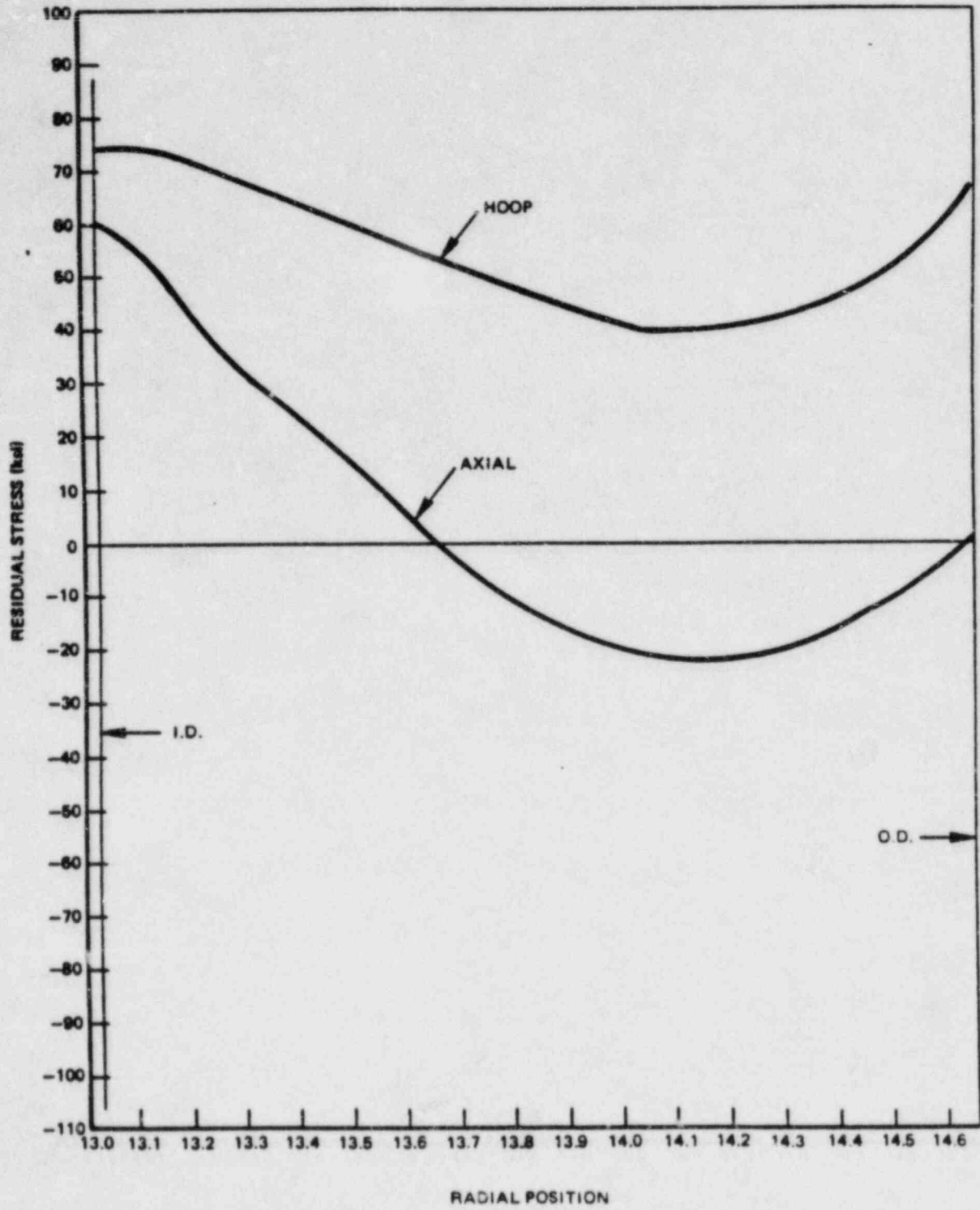


Figure 3.2-9. Throughwall Residual Stress

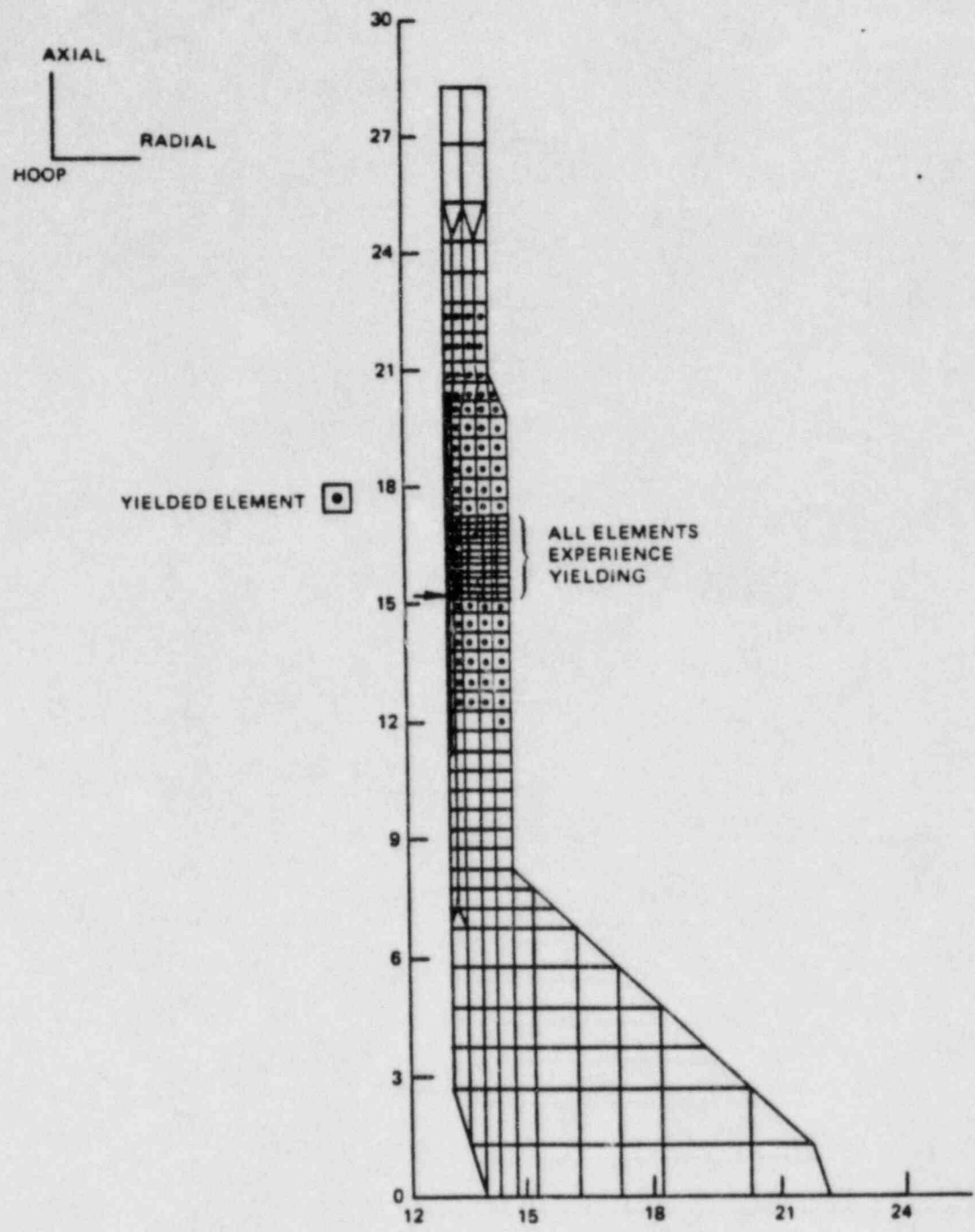


Figure 3.2-10. Region of Yielding

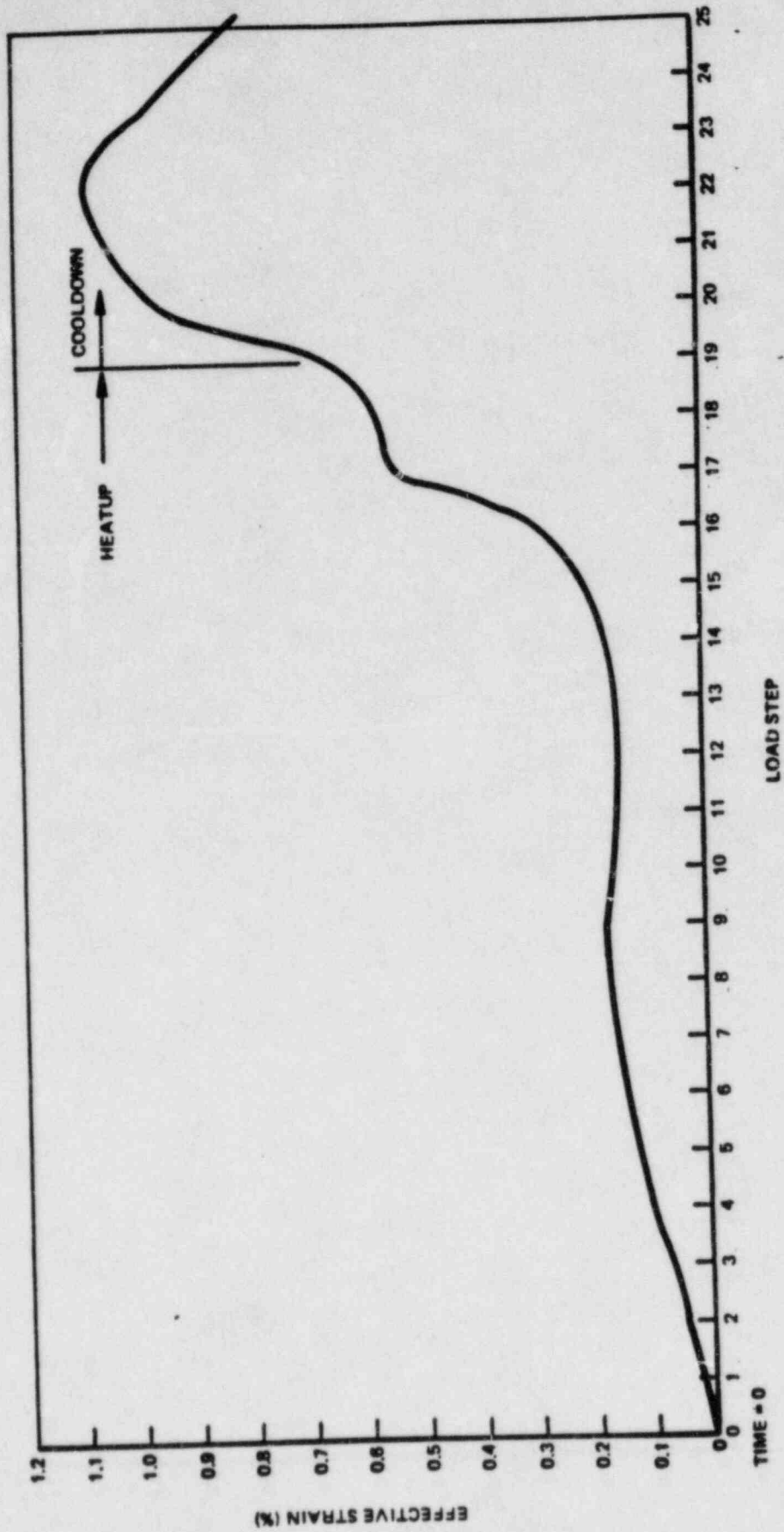


Figure 3.2-11. Effective Strain Versus Load Step (Time)

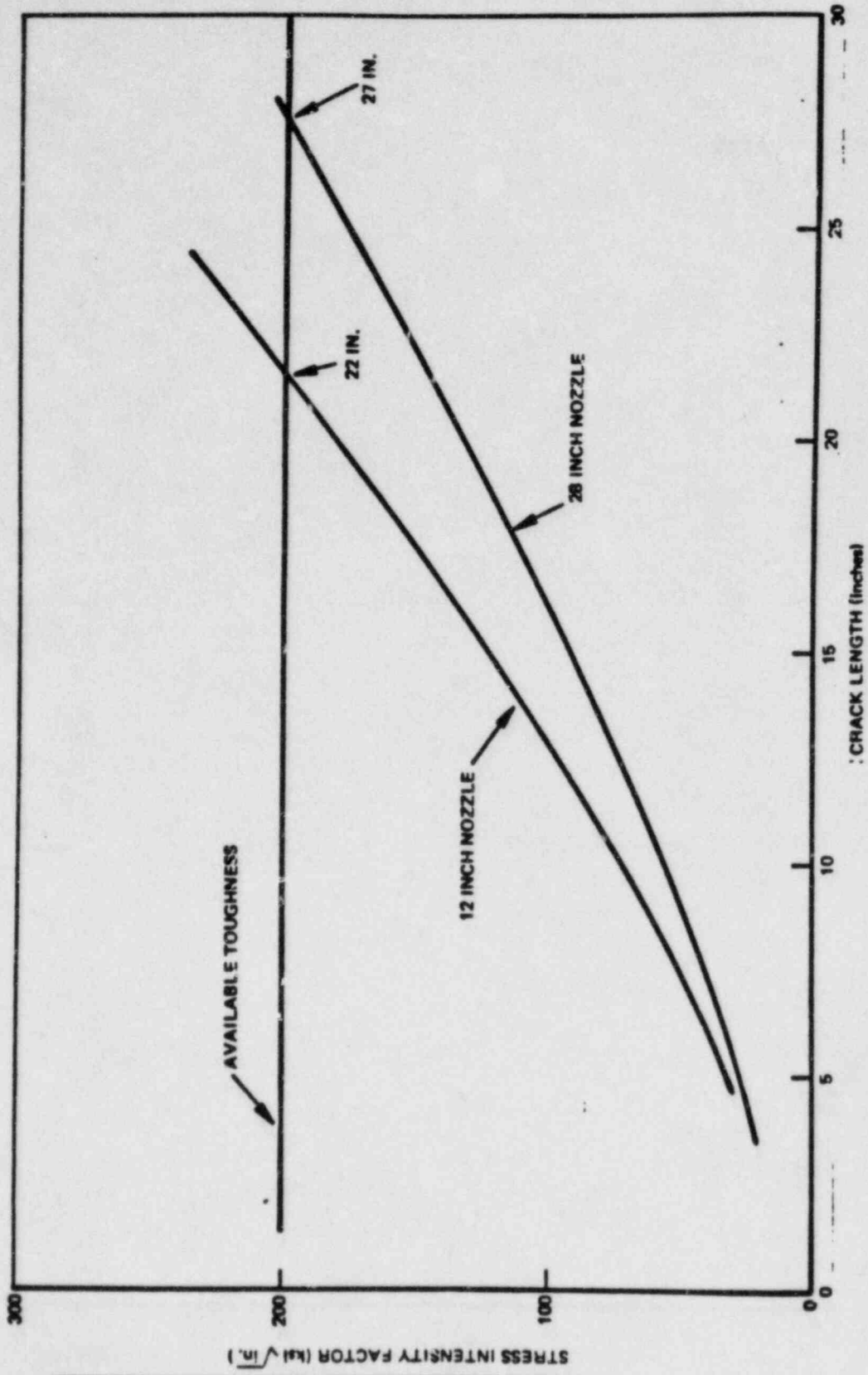


Figure 3.2-12. Critical Flaw Size Assuming LEFM

3.3 RECIRCULATION NOZZLE AND SAFE-END FABRICATION HISTORY

3.3.1 Introduction

The shop fabrication history and field records review for the recirculation inlet and outlet nozzles and safe-ends are described in this section. The scope of the records review included General Electric Quality Assurance records, Combustion Engineering records and site construction records maintained by Boston Edison Company.

The vessel was fabricated by Combustion Engineering and the original safe-ends were post-weld heat treated with the reactor vessel. These furnace sensitized safe-ends were subsequently removed in the shop and new Type 304 stainless steel safe-ends were installed in the field by Bechtel Corporation.

3.3.2 Initial Safe-End Installation

The original safe-ends were welded to the nozzle forgings prior to nozzle installation in the vessel shell. This was accomplished using Combustion Engineering (CE) Detail Weld Procedure (DWP) WC-21466-345-0 (Appendix A). Figure 3.3-1 shows a schematic representation of the joint (actual dimensions are shown in CE drawing E-232-345 - Appendix B). The nozzle forging was first positioned with its centerline vertical to facilitate fit up and tack welding. A single Type 308 stainless steel root pass was then applied as a horizontal (2G) weld. The nozzle with safe-end was then positioned horizontally, preheated to 300°F and welded on in the flat position using Ni-Cr-Fe Alloy 182, 1/8" and 5/32" diameter covered electrodes. Preheat was maintained following weld completion until the joint received an intermediate post-weld heat treatment of 1125°F for 15 minutes. The nozzle safe-end assembly was finished machined except for the piping side of the safe-end, where added length and a modified weld prep was left for hydrotest caps as shown in Figure 3.3-2. The nozzle/safe-end subassemblies were then installed in the vessel shell courses and post-weld heat treated (PWHT) at 1150°F. These nozzles accumulated total times at PWHT temperatures in the range of 9-13 hours.

3.3.3 Furnace Sensitized Safe-End Removal

Following installation in the vessel, a decision was made to remove and replace the furnace sensitized stainless steel safe-ends. This was accomplished in two operations. The first operation was performed in March-May 1969, prior to vessel hydrotest. The second operation was performed in November-December 1969 after vessel hydrotest.

The first operation in safe-end removal was to prepare a 3/8" radius, I.D. groove in the safe-end/weld area to remove the furnace sensitized 304 safe-end and apply additional Ni-Cr-Fe weld. This added weld would provide the desired "butter" thickness for joining a new safe-end without preheat or post-weld heat treatment. The I.D. buildup operation is shown schematically in Figure 3.3-3; it was performed in accordance with CE drawing E-232-345 and DWP WK-21466-345-1 (Appendix C). This procedure permits 1/8" and 5/32" ENi-Cr-Fe-3 (182) covered electrodes, although records indicate that only 5/32" was used, all from the same heat. (Ni-Cr-Fe heat numbers and chemistries are discussed in Section 3.3-6.) The completed I.D. weld buildup was 100% inspected by liquid penetrant and radiographic testing.

The second operation was to machine to remove the safe-end and form a field weld preparation. If required, a weld buildup could be added to the end of each nozzle, as shown schematically in Figure 3.3-4. The buildup was defined in CE drawing E-232-369 (Appendix D) and DWP WA-21466-369-1 (Appendix E). The DWP requires 1/8" ENi-Cr-Fe-3 (182) covered electrodes. Weld inspection and shop traveler records showed that this buildup was applied to N2-A but welding electrode issue records indicate that it could have been applied to other inlet and outlet nozzles.

Following safe-end removal by cutting 1-in. outboard of the weld, the Ni-Cr-Fe butter was machined to the "extended land" configuration, which used a $22\ 1/2 \pm 2^\circ$ prep. angle, 1/16" max. radius, 3/32" \pm 1/64" land face, and 1/16" + 1/32" - 0" land extension (refer to Appendix D, CE drawing E-232-369 Detail "A"). Following machining, all weld preps received liquid penetrant testing per applicable Code requirements.

3.3.4 Replacement Safe-End Fabrication

In parallel to work on the reactor vessel recirculation nozzles, new safe-ends were fabricated from Type 304 stainless steel forgings. The safe-ends were rough machined, weld buttered with Ni-Cr-Fe Alloy 182 then solution heat treated, as shown schematically in Figure 3.3-5. The safe-ends were made in accordance with CE drawing E-232-369, buttering was applied per DWP WB-21466-369-1 (Appendix F), and solution heat treatment was performed per specification M&P 5.5.5.5 (a) (Appendix G). (The solution heat treatment was not required by the engineering specifications and was not called out on the drawings. A review of the shop travelers and heat treat charts confirmed that solution heat treatment was actually performed on all inlet and outlet safe-ends.) Following installation, however, the Alloy 182 butter on the safe-end side ends up in the as-welded metallurgical condition following butt welding.

3.3.5 Field Installation

The safe-ends were installed in the field by Bechtel Corporation in accordance with Welding Procedure Specification P12 P8-AT-Ag (F43) Revision 1 (Appendix H). This procedure is a Gas-Tungsten-Arc Welding (GTAW) or Shielded-Metal-Arc Welding (SMAW) combination procedure. The root pass and the next two layers are made using GTAW with type ERNi-Cr-3 (Alloy 82) filler metal, and the balance of the weld is made using SMAW and ENi-Cr-Fe-3 (Alloy 182) welding electrodes. The root pass was made with the "open butt" technique using spacer blocks to hold the gap and alignment, as shown in Figure 3.3-6. This procedure also required removal of the top half of the land thickness by hand filing.

According to the weld procedure, liquid penetrant examination was performed after the third GTAW pass and on the final I.D. and O.D. surfaces.* Radiography was also performed of the final weld.

3.3.6 Repairs or Other Special Findings

Records were reviewed for conformance to the drawing and specification requirements and to determine whether repairs or other fabrication and

*Thermal sleeves were not installed, so the I.D. of the inlet nozzle to safe-end weld was accessible.

construction operations could be correlated to the stress corrosion cracking found in safe-end to nozzle inlet welds N2-B, N2-F and N2-J, and outlet weld N1-B. From the available shop and field records, there was no evidence of drawing or procedure deviations or field modifications. The methods outlined in the previous sections were those actually used.

Repair records were also reviewed. Detailed maps of repairs were not made; however, repairs were documented by welding inspection and wire/electrode issue ("draw") slips or log sheets. Such records were reviewed and the results can be summarized as: (1) the extent of repair welding required in both the shop and field was not abnormal for Ni-Cr-Fe welding, and (2) weld repairs in a given nozzle did not correlate with the cracking propensity of that nozzle, and similarly, some nozzles found to contain cracking had no evidence of repairs being made.

A detailed review was conducted of all Ni-Cr and Ni-Cr-Fe materials used in the shop and field. In addition to chemistry, material manufacturer was also considered. The findings are summarized in Table 3.3-1 for shop welds and Table 3.3-2 for field welds. All heats of material involved are within specified limits and, with minor exception, are quite consistent in composition (including carbon, phosphorus and sulphur). A slight difference in manganese and iron level is noted between manufacturers (heat codes ending in MD) in Table 3.3-2. This is probably related to electrode coating composition rather than the core wire chemistry. These compositional differences showed no apparent relationship to nozzle weld cracking (these field weld heats of Alloy 182 would not have been exposed initially to the BWR environment, however).

3.3.7 Summary

A complete review of available records has been used to show the series of operations used to fabricate the Pilgrim recirculation inlet and outlet nozzle assemblies. Although no obvious correlation between the fabrication history and cracking has been identified, several operations performed during fabrication may have contributed to cracking. These operations are summarized below:

1. The multiple Alloy 182 welding operations performed on the nozzle side of the joint (weld and PWHT, then I.D. butter buildup in the groove and the deposition of added material for the extended land), could create a more complex metallurgical and residual stress condition than would otherwise be present. However, as pointed out in Subsection 3.2.4, the final residual stress state appears to be dominated by the butt weld and is therefore independent of the weld butter application history.

2. The use of the field, open butt welding procedure for a nozzle to safe-end weld joint is not typical of the integral backing ring or consumable insert practice of most vessel fabricators. Although it cannot be said that open-butt welding per se is unacceptable, it is known that high weld shrinkage tends to close the gap of the open-butt weld (prevention of this is one of the functions of the four spacer blocks shown in Figure 3.3-6). The use of this technique for a Ni-Cr-Fe weld, based on today's technology, would not be approved without additional testing and evaluation.

Table 3.3-1
 ALLOY 182 HEAT NUMBERS FOR PILGRIM
 *** COMBUSTION ENGINEERING SHOP WELDS ***

HEAT NO. ALLOY	SIZE	CHEMISTRY											USED ON			
		C	Mn	Fe	S	P	Si	Cu	Ni	Cr	Al	Ti		Co	Cb	Ta
012-182	182 1/8" Dia.	0.04	8.26	5.79	0.011	0.006	0.44	0.04	67.34	14.56	-	0.41	-	2.09	*	N1A, N1B, N2A, N2B, N2C, N2D, N2E
1907-182	182 1/8" Dia.	0.05	7.64	7.09	0.011	-	0.64	0.01	67.89	14.65	-	0.38	-	1.62	*	N1A(R), N2H(R)
2096-182	182 1/8" Dia.	0.04	7.39	7.05	0.009	0.003	0.55	0.02	68.14	14.53	-	0.49	0.09	1.66	0.01	N2E, N2F, N2J, N2K
2215-182	182 5/32" Dia.	0.03	6.88	7.36	0.010	0.010	0.48	0.02	68.49	14.94	-	0.50	0.07	1.47	0.01	N1A, N1B, N2A, N2B, N2C, N2E(R), N2F(R)
2372-182	182 5/32" Dia.	0.03	7.26	7.05	0.007	0.009	0.53	0.02	68.55	14.40	-	0.44	0.02	1.63	0.02	ALL N1, N2 (SEE NOTE 3)
2216-182	182 5/32" Dia.	0.03	6.98	7.13	0.011	0.010	0.53	0.02	68.88	14.47	-	0.35	0.04	1.53	0.01	N1A, N1B, N2D, N2G, N2H
2275-182	182 5/32" Dia.	0.03	7.05	7.21	0.010	0.011	0.50	0.01	68.07	15.04	-	0.50	0.02	1.53	0.01	N2D(R)
2268-182	182 1/8" Dia.	0.04	7.57	7.10	0.010	0.010	0.49	0.01	68.30	14.27	-	0.46	0.02	1.71	"	N2G(R)
2515-182	182 1/8" Dia.	0.03	7.59	7.26	0.009	0.009	0.49	0.03	67.30	14.86	-	0.58	-	1.79	0.02	(SEE NOTE 4)
2495-182	182 5/32" Dia.	0.03	7.15	7.46	0.007	0.008	0.50	0.03	67.81	14.93	-	0.32	0.02	1.66	0.04	N1A, N1B, N2B, N2C, N2D, N2E
2505-182	182 5/32" Dia.	0.03	7.00	7.83	0.007	0.008	0.49	0.06	67.60	14.76	-	0.52	0.04	1.63	0.01	N2K, N2G, N2H, N2J, N2K
2595-182	182	**CERT. NOT AVAILABLE														

NOTES:

1. RECORDS OBTAINED FROM COMBUSTION ENGINEERING.
2. ALL MATERIAL PRODUCED BY HUNTINGTON ALLOYS.
3. THIS HEAT WAS USED TO RESTORE WELD MATERIAL ON THE I.D. OF THE SAFE END/NOZZLE SUBASSEMBLY AFTER MACHINING A GROOVE TO REMOVE ALL 304 FURNACE SENSITIZED SAFE END MATERIAL.
4. THIS HEAT WAS USED TO MAKE THE EXTENDED WELD LAND BUILDUP ON THE NOZZLE BUTTERS ON N2A AND POSSIBLY OTHER NOZZLES.
5. PHOSPHORUS DATA OBTAINED BY GE THROUGH HUNTINGTON ALLOYS.

Table 3.3-2
ALLOY 82 AND 182 HEAT NUMBERS FOR PILGRIM

*** BECHTEL FIELD WELDS ***

HEAT. NO. ALLOY	SIZE	CHEMISTRY											USED ON NOZZLES			
		C	Mn	Fe	S	P	Si	Cu	Ni	Cr	Al	Ti		Co	Cb	Ta
N103030	62 3/32 X 36"	0.03	2.94	0.34	0.007	0.004	0.19	0.06	73.02	23.42	0.02	0.39	-	2.55	0.01	ALL N1, N2
N103900	62 1/8 X 36"	0.02	2.94	0.65	0.007	0.005	0.14	0.04	73.00	20.38	0.02	0.40	-	2.37	0.01	ALL N1, N2
2450-182	182 3/32" Dia.	0.04	7.65	7.41	0.007	0.010	0.60	0.02	67.35	14.54	-	0.50	0.02	1.62	0.02	N1B
2060-182	182 1/8" Dia.	0.04	7.53	7.13	0.011	0.009	0.62	0.02	67.99	14.38	-	0.45	0.03	1.78	0.01	N1B
2652-182	182 3/32" Dia.	0.02	7.48	7.11	0.010	0.006	0.58	0.01	68.03	14.66	-	0.36	0.03	1.62	0.01	N1A, N2D, N2C, N2J, N2K
2697-182	182 1/8" Dia.	0.03	7.68	7.30	0.012	-	0.54	0.01	68.04	14.28	-	0.36	0.04	1.68	0.01	N1A, N2B, N2C, N2H, N2J, N2K
2722-182	182 1/8" Dia.	0.04	7.35	7.12	0.010	0.008	0.61	0.06	68.27	14.29	-	0.56	0.04	1.51	0.01	N2A, N2E, N2F, N2H
2700-182	182 1/8" Dia.	0.03	7.80	7.54	0.009	0.000	0.56	0.01	67.30	14.30	-	0.55	0.02	1.77	0.01	N1A, N2D, N2E, N2F, N2G, N2J, N2K
2512-182	182 1/8" Dia.	0.03	7.32	7.32	0.007	0.006	0.50	0.03	67.68	14.84	-	0.43	-	1.80	-	N1A
1412MD	182 3/32" Dia.	0.03	7.50	9.00	0.012	-	0.75	0.04	66.00	14.00	-	0.60	0.04	1.90	*	N1A, N2B, N2C, N1B, N2J
LOT NO. L1K919 B 30 D																
1412MD	182 1/8" Dia.	0.03	5.26	8.80	0.011	-	0.72	0.09	68.13	13.95	-	0.04	0.10	1.74	0.04	N1A, N2B, N2C, N1B, N2J
LOT NO. 10006 B 30 D																
2603-182	182 1/8" Dia.	0.03	7.84	7.27	0.010	0.008	0.55	0.01	67.61	14.35	-	0.40	0.02	1.90	0.01	N1A
1278MD	182 3/32" Dia.	0.02	5.34	9.34	0.008	-	0.83	0.05	69.25	13.38	-	0.22	0.02	1.72	0.05	N2A, N2B, N2D, N2F, N2H, N2G, N2J, N2K(?)
2782-182	182 1/8" Dia.	0.06	7.35	7.03	0.012	0.011	0.62	0.02	67.58	14.15	-	0.35	0.03	1.60	0.01	N2E

* Included in Cb

NOTES:

1. RECORDS SEARCHED AND DATA OBTAINED BY BOSTON EDISON.
2. ALL MATERIAL PRODUCED BY HUNTINGTON ALLOYS, EXCEPT HEAT CODES ENDING WITH 'MD'. THESE HEATS WERE MADE BY CHEMETRON/ALLOY RODS DIVISION.
3. PHOSPHORUS VALUES OBTAINED BY GE THROUGH HUNTINGTON ALLOYS.

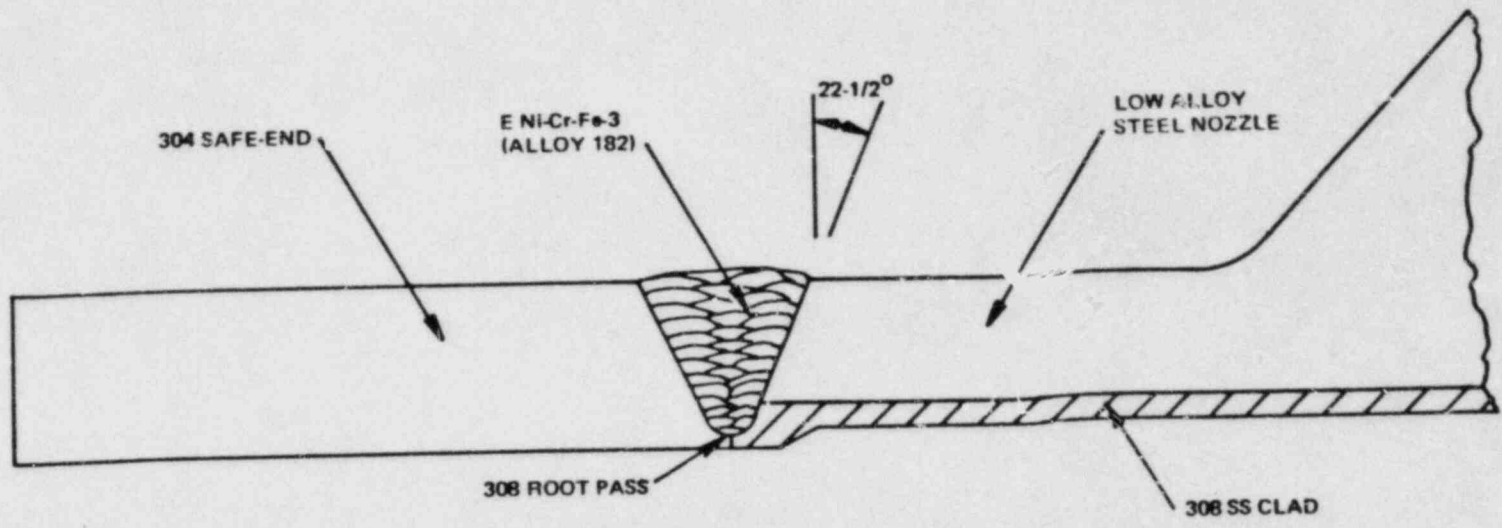
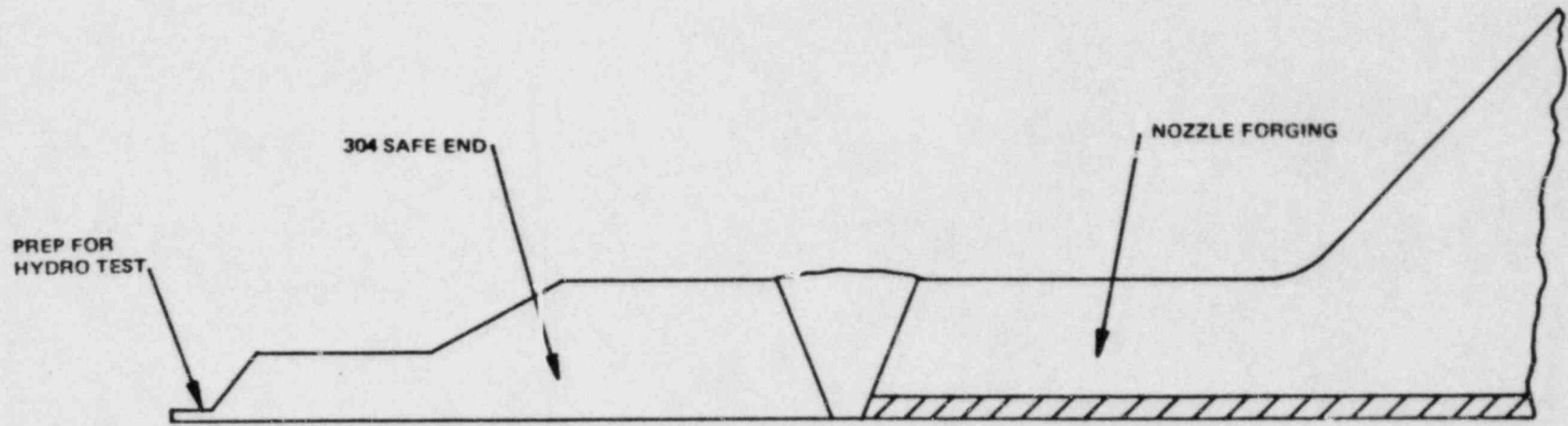


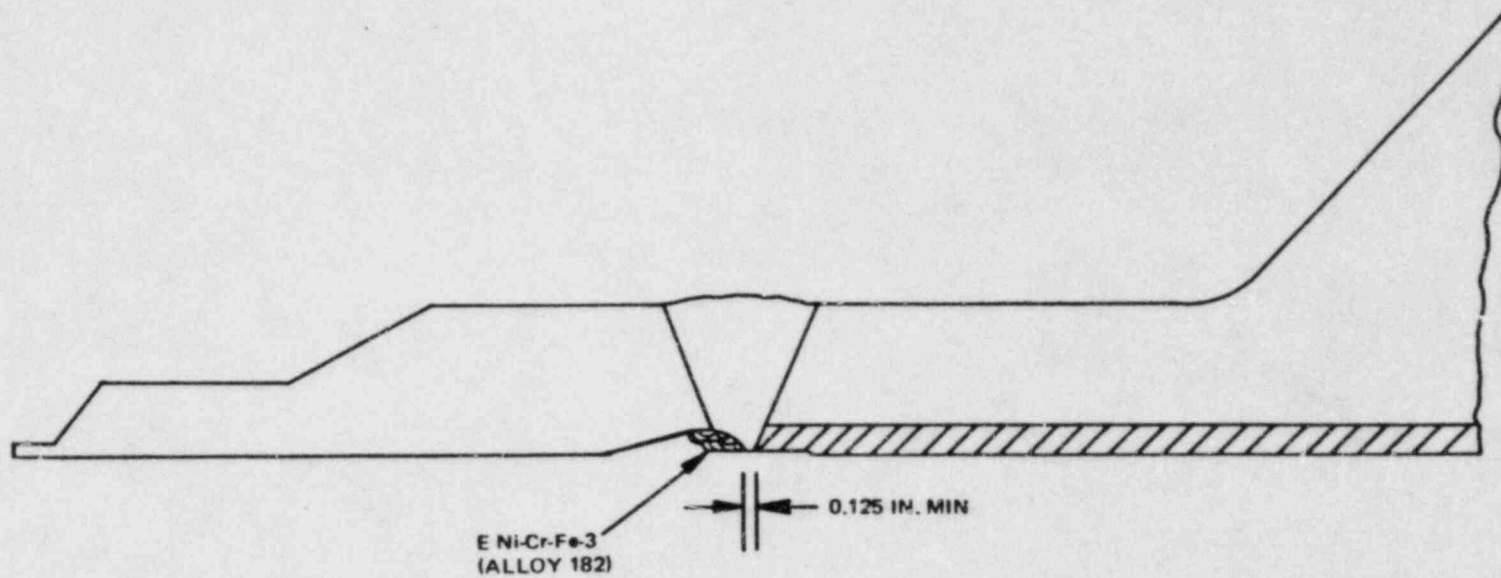
Figure 3.3-1. Shop Fabrication Procedure for Original Furnace Sensitized Safe-End

3-48



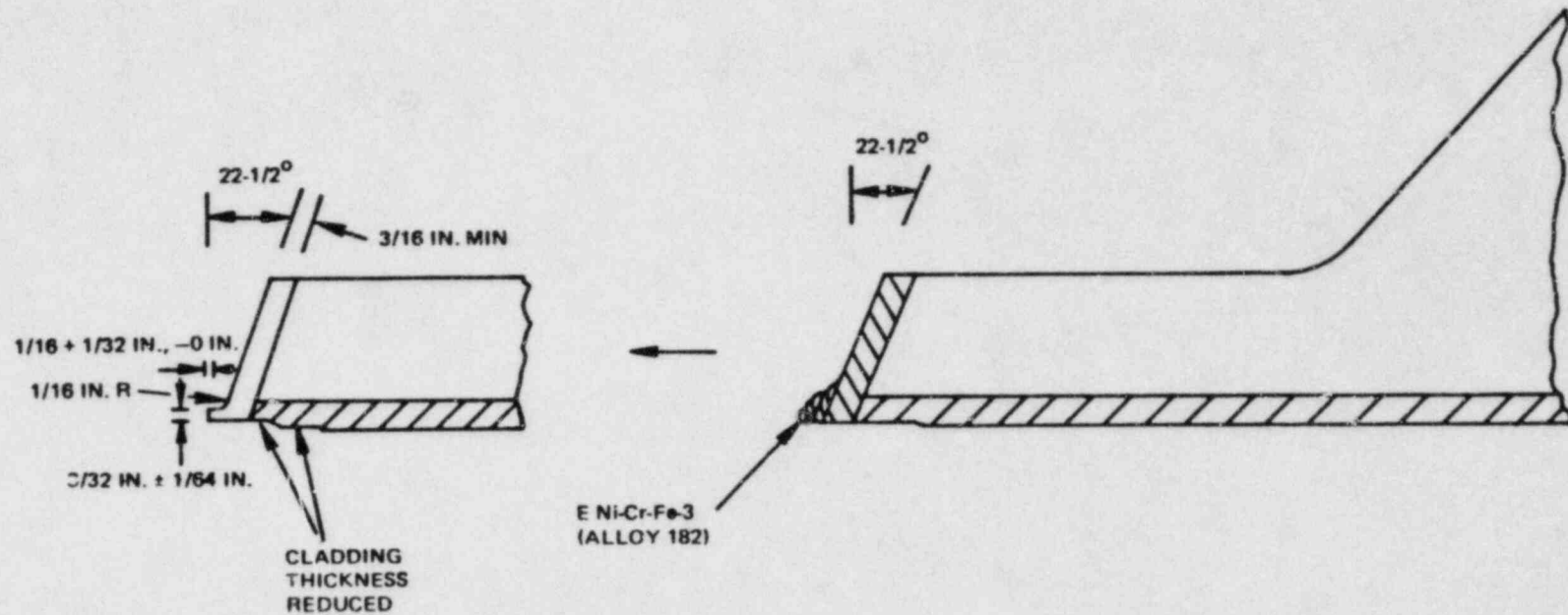
NEDO-30730

Figure 3.3-2. Shop Fabrication: Machine Safe-End Prior to Installation In Vessel Shell Course



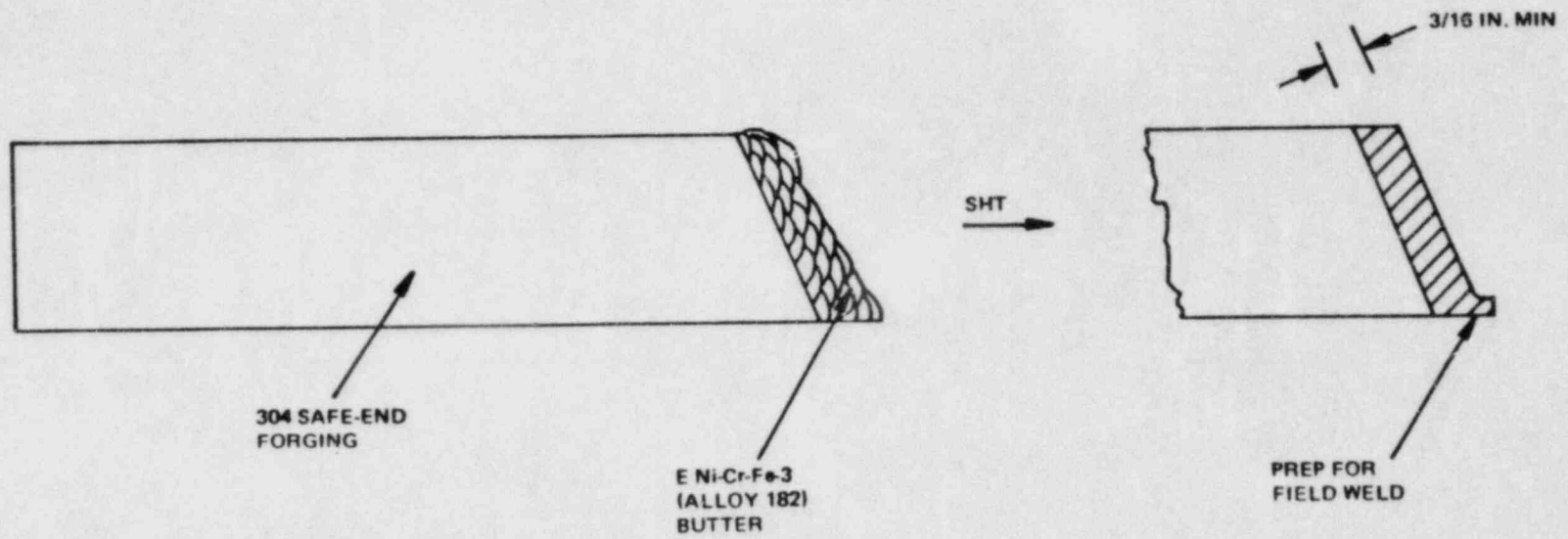
1. **PREPARE I.D. GROOVE TO REMOVE SAFE END FROM I.D.**
2. **ADD ALLOY 182 BUTTER TO INCREASE MINIMUM BUTTER THICKNESS AT I.D.**

Figure 3.3-3. Shop Fabrication After Nozzle Installed in Vessel
(Prior to Vessel Hydrotest)



1. ADD ALLOY 182 BUTTER FOR EXTENDED LAND, IF REQUIRED (SHOP RECORDS REVIEW DETERMINED THIS WAS APPLIED TO N2-A NOZZLE, BUT WELD MATERIAL ISSUE RECORDS INDICATE IT COULD HAVE BEEN USED ON OTHER NOZZLES)

Figure 3.3-4. Shop Fabrication - Cut Off Safe-End and Re-Prep for Field Weld



BUTTER, SOLUTION HEAT TREAT (SHT),
AT 1950°F, WATER QUENCH, FINAL MACHINE

Figure 3.3-5. Shop Fabrication of Replacement Safe-End

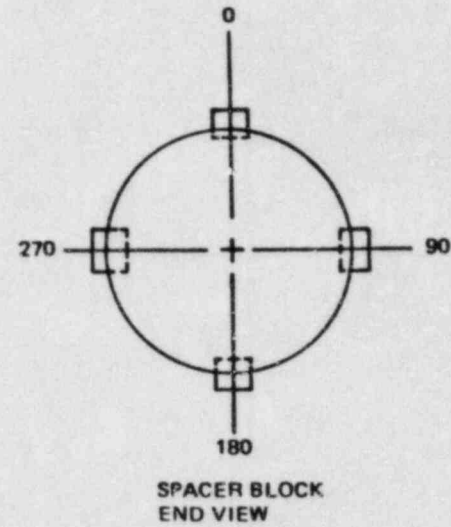
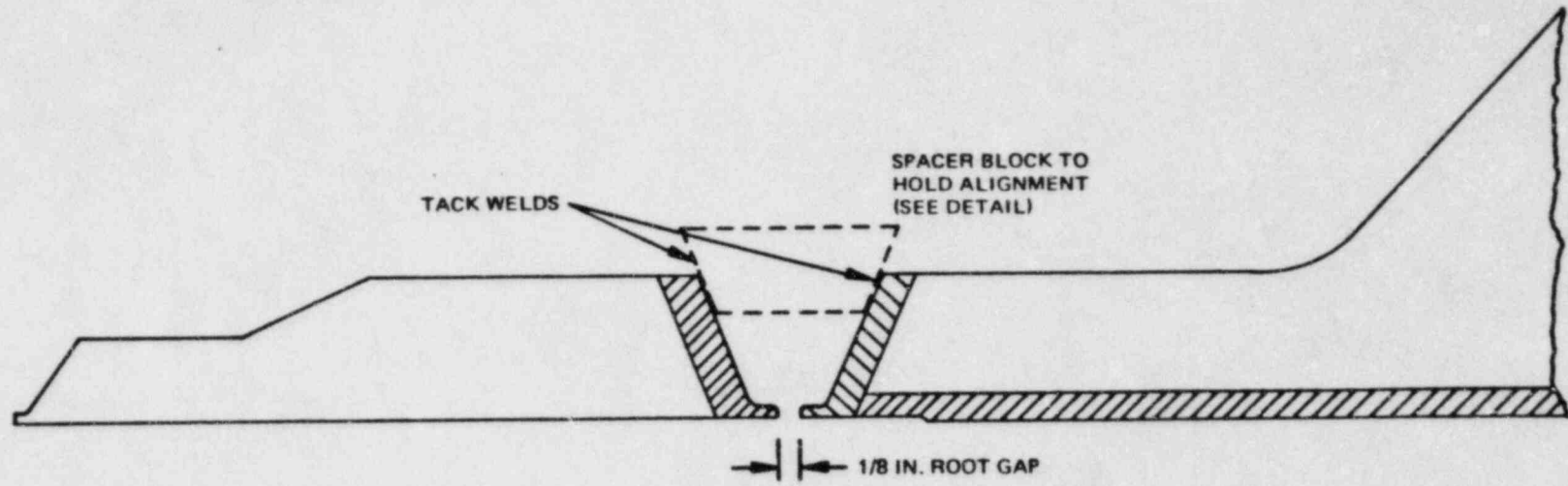


Figure 3.3-6. Field Weld Technique for Safe-End Installation

3.4 WELD BUTTER REPAIR PROGRAM

3.4.1 Introduction

This section describes the weld repair program applied to the Ni-Cr-Fe weld butter cracking. Included is the safe-end removal and examination methods, weld repair techniques (including the half-bead repair and local post-weld heat treatment), and replacement safe-end installation.

3.4.2 Safe-End Replacement Program

Replacement of the high carbon 304 stainless steel safe-ends was performed as part of the piping replacement program. The safe-end replacement program was performed under the rules of ASME Section XI (1980 Edition, Winter 1980 Addenda), Articles IWA7000 and IWB7000. The replacement design, fabrication and installation was performed by General Electric.

The safe-end replacement involves cutting to remove the existing safe-end and machining a new "J" bevel weld preparation for installation of the replacement safe-end. These operations are shown in Figure 3.4-1. In conjunction with machining, etching was performed to verify removal of all 304 stainless steel safe-end material. Note that the final weld preparation may include the nozzle butter as well as portions of the original field weld and safe-end butter, since it is desirable to leave as much Ni-Cr-Fe butter as possible for welding the new safe-end to the low alloy nozzle (Figure 3.4-2). Alternatively, where unacceptable indications are encountered in the field weld, remaining butter thickness is reduced (Figure 3.4-3).

During machining and liquid penetrant examinations of the Ni-Cr-Fe welds, two categories of indications were encountered. The first was axially

oriented stress cracking in the Ni-Cr-Fe weld metal described in Section 3.1. The second was welding-related indications such as slag, lack of fusion and microfissuring, which is typically encountered in Ni-Cr-Fe weldments. The nature and extent of these indications varied, but all required removal or repair prior to safe-end installation. The repair work required is described in the following subsections.

3.4.3 Repair Approach

Following safe-end removal, the Ni-Cr-Fe butters were examined for cracking. In addition to liquid penetrant examination, which detected the deeper axial cracking, ultrasonic examination through the butter face was used to check for circumferential cracking. Internal liquid penetrant examination in the annulus between the nozzle and outer thermal sleeve was performed using borescopes and special tools to check for shallow axial cracking (or shallow circumferential cracking that might not be detectable by U.T.). These examinations confirmed the following:

- (1) Circumferential cracking was not observed in any inlet or outlet nozzle, except for one small circumferential branch of an axial crack on N1-B (Section 3.1).
- (2) All nozzles found to contain cracking (N2-B, N2-F, N2-J and N1-B) showed numerous (>5) cracks distributed randomly about the circumference.
- (3) Cracking did not extend into the low alloy steel nozzle material as determined by dimensional measurements and confirmed by etching.
- (4) The number of affected nozzles and the extent of cracking for each nozzle was sufficiently low to make local repair practical and economical compared with full butter replacement or nozzle to safe-end weld joint redesign to eliminate Ni-Cr-Fe material.

- (5) The extent and depth of cracking observed in the recirculation outlet (28") nozzle made local repair by half-bead welding impractical. As a result, the Ni-Cr-Fe Alloy 182 butter was completely removed and replaced with Ni-Cr (Alloy 82) followed by local post-weld heat treatment.

Repairs were performed according to the requirements of ASME Section XI, Article IWB4000. Unacceptable indications were removed using controlled grinding and, where extensive cracking was encountered, by machining. Removal of indications was confirmed by liquid penetrant examination of all exposed surfaces. Supplemental radiographic and ultrasonic examinations were used where appropriate. Following removal of all indications, repairs were performed using conventional welding, special low penetration welding or the half-bead welding and local post-weld heat treatment processes (details are discussed in the following subsections).

3.4.4 Conventional and Low Penetration Repair Welding

Where the remaining butter thickness on the nozzle was greater than 3/16 in., conventional weld repair using Shielded Metal Arc Welding, or Gas Tungsten Arc welding, was applied. These repairs were examined by liquid penetrant and radiographic methods.

For weld butter thickness less than 3/16 in. but greater than 1/8 in., a special low penetration welding procedure and welder performance qualification techniques were applied in accordance with General Electric specifications. This procedure, which requires special low current, low penetration welding techniques, was qualified on low alloy steel samples (SA508 Cl.2 or SA533, Gr. B) buttered with Ni-Cr-Fe and post-weld heat treated (PWHT). Following PWHT, the test samples were machined to 1/8 in. butter thickness. Each welding procedure and welder was required to successfully qualify on these samples to show no HAZ penetration into the low alloy steel. As for conventional weld repairs, the low penetration repairs were examined by liquid penetrant and radiographic methods.

3.4.5 Half-Bead Weld Repair

When the remaining weld butter thickness was less than 1/8 in., the half-bead welding technique was applied. Since repairs were made in an ASME P-3 to P-8 dissimilar metal weld, the rules of ASME Section XI, IWB4340 were applied. Because the half-bead repair has not been routinely applied to BWR pressure vessels, a number of special tests and evaluations were performed in addition to ASME Code qualification requirements. These tests and evaluations are discussed in the following subsection.

3.4.5.1 Criteria for Half-Bead Welding

The principal advantage of the half-bead welding process is the use of a lower temperature (450-550°F) post-heating cycle in lieu of full PWHT at 1100-1250°F. This was particularly important for recirculation inlet nozzle repairs, where the thermal sleeve interference prohibits the use of local post-weld heat treatment. This is in agreement with the rules of the Code, which permits use of the half-bead welding process when PWHT is impractical (refer to IWB4310).

The key technical considerations for use of half-bead repair are:

(1) heat affected zone BWR environmental stress corrosion cracking performance; (2) potential adverse effects of the higher residual stress associated with the half-bead process; and (3) control of the manual welding and grinding process to obtain the desired HAZ tempering. The first consideration - environmental performance - was not a concern for this application since the I.D. surfaces of the nozzles have been clad with stainless steel. This would prevent exposure of any half-bead repair heat-affected zones to the BWR environment. The second consideration - residual stress - was addressed in two ways. First, the I.D. cladding would again prevent exposure to the BWR environment of any low alloy steel material containing high residual stresses. Secondly, and equally important, analysis confirmed that the residual stresses due to the butt weld are the predominate stresses for this weld joint. Viewed another way, the yielding associated with the butt weld for installing the new safe-end tends to overcome the half-bead repair residual stresses (as discussed

in Section 3.2.4). Finally, the use of hydrogen water chemistry, as discussed in Sections 3.5 and 3.6, would provide significant margin against future stress corrosion of repair weld material or adjacent material.

The third technical consideration - control of the manual welding and grinding process to obtain HAZ tempering - was addressed in the procedure qualification and half-bead application controls, which are discussed in the following subsections.

The development and qualification of half-bead repair included procedure development, ASME Code Section XI testing and HAZ microhardness testing. Mockups and special welder training were also performed and are discussed in Section 3.4.6.

3.4.5.2 Half-Bead Repair Qualification

The repair was performed under the rules of ASME Section XI, Article IWB4340, which applies to dissimilar metal welds. The IWB4340 rules apply rather than IWB4320 (repair to base materials) since the cracking and repair was confined to the Ni-Cr-Fe butter, up to the low alloy steel/butter interface.

The first step in the procedure development was to determine the grinding and welding parameters required to properly temper the HAZ. This work was performed on SA533 Gr. B plate samples in the vertical and horizontal positions. IWB4340 requires 3/32 in. electrode for the first layer, followed by grinding to remove "approximately one-half the first layer thickness" (refer to IWB4323(c)). The Code then requires 1/8 in. electrodes for the second layer and no larger than 5/32 in. for subsequent layers.

Prior General Electric and industry data on the half-bead process was used to select welding parameters and the deposition techniques. Parameters were required not only to effectively temper the HAZ but also must be suitable for all position welding (vertical, horizontal and overhead), which restricts welding current to the lower ranges compared to flat position or "downhand"

welding. The parameters developed for this repair are discussed in sequence starting with the first layer.

Another parameter variable for layer disposition is bead overlap, which affects HAZ uniformity and controls interbead tempering. Based on prior GE test work with this process, this is a key factor in the overall HAZ hardness improvement (Figure 3.4-4). For the first and all subsequent layers, _____

For grinding or machining the first layer, a number of factors were considered. The most important requirement is to establish a procedure that produces reproducible results. For local repair grindouts, machining is not practical, so manual grinding was applied. Prior GE and industry experience indicated that grinding could be controlled by weld surface contour. Smoothing the first layer surface to remove the surface of the beads while leaving some valleys between beads reduced the first layer thickness by 20-35%. This procedure was considered since it is closer to the temperbead process (no first layer grinding) recently shown by research at the Central Electricity Generating Board⁴ (CEGB) to both temper and refine the grain structure of the HAZ. However the lower current parameters required for all position welding were judged inadequate to achieve the level of grain refinement demonstrated by the CEGB tests using higher welding currents and larger electrodes.

Subsequent tests were performed using additional grinding of the first layer. The procedure involved grinding to remove bead ripples and valleys between beads which _____ This procedure was readily controlled and repeated in both the vertical and horizontal welding positions. Heat-affected zone hardness testing, discussed later, proved the effectiveness of this procedure in improving HAZ hardness over the as-welded hardness. _____

_____ which was in agreement with the current rules of the Code (refer to IWB4323(c)).

Additional technical guidance in selecting the above grinding procedure was taken from recent work published by Oak Ridge National Laboratory.⁵ The data showed acceptable half-bead HAZ properties for complete removal of the first layer as well as for a full thickness first layer. Efforts were therefore focused on other variables such as electrode size, current, and deposition technique to select the final parameters for qualification and application.

was high enough to properly temper the first layer HAZ yet low enough to avoid extreme penetration, which would form a new HAZ. The second layer was lightly dressed by grinding to remove excessive bead crowns and provide a suitable surface for the third layer.

Prior General Electric tests had shown the benefit of _____ tempering. Accordingly, the _____ parameters were selected to provide additional HAZ tempering.

The final welding technique control was the tie-in along the length of the beads at start and stop locations. For most repair cavities, the length was short enough to travel the entire length without a start and stop due to change of electrodes. When required, start and stop areas were handled by first stopping the bead and grinding the crater smooth to remove any crater indications and provide a smooth surface for the next bead. _____

In this manner, the underlying heat-affected zone in the start/stop region was made as uniform as possible for subsequent tempering by the second and third layer. The resulting excess reinforcement in this area would then be ground flush prior to the next layer deposition. A summary of the parameters and technique development for the half-bead process is shown in Table 3.4-1.

Following parameter development, ASME Code qualification was performed. This qualification and the microhardness testing are discussed in the next two sections.

3.4.5.3 Half-Bead Repair Procedure Qualification

All ASME code qualification was performed in accordance with IWB4340 of Section XI, plus applicable ASME Section IX requirements invoked by IWB4340.

Electrode handling and moisture control requirements of IWB4331(b) were applied to all qualifications and repairs. This involved baking all electrodes upon removal from hermetically sealed containers at $550^{\circ}\text{F} \pm 50^{\circ}\text{F}$ for 2 hours, followed by holding at a temperature of $225^{\circ}\text{F} - 350^{\circ}\text{F}$. Portable ovens at $225^{\circ}\text{F} - 350^{\circ}\text{F}$ were used at welding stations to limit electrode exposure to a maximum of 20 minutes.

In order to provide the required material (SA508 Cl 2) and restraint for the qualification weld, a 12-inch size nozzle forging as shown in Figure 3.4-5 was used. Both horizontal and vertical weld grooves were prepared to evaluate the process in both positions and provide the length of weld required for removal of weld and HAZ test specimens. The base material was certified by impact and dropweight testing according to ASME Section III, NB2300 requirements for a T_{NDT} of -30°F .

The nozzle forging test specimens were certified using a post-weld heat treatment of 40 hours at 1150°F , however, the forging itself had not been installed in a vessel and therefore had not received post-weld heat treatment. To comply with IWB4322.1(a) requirements, the forging was given a post-weld heat treatment of 1150°F for 24 hours. The 24 hours was more than adequate, since records for the Pilgrim reactor vessel show that all nozzles in the lower shell assembly (which includes recirculation inlet and outlet nozzles) received from 9-13 hours of post-weld heat treatment.

Weld groove design for half-bead qualification (and repair application) was selected from prior GE testing. _____

Prior to welding, the nozzle forging was uniformly heated to 300°F minimum preheat as required by IWB4343(a). Welding was completed following the technique shown in Figures 3.4-7 and 3.4-8 with a maximum welding interpass temperature of 400°F. Following welding the entire forging was post heated to 450°F - 550°F for 2 hours minimum as required in IWB4343(d). The weld sample was allowed to cool to ambient temperature at which time radiographic examination and mechanical test specimen removal was initiated.

Mechanical testing included transverse side bend and tensile testing per ASME Section IX, and all weld metal tensile and heat-affected zone/base metal impact testing per IWB4322.1(j) and IWB4322.1(c) respectively. Mechanical test results are shown in Table 3.4-2.

The acceptance criteria for the transverse tensile tests (specimens TT4 and TT5 of Table 3.4-2) are defined in QW-153 and Table QW-422 of ASME Section IX. For the SA508 Cl 2 (P-3 Group 3 material) the specified minimum tensile strength is 80,000 psi, which was met for both test specimens. A specific acceptance criteria is not defined for the all weld metal tensile specimen LT1, so the value of 93,800 in Table 3.4-2 is recorded for information. Side bend test criteria are defined in QW-163 of ASME Section IX. The criteria has no open defects exceeding 1/8 inch length on the bend specimen surfaces. The small defects reported, typical of Ni-Cr-Fe weldments are well within the acceptance criteria.

Impact test procedures and acceptance criteria are defined in IWB4322(1c) of ASME Section XI. The test temperature for impact testing was selected based on the dropweight testing performed on SA508 Cl 2 actual base material. Test temperature was $T_{NDT} + 60^{\circ}\text{F}$, or $+30^{\circ}\text{F}$ for the base material T_{NDT} of -30°F .

Tests were performed using the standard 10 x 10 mm Charpy V specimens. Specimens were removed from the vertical weld transverse to the weld line and parallel to the plate surface. The notch was located in the HAZ, _____

_____ to cover the desired HAZ area. Companion base metal specimens were obtained from adjacent locations while maintaining forging working and quenching orientation comparable to those for the weld HAZ specimen.

The acceptance criteria for impact tests requires that the average mils lateral expansion for the HAZ equal or exceed the unaffected base material. From Table 3.4-2, it can be seen that the criteria has been met. The HAZ

_____ Since this criteria has been met, additional Charpy testing was not required.

Hardness testing was also performed to confirm the effectiveness of the half-bead procedure in tempering the heat-affected zone. Those tests are described in the next subsection.

3.4.5.4 Half-Bead Hardness Testing

Locations for hardness testing are shown in Figure 3.4-9. Hardness traverses were normally made starting at the fusion line moving outward into the heat-affected zone in increments of 0.008 inch. Readings were taken at central bead locations (traverses B, C, D in Figure 3.4-9) and on edge beads (traverses A, E in Figure 3.4-9). Hardness test results are plotted in Appendix I.

In these figures, individual measurements are plotted. Lower and upper bound lines are then constructed to encompass the range of the individual data points. The hardness test results are discussed in detail in the following subsections. The chemical compositions of the SA533 and SA508 materials are shown in Table 3.4-3.

Bead on plate tests were performed to establish a baseline "as-welded" hardness condition to compare the effectiveness of the half-bead procedure. Figures I-1 and I-2 show the results of bead on SA533 Gr. B plate tests for a single weld bead using 3/32 in. ENiCrFe-3 electrode and the welding parameters of Table 3.4-4. These tests demonstrate the untempered HAZ hardness using the lower and upper limit of the parameters for the half-bead first layer. _____

_____ A Knoop to equivalent Rockwell "C" hardness conversion table is shown in Table 3.4-5.

Using the _____ procedure described in previous sections, a significant improvement in HAZ hardness was achieved. Figures I-3 and I-4 show the results for horizontal half-bead groove welds on the SA533 Gr. B plate material. For the central beads (refer to Figure 3.4-9) results in Figure I-3 show _____

_____ For the edge beads, where less interbead tempering is present, results in Figure I-4 show _____

Using the vertical _____ half-bead procedure, results for central and edge bead locations on SA533 Gr. B plate are shown in Figures I-5 and I-6 respectively. Note in Figure I-5 that significant tempering has been achieved at all locations with _____ over the entire HAZ area. At edge bead locations, desired results were again achieved with _____

For the SA508 Cl 2 material, baseline bead on plate tests were also performed using the parameters of Table 3.4-4, and are shown in Figures I-7 and I-8. For low heat input, results in Figure I-7 showed _____

_____ The higher heat input parameters again produced hardnesses above _____

Results of hardness testing on the SA508 Cl 2 procedure qualification half-bead weldments are shown in Figures I-9 and I-10. For the vertical half-bead the significant hardness improvement can be seen by comparing results in Figure I-9 to Figures I-7 and I-8. _____

For the horizontal half-bead of Figure I-10 hardness results showed more variability than the vertical beads, but again showed significant improvement over the as-welded baseline condition. _____

For comparison purposes, post-weld heat treated samples were measured by the same microhardness techniques. These samples were prepared by buttering SA533 Gr. B plate with two layers of ENiCrFe-3 using 1/8" electrode at 80-95 amps. The samples were then post-weld heat treated at 1150°F for four hours. (These samples were actually used to qualify the low penetration welding procedures and welders described in Section 3.4.4.)

Results for the post-weld heat treated samples are shown in Figures I-11 and I-12.

These results show that the high hardenability of these materials results in a moderately hardened HAZ even in the post-weld heat treated condition.

The overall results of the microhardness testing can be viewed in several ways. First, the results clearly showed the effectiveness of the selected half-bead parameters in improving the HAZ hardness. As-welded bead on plate peak hardnesses ranged

For this application, the half-bead repair was found to be fully acceptable in terms of ASME Code and other technical criteria. In addition to ASME Section IWB4340 requirements, residual stress and HAZ hardness were evaluated.

Analysis showed that the butt weld residual stresses predominate or "overwhelm" the majority of the half-bead residual stresses. In addition, the I.D. stainless steel cladding on the nozzle bore prevents exposure of half-bead low alloy steel HAZ or low alloy steel with high residual stress to the BWR environment.

3.4.6 Application of Half-Bead Repair

Additional work was performed to apply the qualified half-bead procedure to the recirculation inlet nozzles. This included weld joint and backing material design, welder training and mockup testing.

The narrow annulus (0.25" nominal) between the nozzle bore and the outer thermal sleeve (see Figure 3.0-1) required special tooling to apply the half-bead procedure. Local excavations were made to remove cracking (or in some cases welding defects) as required. These excavations were from 1-4 inches wide and from about 0.25-0.8 inches in depth, depending on the actual extent of cracking and remaining butter thickness.

To repair a given cavity, a backing material between the nozzle bore and thermal sleeve is required.

The basic weld repair scheme is shown in Figures 3.4-10 and 3.4-11. For all repairs, the minimum cavity dimensions (angle, root opening and root radius) that were qualified in the ASME Code testing must be applied to actual grindouts. Following this criteria, the short horizontal repair in Figure 3.4-10 would be

made using a _____ with a horizontal welding. A longer horizontal repair cavity in Figure 3.4-11 would be made using the _____ with a vertical up welding technique. Similarly, short or long vertical repair cavities (i.e., at the top or bottom of the nozzle) would be made using the corresponding groove design and welding progression.

Because of the complexity of these repairs, all welders were qualified for all position NiCrFe welding to the required thicknesses per ASME Section IX. In addition, each welder had to practice and demonstrate proficiency at performing the half-bead procedure in groove plates in the vertical up and horizontal welding positions. Finally, all welders were trained _____ on mockups containing the nozzle and thermal sleeve. Where appropriate, this training and practice was performed with face masks and other radiation protective gear that would interfere with welding.

3.4.7 Additional Half-Bead Repair Requirements

To achieve the 300°F preheating and the 450-550°F post-heating for the half-bead process, electrical resistance methods were qualified and applied. Special machining and examinations were also required.

All heating work was performed using electrical resistance heaters and temperature controllers. First, finite element analysis was performed to determine heater requirements and temperature distributions. This analysis also confirmed that unacceptable thermal stress would not be generated in the nozzle or vessel wall as a result of local heating. Heating procedures were then developed and checked out on a mockup. During the repair, nozzle temperatures were continuously monitored by ten thermocouples (plus spares) to confirm the Code required preheat, interpass and post-heat temperatures are obtained and to provide data for a final verification analysis. The verification analysis was performed for all nozzles to again confirm acceptable levels of thermal stress (so that unacceptable nozzle or vessel wall residual stresses are not produced as a result of the heating).

Following the repair and cooldown from the post-heat cycle, the first step was to machine the buttering repairs to provide surfaces suitable for non-destructive examination (NDE) and prepare a final machined weld preparation for a new safe-end installation. Special tooling was developed to machine the I.D. of the repairs (with a tool in the narrow, 0.25" or less annulus). After machining, the butter and accessible I.D. surfaces were liquid penetrant examined and any blending or "touch up" repairs were performed if required.

Final NDE must be performed a minimum of 48 hours (per Code) after the nozzle cools down to ambient temperature to assure delayed cracking is not present. The final examination included radiographic and liquid penetrant examinations of the butter and the "3T" heating zone on the nozzle, adjacent to the butter. Finally, ultrasonic examination was performed of the "3T" band per Code requirements.

After half-bead repairs and examinations were completed, the new safe-ends were installed with automatic Gas Tungsten Arc Welding (GTAW) using ASME SFA 5.14 ERNiCr-3 consumable inserts and filler metal. The safe-ends themselves are General Electric 316 Nuclear Grade material, which is pre-buttered on the end in the shop using ERNiCr-3 (so that a similar metal field weld can be made).

3.4.8 Local Post-Weld Heat Treatment Repair

For the recirculation outlet nozzle found to contain cracking (N1-B), re-buttering using ERNiCr-3 (Alloy 82) filler material and local post-weld heat treatment (PWHT) was applied. This work was performed under the rules of ASME Section III, Article NB4000.

This repair was selected because the extent of cracking on this nozzle would have required considerable half-bead repair area. The time and potential difficulties associated with such a repair made local half-bead impractical. Accordingly, the original NiCrFe (Alloy 182) was removed by machining, down to the original low alloy steel material. A specially designed backing ring pre-buttered with NiCr (Alloy 82) was installed to provide a good surface for the new buttering buildup, and to prevent distortion of the nozzle end

radially inward. The nozzle was locally preheated to 250°F, and the new butter was applied using SFA 5.14 ERNiCr-3 and automatic GTAW. Preheat was maintained continuously until the start of PWHT at 1150°F for one hour per inch of thickness.

As for the heating work performed on recirculation inlet nozzles, thermal analysis and mockup testing were performed to confirm acceptable thermal stresses and develop the required heater position and power requirements. During the preheat and post-weld heat treatment 19 thermocouples (plus spares) were applied at key nozzle locations to monitor and control all heaters and provide data for final thermal stress analysis.

Based on measured nozzle temperature and heating/cooling cycles, thermal stress analysis was performed to confirm acceptable stress levels. This analysis showed that allowable thermal stress gradients were maintained throughout the process, and that unacceptable residual stresses were not produced in the nozzle or vessel wall.

Following heat treatment, the backing ring and butter were machined and examined by liquid penetrant and radiographic methods per applicable NB5000 requirements. The new safe-end was then installed using NiCr (Alloy 82) material and automatic GTAW as was applied to the inlet safe-ends.

3.4.9 Summary

A complex nozzle buttering repair program was successfully qualified and implemented on the Pilgrim recirculation inlet and outlet nozzles.

The use of controlled grinding and machining to remove all unacceptable cracking or welding defects prepared the nozzles for conventional, low penetration or half-bead and local post-weld heat treatment repair as required.

All procedures were qualified and performed under the rules of ASME Section XI or III as applicable under the Owner's Repair Program. In addition

to Code requirements, special evaluation, test work, training, examinations and finite element analyses were performed by General Electric to support these complex repairs. Repair of NiCrFe to original condition using the same material was technically supported by extensive failure analysis to understand the nature of the cracking and special analyses showing residual stress conditions and their influence on cracking. The final, long term justification for the repair, however, is the elimination of the susceptible environment through the application of hydrogen water chemistry.

Table 3.4-1
HALF-BEAD WELDING PARAMETERS
(GE COMPANY PROPRIETARY)

Table 3.4-2
 HALF-BEAD REPAIR QUALIFICATION - MECHANICAL TEST RESULTS

Tensile Tests

Specimen No.	Type	Area	Ultimate Total Load (lb.)	Ultimate Unit Stress (psi)	Character of Failure & Location*
TT4	Transverse	0.192	16,012	83,400	BM Ductile
TT5	Transverse	0.193	16,096	84,400	BM Ductile
LT1	All Weld Metal	0.192	18,009	93,800	WM Ductile

Guided Bend Tests

Type	Results	Comment
Side Bend	One defect, 1/64"	Acceptable
Side Bend	Three defects, 1/32", 1/32", 1/64"	Acceptable
Side Bend	Two defects, 1/16", 1/32"	Acceptable
Side Bend	One defect, 1/32"	Acceptable

Toughness Tests

Specimen No.	Notch Location	Notch Type	Test Temp.	Impact Values	Lateral Exp.	
					% Shear	Mils
CH-7	HAZ	45°V	29.5°F	78	53	50
CH-8	HAZ	45°V	29.5°F	80	69	44
CH-9	HAZ	45°V	29.5°F	81	72	43
CB-1	Base Metal	45°V	29.3°F	43	34	37
CB-2	Base Metal	45°V	29.3°F	31	35	28
CB-3	Base Metal	45°V	29.3°F	67	48	53

*BM - Base Metal
 WM - Weld Metal
 HAZ - Heat Affected Zone

Table 3.4-3

CHEMISTRY OF LOW ALLOY STEELS USED IN HALF-BEAD REPAIR PROGRAM

<u>Material</u>	<u>Heat No.</u>	<u>Type</u>	<u>C</u>	<u>Mn</u>	<u>P</u>	<u>S</u>	<u>Si</u>	<u>Ni</u>	<u>Cr</u>	<u>Mo</u>	<u>V</u>
SA533 Gr. B	C4132	Mill	0.21	1.32	0.013	0.004	0.26	0.61	--	0.58	--
		Check	0.20	1.26	--	--	0.25	0.59	0.22	0.56	--
SA508 Cl. 2	Q2QL23QT (Forging 402H-1)	Ladle	0.18	0.74	0.008	0.010	0.23	0.37	0.78	0.65	0.01
		Check	0.17	0.74	0.015	0.013	0.23	0.35	0.84	0.62	0.01

Table 3.4-4

PARAMETERS FOR BEAD ON PLATE TEST FOR AS-WELDED HAZ HARDNESS
(GE COMPANY PROPRIETARY)

Table 3.4-5
EQUIVALENT HARDNESS CONVERSIONS

<u>Knoop 500g</u>	<u>Rockwell C</u>
520	50.5
510	49.8
500	49.1
490	48.4
480	47.7
470	46.9
460	46.1
450	45.3
440	44.5
430	43.6
420	42.7
410	41.8
400	40.8
390	39.8
380	38.8
370	37.7
360	36.6
350	35.5
340	34.4
330	33.3
320	32.2
310	31.0
300	29.8
290	28.5
280	27.1
270	25.6
260	24.0
250	22.2
240	20.3

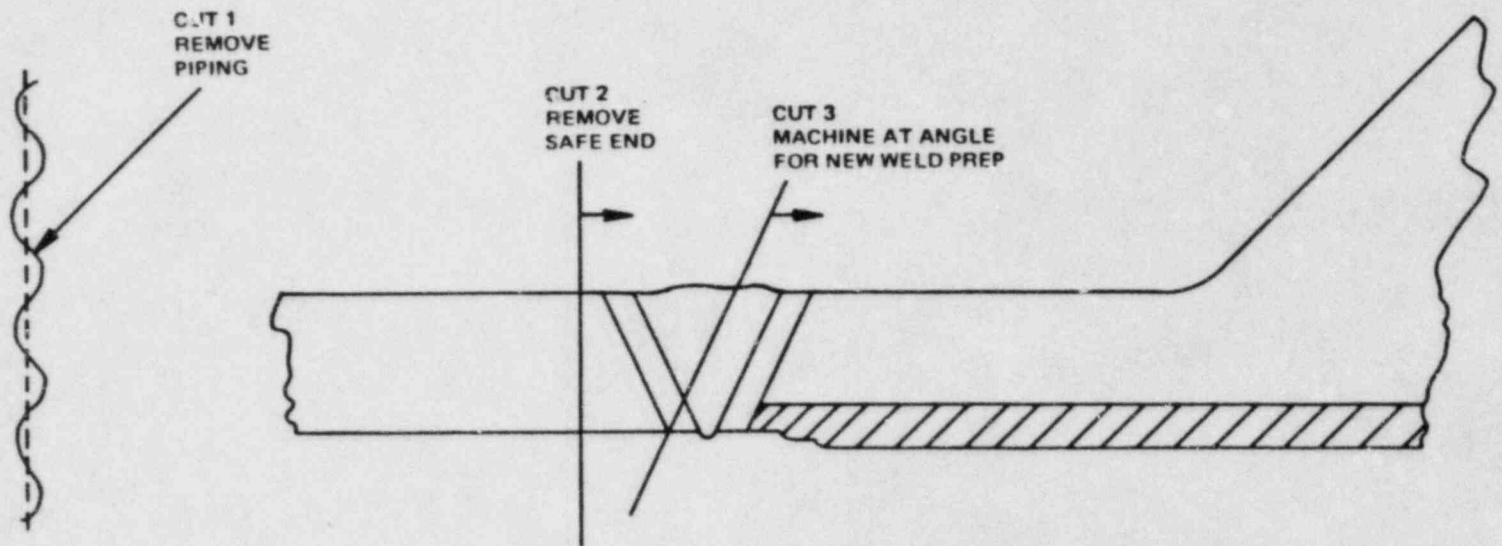


Figure 3.4-1. Safe-End Removal and Weld Preparation Technique

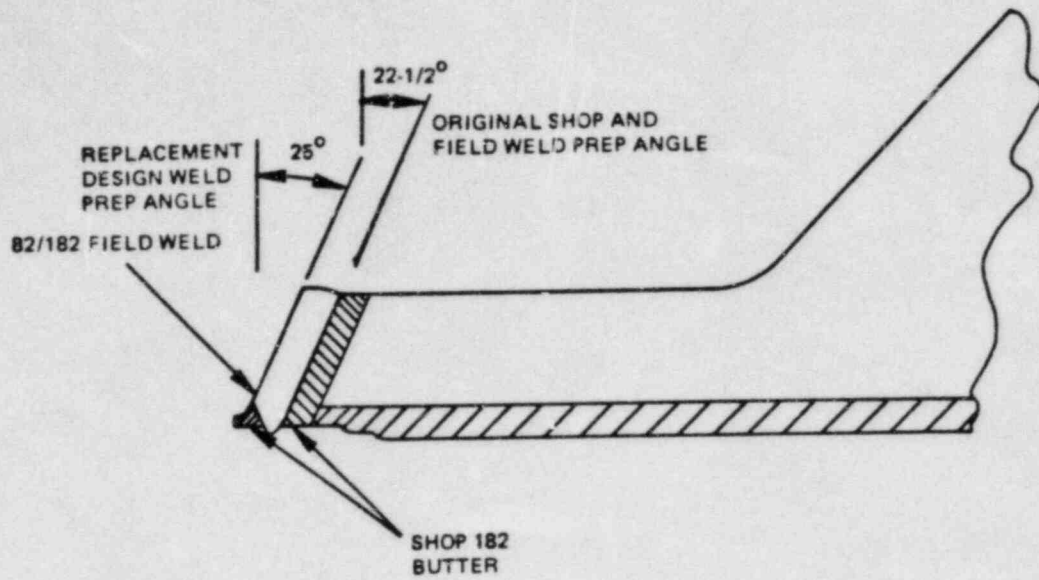


Figure 3.4-2. Configuration for Nozzles Where Field Weld and Original Safe-End Weld are Acceptable to Retain Desired Butter Thickness

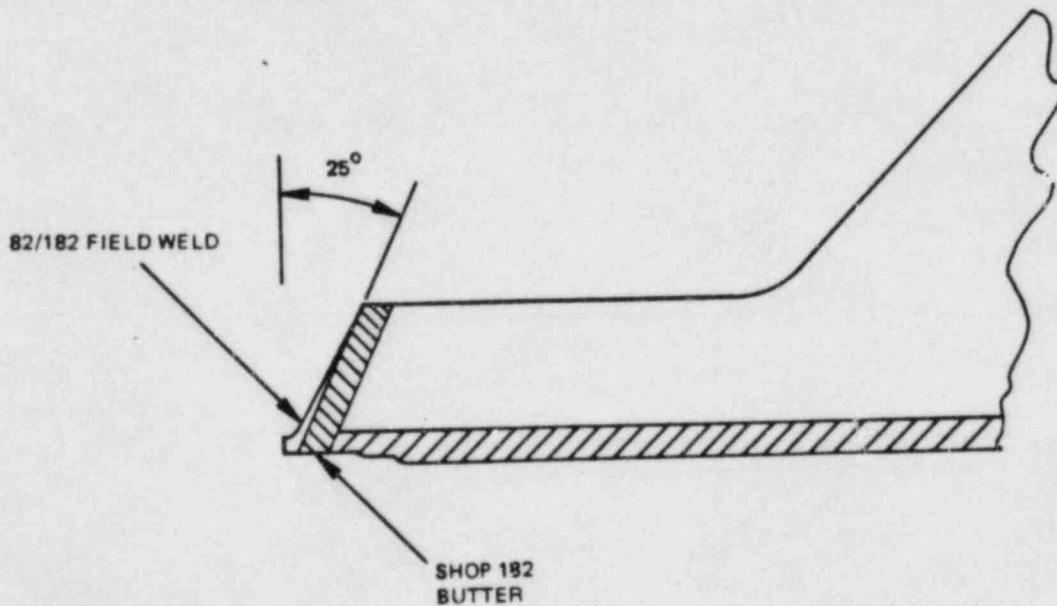


Figure 3.4-3. Configuration for Nozzles Where Unacceptable Indications in Field Weld Require Removal by Machining, Resulting in a Reduced Butter Thickness

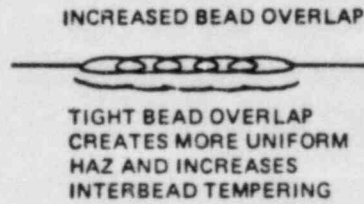
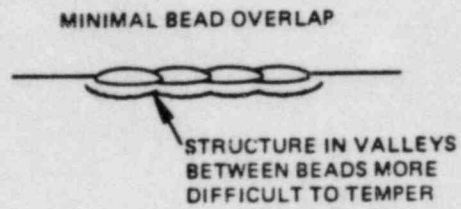


Figure 3.4-4. Effect of Bead Overlap on Half-Bead Tempering Process

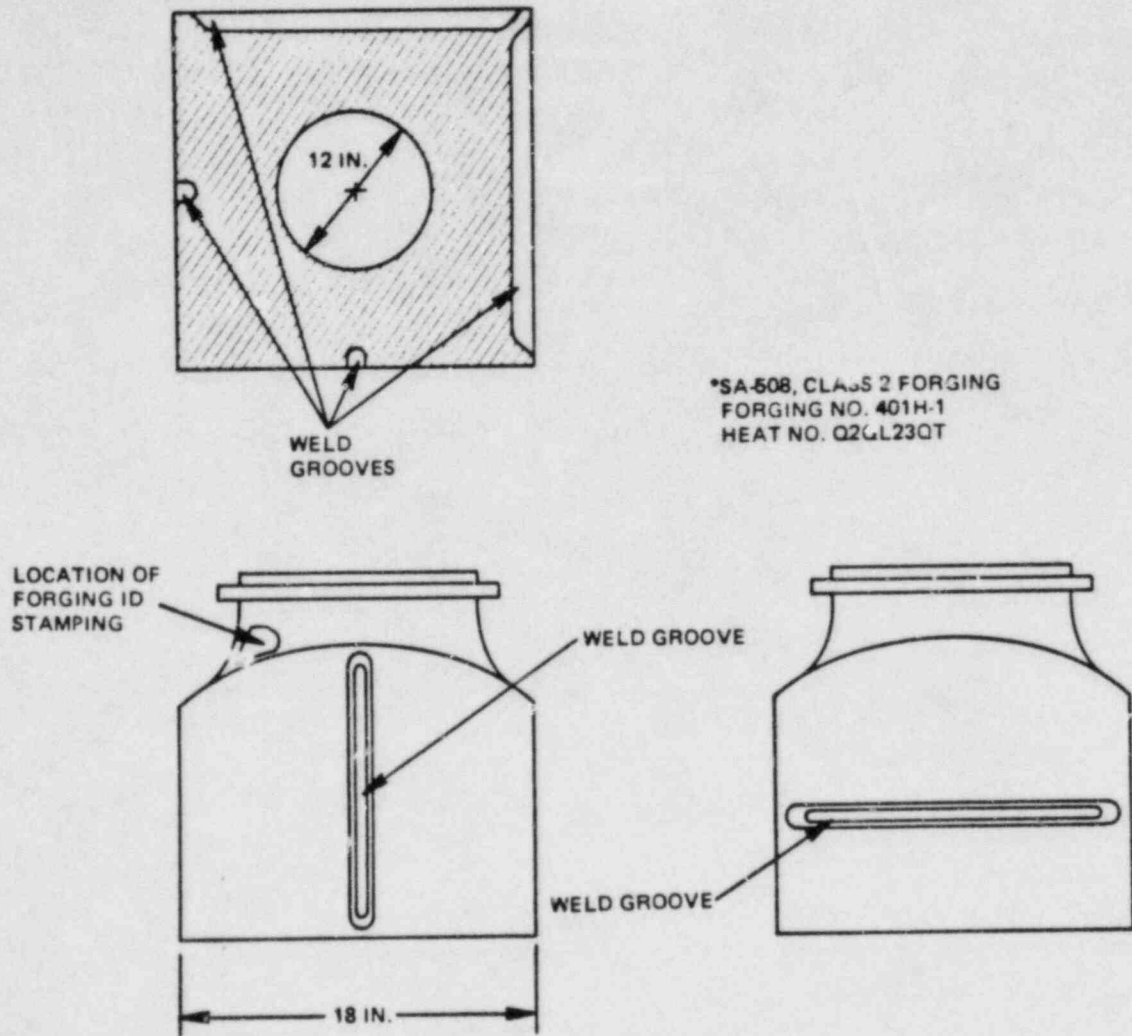


Figure 3.4-5. Half-Bead Weld Procedure Qualification Sample

Figure 3.4-6. Weld Groove Design for Half-Bead Qualification
(GE COMPANY PROPRIETARY)

Figure 3.4-7. Half-Bead Welding Procedure for Horizontal Weld Grooves
(GE COMPANY PROPRIETARY)

Figure 3.4-8. Half-Bead Welding Procedure for Vertical Weld Grooves
(GE COMPANY PROPRIETARY)

Figure 3.4-9. Locations for Half-Bead HAZ Microhardness Traverses
(GE COMPANY PROPRIETARY)

Figure 3.4-10. Half-Bead Repair Technique for Short Horizontal Repair Cavity
(Thermal Sleeve not Shown) (GE COMPANY PROPRIETARY)

Figure 3.4-11. Half-Bead Repair Technique for Longer Horizontal Repair Cavity (GE COMPANY PROPRIETARY)

3.5 QUALIFICATION OF HYDROGEN WATER CHEMISTRY

3.5.1 Introduction

The recirculating coolant in boiling water reactors (BWRs) is high-purity (no additive) neutral pH water containing radiolytically produced dissolved oxygen (100-300 ppb). This level of dissolved oxygen is sufficient to provide the electrochemical driving force needed to promote intergranular stress corrosion cracking (IGSCC) of sensitized austenitic stainless steel piping and similar structural components if the other two prerequisites for IGSCC [a sensitized microstructure (chromium depletion at the grain boundaries) and a tensile stress above the yield stress] are also present. A variety of IGSCC remedies have been developed and qualified which address the sensitization and tensile stress aspects of stress corrosion cracking, including Nuclear Grade Type 316 and 304 stainless steels, solution heat treatment (SHT), corrosion-resistant cladding (CRC), heat sink welding (HSW) and induction heating stress improvement (IHSI). It should also be possible to suppress IGSCC by reducing the electrochemical driving force for IGSCC (i.e., by modifying the BWR coolant environment).

The demonstration of an IGSCC remedy based on modifying the chemistry of the BWR coolant is the objective of an ongoing materials test program. The basic concept is to reduce the aggressiveness of the BWR environment by adding hydrogen gas to the feedwater to reduce the dissolved oxygen level and reducing the coolant conductivity to a low value by improved operational practices. This approach appears to have the potential for "blanket" protection of all types of BWR structural materials during power operation of the plant and may arrest the growth of incipient cracks.

To evaluate and quantify the beneficial effects of oxygen suppression through hydrogen additions, numerous laboratory and Dresden-2 in-reactor testing techniques have been used to study a broad range of BWR structural materials and corrosion phenomena. The results of these laboratory materials programs and Dresden-2 operational results are the subject of this subsection.

3.5.2 Research Objectives and Principal Findings

3.5.2.1 Full-Size Welded Stainless Steel Pipe Tests

Pipe testing has been performed to quantify the effect of H_2WC on the IGSCC performance of Type 304 stainless steel piping. The general approach is similar to that used for the General Electric/EPRI Program, "Alternate Alloys for BWR Pipe Applications",⁶ EPRI Project RP-968. However, instead of selecting and qualifying a particular alternative piping alloy, the thrust of the present program was to qualify an alternative environment using hydrogen addition to reduce the dissolved oxygen concentration.

To reliably demonstrate the improved IGSCC performance of Type 304 stainless steel in H_2WC in a reasonable period of time, a reliable, accelerated test representative of actual field piping conditions was required. The full-size welded pipe test which was developed for EPRI RP-968 fits this requirement. A statistical method was used for developing factors of improvement (FOI) by comparing times-to-failure for alternate alloy with similar data for the reference alloy, Type 304 stainless steel. Similarly, the method was used to establish a FOI for H_2WC vis-a-vis the normal 200 ppb $O_2/288^\circ C$ ($550^\circ F$) BWR steady-state environment by comparing times-to-failure for the reference alloy in the two environments.

The pipe tests were conducted in simulated BWR high temperature water environments in the Pipe Test Laboratory (PTL) as described in detail elsewhere.⁷ This facility was modified to provide control and monitoring capability for hydrogen addition and the lower O_2 and conductivity levels required for H_2WC .

Initially, the H_2WC environment was selected as 50-70 ppb O_2 with a conductivity of $0.6 \pm 0.3 \mu S/cm$. This environment was established at a time when it was not certain if lower O_2 levels could economically be established in a plant and was expected to provide conservative data. Four H_2WC crack growth specimens, six H_2WC crack initiation specimens and four reference specimens exposed to 200 ppb O_2 environments were initially included in the program.

Of the four crack growth specimens, two were sectioned metallographically after precracking in 200 ppb O_2 water to determine pre-crack depth and two were continued on test in the 50-70 ppb O_2 H_2WC environment.

As described in additional detail later in this section, premature cracking occurred in the initial 50-70 ppb O_2 H_2WC environment and it was determined that dissolved oxygen and conductivity must be lowered to 20 ppb and $<0.2 \mu S/cm$, respectively, to demonstrate improvement. Exposure of all cracked specimens was then continued in the new specification H_2WC environment to determine if crack arrest would occur. Additionally, two new crack growth specimens and three new crack initiation specimens were added to the program for testing in the new H_2WC environment.

The total test matrix is shown in Table 3.5-1. Four heats of Type 304 stainless steel were included in the program. One heat of Type 316 Nuclear Grade stainless steel was included in the crack initiation tests.

The 10-cm (4-in.) Schedule 80 pipe specimens were assembled using eleven 10-cm (4-in.)-long test pieces from one heat, two transition pieces, and top and bottom end caps joined by circumferential welds as illustrated in Figure 3.5-1.

The pipe specimens were cyclically loaded at one cycle per day in a pipe test stand (Figure 3.5-2). The loaded waveform is shown in Figure 3.5-3. A long hold time was used to prevent fatigue failure during long exposure to develop factors-of-improvement (FOI). To accelerate cracking, axial test loads were applied to attain a maximum nominal pipe section stress equal to 233.2 MPa (33.8 ksi) $2S_M$ (S_M = ASME Code allowable), as determined at the smallest cross section of the specimen, the weld counterbore.

The results were evaluated by ultrasonic test (UT) and metallography. Specimens were given an initial baseline UT before going on test. The pipe tests were conducted until through-wall cracks occurred or until the test objectives were achieved and removed for destructive metallographic evaluation.

The longer exposure specimens were periodically removed from test for UT inspection to estimate crack growth.

Crack growth pipe specimen AWC-1 failed by IGSCC at HAZ location designated J-1 after 30 cycles, 844 hours exposure to the 50-70 ppb O_2 /0.6 $\mu S/cm$ conductivity H_2WC environment. This specimen had a precrack initiated in the 200 ppb oxygen environment estimated by UT evaluation to be 0.38 mm (15 mils) deep. During the 50 to 70 ppb O_2 /0.6 $\mu S/cm$ conductivity H_2WC exposure, the intergranular portion of the crack grew to a maximum depth of 4.8 mm (190 mils) and extended to 360° around the pipe, after which the pipe failed in ductile tension.

Because failure of Specimen AWC-1 occurred earlier than expected for H_2WC exposure, testing of all pipe specimens in this environment was interrupted and UT evaluations were conducted. Table 3.5-2 lists the accumulated exposures of the specimens and estimated maximum crack depths from UT inspections.

It can be seen that all specimens tested in the 50 to 70 ppb O_2 high conductivity H_2WC environment exhibited early cracking except Specimen AWC-14, which was fabricated from Type 316 Nuclear Grade (NG) stainless steel pipe. This specimen showed no crack indications for UT examination at maximum sensitivity. Subsequent metallographic examination on specimen AWC-14 verified the UT results.

The remaining unfailed, but cracked specimens from this environment were transferred to the lower oxygen/conductivity environment described above to determine if crack arrest would occur in this environment.

The results of exposure of the precracked specimens to typically 20 ppb O_2 /0.2 $\mu S/cm$ conductivity environment are also listed in Table 3.5-2. None of these specimens failed during exposure times significantly longer than the failure times for the four reference 200 ppb oxygenated water specimens listed in Table 3.5-2. All of the precracked specimens, except AWC-11, showed some

crack extension in the lower oxygen environment. Specimens AWC-9 and AWC-12 had one weld removed from each four metallographic sectioning to characterize the cracking.

The metallographic sections of Specimens AWC-9 and AWC-12 showed intergranular cracks with a transition to transgranular during the later stage of cracking. SEM examination also showed intergranular thumbnail cracks with a transition through mixed mode to total transgranular cleavage fracture at the root of the cracks and, in most instances, showed striations which are indicative of fatigue associated with the cleavage fracture.

Two additional crack growth specimens (AWC-15 and AWC-16) were precracked in 0.2 ppm O₂ water to depths of approximately 1.27 and 1.02 mm (50 and 40 mils), respectively. Specimen AWC-15 was exposed to the low oxygen/ conductivity H₂WC environment for 5310 hours (including 343 hours in 200 ppb O₂) and Specimen AWC-16 was exposed to the 0.2 ppm O₂ water control environment at constant load to evaluate the fatigue component of crack propagation. Specimen AWC-16 failed in 1285 hours, while the precracked specimen AWC-15 did not fail during the total 5653 hours of exposure.

Due to premature failure of the original crack initiation specimens in the 50-70 ppb O₂ water, three new crack initiation specimens (one from each of three heats, Specimens AWC-17, -18, and -19) were tested in the low oxygen/ conductivity environment. Specimen AWC-17 was removed from test after 1693 hours for interim UT examination and removal of one weld for dye penetrant test and sectioning. No evidence of crack initiation could be seen at this time. It was repaired and returned to test. Specimens AWC-17, -18, and -19 have obtained 5122, 7580, and 7585 hours of exposure, respectively, with no UT indications of cracking (FOI of at least 25). Through-wall failures of these pipes in the reference environment would be expected in approximately 1500 hours.

3.5.2.2 Crack Propagation Studies

The series of tests performed under the general heading of crack propagation studies had two major objectives: (1) determine the effects of a reduction in the dissolved oxygen level in the coolant on the crack propagation rates for key BWR structural materials, and (2) determine the crack arrest and retardation behavior in this reduced oxygen environment. The types of testing techniques utilized to provide this information included low cycle fatigue tests, constant load stress corrosion crack growth tests and fatigue crack growth tests.

3.5.2.2.1 Low Cycle Fatigue Tests on Carbon Steel. A series of fatigue crack initiation tests was performed to determine the effect of dissolved oxygen on the fatigue lifetime of carbon steel piping in high purity water. Tests were conducted on notched and unnotched specimens of SA 106-B carbon steel at low (11.1 cph) and high (277 cph) frequencies. The specimens were cyclically loaded with a R* ratio of 0.08.

The test revealed that H₂WC should not adversely affect the notched or unnotched fatigue crack initiation behavior of carbon steels. Indeed, a H₂WC specification of 20 ppb O₂ and 0.2 µS/cm conductivity clearly inhibits crack initiation and lifetimes approach those obtained in air tests. The service lifetime of carbon steel piping in BWRs probably can be extended by controlling the dissolved oxygen and conductivity levels to low values.

3.5.2.2.2 Stress Corrosion Crack Growth Tests. One standard 1T-WOL specimen (Figure 3.5-4) was fabricated from each of four typical BWR structural materials: (1) furnace sensitized [621°C (1150°F)/12 hr] Type 304 stainless steel; (2) furnace sensitized [621°C (1150°F)/2 hr] Type 316 nuclear grade stainless steel, (3) SA508 Class 2 low alloy steel; and (4) SA333 Grade 6 carbon steel. Each specimen was fatigue precracked in room temperature air to ensure that an active fatigue crack was present prior to environmental testing.

$$*R = \frac{\text{minimum load}}{\text{maximum load}}$$

The SCC test was performed in six loading phases (three slow cyclic loading phases and three constant load phases) as shown in Figures 3.5-5a, b, c. The slow cyclic loading (SCL) phase prior to each of the three constant load (CL) phases ensured that each specimen had an active crack growing in the environment prior to switching to constant load. The loading during each of the constant load phases was selected so that the stress intensity (K) for each specimen corresponded to the K levels used in previous 288°C (550°F)/200 ppb oxygenated water baseline tests.⁸ Therefore, a direct comparison of crack growth rates in the 200 ppb oxygenated water baseline environment and H₂WC could be made. The results of these tests are summarized in Tables 3.5-3 and 3.5-4 for the H₂WC and nominal environment, respectively.

The results of the SCC growth tests revealed that the H₂WC environment was detectably less aggressive than the 200 ppb O₂ environment for three of the four materials tested; the Type 316 Nuclear Grade stainless steel showed no detectable growth in either environment.

3.5.2.2.3 Fatigue Crack Growth Tests. A total of ten compact tension (CT) fracture mechanics specimens and two 1T-WOL fracture mechanics specimens were tested at two cyclic frequencies. Each specimen was fatigue precracked a minimum of 1.9 mm (0.075 in.) in room temperature air to ensure that an active fatigue crack was present prior to testing in the H₂WC environment. The materials tested were annealed, furnace sensitized, welded and low temperature sensitized [482°C (900°F)/24 hr] Type 304 stainless steel, furnace sensitized Type 316 Nuclear Grade stainless steel, SA508 Class 2 low alloy steel and SA333 Grade 6 carbon steel (only 1T-WOL specimens).

Six specimens were loaded at a time in a series chain using the skewed sawtooth waveform shown in Figure 3.5-6. The cyclical frequency was 0.74 cph (81-minute period) and 7.5 cph (8-minute period) with R = 0.6. Initial stress intensity values were selected to obtain a direct comparison of crack growth rates in H₂WC with growth rates generated previously for the same materials in a 200 ppb oxygenated water environment under identical loading conditions.

The six 0.74 cph specimens were subjected to 1349 loading cycles in H_2WC , while the remaining 7.5 cph specimens were characterized by 15,000 cycles.

- Compliance-based crack length data for the 12 specimens, as well as eight specimens tested in the nominal environment, were analyzed for average crack growth rate as shown in Table 3.5-5. These average cyclic crack growth rates are plotted as a function of stress intensity range (ΔK) in Figures 3.5-7 through 3.5-10 for austenitic stainless steels and ferritic materials at the two cyclic frequencies.

Figure 3.5-7 shows that the 0.74 cyclic crack growth rates for the two sensitized Type 304 stainless steel specimens tested in 200 ppb O_2 reference environment were three times greater than the cyclic crack growth rate of sensitized Type 304 stainless steel tested in H_2WC . The solution annealed and weld HAZ Type 304 stainless steel specimens which had a low degree of sensitization had H_2WC cyclic crack growth rates similar to the specimen which was highly sensitized. Therefore, the degree of sensitization of Type 304 stainless steel seems to have little effect on cyclic crack growth rate in H_2WC under the loading conditions tested. The cyclic crack growth rate for Type 316 Nuclear Grade stainless steel in H_2WC was only slightly less than the Type 304 stainless steel data.

A more dramatic difference in cyclic crack growth rate in H_2WC versus the 200 ppb O_2 reference environment was seen in the carbon steel and low alloy steel specimens (Figure 3.5-8). The 0.74 cyclic crack growth rate in H_2WC was 20 times less for carbon steel and 7 times less for low alloy steel than in the 200 ppb O_2 reference environment. Similar differences in cyclic crack growth in H_2WC versus the 200 ppb O_2 reference environment were seen at higher 7.5 cph, where the factor of improvement for Type 304 stainless steel was similar to that obtained at the lower frequency, but significantly higher (450 and 1000X) for the ferritic materials (Figures 3.5-9 and 3.5-10).

3.5.2.3 Corrosion Potential Measurements and Slow Strain Rate Tests (CERT and SET)

The objective of this part of the program was to determine whether stress corrosion or other forms of localized corrosive attack can occur in H_2WC . The task included three subtasks: (1) measurement of the corrosion potentials of Type 304 stainless steel, Alloy 600, carbon steel, Zircaloy-2, and low chromium (simulated sensitized grain boundary) Type 304 stainless steel in six water environments covering the expected range of H_2WC dissolved oxygen and hydrogen contents; (2) Constant Extension Rate Technique (CERT) testing of Type 304 stainless steel, Alloy 600 and low alloy and carbon steels, in three O_2-H_2 water environments selected from subtask (1), plus additional CERT tests on low alloy and carbon steel to support the Dresden-2 tests and (3) limited Straining Electrode Technique (SET) testing of Type 304 stainless steel, Alloy 600 and Alloy X-750 at various test potentials simulating the nominal and H_2WC environments.

3.5.2.3.1 Corrosion Potential Measurements. The decrease in dissolved oxygen content in the BWR coolant as a result of hydrogen additions to the feedwater should significantly reduce the corrosion potential, which is a measure of the thermodynamic driving force for corrosion reactions. Figure 3.5- 1 from Indig and McIlree⁹ indicates that there is a rapid drop in the corrosion potential of Type 304 stainless steel when the dissolved oxygen content falls below approximately 40 ppb.

The corrosion potentials of Type 304 stainless steel, Alloy 600, carbon steel (SA333, Gr. 6), Fe-10Ni-8.1Cr, Zircaloy-2 and platinum were measured against a high temperature Ag/AgCl reference electrode in high purity water and in a 0.01N Na_2SO_4 solution. The high purity water and sodium sulfate solutions contained specific concentrations of dissolved oxygen and hydrogen and were heated to 274°C (525°F). In the Na_2SO_4 solutions, the potential of pressure vessel steel (SA533 Gr. B) was also determined.

In high purity water, the electrochemical potentials for stainless steel tended to be below the potentials previously reported when the dissolved

IMAGE EVALUATION
TEST TARGET (MT-3)

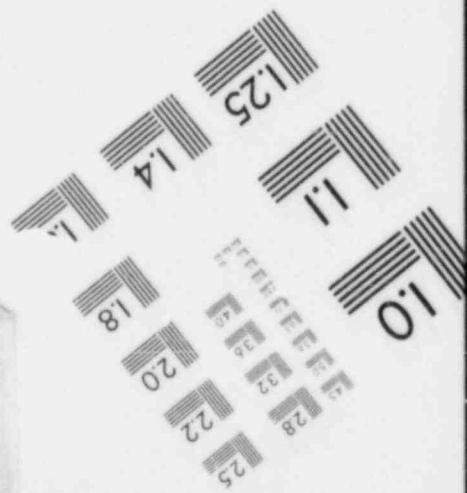
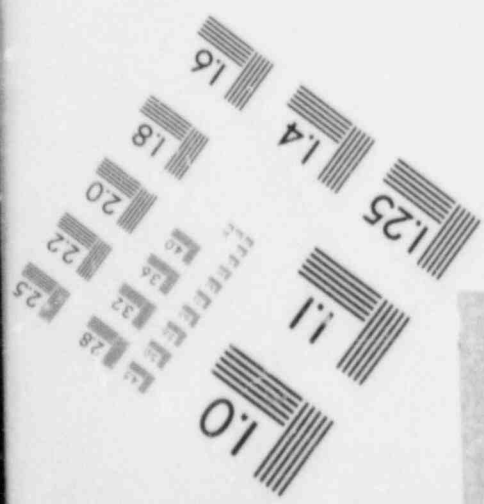
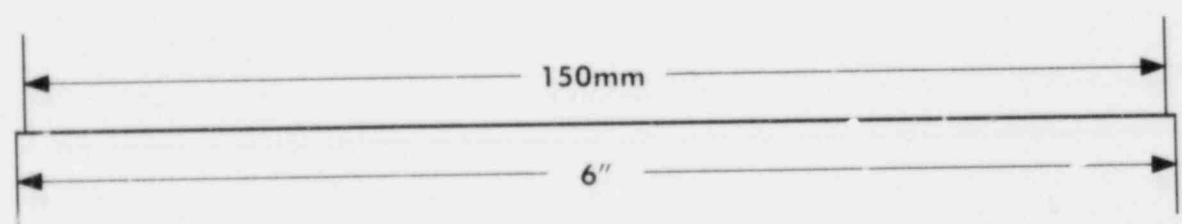
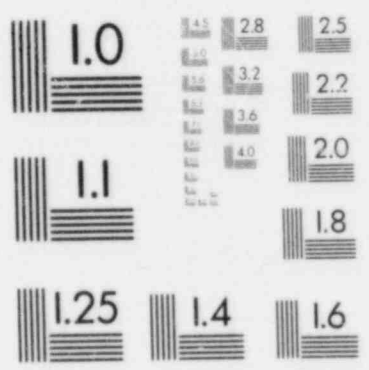
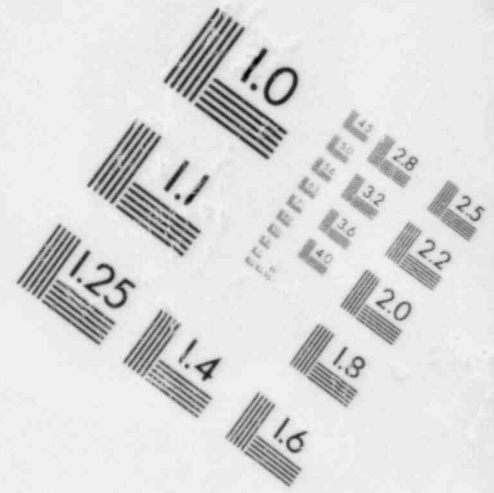
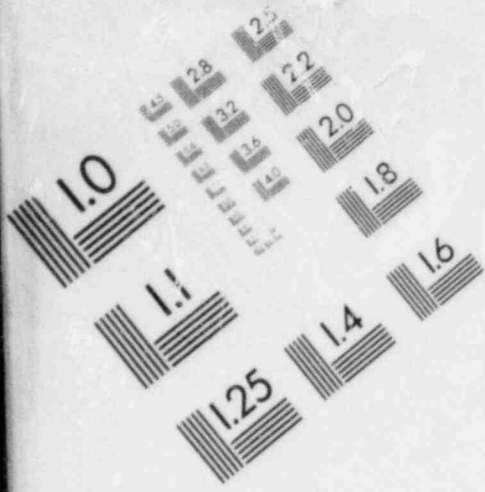
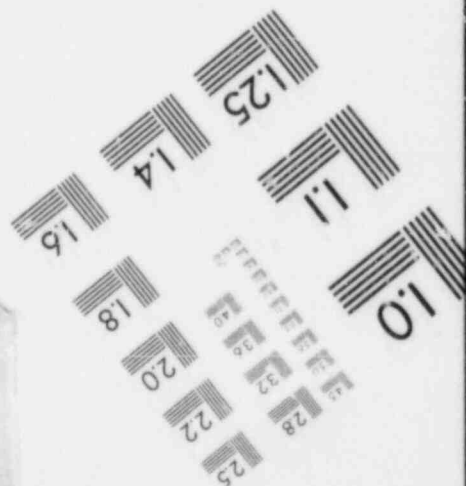
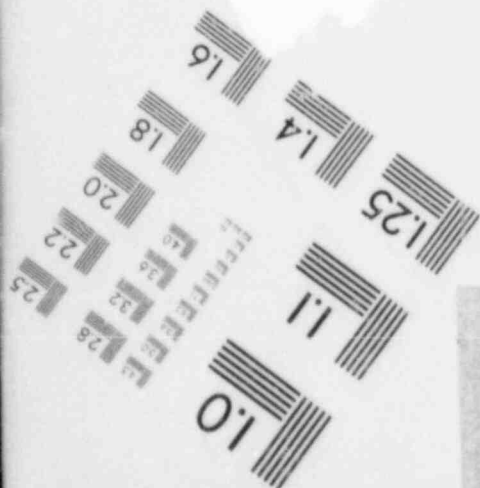
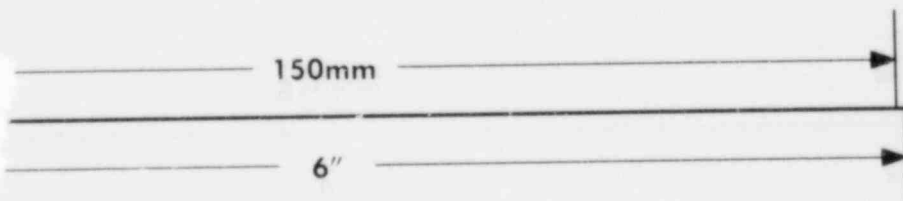
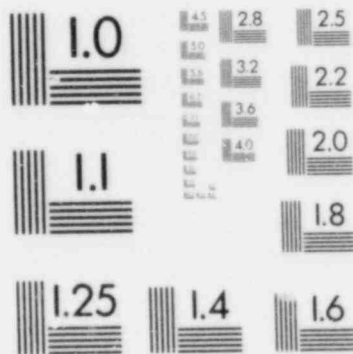
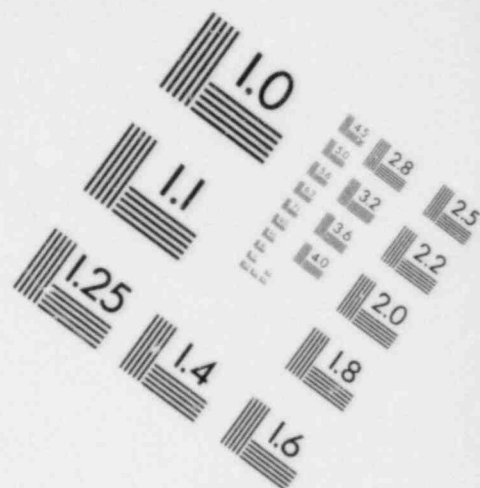
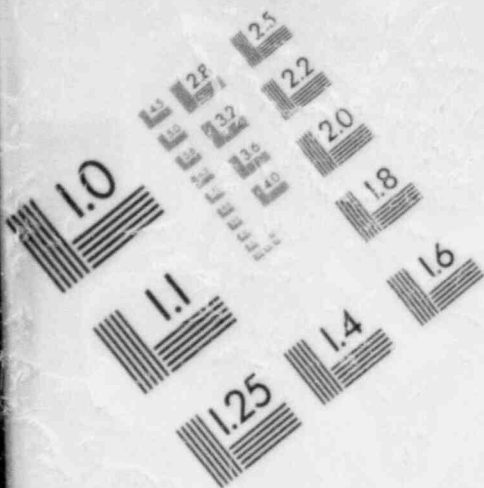


IMAGE EVALUATION
TEST TARGET (MT-3)



oxygen concentration was >100 ppb. At very low dissolved oxygen concentrations, the opposite effect occurred; the potentials were above previous values. The other iron and nickel base alloys behaved similarly. The net effect was to limit the response of electrochemical potential with changing dissolved oxygen concentration. The corrosion potentials in 0.01N Na₂SO₄ were lower than in high purity water. In part, this decrease in potential is related to an increase in p^H because the Na₂SO₄ forms a basic solution in high temperature water. It appeared that hydrogen had only an indirect effect on the electrochemical potential of the corrosion electrodes as measured in these laboratory tests. In-reactor the major effect of hydrogen will be in recombination with oxygen, and as the oxygen decreases, a decrease in the chemical driving force for IGSCC.

3.5.2.3.2 Constant Extension Rate Tests. The constant extension rate test (CERT) facility used for studying stress corrosion cracking behavior of alloys in simulated BWR environments was described by Clarke, Cowan, and Danko.¹⁰ To minimize oxygen gettering due to chemical reaction with heated surfaces, the regenerative heat exchanger was fabricated from titanium tubing and the pressure vessel and load frame internals were made from Ti-6Al-4V alloy.

All CERTs (apart from the Dresden-2 support tests) were conducted at 274°C (525°F) in controlled aqueous environments (both water purity and dissolved gas concentrations) at a strain rate of $2 \times 10^{-5} \text{ min}^{-1}$. CERTs were conducted on Type 304 stainless, Alloy 600, pressure vessel low alloy steel (SA533) and carbon steel SA333, Gr. 6.

Table 3.5-6 presents a summary of the experimental conditions and the CERT results for the materials tested. The CERT results tabulated are the mechanical properties, failure times, and failure morphologies. Lower values of the mechanical properties and shorter CERT testing times are indications of stress corrosion cracking. Verification of stress corrosion cracking is obtained by post-test examination.

The most important result of these tests was that none of the alloys exhibited any sign of stress corrosion cracking in the hydrogen water chemistry environment. Except for Alloy 600, all of the alloys exhibited some degree of stress cracking in a simulated normal BWR environment.

The CERT tests performed in support of the Dresden-2 H₂WC demonstration used SA508 Class 2, SA533 Grade B Class I low alloy steel and SA106 Grade B carbon steel tested in the creviced and uncreviced condition. The crevice was produced by wrapping and spot welding thin stainless steel shim stock around the test section. The test conditions and results are presented in Table 3.5-7. Comparison of these data with previous low alloy steel CERT data in 200 ppb O₂ water, 8.0 ppm O₂ water and air shows the benefit of the H₂WC (50 ppb O₂, 230 ppb H₂, <1 μS/cm). In contrast to the roughly 20% transgranular stress corrosion cracking (TGSCC) in 0.2 ppm O₂, these H₂WC CERT test results reveal the 100% ductile behavior and appear to be essentially the same as 288°C (550°F) air test results.

The CERTs clearly indicated that in high purity water, intergranular stress corrosion cracking of weld-sensitized Type 304 stainless steel and TGSCC of pressure vessel and carbon steel can be prevented by hydrogen water chemistry.

The indications from CERTs run in the present and previous programs are that the low alloy and carbon steel are more resistant to stress corrosion cracking in higher dissolved oxygen concentrations than stainless steel.

Alloy 600 in the welded + LTS condition did not show any indications of IGSCC in any of the CERTs. This was not surprising, since the only instance of IGSCC of this alloy in the field was related to the presence of crevice and high concentrations of an impurity (resins).

3.5.2.3.3 Straining Electrode Tests. The straining electrode test (SET) is a CERT conducted under potential control rather than chemical control. Because potential control requires the passage of current through the solution in contact with the specimen, a conductive electrolyte is used to minimize IR drops.

A circulating deaerated 0.01N solution of Na_2SO_4 maintained at 274°C (525°F) was the electrolyte. The control potentials simulated either normal BWR or H_2WC environments. All specimens were pulled to failure at a strain rate of $2 \times 10^{-5} \text{ min}^{-1}$ in an austenitic stainless steel pressure vessel. Since deaerated test solutions were used, titanium alloys in the high temperature SET system were not necessary.

The results of the SETs are presented in Table 3.5-8. The critical findings in these tests were that no SCC occurred at potentials that simulated the hydrogen water chemistry environment for Type 304 stainless steel, Alloy 600 or Alloy X-750. IGSCC did occur in the simulated nominal environment for Type 304 stainless steel and Alloy 600. No cracking of Alloy X-750 occurred in the SETs at -0.100 and $-0.700\text{V}_{\text{SHE}}$.

3.5.3 In-Reactor H_2WC Test Results

Materials tests have been conducted at Dresden-2 under H_2WC conditions to confirm the results of the laboratory H_2WC investigations. These tests indicate the laboratory data appear to be directly applicable for predicting materials behavior in an operating BWR.

The first set of hydrogen injection verification studies was run at the Dresden-2 nuclear power plant of the Commonwealth Edison Co. from May 19 to July 7, 1982.¹¹ Hydrogen was added to the reactor feedwater via injection taps in the condensate booster pump casings. Initially, hydrogen was added for five consecutive steady-state periods, during which feedwater hydrogen concentrations in parts per billion were: <5 (two days), 200 (two days), 400 (two days), 1000 (four hours) and 1800 (four hours). Reactor power during this sequence was held at about 83% of full power (2527 MWTh).

The remainder of the initial demonstration testing with hydrogen was done from June 3 to June 29 to support electrochemical potential (ECP) measurements and CERT tests in the reactor autoclaves. Except for power decreases for

maintenance or weekend surveillance testing, reactor power was close to 100% during this time. The hydrogen addition rate was adjusted to produce the required oxygen concentrations in the test autoclaves (reactor recirculation system water) and ranged from 0.6 to 1.3 ppm in the reactor feedwater. After the cessation of hydrogen addition, there were 10 additional days of CERT testing under normal reactor conditions to provide baseline comparison data.

In April 1983, Dresden-2 initiated full time operation on hydrogen water chemistry. From October 1983 through April 1984, a second series of ECP measurements and CERT tests were performed in the same reactor autoclaves.

3.5.3.1 Corrosion Potential Measurements

Electrochemical potentials (ECP) of Type 304 stainless steel, Alloy 600, SA533-B low alloy steel, and platinum were measured against an AgCl reference electrode in an autoclave containing flowing reactor water. In general, the ECPs decreased directly with oxygen concentrations in a manner similar to that obtained in the laboratory (Figure 3.5-12). With time, however, at any constant oxygen concentration and conductivity, the corrosion potential of film-forming materials drifted upward. The platinum potential was unique and more sensitive to hydrogen than oxygen concentration. Based on these potential measurements, and the stress corrosion cracking results (discussed below), it appears that intergranular stress corrosion cracking (IGSCC) of furnace-sensitized Type 304 stainless steel in boiling water reactors can be prevented at corrosion potentials less than $-325\text{mV}_{\text{SHE}}$, in agreement with the laboratory test data presented earlier.

During the second ECP measurement campaign at Dresden-2 (October 1983 - April 1984), the ECPs of stainless steel were measured for 3330 hours (~139 days). Potentials obtained during this extensive coverage were similar to those measured during the first demonstration campaign. The normal Dresden-2 environment was characterized by an ECP range for Type 304 stainless steel of -100 to $-200\text{mV}_{\text{SHE}}$, while the hydrogenated Dresden-2 environment reduced the Type 304 stainless steel potential to -370 to $-460\text{mV}_{\text{SHE}}$. It appears that, during times when H_2WC is terminated, a "memory" effect occurs in that the

potential does not suddenly rise into the range where IGSCC of sensitized Type 304 stainless steel can occur. Instead, the potential rises slowly, which creates a window of time prior to rising into the cracking potential region. Typically, this window is ~10 hours (Figure 3.5-13).

The ECP measurements obtained during the second campaign also revealed that at Dresden-2 there is no significant difference between the ECPs of filmed or unfilmed Type 304 stainless steel and Type 316 stainless steel. This differs from some of the data obtained by ASEA-ATOM at Ringhals-1, which suggests that Type 316 stainless steel reaches a significantly lower potential in H_2WC than Type 304 stainless steel.

3.5.3.2 In-Reactor CERT Test Results

Two low alloy steel and three furnace-sensitized Type 304 stainless steel specimens were tested in Dresden-2 environments modified by hydrogen injection, and in the normal BWR environment that contained approximately 200 ppb dissolved oxygen during the initial H_2WC demonstration. In the modified BWR environments, two different H_2 injection rates resulted in dissolved oxygen concentrations of 40 ± 5 and <20 ppb dissolved oxygen. Type 304 stainless steel tensile samples were run in both of the modified environments, while the SA533 Grade B low alloy steel was tested in the aqueous environment that contained <20 ppb O_2 .

For Type 304 stainless steel, suppressing the dissolved oxygen to 40 ppb resulted in a decrease in the amount of IGSCC, but elimination of the phenomenon did not occur until the dissolved oxygen concentration was <20 ppb. Stress versus time plots, normalized to a crosshead speed of $25 \mu\text{m/hr}$ (0.001 in./hr) (Figure 3.5-14) are shown for the three different reactor environments. The vertical dashed lines indicate the times the load was removed from the tensile specimen when the hydrogen injection system was shut off. The "x"s indicate CERT data obtained in 288°C air. When the curves are converted to stress-strain curves at a crosshead speed of $25 \mu\text{m/hr}$ (0.001 in./hr), each 100 hours of the testing results in a 13.3% specimen strain. The curves

clearly show the increased ductility and tensile strength (decreased IGSCC) with decreasing dissolved oxygen concentration. The <20 ppb oxygen data is similar to that obtained in high temperature air. The CERT at the lowest dissolved oxygen concentration was terminated before specimen failure.

The low alloy steel samples during the 1982 campaign clearly showed the benefit of reduced oxygen concentration in stress corrosion response. Both laboratory and in-reactor studies are in agreement, as the transgranular stress corrosion cracking was eliminated as the oxygen decreased to <20 ppb. Since the pressure vessel steel was tested at 75 $\mu\text{m/hr}$ (0.003 in./hr), each 10 hours of extension should produce about 4% strain. Transgranular cracks were found in the sample tested in the laboratory in water containing 200 ppb dissolved oxygen, but no cracks were found in the samples tested in the laboratory or reactor in the low dissolved oxygen environment. Since low alloy steel is more tolerant of higher oxygen concentrations and lower water purity than sensitized stainless steel, any oxygen-conductivity environment which provides SCC protection for sensitized stainless steel will also provide protection for the low alloy steel.

The 1983-1984 CERT test campaign at Dresden-2 was characterized by a similar set of seven experiments. Four furnace-sensitized Type 304 stainless steel specimens, one furnace-sensitized Type 304 stainless steel specimen precracked by IGSCC in a 0.2 ppm oxygen water laboratory autoclave and shipped to the site, one SA106 Grade B carbon steel and one SA508 Class 2 low alloy steel specimens were tested. The results of these CERT tests plus the results of the first campaign and comparable laboratory tests are summarized in Table 3.5-9.

Table 3.5-9 clearly indicates an excellent correlation between Dresden-2 and laboratory CERT test results. It also clearly shows that H_2WC provides mitigation of IGSCC in furnace sensitized Type 304 stainless steel even in instances where hydrogen addition has been interrupted. For example, in one CERT study (line No. 6) 396 hours of test time and 45% strain were accumulated with >10% of the test time in oxygenated water (30 hours with no H_2 and O_2 >200 ppb and 15.5 hours with O_2 at 25-41 ppb) and no IGSCC was identified.

However, in CERT No. 5, a 12-hour continuous test period with the hydrogen injection terminated produced minor IGSCC damage. (This test result is also marred by a thermal overload problem which resulted in extremely high thermal stress.) The precracked furnace-sensitized Type 304 stainless steel specimen (No. 8) (67 hours in 200 ppb O_2) failed by ductile tearing after 301 hours in Dresden-2. The mechanical parameter of this specimen is similar to non-precracked specimens. It is also important to note that this test included 10 hours >40 ppb oxygen. Finally, no IGSCC was identified in either SA508-2 and SA533-B low alloy steel and SA106-B carbon steel in H_2WC at Dresden-2 despite interruptions in hydrogen injections.

3.5.3.3 In-Reactor DC Potential Drop Crack Growth Test

Crack growth data versus time and environment on precracked furnace-sensitized Type 304 stainless steel is being obtained at Dresden-2 using the reversing DC potential drop technique as developed by GE Corporate Research and Development. The specimen was precracked in San Jose in the nominal 200 ppb O_2 and then transported to Dresden-2 for testing. The K_I level for the specimen bounds the crack previously identified in Dresden-2 safe-end at 27.5 MPa \sqrt{m} (25 ksi $\sqrt{in.}$). To supplement this program, bolt-loaded WOL specimens (one each) of Alloy 600 and unclad SA508 Class 2 low alloy steel have also been inserted into the autoclave.

Figure 3.5-15 presents the early DC potential drop crack growth data of the precracked furnace-sensitized Type 304 stainless steel specimen. Although the data is preliminary and is clouded by a reactor scram which occurred approximately 120 hours into the test and some other interruptions in hydrogen injection, no significant crack growth has occurred on the specimen. This preliminary result verifies the result of the Dresden-2 precracked CERT test discussed above and the results of the mid-cycle in-service inspection (ISI) as presented in Table 3.5-10.

This mid-cycle ISI was performed as required by the NRC to verify the mitigation of IGSCC growth by H_2WC . The inspection was performed on November 12, 1983, after approximately 5.5 months of operation with hydrogen

injection. The results presented in Table 3.5-10 indicate that, despite interruptions in hydrogen injection, no crack growth was detected by ultrasonic testing.

3.5.4 Summary

Overall, the results of these laboratory and in-reactor H_2WC materials programs are highly encouraging. Hydrogen water chemistry clearly improves the stress corrosion cracking performance of several BWR structural materials as follows:

- (1) The ECPs of all the tested BWR structural materials decrease with decreasing oxygen content. During times when H_2WC is terminated, a "memory" effect occurs in that the potential of Type 304 stainless steel does not rapidly rise into a range ($> -325 \text{ mV}_{SHE}$) where IGSCC can occur. This "safety" window of time appears to be ~ 10 hours.
- (2) H_2WC clearly provides mitigation of IGSCC in furnace-sensitized Type 304 stainless steel and IGSCC of carbon steel and low alloy steel at Dresden-2. These results are in exact agreement with laboratory studies.
- (3) For pre-cracked furnace-sensitized Type 304 stainless steel, a Dresden-2 CERT test and preliminary DC potential drop studies indicated mitigation of crack propagation in-reactor. These results, combined with laboratory pre-cracked pipe tests results and the ISI data at Dresden-2, indicate that pre-existing cracks at Dresden-2 or other BWRs should not propagate during H_2WC operation.
- (4) H_2WC prevents initiation and propagation of IGSCC in welded Type 304 stainless steel piping at high stress levels (twice ASME Code allowable). A FOI of > 25 has been achieved on crack initiation for full size Type 304 stainless steel piping in the H_2WC environment.

- (5) H_2WC prevents IGSCC of sensitized Type 304 stainless steel and Alloy 600 and TGSCC of low alloy and carbon steel.
- (6) For Type 304 and Type 316 Nuclear Grade stainless steels, low alloy steel and carbon steel, no measurable crack growth is observed in H_2WC even at high stress intensities. Measurable crack growth is observed for Type 304 stainless steel and carbon steel in the normal BWR environment.
- (7) Cyclic crack propagation rates are significantly reduced in H_2WC for stainless, low alloy and carbon steel even at high stress intensities.
- (8) No detrimental effects such as hydrogen embrittlement have been found for high strength materials such as Alloy 600 and Alloy X-750 in the H_2WC environment.

The results obtained from in-reactor studies and from the laboratory test conducted under this program correlate well, and it appears that the laboratory results are directly applicable for predicting materials behavior in Dresden-2 and other BWRs.

All evidence available to date suggests that H_2WC has been effective in mitigating IGSCC during reactor power operation at the Dresden-2 station. It is anticipated that the beneficial effects of H_2WC would apply to all BWRs.

Table 3.5.1
TEST MATRIX FOR HYDROGEN WATER CHEMISTRY PIPE TESTS

Material	Heat Number	Test Condition/Specimen Number		
		Normal BWR Water	Hydrogen Water Chemistry	
		200 ppb O ₂	50 ppb O ₂	20 ppb O ₂
<u>Reference Specimens</u>				
Type-304 SS	04836	AWC-5		
Type-304 SS	04836	AWC-6		
Type-304 SS	51416	AWC-7		
Type-304 SS	M2152	AWC-8		
<u>Crack Growth Specimens</u>				
Type-304 SS	04836	AWC-1 (Precrack)	→	AWC-1
Type-304 SS	04836	AWC-2 (Precrack)*		
Type-304 SS	04836	AWC-3 (Precrack)	→	AWC-3
Type-304 SS	04836	AWC-4 (Precrack)*		
Type-304 SS	04836			AWC-9 (Precrack) → AWC-9
Type-304 SS	04836			AWC-10 (Precrack) → AWC-10
Type-304 SS	04836			AWC-11 (Precrack) → AWC-11
Type-304 SS	51416			AWC-12 (Precrack) → AWC-12
Type-304 SS	M2152			AWC-13 (Precrack) → AWC-13
**Type-304 SS	04836	AWC-15 (Precrack)	→	AWC-15
**Type-304 SS	04836	AWC-16 (Precrack)	→	
		AWC-16	←	
<u>Crack Initiation Specimens</u>				
Type-316 NG SS	03165			AWC-14 → AWC-14
**Type-304 SS	04836			AWC-17
**Type-304 SS	M1989			AWC-18
**Type-304 SS	M2152			AWC-19

*For metallographic crack depth determination

**New tests

Table 3.5-2
EXPOSURES AND RESULTS OF H₂WC PIPE TESTS⁽¹⁾

Specimen Number	Heat Number	200 ppb O ₂ Water		50-70 ppb O ₂ Water		20 ppb O ₂ Water (H ₂ WC)	
		Hours Exposure	Maximum Depth, mm (mils) ²	Hours Exposure	Maximum Depth, mm (mils) ²	Hours Exposure	Maximum Depth, mm (mils) ²
<u>Reference Specimens</u>							
AWC-5	04836	2044	Failed				
AWC-6	04836	1645	Failed				
AWC-7	51416	1059	Failed				
AWC-8	M2152	1339	Failed				
<u>Crack Growth Specimens</u>							
AWC-1	04836	308	0.38(15) ³	844	Failed		
AWC-2	04836	308	1.40(55) ³				
AWC-3	04836	1075	0.25(10) ³	877	1.52(60)	3955	2.54(100)
AWC-4	04836	654	1.12(44) ³				
AWC-9	04836			847	1.27(50) ³	3974	2.67(105) ⁴
AWC-10	04836			847	1.95(77) ³	4113	1.95(77)
AWC-11	04836			848	1.42(56) ³	3082	1.42(56)
AWC-12	51416			847	2.54(100) ³	3911	>5.08 (>200)
AWC-13	M2152			848	>5.08 (>200) ³	3082	>5.08 (>200)
AWC-15	04836	343	1.27(50) ³			5310	(5)
AWC-16	04836	343	1.02(40) ³				
		1285	Failed				
<u>Crack Initiation Specimens</u>							
AWC-14	03165			847	No Cracks (UT)	4047	
AWC-17	04836				No Cracks (UT)	5122	
AWC-18	M1989				No Cracks (UT)	7580	
AWC-19	M2152				No Cracks (UT)	7585	

3-104

NEDO-30730

NOTES FOR TABLE 3.5-2

- (1) All except AWC-14 are Type-304 stainless steel. AWC-14 is Type-316 NG stainless steel.
- (2) As estimated by UT inspection unless noted otherwise.
- (3) Precrack depth.
- (4) Measured on metallographic section.
- (5) UT complete, metallography initiated.

Table 3.5-3
SCC CRACK GROWTH TEST RESULTS IN H₂WC

H₂WC (20 ± 15 ppb O₂, 125 ± 25 ppb H₂, <0.2 μS/cm)

Material	Growth Rate	Stress Intensity
FS Type 304	No Growth*	$K \leq 31.2 \text{ MPa } \sqrt{\text{m}}$ (28.4 ksi $\sqrt{\text{in.}}$)
FS Type 316 NG	No Growth	$K \leq 30.1 \text{ MPa } \sqrt{\text{m}}$ (27.4 ksi $\sqrt{\text{in.}}$)
SA508	No Growth	$K \leq 50.9 \text{ MPa } \sqrt{\text{m}}$ (46.3 ksi $\sqrt{\text{in.}}$)
SA333-6	No Growth	$K \leq 44.8 \text{ MPa } \sqrt{\text{m}}$ (40.3 ksi $\sqrt{\text{in.}}$)

*Below detectable limit, i.e., growth rate < 8×10^{-8} mm/sec (3×10^{-9} in./sec.).

Table 3.5-4
SCC CRACK GROWTH TEST IN 200 PPB OXYGEN WATER

Material	Growth Rate	Stress Intensity
FS Type 304	8.9×10^{-8} mm (3.5×10^{-9} in.)/sec	$K = 17.3 \text{ MPa } \sqrt{\text{m}}$ (15.7 ksi $\sqrt{\text{in.}}$)
FS Type 316 NG	No Growth	$K \leq 26.7 \text{ MPa } \sqrt{\text{m}}$ (24.3 ksi $\sqrt{\text{in.}}$)
SA 508	Incipient Growth	$K = 49.1 \text{ MPa } \sqrt{\text{m}}$ (44.7 ksi $\sqrt{\text{in.}}$)
SA 106-B	1.4×10^{-7} mm (5.2×10^{-9} in.)/sec	$K = 44.0 \text{ MPa } \sqrt{\text{m}}$ (40.0 ksi $\sqrt{\text{in.}}$)

Table 3.5-5
FATIGUE CRACK GROWTH TEST RESULTS

Material	Cyclic Frequency (cph)	Environment	Stress Intensity MPa \sqrt{m} (ksi $\sqrt{in.}$)	Crack Growth Rate		Factor of Improvement
				mm/cycle $\times 10^{-5}$	(in./cycle) $(\times 10^{-5})$	
FS Type 304	0.74	H ₂ WC	30.9 (28.1)	69	(2.7)	~3
		200 ppb O ₂	30.3 (27.6)	254	(10)	--
	7.5	H ₂ WC	25.8 (23.5)	16	(0.63)	~3
		200 ppb O ₂	36.5 (33.2)	50	(2.0)	--
SA 508-2	0.74	H ₂ WC	34.1 (31.0)	7.6	(0.3)	~7
		200 ppb O ₂	37.6 (34.2)	50.8	(2.0)	--
	7.5	H ₂ WC	33.8 (30.8)	1.7	(0.07)	~450
		200 ppb O ₂	33.7 (30.7)	760	(30)	--
SA 333-6	0.74	H ₂ WC	30.4 (27.7)	5.6	(0.22)	~20
		200 ppb O ₂	30.6 (27.8)	109	(4.3)	--
	7.5	H ₂ WC	24.2 (22.0)	0.33	(0.013)	~1000
		200 ppb O ₂	23.7 (21.6)	330	(13)	--

3-107

NEDO-30730

Table 3.5-6

CERT RESULTS FOR MATERIALS TESTED IN HIGH PURITY WATER AT 274°C (525°F)

Material and Condition	Dissolved Gases (ppb)				Fracture ⁽¹⁾ Stress		UTS ⁽²⁾		T _f ⁽³⁾ h	R.A. ⁽⁴⁾ (%)	Elongation (%)	Fracture Morphology
	Inlet		Effluent		MPa	ksi	MPa	ksi				
	O ₂	H ₂ *	O ₂	H ₂ *								
T-304SS, W	200	0	180	0	610	88.6	429	62.2	246	29.8	29.2	20% IGSCC; 80% Ductile
T-304SS, W+LTS	200	0	180	0	600	87.1	409	59.3	244	31.5	26.8	30% IGSCC; 70% Ductile
T-304SS, W+LTS	200	100	100	100	694	100.7	403	58.5	236	41.9	27.1	25% IGSCC, **75% Ductile
T-304SS, W+LTS	45	112	19	112	1570	228	409	59.3	294	74	36.3	Ductile
SA533B	210	0	205	0	895	129.9	601	87.3	150	32.8	17.2	16% IGSCC; 84% Ductile Shallow pits, deep auxiliary cracks
SA533B	200	100	65	100	1700	246.7	637	92.5	203	62.8	21.9	100% Ductile
SA533B	45	112	13	112	1699	246.6	623	90.4	188	63.3	24.4	100% Ductile; minor pits
A 600, W+LTS	187	0	180	0	1072	155.6	559	81.1	362	47.9	42.8	100% Ductile
A 600, W+LTS	30	125	10	125	1103	160.1	525	76.2	342	52.4	40.7	100% Ductile
SA333 Grade 6	40	125	5	125	1076	156.2	471	68.4	262	56.2	29.6	100% Ductile

(1) Maximum load/failure cross section

(2) Maximum load/original cross section

(3) Failure time in hours

(4) Reduction in area

* H₂ concentration calculated

** 5% IGSCC also noted

Table 3.5-7
CERT TEST RESULTS IN H₂WC*

Spec I.D.	Material	Strain Rate (min ⁻¹)	Time to Failure (hr)	Max. Stress MPa (ksi)	RA (%)	Elongation (%)	Fracture Mode
A106-1	SA106B ⁽¹⁾ Carbon Steel	1 x 10 ⁻⁴	46	496 (72.0)	41.6	28.6	100% Ductile
A106-2	SA106B ⁽²⁾ Carbon Steel	1 x 10 ⁻⁴	39.5	494 (71.7)	35.6	26.3	100% Ductile
A533-1	SA533B C1 I ⁽¹⁾ Low Alloy Steel	1 x 10 ⁻⁴	47	571 (82.8)	70.4	32.0	100% Ductile
A508-1	SA508 C1 II ⁽¹⁾ Low Alloy Steel	1 x 10 ⁻⁴	43.5	581 (84.3)	75.0	28.6	100% Ductile

Notes: * 50 ppb O₂, 230 ppb H₂, <1 μS/cm conductivity at 288°C (550°F).

(1) Specimen was creviced by wrapping and spot welding thin stainless steel shim stock around the 3.1 mm (1/8 in.) diameter test section.

(2) This specimen was tested without a crevice.

Table 3.5-8

SET RESULTS IN 0.01N Na₂SO₄ AT 274°C (525°F)
(STRAIN RATE 2 x 10⁻⁵/MIN)

Material and Metallurgical Condition	Electro- Chemical Potential	Fracture ⁽¹⁾ Stress		UTS ⁽²⁾		T _f ⁽³⁾ h	R.A. ⁽⁴⁾ (%)	Elongation (%)	Fracture Morphology
		ksi	MPa	ksi	MPa				
Type-304SS, W+LTS	-0.100	35.1	242	33.7	232	36	3.9	4.8	100% IGSCC
Type 304SS, W+LTS	-0.500	178.3	1228	68.3	471	277	61.1	36.4	>95% Ductile, some TGSCC Initiation
Alloy 600 W+LTS	-0.100	111.3	767	77.3	533	233.5	30.6	31.1	70% IGSCC, 30% Ductile
Alloy 600 W+LTS	-0.500	180	1240	83.2	573	320	53.8	43.3	100% Ductile
Alloy X-750 3-step heat treated	-0.100	275	1895	168.5	1161	306	39.1	31.2	100% Ductile
Alloy X-750 3-step heat treated	-0.700	258.4	1780	165.4	1140	283	36.0	31.5	100% Ductile

- (1) Maximum load/failure cross section
(2) Maximum load/original cross section
(3) Failure time in hours
(4) Reduction in area

Table 3.5-9

RESULTS OF DRESDEN-2 AND LABORATORY H₂WC CERT TESTS

	Material	Test Location	O ₂ , ppb	K ¹ μS/cm	Time to Failure, hrs	Time Off H ₂ WC, hrs	Elongation %	Result
1)	FS ² T-304	D-2	268	0.29	108	0	12	70% IGSCC
2)	FS T-304	D-2	40	0.37	143	2	20	35% IGSCC
3)	FS T-304	D-2	<20	0.29	>297	4	38	Ductile Fracture
4)	FS T-304	D-2	5-20	0.19	208 ³	5	NM ⁴	Ductile Fracture
5)	FS T-304	D-2	5-23	0.17	181	15	NM	Minor IGSCC along gauge
6)	FS T-304	D-2	3-30	0.13	396	36	45	Ductile Fracture
7)	FS T-304	D-2	7-19	0.09	400	25	46	Ductile Fracture
8)	FS T-304PC ⁵	D-2	12-20	0.09	301 ⁶	7	40	No IGSCC Extension
9)	FS T-304	VNC ⁷	195	<0.1	156	NA ⁸	17	85% IGSCC
10)	FS T-304	VNC	15	<0.1	262	0	NA	Ductile Fracture
11)	SA 533B	D-2	150-280	0.29	37 ⁹	NA	12	40% TGSCC
12)	SA 533B	D-2	5-20	0.29	63	0	24	Ductile Fracture
13)	SA 533B	VNC	200	<0.1	43	NA	11	40% TGSCC
14)	SA 533B	VNC	12	<0.1	60	0	22	Ductile Fracture
15)	SA 508-2	D-2	12-18	0.08	52 ¹⁰	0	NM	Ductile Fracture
16)	SA 508-2"	VNC	50	<1	44	0	29	Ductile Fracture
17)	SA 106B	D-2	8-14	0.12	94	2	NA	Ductile Fracture
18)	SA 106B	VNC	50	<1	40	0	29	Ductile Fracture

(1) K = Conductivity

(2) FS = Furnace Sensitized 621°C (1150°F)/24 hr

(3) Thermal Overload Ended Test

(4) NM = Not Measured to Date

(5) PC = Pre-cracked in 200 ppb O₂

(6) Plus 67 Hours Pre-cracking (368 hr total)

(7) VNC = Vallecitos Nuclear Center

(8) Not Applicable, i.e., not a H₂WC Test

(9) Extension rate was 3 mils/hr for SA 533, SA 508-2, SA 106B and 1 mil/hr for Type 304 Stainless Steel

(10) Motor Failure, Specimen Fractured Manually

(11) Crevice

Table 3.5-10
MID-CYCLE ISI RESULTS FROM DRESDEN-2

<u>Weld</u>	<u>Date</u>	
	<u>April 29, 1983</u>	<u>November 12, 1983</u>
28-in. Safe End PS2-201-1	1-in. long, 16% deep ¹	1-in. long, 13% deep
17-in. Riser (Two Cracks) PD5-D20	0.25-in. long, 17% deep	0.25-in. long, 15% deep
	0.25-in. long, 19% deep	0.25-in. long, 17% deep
12-in. Riser (Two Cracks) PD5-D5	0.50-in. long, 19% deep	0.50-in. long, 18% deep
	0.25-in. long, 14% deep	0.25-in. long, 16% deep

¹Percentage Through-Wall

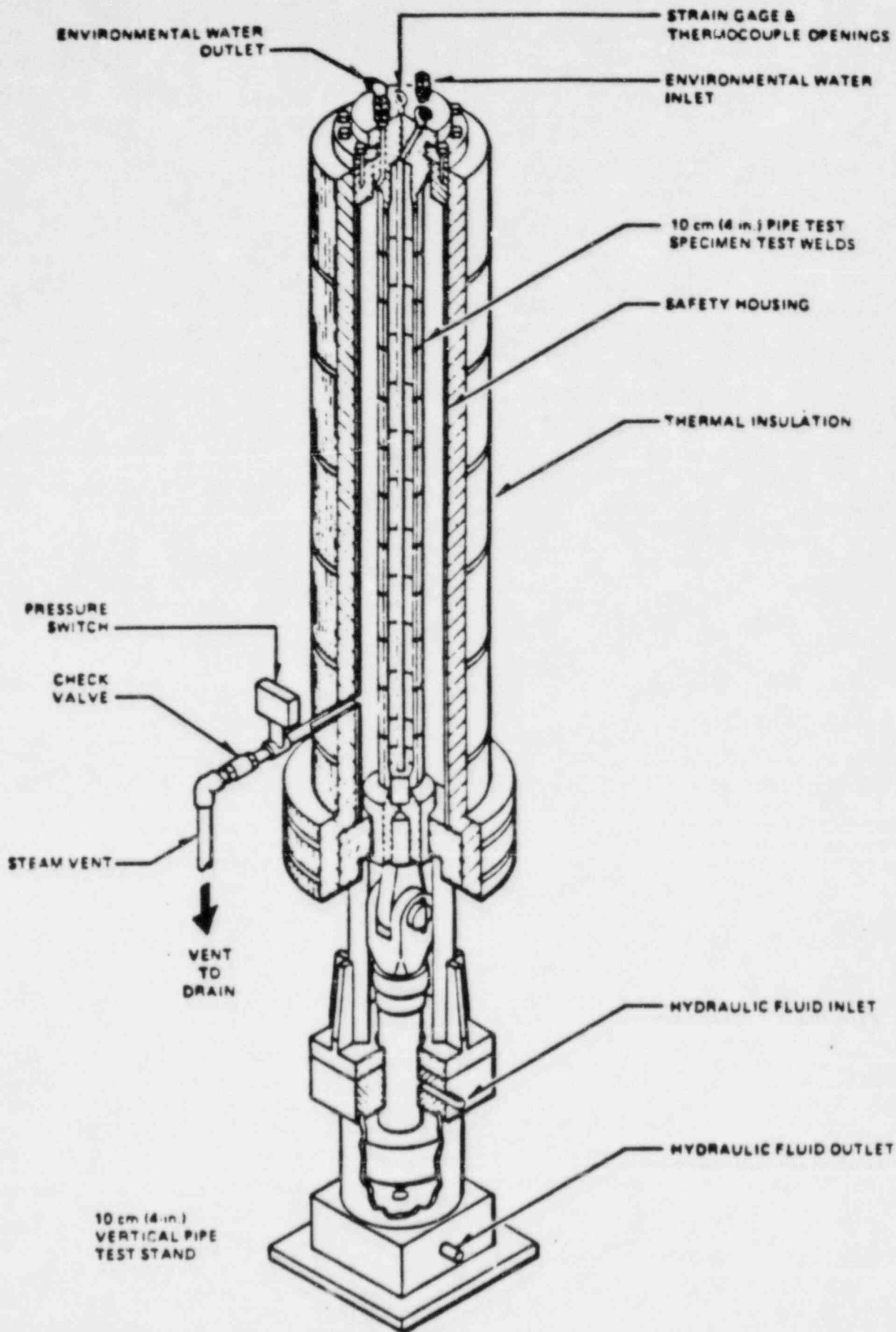


Figure 3.5-2. Pipe Test Specimen Loading Stand

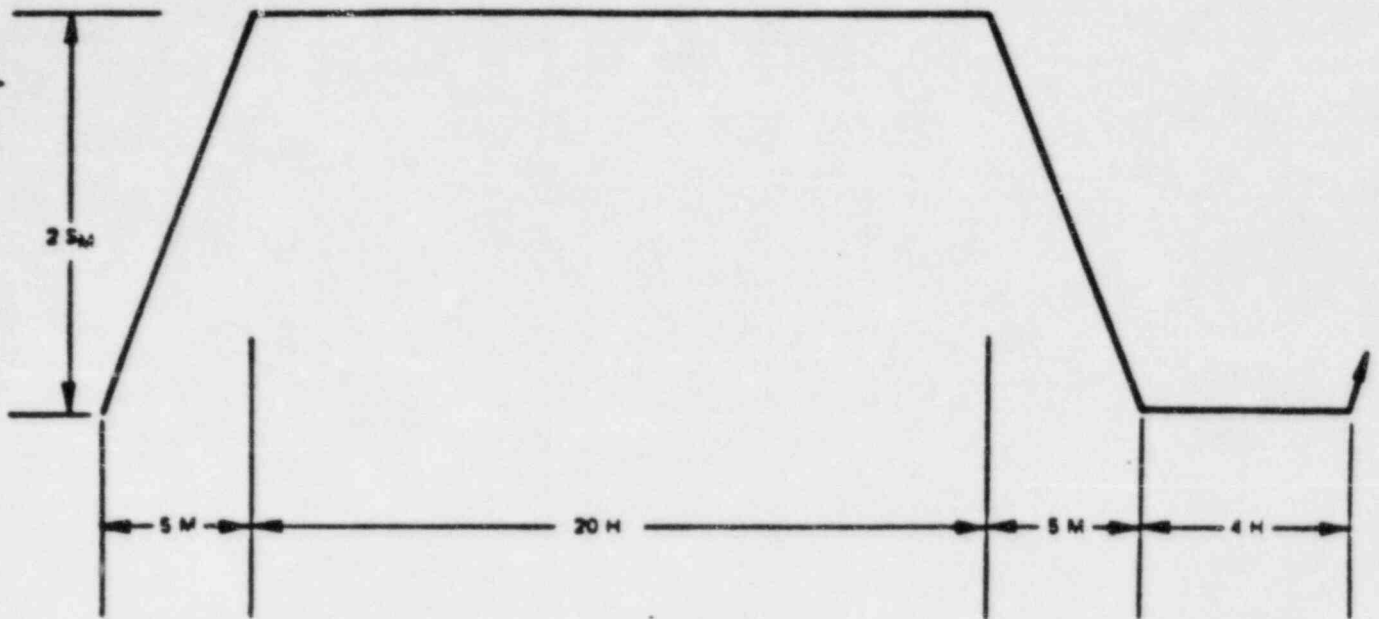


Figure 3.5-3. Loading Waveform Used for Hydrogen Water Chemistry Pipe Tests (M = minutes, H = hours, S_M = ASME Code Allowable Stress)

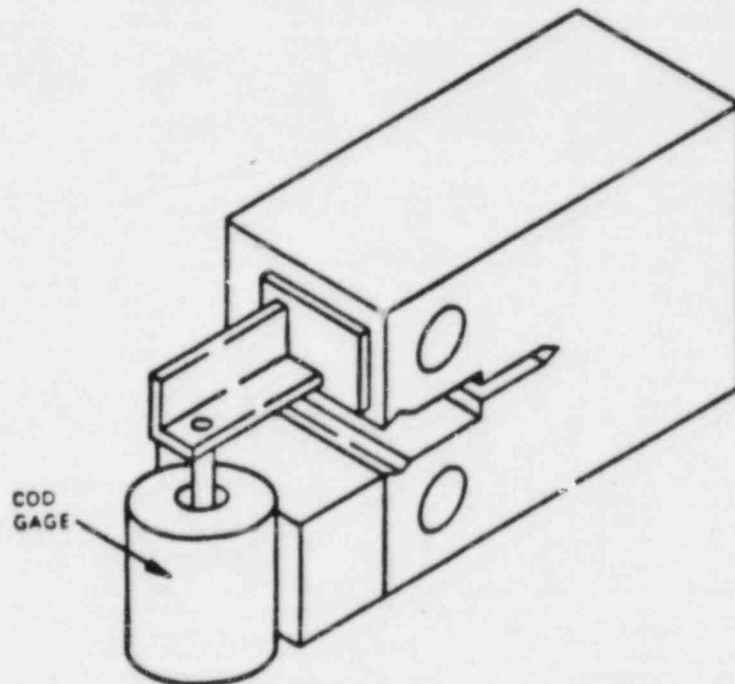


Figure 3.5-4. Typical WOL or Compact Tension Specimen for Crack Growth Rate Study

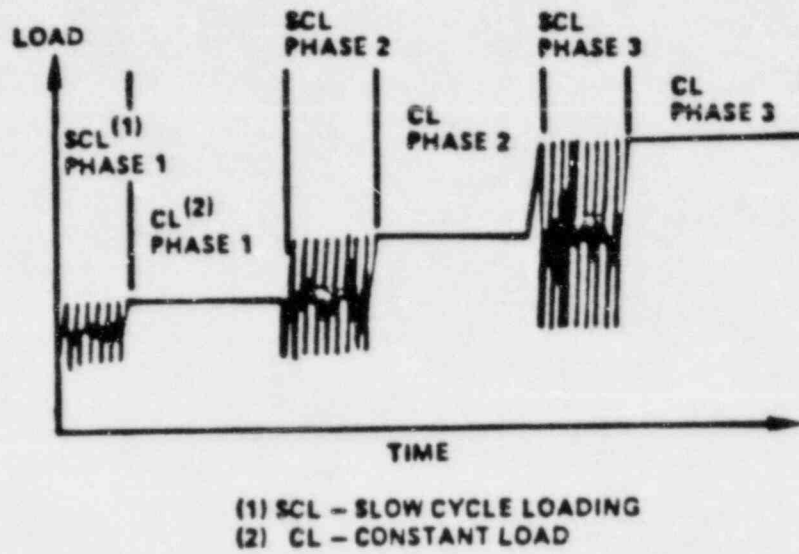


Figure 3.5-5a. Stress Corrosion Test Loading History

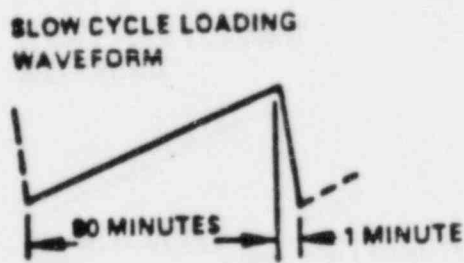


Figure 3.5-5b. Slow Cyclic Loading Waveform Detail

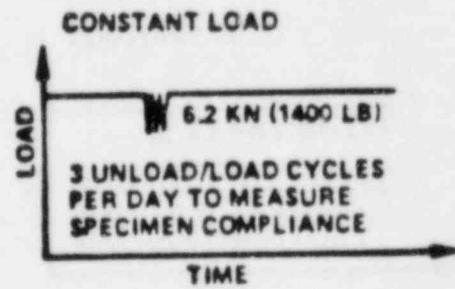


Figure 3.5-5c. Constant Load Detail

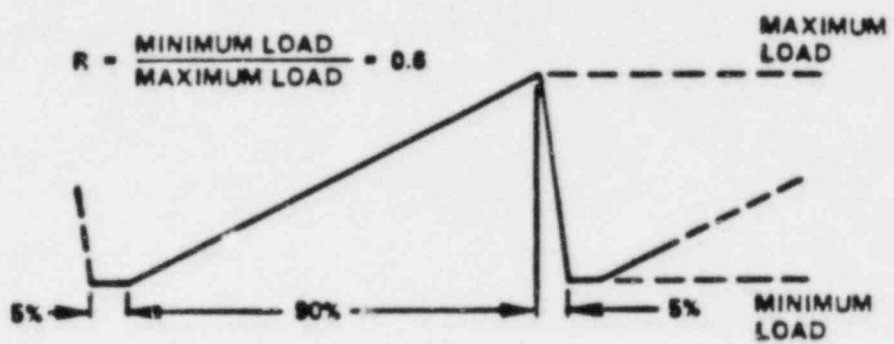


Figure 3.5-6. Cyclic Loading Waveform

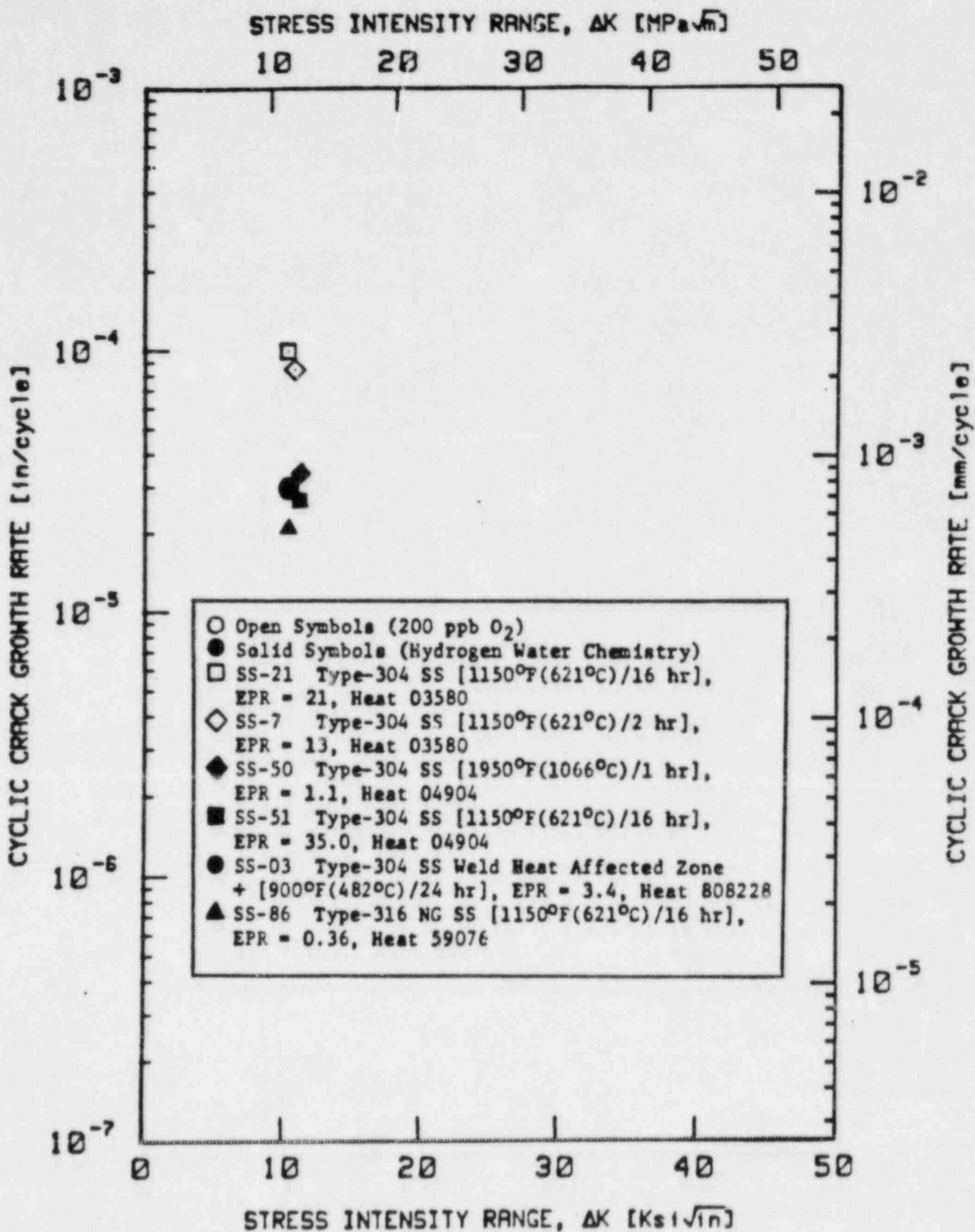


Figure 3.5-7. Comparison of Cyclic Crack Growth Data (0.74 cph, R=0.6) in H₂WC versus Nominal Environment for Furnace Sensitized Stainless Steel

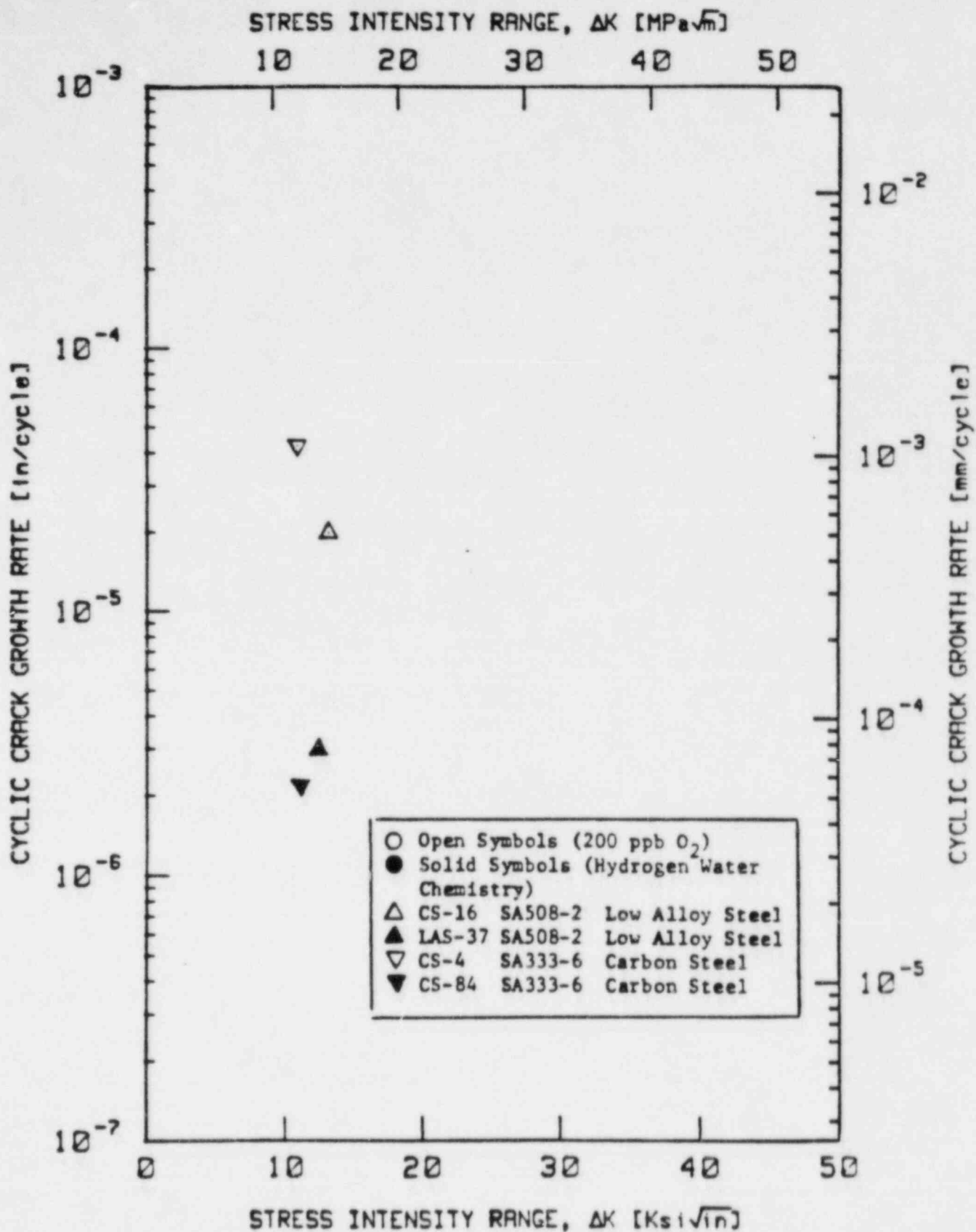


Figure 3.5-8. Comparison of Cyclic Crack Growth Data (0.74 cph, R=0.6) in H₂WC versus Nominal Environment for Carbon and Low Alloy Steel

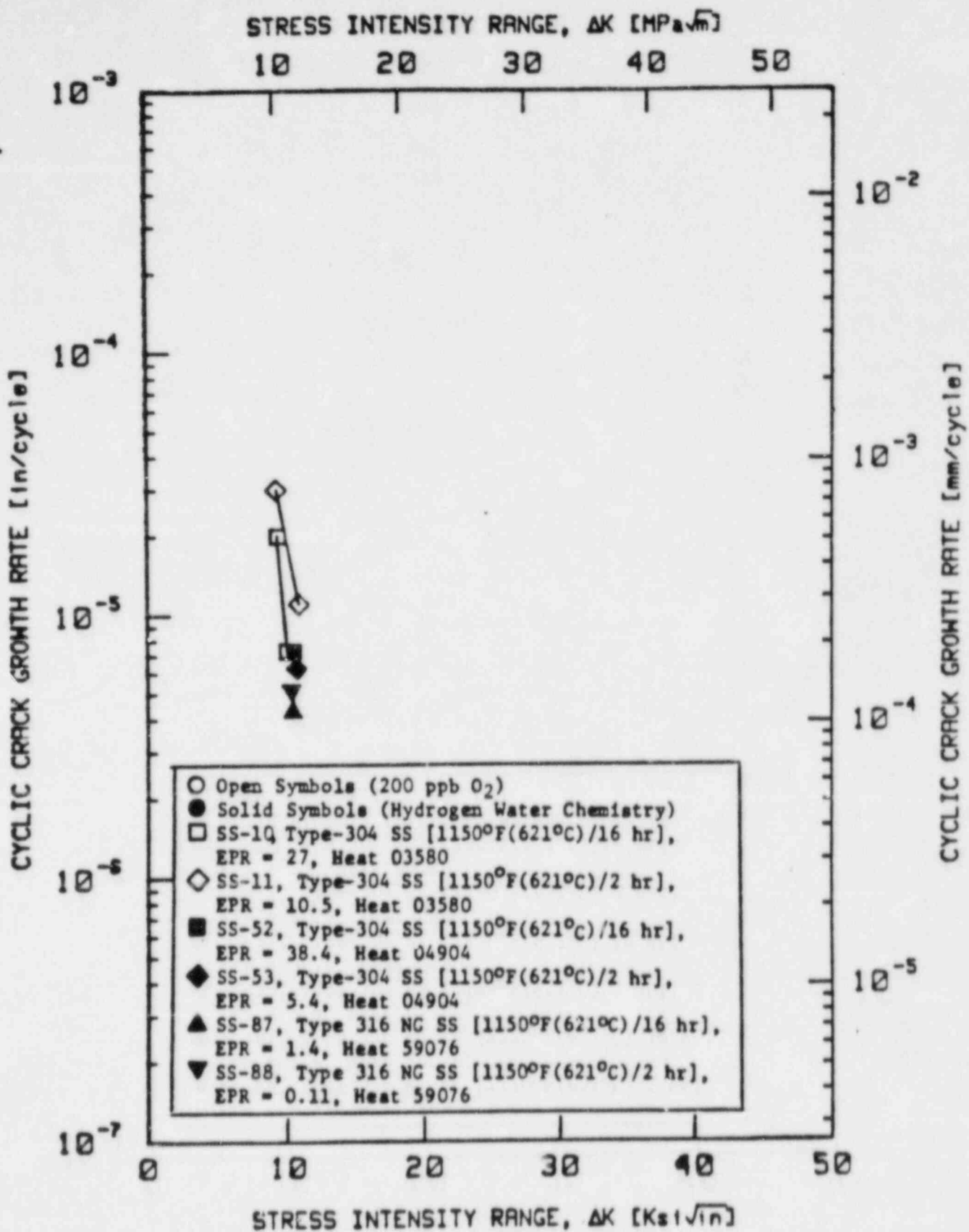


Figure 3.5-9. Comparison of Cyclic Crack Growth Data (7.5 cph, R=0.6) in H_2WC versus Nominal Environment for Furnace Sensitized Stainless Steel

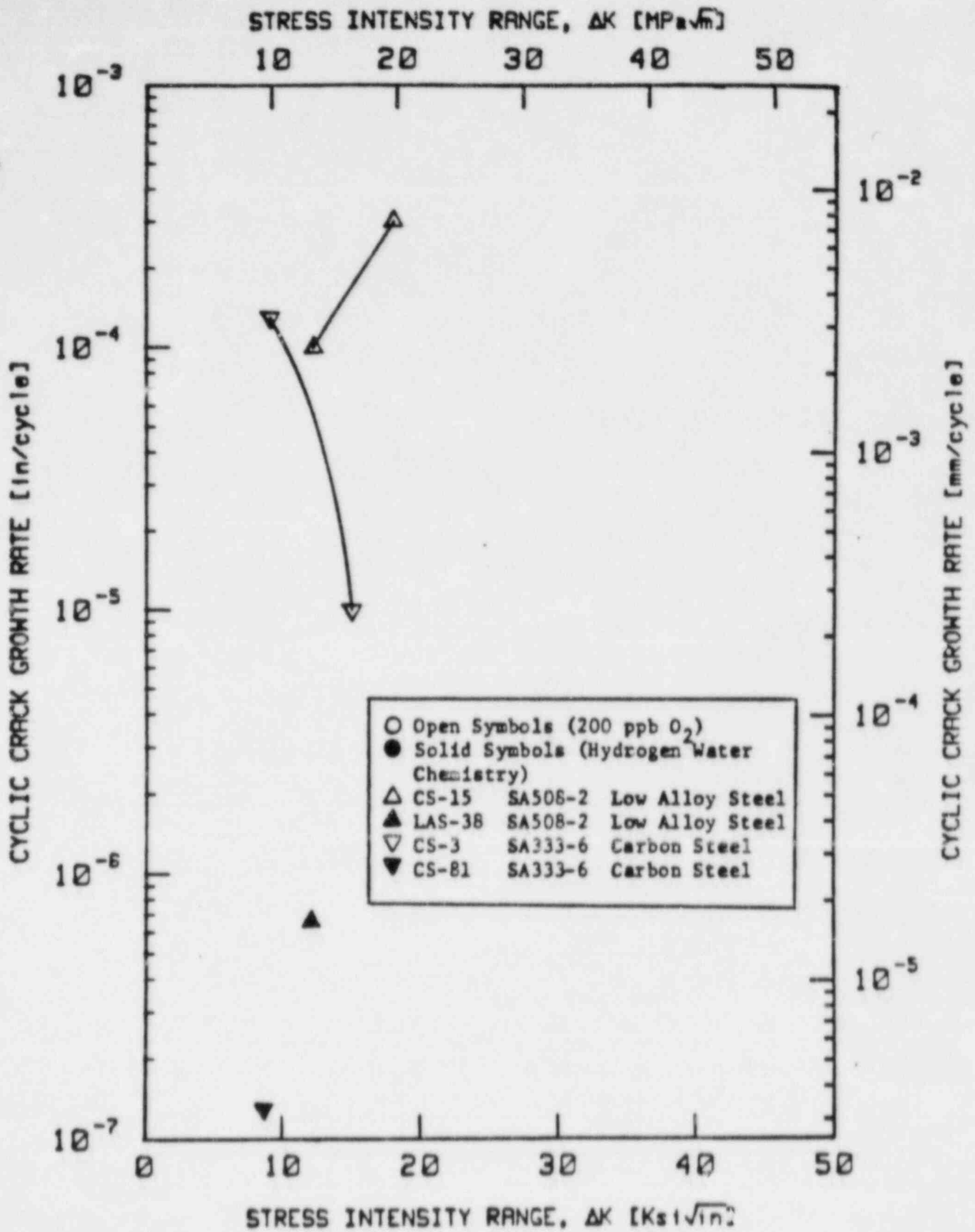


Figure 3.5-10. Comparison of Cyclic Crack Growth Data (7.5 cph, R=0.6) in H₂WC versus Nominal Environment for Carbon and Low Alloy Steel

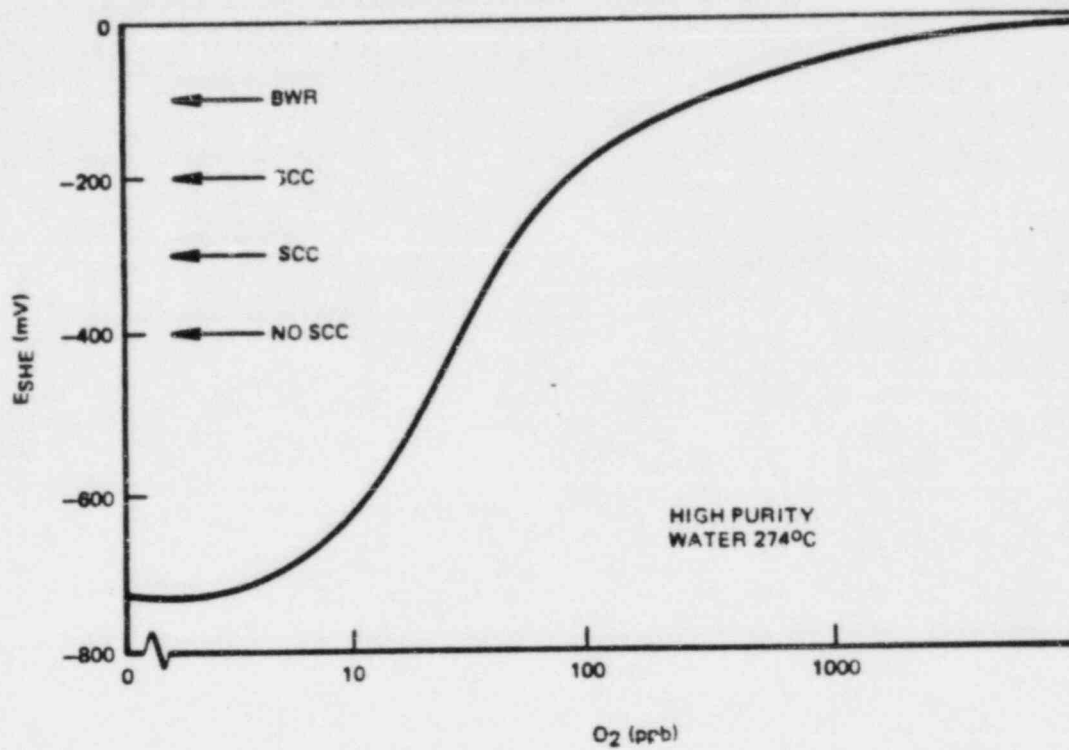


Figure 3.5-11. Relationship Between Dissolved Oxygen and Potential to IGSCC of Welded Type 304 Stainless Steel

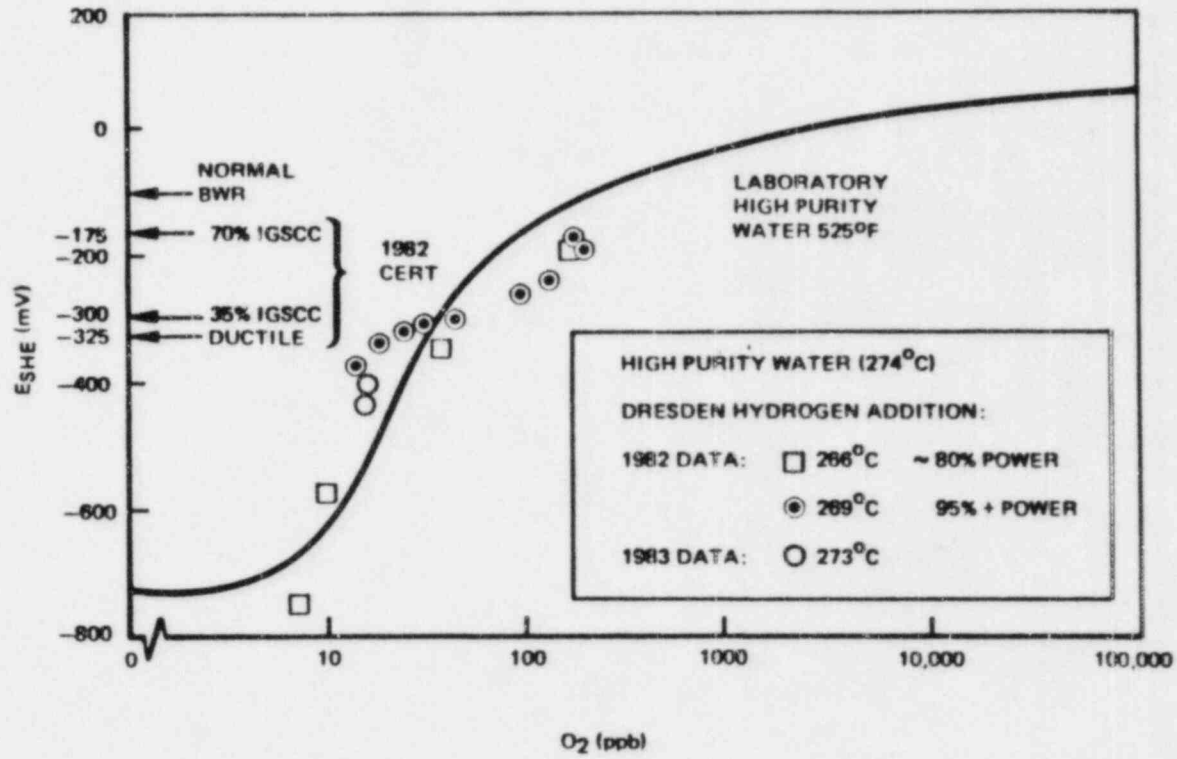


Figure 3.5-12. The Effect of Dissolved Oxygen on the Corrosion Potential of Type 304 Stainless Steel in High Purity Water at 274°C (525°F)

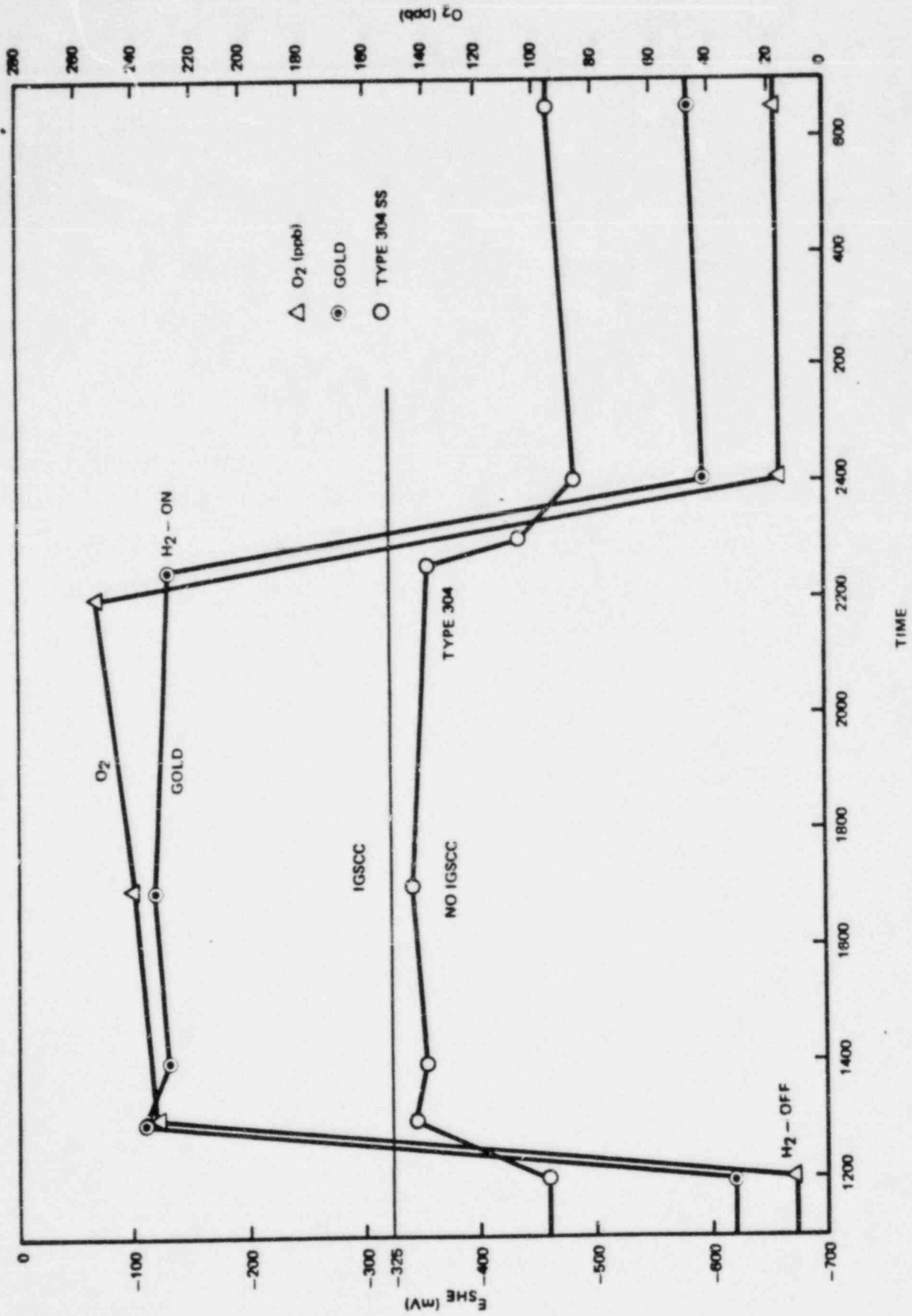


Figure 3.5-13. Example of ECP Memory Effect During H₂WC

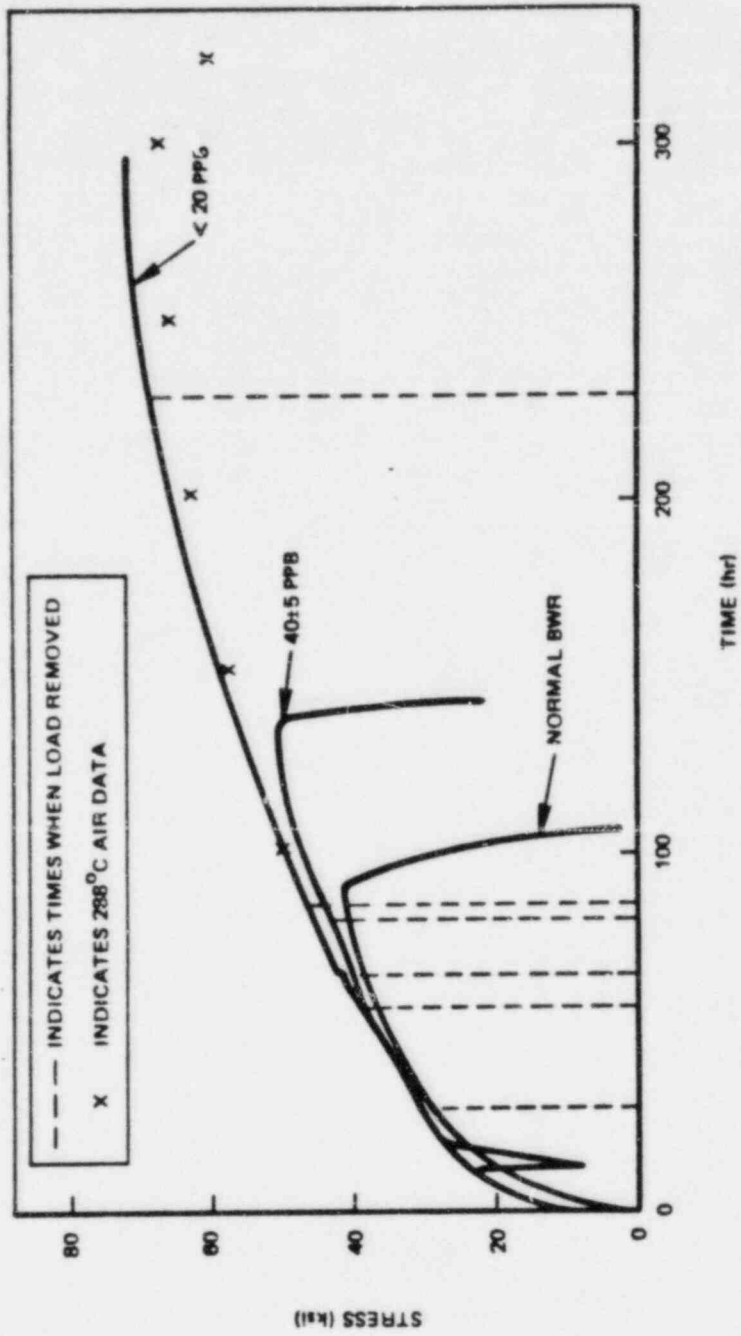


Figure 3.5-14. IGSCC Behavior of Sensitized Stainless Steel in Dresden-2 Tests

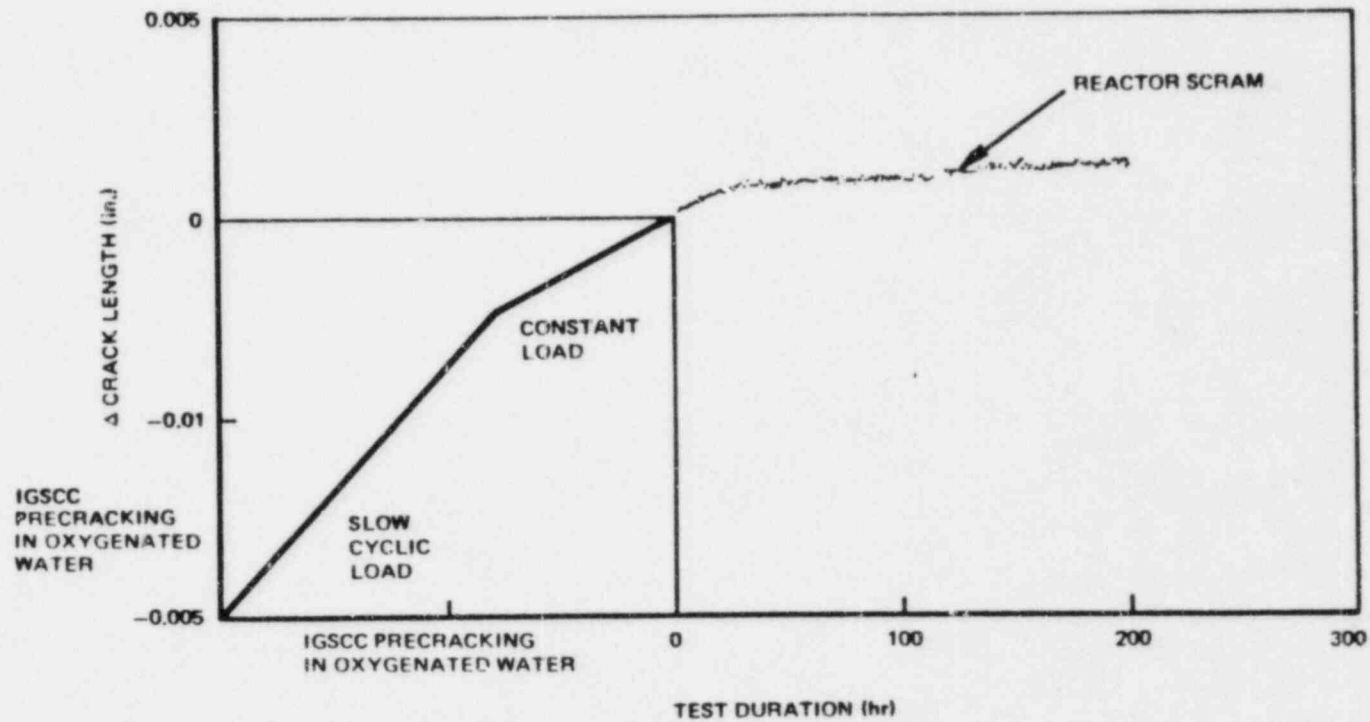


Figure 3.5-15. Dresden-2 H₂WC Crack Growth Test - Furnace Sensitized Type 304 SS
(K = 25 ksi $\sqrt{\text{in.}}$)

3.6 BEHAVIOR OF Ni-Cr-Fe ALLOYS IN HYDROGEN WATER CHEMISTRY

3.6.1 Introduction

Alloy 600 and its weld metal, Alloy 182, can be susceptible to stress corrosion cracking in the oxygenated BWR environment. Studies at General Electric Company have been performed to evaluate the behavior of these materials in the normal BWR environment to allow comparison with the behavior of Type 304 stainless steel. In addition, tests to evaluate the effect of Hydrogen Water Chemistry (H_2WC) on eliminating stress corrosion cracking have also been performed. The objective of this subsection is to present the understanding on SCC of these susceptible alloys in BWR environment and to establish that the existing data in the H_2WC low oxygen environment demonstrates arrest of IGSCC.

3.6.2 Background on the Physical and Corrosion Properties of Alloy 600 and its Weld Metal - Alloy 182

The wrought alloy and its Shielded Metal Arc Weld material Alloy 182 are of very similar composition. Table 3.6-1 shows that the materials have similar chromium and carbon contents. The strength properties are also listed in Table 3.6-1. The strength levels of the weld metal are higher than those of the wrought material. The environmental performance of these materials is generally excellent. At elevated temperatures when high tensile stresses are found in combination with oxygenated environments and tight crevices, these alloys can exhibit IGSCC. (In the case of weld metals, the failure mode is really interdendritic along the columnar boundaries formed during solidification.) Copson and Economy first investigated these alloys in double U-bend specimens in aerated 316°C water.¹² They found that, when high stress and aerated environment were present, both materials cracked in the tight crevices. They also tested Alloy 600 in an oxygen-free environment. The removal of oxygen eliminated the crevice cracking. Later studies have been performed by Page in which he evaluated the behavior of Alloy 600 and Alloy 182 along with other

alloys at 288°C in 16 ppm oxygen, using slow extension rate tests (CERT).¹³ Both materials exhibited cracking only if the specimen had been creviced. This is consistent with the earlier test results. Page concluded that, as the corrosion potential was reduced consistent with reduced oxygen levels, the cracking tendency would be reduced or eliminated.

3.6.3 Evaluation of Baseline Behavior of Alloy 600 and Alloy 182 in Oxygenated High Temperature Water at GE San Jose

A significant effort has been on-going at GE to evaluate the behavior of structural materials in oxygenated BWR water. The initiation behavior of these nickel base alloys have been examined in both small specimens and in full-size pipe tests in uncreviced and creviced conditions, and in 0.2 ppm oxygen as well as 8 ppm oxygen levels in high temperature, high purity water. In general, tests similar to those performed on stainless steel have been conducted.^{14,15} In addition, crack growth studies have been performed to evaluate the rate of crack growth of initiated cracks in Alloy 600 and Alloy 182. These tests also parallel evaluations made on sensitized stainless steel. An abbreviated discussion of the SCC initiation behavior follows.

3.6.3.1 Comparison of Susceptibility of Nickel-Chrome-Iron Alloys with Sensitized Type 304 Stainless Steel

As part of surveillance programs to evaluate structural materials used in the BWR, small specimen tests as well as full-size pipe tests have been conducted on Alloy 600 and on Alloy 182 weld metal. The majority of laboratory tests were performed in 8 ppm oxygen, 288°C water, although surveillance tests have been conducted in-reactor on Alloy 600. The behavior of both materials is similar. Figure 3.6-1 displays a summary of the test results for Alloy 182 in 8 ppm oxygen, as well as the general behavior of sensitized Type 304. The comparisons are made using a stress rule index to rank the two alloys. The data clearly establishes that failure occurs earlier in the stainless steel. In 0.2 ppm oxygen environment the data is limited for Alloy 182. While Page could not initiate SCC without a crevice,

IGSCC was promoted in the 182 weld metal in full-size pipe components at high stress at GE. Figure 3.6-2 displays the test data. Pipe tests and small specimen IGSCC tests for Alloy 600 show this wrought material is significantly more resistant to crack initiation than Alloy 182.

3.6.4 Crack Growth Behavior in Oxygenated Environment

Crack growth tests have been performed on both Alloy 600 and Alloy 182 in 0.2 ppm oxygenated 288°C water as well as in hydrogen water chemistry environments.^{8,16-18} The procedures used have also been used to evaluate crack growth rates in sensitized stainless steel.¹⁹ Prior to presenting the data, some discussion of the test methods is appropriate.

3.6.4.1 Crack Growth Test Techniques

Environmental crack growth data were generated using standard 1T-WOL fracture mechanics specimens (Figure 3.6-3). Each specimen was fatigue pre-cracked, in room temperature air, to ensure that an active fatigue crack was present at the start of testing. In order to obtain the desired crack growth data in all cases but one, each specimen was provided with an in-situ transducer for remotely measuring the crack opening displacement (COD) which accompanies specimen loading. These transducers are high temperature "canned" linear variable differential transformers (LVDTs). Calibration curves, based on previous work, were used to translate the COD/load (i.e., compliance) data to crack length data.

The compliance data were automatically recorded and converted to crack length data, using an on-line, mini-computer based data acquisition system (Figure 3.6-4). This system is used in conjunction with the multi-specimen, closed loop, servo-controlled loading system also shown in Figure 3.6-4. The loading system has the capability to apply a variety of loading waveforms to a chain of up to eight test specimens. The load on the specimen chain is constantly monitored and serves as the controlling feedback variable in the loading system.

An existing GE environmental test loop was used to provide the different test environments studied (Figure 3.6-5). This loop has a high flow capability and can supply up to 10 gpm of high temperature/pressure demineralized water to any of several autoclaves. This high flow capability maximizes chances that each specimen will be subjected to a fully refreshed bulk environment condition. The loop is capable of monitoring and controlling the following water chemistry parameters: dissolved oxygen level, dissolved hydrogen level, pH, hydrogen peroxide and conductivity.

Only one series of tests was performed using bolt-loaded WOL specimens instead of actively loaded specimens. These tests were conducted in a refreshed autoclave and inspected periodically to evaluate crack growth using interim compliance measurements. These tests contributed to the 0.2 ppm oxygen data base.

3.6.4.2 Material Conditions Tested

The Alloy 600 and Alloy 182 materials have been tested in several conditions. However, the majority of crack growth tests were conducted on Alloy 600 material that was mill annealed followed by a 200-hour treatment at 750°F or on Alloy 182 that was as-deposited followed by 24 hours at 1150°F followed by 200 hours at 750°F. This was established to give the most susceptible condition. For these alloys the material mill annealed (or as deposited) processing can impart substantial sensitization. In particular, studies in Alloy 182 have demonstrated similar behavior between the as-deposited and as-deposited plus heat treatment condition.

3.6.4.3 Crack Growth Rates in 0.2 ppm O₂ High Purity, High Temperature Water

Tests have been conducted on Alloy 600, Alloy 182 and T-304 stainless steel in 0.2 ppm oxygen level at 400°F (205°C), and 550°F (288°C). Table 3.6-2 lists the environment and the associated constant growth rates for the three materials at a similar stress intensity level of $\sim 30 \text{ ksi}\sqrt{\text{in}}$. In all cases, the materials demonstrated IGSCC crack growth in the oxygenated environment.

At the lower temperature, there is some reduction in rates but the stress corrosion cracking behavior is clearly demonstrated in the oxygenated environment.

3.6.5 Crack Growth Rates in Hydrogen Water Chemistry Environments

Hydrogen additions (H_2WC) to the feedwater lead to a reduction in oxygen level in the coolant environment, thus leading to a reduction in corrosion potential and eliminating the driving force for stress corrosion cracking in both sensitized stainless steel and Ni-Cr-Fe alloys. The investigations into its effect in the IGSCC behavior of sensitized Type-304 stainless steel are extensive. Both small specimen crack growth tests, as well as pre-cracked pipe tests, have demonstrated that reduction in oxygen will arrest IGSCC.¹⁷ (see Section 3.5).

The data base for Ni-Cr-Fe alloys is not as extensive. However, the data that do exist clearly demonstrate that H_2WC environments with their associated low oxygen (~ 20 ppb O_2) arrest IGSCC. Table 3.6-3 lists the test environments and associated crack growth rates for Type-304 stainless steel, Alloy 600, and Alloy 182. Tests have been conducted at 400°F (205°C), 500°F (260°C) and 550°F (288°C).⁹

For all tests on the Type-304 stainless steel and Alloy 600, crack growth monitoring techniques substantiated no growth. For Alloy 182, compliance evaluation was only performed in the 500°F H_2WC environment where no constant load crack growth was detected. In the 550°F environment, failure of the transducer early in the test led to difficulties in evaluating continuously whether any crack growth had taken place during the constant load phase. However, examination of the final post-test crack fracture surface revealed that the extent of cracking was limited to that expected from the initial cyclic loading prior to constant load testing in H_2WC . Based on this observation, IGSCC cracking was judged to have been arrested by the H_2WC environment.

3.6.6 Summary

In order to promote stress corrosion cracking in high temperature high purity water, oxygen must be present. Reduction of oxygen to 20 ppb through hydrogen additions eliminates the conditions for either crack initiation or crack growth. The evidence of this arrest of IGSCC is extensive for sensitized Type-304 stainless steel. For Ni-Cr-Fe alloys, the available data clearly establish behavior analogous to that for stainless steel.

Of particular interest is the crack growth data. The specialized techniques needed to evaluate crack growth behavior in high temperature environments have been used to evaluate the behavior of the alloys. In the H_2O environments, studies have substantiated that reduction of oxygen to the 20 ppb level will, in turn, arrest IGSCC in Alloy 600 and Alloy 182 weld metal.

Table 3.6-1

SUMMARY OF COMPOSITION AND MECHANICAL PROPERTIES

A. TYPICAL CHEMISTRY (NICKEL BASE ALLOYS)

<u>Alloy</u>	<u>C</u>	<u>Ni</u>	<u>Cr</u>	<u>Mn</u>	<u>Fe</u>	<u>S</u>	<u>P</u>	<u>Nb + Ta</u>	<u>Ti</u>	<u>Si</u>
600	0.05	76	15	0.2	9	0.003	0.005	--	0.2	0.15
182* Weld Metal	0.04	69	15	7	8	0.005	0.010	1.75	0.43	0.44

B. MECHANICAL PROPERTIES

<u>Alloy</u>	<u>Minimum R.T. ASME Code Values</u>			<u>Typical 550°F Properties</u>		
	<u>0.2% Y.S.</u>	<u>UTS</u>	<u>Elong.</u>	<u>0.2% Y.S.</u>	<u>UTS</u>	<u>Elong.</u>
600	35	80	30	32	90	45
182	45	80	30	54	87	44

*Typically SMAW electrode material

Table 3.6-2

CRACK GROWTH RATES IN 0.2 PPM O₂, HIGH TEMPERATURE WATER
(GE COMPANY PROPRIETARY)

Table 3.6-3

CRACK GROWTH RATES IN HYDROGEN WATER CHEMISTRY ENVIRONMENTS
(GE COMPANY PROPRIETARY)

3-135

NEDD-30730

3-136

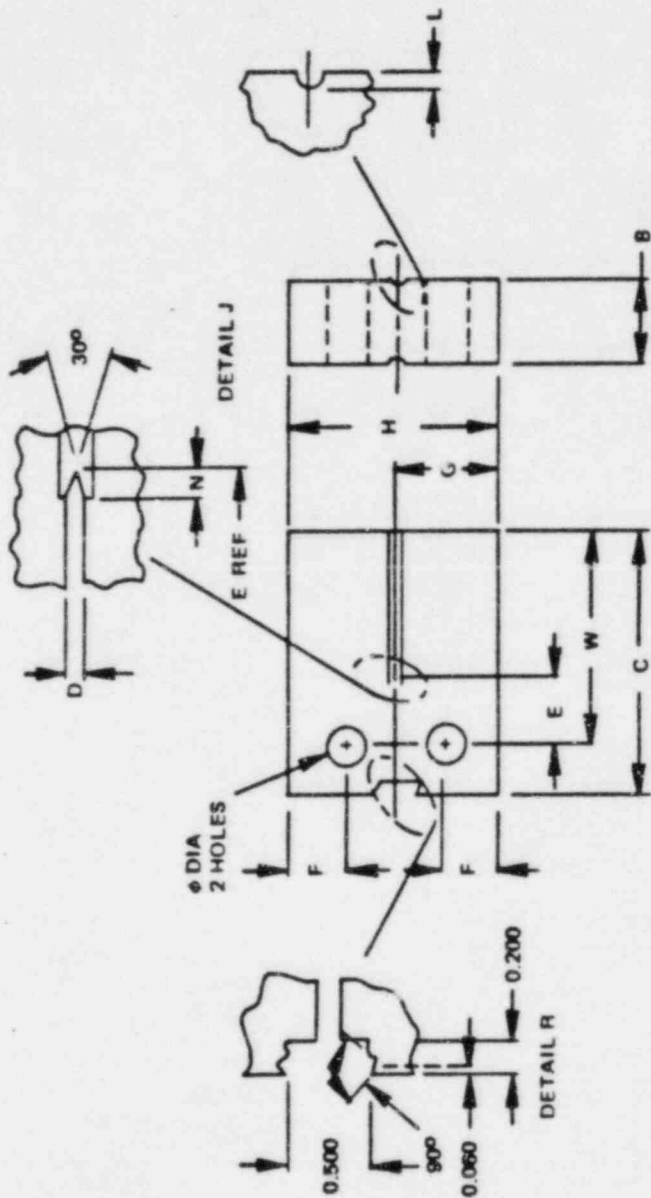
NEDO-30730

Figure 3.6-1. Stress Dependency of Materials in 288°C, 8 ppm Oxygenated Water
(GE COMPANY PROPRIETARY)

3-137

NET-0-30730

Figure 3.6-2. Pipe Test Results, 0.2 ppm O₂, 288°C
(GE COMPANY PROPRIETARY)



SPEC NO.	B	W	C	D	E	F	G	H	L	M	N	O	P	H
----------	---	---	---	---	---	---	---	---	---	---	---	---	---	---

1T-WOL	1.000±0.010	2.55	3.200	0.094	0.767	0.650	1.240	2.480	0.050	0.947	0.175±0.020	0.500 ^{+0.005} _{-0.000}	-	YES
--------	-------------	------	-------	-------	-------	-------	-------	-------	-------	-------	-------------	---	---	-----

Figure 3.6-3. WOL Specimen for Crack Growth Rate Study

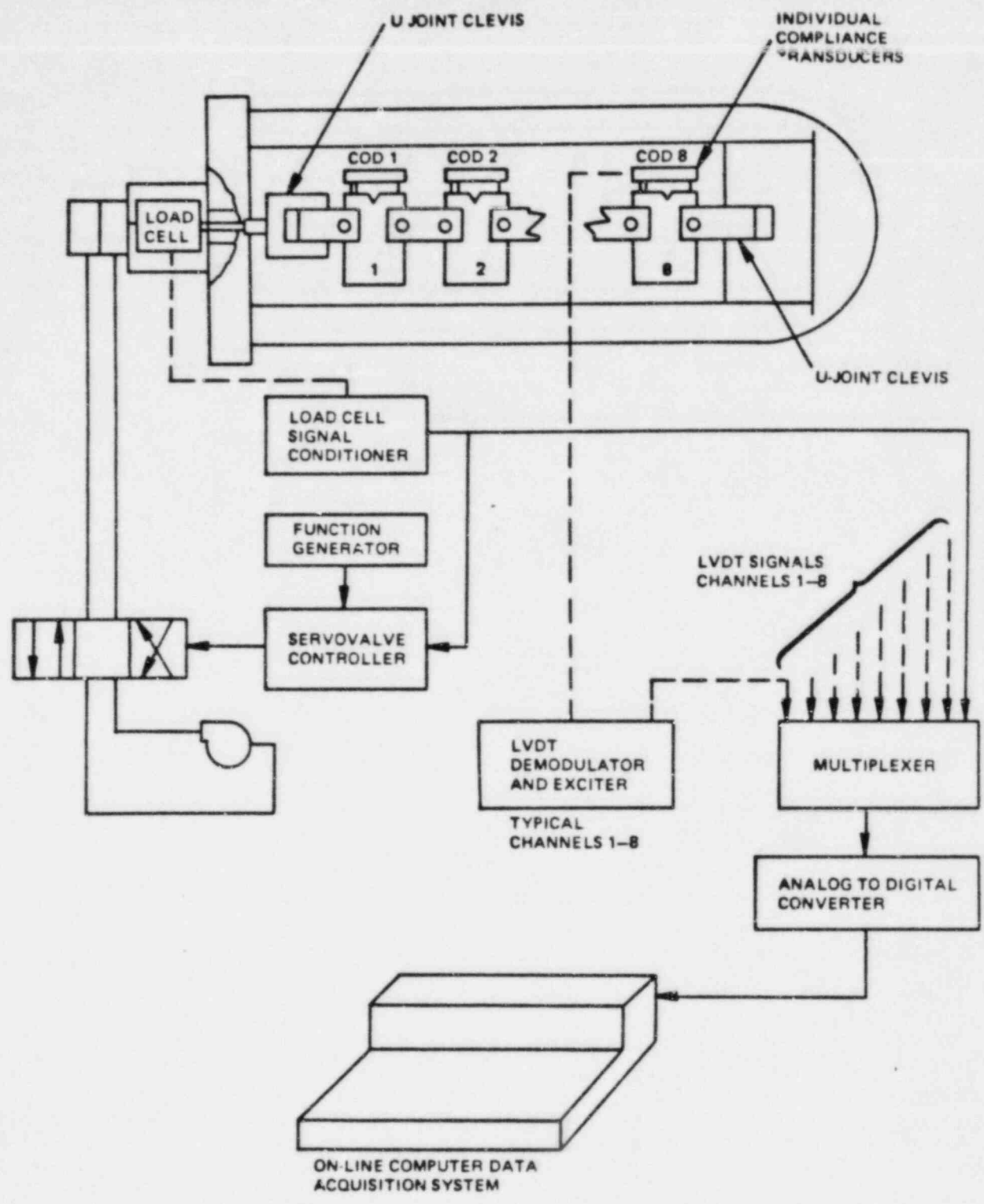


Figure 3.6-4. Schematic of Test Vessel VI, Multispecimen Environmental Test Facility

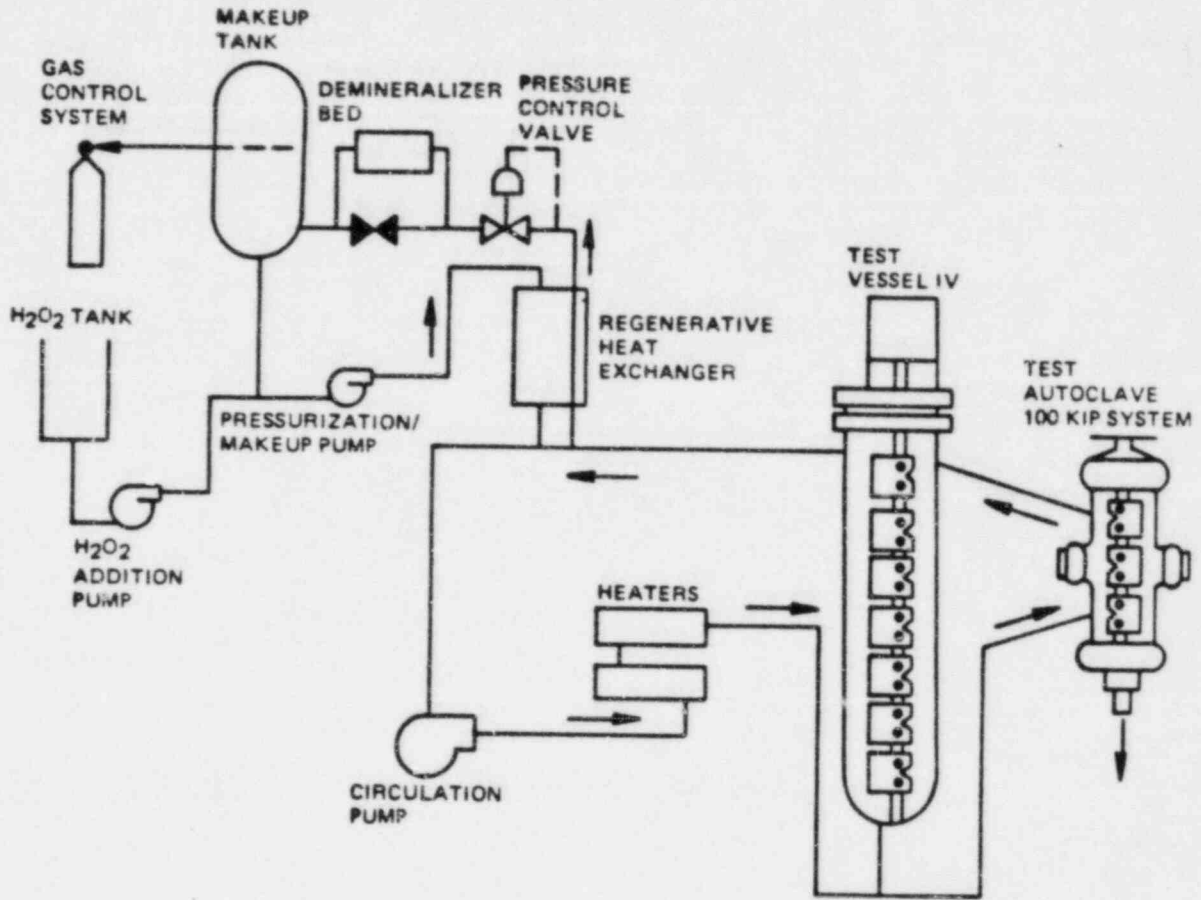


Figure 3.6-5. High Pressure/Temperature Environmental Test Loop

3.7 NOZZLE TO SAFE-END DISSIMILAR WELD INSPECTION PROGRAM

3.7.1 Introduction

The General Electric Company is currently pursuing the development of nondestructive (NDE) volumetric procedures which will reliably detect axial and circumferential cracking in dissimilar metal welds. This program is directed primarily at the examination of Alloy 182 weld metal attaching low alloy steel nozzle material to stainless steel safe-ends.

3.7.2 UT Technique Development Approach

A successful program requires mockups which are representative of the actual safe-end to nozzle dissimilar metal welds, as found in the field. The mockups must also have dissimilar metal welds which contain either machined notches, side drilled holes or induced IGSCC. Mockups which are either available or can be fabricated for this program are listed in Table 3.7-1.

Using 12 in. and 28 in. calibration blocks made from dissimilar metal welds containing ID notches and side drilled holes, a data base will be generated by scanning these blocks using conventional ultrasonic (UT) methods. These will include the use of 45°, 60° pulse-echo, shear wave 1.0, 1.5 and 2.25 MHz transducers pulsed by portable flaw detectors and large nonportable flaw detectors. Then a selection of unique UT techniques will be investigated, such as:

1. Conventional pitch/catch, 0.5 through 5 MHz at various incident angles
2. Refracted L-wave pulse-echo, 0.5 through 5 MHz at various incident angles
3. Refracted L-wave pitch/catch, 0.5 through 5 MHz at various incident angles

4. Polarized shear waves
5. Other more exotic techniques as they are identified.

In addition, computer controlled, automated techniques will be employed to incorporate state-of-the-art automated systems in the program.

For each technique a scan of each mockup will be made in the circumferential and axial direction. Data will be recorded along the length of each indication at 1/4 inch intervals or less to obtain at least 4 sets of data for each indication. Data will be input to a living matrix for each mockup to show detectability. The length and through-wall dimensions of the indications will be sized on a best effort basis.

When penetration and detection capabilities are demonstrated on mockups containing notches and side drilled holes using a certain system, that system will then go through a qualification step using mockups containing real IGSCC.

As a backup to this program, the qualification of specialized radiographic (RT) and /or a combination of RT and UT techniques will be investigated.

Note: If notches are not detected with signal amplitude \geq than 2 to 1 or some other unique signal characteristic is not identified, the test system shall not be used on other test samples containing IGSCC. In other words, a test system must demonstrate its ability to detect circumferential and axial notches within the Ni-Cr-Fe weld material before that system is applied to a sample with real IGSCC.

Table 3.7-1
 MOCKUPS FOR UT TECHNIQUE DEVELOPMENT PROGRAM

MOCKUPS AVAILABLE AT G.E. FOR THIS PROGRAM:

<u>Mockup</u>	<u>Size</u>	<u>Defects</u>
Pilgrim PIL-34	12" OD	ID notches Side drilled holes
GE (2 ea.) Cal Blocks from PIL-34	12" OD	ID notches Side drilled holes
GE Cal Block from PIL-34	12" OD	Induced IGSCC

MOCKUPS WHICH CAN BE FABRICATED BY G.E. FOR THIS PROGRAM:

<u>Mockup</u>	<u>Size</u>	<u>Defects</u>
GE Cal Block from 28" Outlet	28" OD	ID notches Side drilled holes
GE Block from 28" Outlet	28" OD	Induced IGSCC

4. THERMAL SLEEVE INDICATIONS

The ten recirculation inlet nozzles have thermal sleeves to facilitate connection to the jet pump riser pipes. The thermal sleeve assembly/safe-end configuration is shown in Figure 3.0-1. The inner and outer sleeves consist of Type 304 stainless steel and are attached to one another by a fillet weld. Shop welded pads were applied to the outside of the outer thermal sleeve to aid in alignment with the safe-end (Figures 4.0-1 and 4.0-2).

Following removal of the piping from the safe-ends, the accessible areas of the thermal sleeve were examined and found acceptable. However, subsequent dye penetrant (PT) examinations revealed intermittent cracking on the outer thermal sleeve O.D. Based on a conservative analysis of crack growths during the interim period until hydrogen water chemistry (H₂WC) is implemented, Boston Edison Company has elected not to repair the thermal sleeves during the pipe replacement outage.

This section presents the results of the nondestructive examinations of the thermal sleeves, the residual stress analysis and the structural integrity evaluation. In addition, justification is provided for continued operation without thermal sleeve repair.

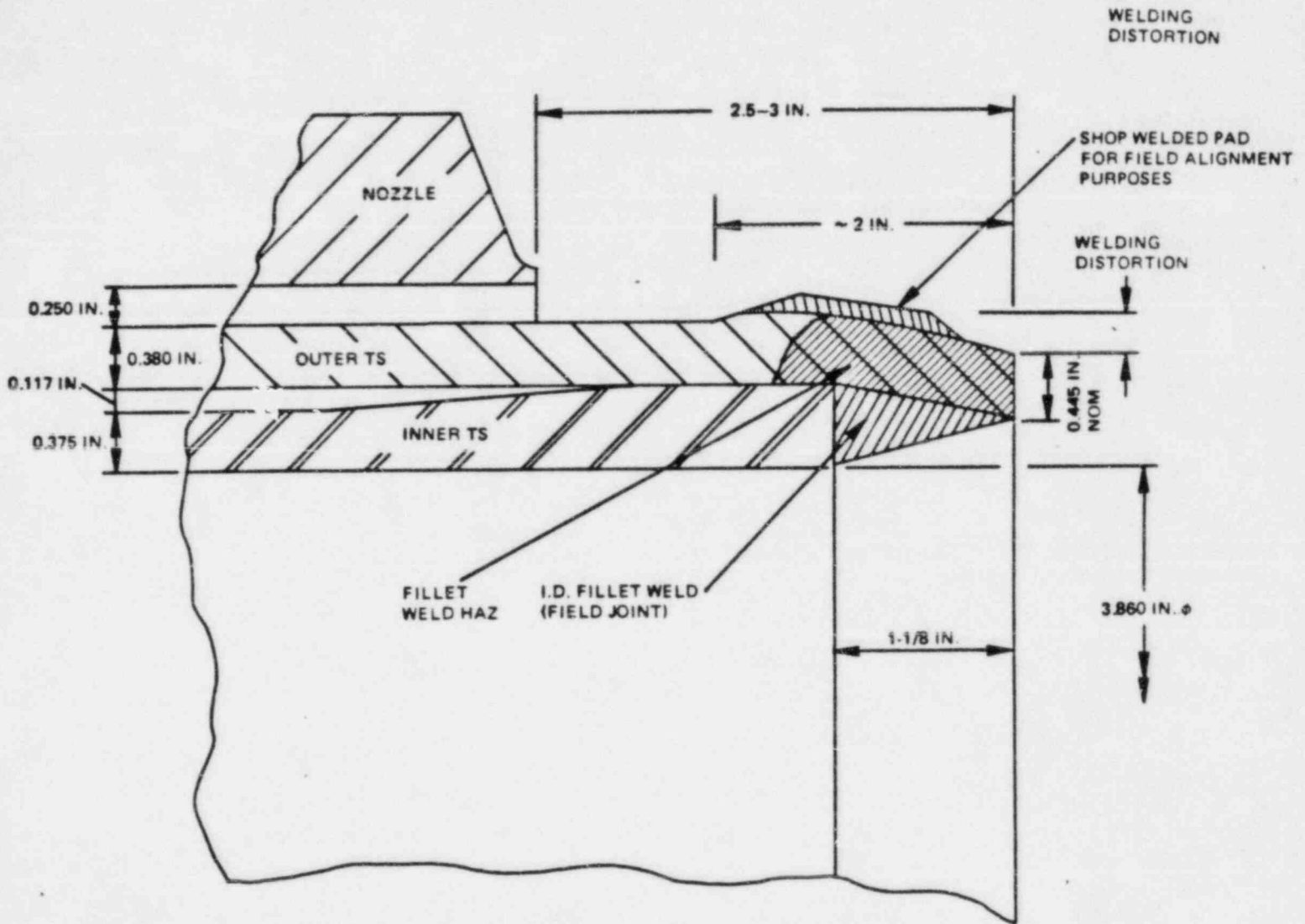
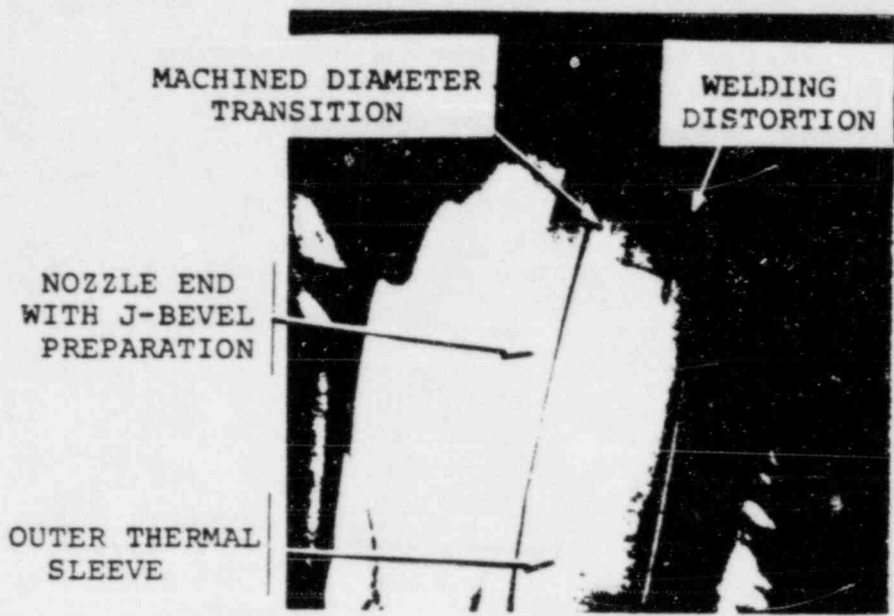


Figure 4.0-1. Cross-section of Pilgrim Recirculation Inlet Thermal Sleeve/Nozzle at Alignment Pad Locations

NOZZLE N2-E
(SIDE VIEW)



NOZZLE N2-E
(TOP VIEW)



Figure 4.0-2. Thermal Sleeve Pad Configuration and Welding Distortion

4.1 NON-DESTRUCTIVE EXAMINATION RESULTS

Liquid penetrant (PT) examination of accessible areas of the Type 304 stainless steel thermal sleeves revealed linear indications in seven of the eight thermal sleeves examined. The indications were located in the sensitized material near the pad and the fillet weld heat affected zones (HAZ). The lengths were typically between 0.25 and 1.0 inches.

Radiographic (RT) examination was used to confirm the PT results and to aid in the determination of the extent of cracking. The RT results showed no indications in the inner thermal sleeves. However, one indication was found by RT in each of the two outer thermal sleeves not examined by PT. These indications were also associated with the sensitized zone near the pad and fillet weld. Thus, non-destructive examination (NDE) identified limited cracking in nine of the ten recirculation inlet nozzle thermal sleeves.

The thermal sleeve NDE results are summarized in Table 4.1-1. The PT and RT cracking maps are provided in Appendix J.

Table 4.1-1
THERMAL SLEEVE NDE

	<u>UT TS/TS Weld</u>	<u>PT OD Cracks (Number)</u>	<u>PT ID</u>	<u>PT FACE</u>	<u>RT Cracks (Number)</u>	<u>UT TS/Noz Weld</u>	<u>Remarks</u>
N2-A	OK	7	OK	OK	1	OK	Cracks in HAZ
N2-B	OK	0	OK	OK	0	OK	
N2-C	OK	4	OK	OK	4	OK	Cracks in HAZ
N2-D	OK	3	OK	OK	3	OK	Cracks in HAZ
N2-E	OK	11	OK	OK	7	OK	Cracks in HAZ
N2-F	OK	4	OK	OK	3	OK	Cracks in HAZ
N2-G	OK	1	OK	OK	0	OK	Cracks in HAZ
N2-H	OK	Not Done	OK	OK	1	OK	Cracks in HAZ
N2-J	OK	7	OK	OK	7	OK	Cracks in HAZ
N2-K	OK	Not Done	OK	OK	1	OK	Cracks in HAZ

4.2 RESIDUAL STRESS ANALYSIS OF THE THERMAL SLEEVE FILLET WELD

A residual stress analysis was performed to determine the stresses resulting from the thermal sleeve fillet weld. Figure 3.0-1 shows the Pilgrim thermal sleeve configuration. For the purposes of analysis, the nozzle/safe-end and the effect of the weld pad were not included in the axisymmetric analysis described here. The analysis considered a single pass weld only whereas the actual weld included multiple passes and showed much higher shrinkage (approximately 1/4-in. radial) than that expected in a single pass weld. Thus, the results presented here underestimate the actual residual stress magnitudes. Nevertheless, the results describe the general trend and explain the observed cracking.

The residual stress analysis consists of two parts: (i) thermal analysis to determine the temperatures following the weld deposit, (ii) elastic-plastic stress analysis to determine the final stress after cooldown. The analysis assumes axisymmetric conditions. Even though this does not consider the three dimensional nature of the welding process, the axisymmetric predictions have been shown to be in good agreement with experimental results.

4.2.1 Thermal Analysis

The finite element computer code ANSYS (Reference 1) was used to develop an axisymmetric model to simulate the Pilgrim recirculation inlet nozzle thermal sleeve. The isoparametric heat conduction element STIF 55 is used. The same model with an isoparametric stress element was subsequently used for the stress analysis.

As in the case of the safe-end to nozzle weld thermal analysis (Section 3.2.2.2), the Nugget Area Heating (NAH) method was used to simulate the welding process by heating each node modeled in the finite element end weld to the melting temperature of the weld material and holding it at that temperature for a specified time duration. After this hold period, the nodal temperature boundary conditions are released and the thermal sleeve

cools down to ambient temperature by natural conduction. The representation of the welding process is shown in Figures 4.2-1 and 4.2-2. The environment surrounding the thermal sleeve is air retained at 70°F throughout the welding process. Heat transfer through the annulus between the two thermal sleeves was judged to be insignificant and was not included in the analysis.

The temperature distribution is determined at several times following the weld deposit. Isotherms at different times throughout the transient are shown in Figures 4.2-3 through 4.2-8. These figures graphically describe the change in the thermal sleeve temperature gradient as time progresses. Each isotherm represents a temperature gradient of 100°F. These isotherms clearly indicate that the end of the thermal sleeve, in the region of the weld, is quickly heated to 2500°F, resulting in a steep temperature gradient. As the thermal sleeve returns to ambient temperature the region of the weld is gradually cooled by conduction horizontally through the thermal sleeve away from the weld region. As shown in Figure 4.0-1, the temperature changes and the associated stresses result in significant permanent deformation.

4.2.2 Stress Analysis

Results of the thermal analysis were applied to the finite element model to determine the residual stresses. The isoparametric stress element STIF 42 was used in the stress analysis. The thermal sleeve was modeled as an axisymmetric finite element mesh. As shown in Figure 4.2-9, the nodes at the end of the outer thermal sleeve are fixed to simulate the attachment to the nozzle while the nodes at the end of the inner thermal sleeve are coupled in the Y-axis direction to simulate plane strain. A full 13.81-in. of the thermal sleeve was modeled for two reasons. The first was to model the sleeve up to the place of attachment to the nozzle. The second was to avoid the influence of end effects on the stresses where the yielding occurs (approximately the first two inches of the thermal sleeve). This is done by assuring that the length of the thermal sleeve model is at least $3\sqrt{Rt}$, where R is the radius and t is the thickness of the thermal sleeve.

Elastic-plastic analysis was performed based on the von Mises yield criterion and the Prandtl-Reuss equations. Subsequent yielding was evaluated using a kinematic hardening model and a bilinear temperature dependent stress-strain curve.

The nodal temperature time history from the thermal analysis was provided as input to the stress analysis model. Sufficiently small time steps were chosen to assure numerical convergence and to provide a proper description of the cyclic thermal loading.

The analysis simulated a single pass welding operation and predicted significantly lower shrinkage than that observed in the thermal sleeve. Analysis using multipass welding would have predicted better agreement on deflections. However, comparison with test data has shown that even with the single pass analysis the predicted weld residual stresses are in good agreement with the measured values.

The resulting stress distribution on the outside surface of the outer thermal sleeve is shown in Figure 4.2-10.

The observed circumferential cracking is in the general area where the high axial stresses were noted. Although the maximum stress location does not necessarily coincide with the actual crack areas, the local weld residual stress and additional stiffness due to the weld pad is likely to move the high stress location closer to the weld pad where cracking has been observed. Figure 4.2-11 shows the through-wall axial stress distribution in the outer thermal sleeve.

Since other membrane stresses in the sleeve are negligible, IGSCC crack growth is likely to slow down as the crack tip moves into the compressive stress region. Thus it is expected that the observed cracks are part through-wall cracks with a remaining uncracked ligament.

This is consistent with the fact that no axial cracks have been found during inspection.

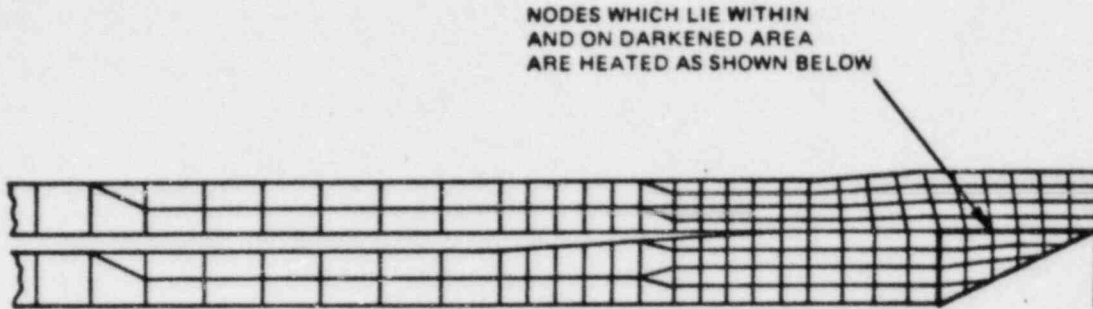


Figure 4.2-1. Nuggett Area Modelling

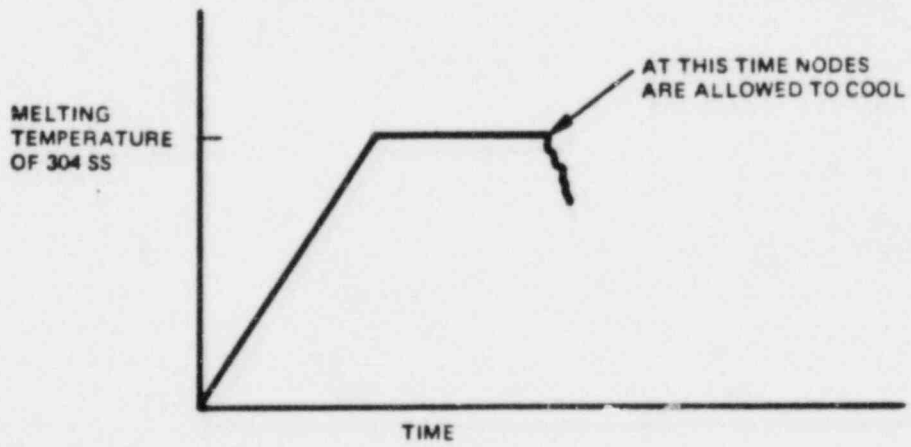


Figure 4.2-2. Nuggett Area Heating Temperature History

Figure 4.2-3. Isotherms at Time = 5 Seconds
(GE COMPANY PROPRIETARY)

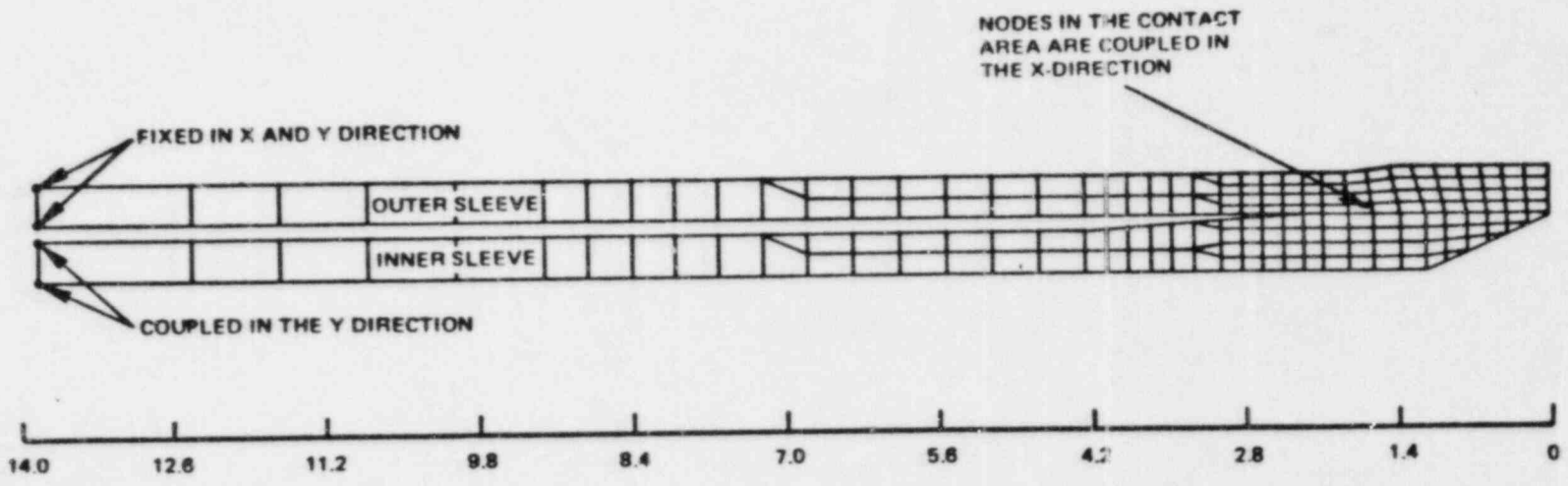
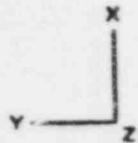
Figure 4.2-4. Isotherms at Time = 9 Seconds
(GE COMPANY PROPRIETARY)

Figure 4.2-5. Isotherms at Time = 12 Seconds
(GE COMPANY PROPRIETARY)

Figure 4.2-6. Isotherms at Time = 25 Seconds
(GE COMPANY PROPRIETARY)

Figure 4.2-7. Isotherms at Time = 70 Seconds
(GE COMPANY PROPRIETARY)

Figure 4.2-8. Isotherms at Time = 192 Seconds
(GE COMPANY PROPRIETARY)



4-12

NED0-30730

Figure 4.2-9. Pilgrim Recirculation Inlet Nozzle Element Mesh

Figure 4.2-10. Calculated Residual Stress Due to End Weld
(GE COMPANY PROPRIETARY)

Figure 4.2-11. Calculated Through-Wall Residual Stress
Due to End Weld Outer Sleeve
(GE COMPANY PROPRIETARY)

4.3 STRUCTURAL INTEGRITY OF THE THERMAL SLEEVE

The effect of the observed cracking on the structural integrity of the thermal sleeve is evaluated in this section. The cracking is predominantly in the vicinity of the four weld pads which are located at 45° to the vertical vessel axis. Therefore the effect on the structural margin of the vessel can be determined by considering four separate cracks located symmetrically at 45° to the vessel axis. While this is a realistic description of the cracking an alternate premise that assumes one long continuous crack provides a lower bound safety margin. The two assumptions are evaluated separately in this section.

Primary loads on the thermal sleeve include the seismic and hydraulic loads on the sleeve and the stresses due to differential pressure. The primary stresses in the thermal sleeve and the safety margins in the cracked thermal sleeve are described in the following paragraphs.

4.3.1 Applied Loading

Stresses in the thermal sleeve are mainly due to hydraulic loads and seismic loads at the end of the inside thermal sleeve. Pressure stresses are negligible since the pressure is the same on both sides of the thermal sleeve. Pressure fluctuations are small and are unlikely to cause crack growth. All loads were obtained from the Pilgrim design report. The stresses in this region are as follows:

The membrane stress (σ_m) due to the axial force is compressive since the hydraulic force tends to close the indication in the outer sleeve.

$$\sigma_m = -1.0 \text{ ksi}$$

The bending stress is due to the applied moment (including seismic and hydraulic and the effect of the axial force due to the pressure in the riser):

$$\sigma_b = 8.30 \text{ ksi}$$

The calculated primary stresses were used in computing the allowable flaw parameters for the thermal sleeve.

4.3.2 Allowable Flaw Parameters Assuming Four Separate Indications

As described earlier, four separate indications (corresponding to the location of the pads) were assumed in determining the critical flaw sizes (Figure 4.3-1). The allowable flaw parameters can be determined by applying a safety margin on the conditions that define net section collapse. The general evaluation methodology is described in Reference 20. The following equation defines the crack depth and length corresponding to the limiting moment of the cracked section. The bending stress, P_b , at net section collapse is given by

$$\text{_____} \quad (4.3-1)$$

where a/t is the crack depth ratio and 2α is the crack angle corresponding to each of the cracked segments as shown in Figure 4.3-1. (Crack growth points shown in the figure are discussed in Section 4.4.) The flow stress, σ_f , can be approximated by $3 S_m$ where S_m is the ASME Code design stress intensity for the thermal sleeve material. In the above equation the effect of the compressive membrane stress is conservatively neglected. Also, to simplify the analysis, it is assumed that cracks do not carry compression. This is conservative for long cracks since the moment carrying capability of the compressive forces on the crack is ignored.

Figure 4.3-2 shows the crack size corresponding to net section collapse as well as the allowable crack length and depth for a safety factor of 3. It is seen that the total crack length of all four segments can be _____ the circumference for a through-wall crack and still maintain the ASME Code safety margin.

Clearly the inherent safety margin in the structure is demonstrated by the ability to tolerate large cracks.

4.3.3 Allowable Flaw Parameters Assuming One Continuous Indication

For the limiting case when all the cracks are sufficiently close to form one indication the evaluation from Reference 20 can be used. The following equations define the crack length and depth corresponding to net section collapse:

for $\alpha + \beta < \pi$

$$\beta = \frac{(\pi - \frac{\alpha a}{t}) - (\frac{P_m}{\sigma_f})\pi}{2} \quad (4.3-2)$$

$$P_b = \frac{2 \sigma_f}{\pi} (2 \sin \beta - \frac{a}{t} \sin \alpha) \quad (4.3-3)$$

for $\alpha + \beta > \pi$ (assume crack takes compression)

$$\beta = \frac{\pi (1 - \frac{a}{t} - \frac{P_m}{\sigma_f})}{2 - \frac{a}{t}} \quad (4.3-4)$$

$$P_b = \frac{2 \sigma_f}{\pi} (2 - \frac{a}{t}) \sin \beta \quad (4.3-5)$$

P_m is the primary membrane stress and P_b is the primary bending stress. All other parameters are defined in Figure 4.3-3. The critical flaw sizes and the flaw depth and length corresponding to a safety factor of 3 are shown in Figure 4.3-4. Even with the conservative assumption of one long crack, a through-wall crack of up to _____ can be permitted.

4.3.4 Structural Significance of the Observed Cracking

The averaged crack length (cumulative value for all cracks that are approximately in the same circumferential plane) for the indications in the different thermal sleeves is less than 6 inches. This is less than 20% of the circumference. The crack depth corresponding to the indications is not known. Based on the predicted bending residual stress it is likely that the cracks are part-through cracks. However even if it is assumed that all the indications are through-wall cracks, the total length of 20% of the circumference is well within the allowable value _____

_____ Clearly the observed indications do not pose any concerns on the integrity of the thermal sleeve.

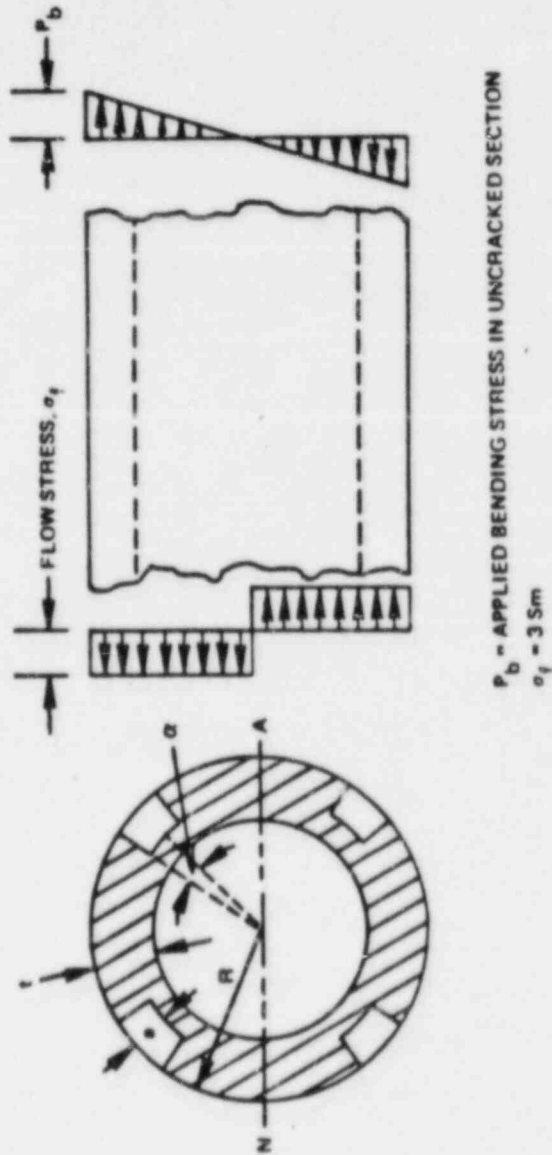


Figure 4.3-1. Crack Configuration for Four Separate Indications

Figure 4.3-2. Allowable Flaw Sizes for Pilgrim Recirculation
Inlet Thermal Sleeve (Four Separate Indications)
(GE COMPANY PROPRIETARY)

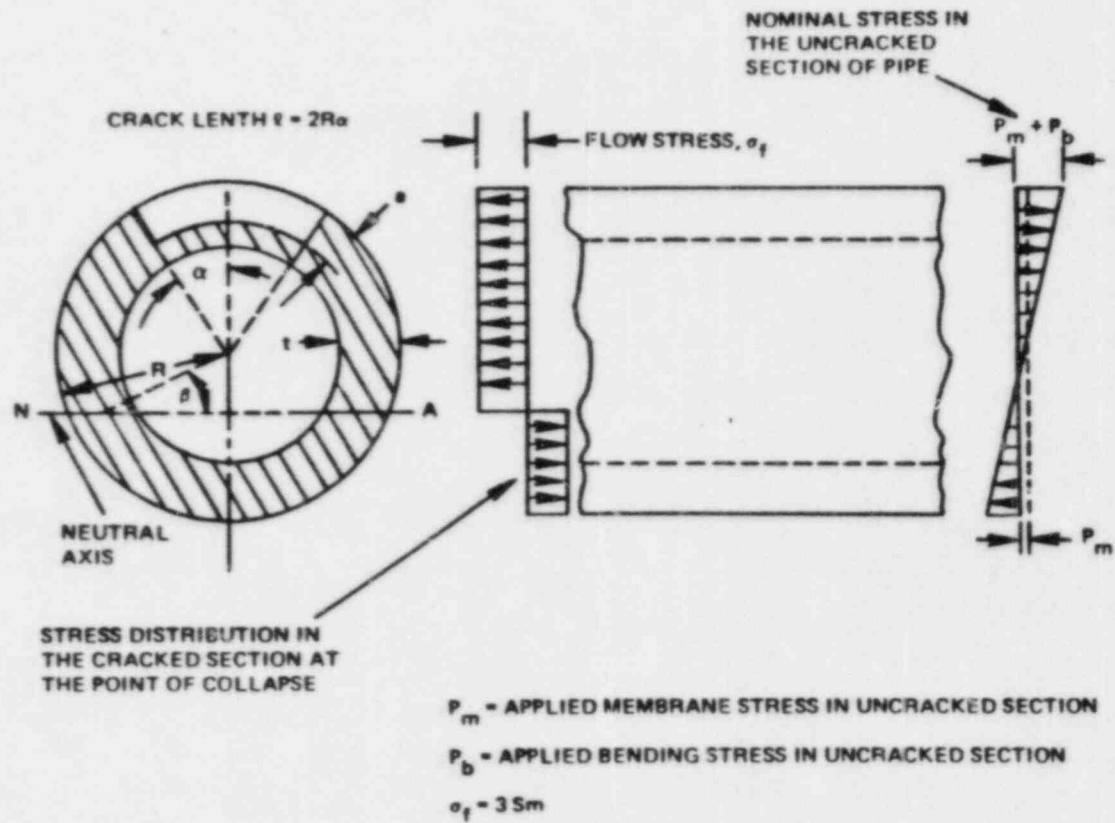


Figure 4.3-3. Crack Configuration for One Continuous Indication

Figure 4.3-4. Allowable Flaw Sizes for Pilgrim Recirculation
Inlet Thermal Sleeve (One Continuous Indication)
(GE COMPANY PROPRIETARY)

4.4 CRACK GROWTH ASSESSMENT

It is expected that hydrogen water chemistry (H_2WC) would be implemented after the next eighteen months. IGSCC crack growth is expected to be arrested after H_2WC is implemented. However, to assess the effect of potential IGSCC growth in the next 18 months before implementation of H_2WC , a conservative crack growth analysis was performed. The initial crack depth was assumed to be 20% of wall thickness and the total crack length was assumed to be 6-in. Crack growth analysis was performed using upper bound data for sensitized material in 0.2 ppm oxygenated water at 550°F (Reference 21). Stress intensity factors corresponding to the maximum calculated residual stress value of 40 ksi were used in the analysis. It should be emphasized that the predicted crack growth is extremely conservative since it assumes upper bound residual stress, upper bound crack growth rates and ignores the potential benefit of compressive radial stress between the two thermal sleeves. The crack growth results are shown in Figures 4.3-2 and 4.3-4.

This conclusion would not be changed even if a through-wall crack is initially assumed.

Thus, operation without the benefit of H_2WC for 18 months is acceptable, even with conservative crack growth projections. Once H_2WC is implemented further crack growth is suppressed and no reduction in structural capability is expected.

4.5 JUSTIFICATION FOR OPERATION WITH CRACKED THERMAL SLEEVES

Due to the limited extent of the observed cracks and the following arguments which conclude that there are no safety concerns for continued operation with the existing cracked thermal sleeves, repair of the thermal sleeves is not necessary.

4.5.1 Pressure Boundary Integrity

Thermal sleeves are not part of the primary pressure boundary. Thus, even if the cracks propagate through-wall, there would be no effect on the primary pressure boundary.

4.5.2 Thermal Sleeve Structural Integrity

The thermal sleeve structural integrity evaluation (section 4.4) concludes that the observed cracks are well within the ASME Code allowable values. Even when considering potential crack growth during the next 18 months of operation prior to implementation of H₂WC, the final crack size would not reduce the structural margin to less than that required by the Code applicable to original construction. Subsequent to H₂WC implementation, initiation and further propagation of pre-existing IGSCC will be prevented in sensitized Type 304 stainless steel (section 3.5).

4.5.3 Thermal Sleeve Leakage

Leakage due to IGSCC at either thermal sleeve weld is limited by the configuration of the thermal sleeve assembly. This leakage would probably not be detectable with the existing jet pump instrumentation. However, no significant degradation in jet pump operational characteristics would result. Furthermore, there would be no detrimental effects on the nozzle since there is an insignificant temperature difference between the incoming recirculation flow and the reactor vessel fluid.

4.5.4 Postulated Thermal Sleeve Separation

The worst case failure scenario postulates a 360° circumferential throughwall crack which results in the separation of the inner and outer thermal sleeves. Gross movement of the inner sleeve would be restrained by the restrainer gate, riser brace and shroud wall. As stated above, leakage due to the complete separation of the inner thermal sleeve would probably not be detectable. However, a secondary consideration is the potential for flow induced vibration as a result of circumferential sleeve separation. Eventually, circumferential failure of the riser piping inside the vessel is postulated to occur. However, this failure would not threaten the capability to maintain core floodability. Furthermore, the jet pump instrumentation would detect this event. Plant technical specifications identify the appropriate mitigating operator actions. No safety limits would be violated and the reactor coolant pressure boundary would not be threatened.

4.5.5 Summary

There are no safety concerns associated with continued full power operation of Pilgrim Nuclear Power Station with the currently cracked thermal sleeves. Implementation of H₂WC will ensure that sufficient margin to the ASME Code allowable limits for structural integrity is maintained.

5. REFERENCES

1. ANSYS Engineering Analysis System, Swanson Systems, Inc., March 1, 1975.
2. M. L. Herrera, H. S. Mehta, S. Ranganath, "Residual Stress Analysis of Piping with Pre-Existing Cracks Subjected to the Induction Heating Stress Improvement Treatment", ASME Paper 82-PVP-60.
3. EPRI Research Program, "Last Pass Heat Sink Welding", Final Report, Report No. NP-3479-LD, March 1984.
4. P. J. Alberry and R. D. Nicholson, "A Heat Affected Zone Computer Model Comparison of ASME III and CEGB Two Layer Refinement Procedures for BWR and PWR Cladding Repairs", CEGB RD/M/1156R81, Central Electricity Generating Board, Marchwood, U.K., June 1981.
5. Hobson, D. O., Nastad, R. K., "Effects of Off-Specification Procedures on the Mechanical Properties of Half-Bead Weld Repairs", ORNL/TM-8661, NUREG/CR-3265, July 1983.
6. J. Alexander, et al., Alternate Alloys for BWR Pipe Applications, EPRI, October 1982 (EPRI NP-2671-LD).
7. J. C. Danko, et al., "A Pipe Test Method for Evaluating the Stress Corrosion Cracking Behavior of Welded Type 304 Stainless Steel Pipes", Properties of Steel Weldments for Elevated Temperature Pressure Containment Applications, MPC-9, ASME Winter Meeting, San Francisco, California, December 1978.
8. D. A. Hale and A. E. Pickett, "Materials Performance in a Startup Environment First Semiannual Progress Report May 1981 - January 1982", NEDC-23492-1, EPRI Contract RP-1332-2, April 1982.
9. M. E. Indig and A. R. McIlree, *Corrosion*, 35 28, 1979.
10. W. L. Clarke, R. L. Cowan, and J. C. Danko, "Dynamic Straining Stress Corrosion Test for Predicting Boiling Water Reactor Materials Performance", Stress Corrosion Cracking - The Slow Strain Rate Technique. G. H. Ugiansky and J. H. Payer, Eds, ASTM 1979 (ASTM STP 665).
11. E. L. Burley, et al., "Oxygen Suppression in Boiling Water Reactors - Phase 2 Final Report", DOE/ET/34203-47 (NEDC-23856-7), October 1982.
12. H. R. Copson and G. Economy, *Corrosion*, Vol. 24, p. 55-56, 1968.
13. R. A. Page, "Stress Corrosion Cracking of Alloys 600, and 690 and Weld Metals No. 82 and No. 182 in High Temperature Water", Interim Report, EPRI NP2617, September 1982.

14. H. H. Klepfer, et al., "Cause of Cracking in Austenitic Stainless Steel Piping", NEDO-21000, General Electric Company, 1975.
15. R. M. Horn, "Parametric Studies for Stress Corrosion in Type-304 Stainless Steel Pipe", Final Report, EPRI-NP-3451, January 1984.
16. D. A. Hale, "Materials Performance in a Startup Environment", Final Report, NEDC-30676, General Electric Company, June 1984.
17. B. M. Gordon, et al., "Hydrogen Water Chemistry for Boiling Water Reactors", Interim Report, General Electric Company, NEDE-30261, September 1983.
18. B. M. Gordon, "EPRI Second Seminar on Countermeasures for BWR Pipe Cracking", paper 72, Palo Alto, CA., November 15-18, 1983.
19. R. M. Horn, et al., "The Growth and Stability of Stress Corrosion Cracks in Large Diameter BWR Piping", Final Report, EPRI 2472, July 1982.
20. Ranganath, S. and Mehta, H. S., "Engineering Methods for the Assessment of Ductile Fracture Margin in Nuclear Power Plant Piping", Proceedings of the ASTM Symposium on Elastic Plastic Fracture: Philadelphia, PA November 1981 (STP-803).
21. "The Growth and Stability of Stress Corrosion Cracks in Large Diameter BWR Piping", EPRI NP-2472 Project T118-1, Final Report, June 1982, Electric Power Research Institute, Palo Alto, CA.

APPENDICES
(COMBUSTION ENGINEERING DOCUMENTS AND
BECHTEL FIELD WELDING PROCEDURES)

APPENDIX A
COMBUSTION ENGINEERING DETAIL WELD PROCEDURE
WC-21466-345-0

COMBUSTION ENGINEERING, 7.
 MATERIALS & WELDING ENGINEERING SECTION

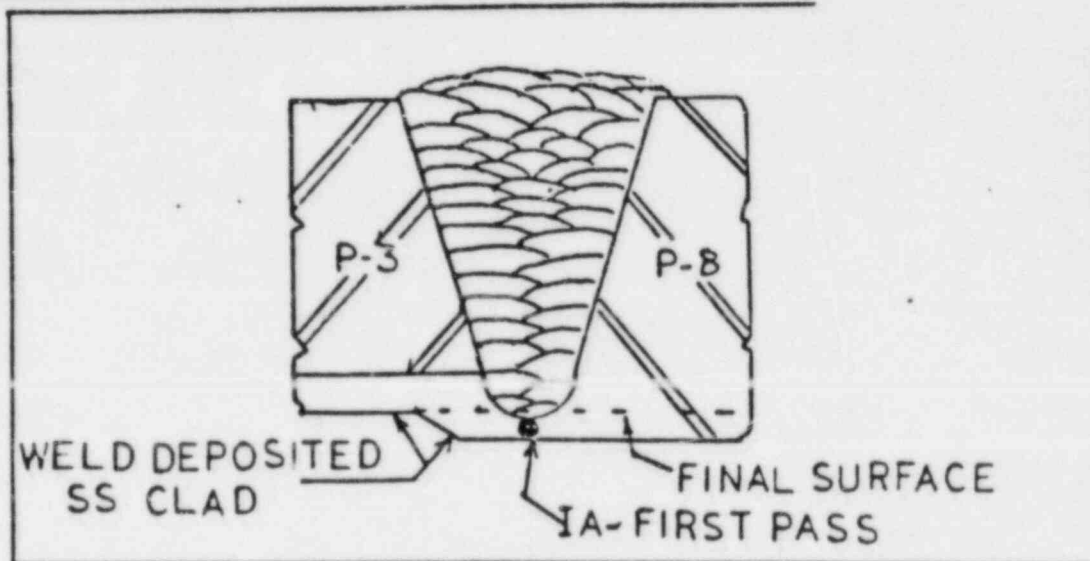
E-232-345
 Nozzle Extension Welds

DETAIL WELDING PROCEDURE
 NO.: WC-21466-345-0
 DATE: June 28, 1967

Weld No.: 3-345 A & B, 8-345 A-K, 13-345 A & B

References: M&P 4.3.8.5(b), M&P 6.1.1.2(b), IA-MA-38-6, IA-MA-38A(6)

Joint Configuration:



Welding Sequence:

	<u>Amps*</u>	<u>Volts*</u>
1st Increment - 1/16"∅ E-303 Single Pass Layer**	95 DC-SP	14
2nd Increment - 1/8"∅ Inco 182	75-105 DC-RP	24
Remainder - 5/32"∅. Inco 182	105-135 DC-RP	24

QIA-88A(3)
 QMA-3.43B(1)

Welding Position: First Pass: Horizontal
 Remainder: Flat

** Gas - Argon at 15 CFH
 Tungsten - 3/32"∅
 Cup Size - 1/4" I.D.
 Cup to Work - 1/4"

Non-Destructive Testing:

Visual:

Magnetic Particle:

Liquid Penetrant: M&P 2.4.3.9(c) (R,FF)

Ultrasonic:

Radiographic: M&P 2.4.1.3(a) (F)

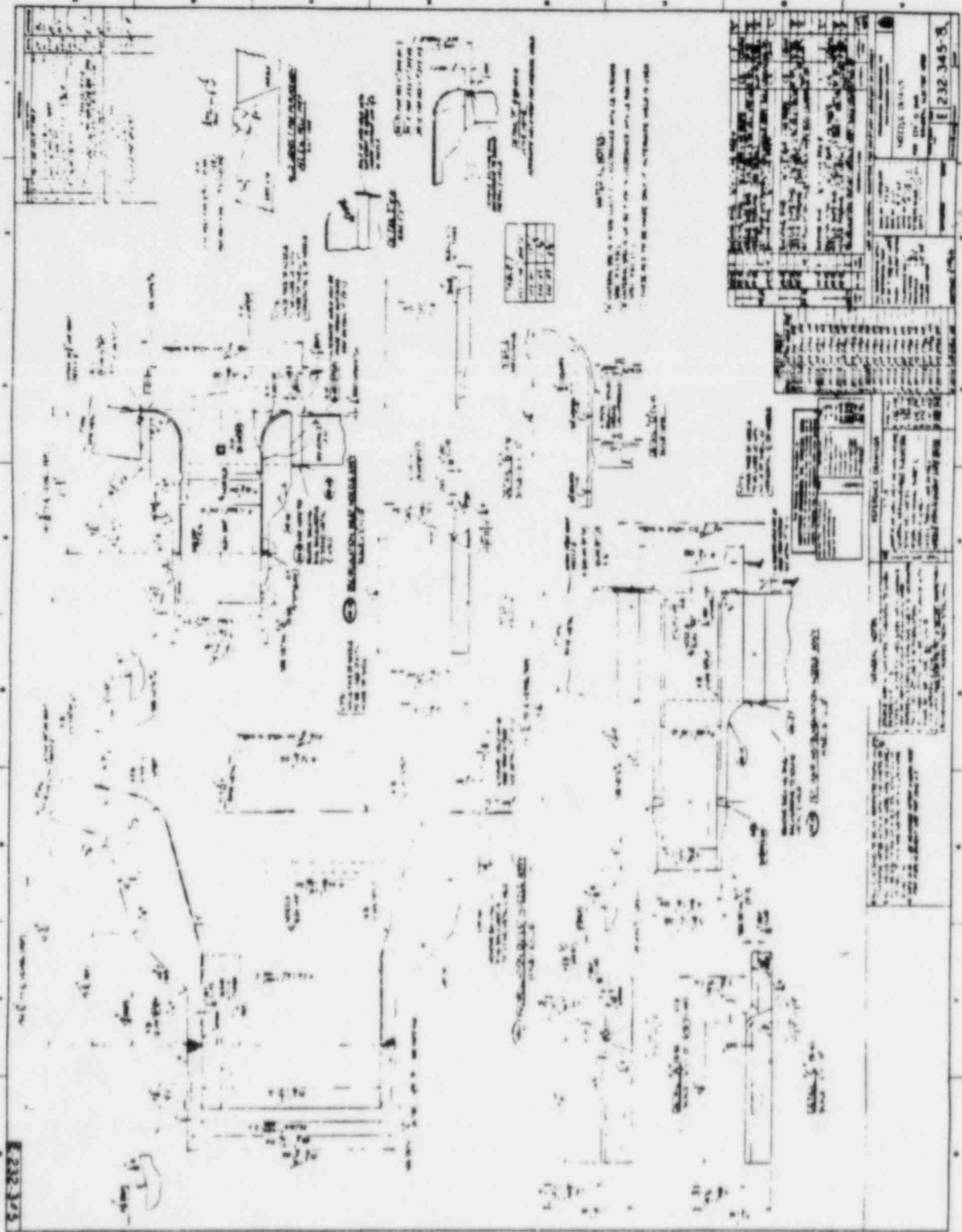
* +10% of value shown.

(P.T. of root layer
 for C.E. information)

TOLERANCES: FRACTIONS: ± ; DECIMALS: + ; ANGLES: ±

APPENDIX B

COMBUSTION ENGINEERING DRAWING E-232-345



APPENDIX C
COMBUSTION ENGINEERING DETAIL WELD PROCEDURE
WK-21466-345-1

COMBUSTION ENGINEERING, INC.
 MATERIALS & WELDING ENGINEERING SECTION

APPROVED FOR
 FABRICATION BY

V. 70095-46

E-232-345

Machining and Welding For Safe
 End Replacement Lower Shell

DETAIL WELDING PROCEDURE

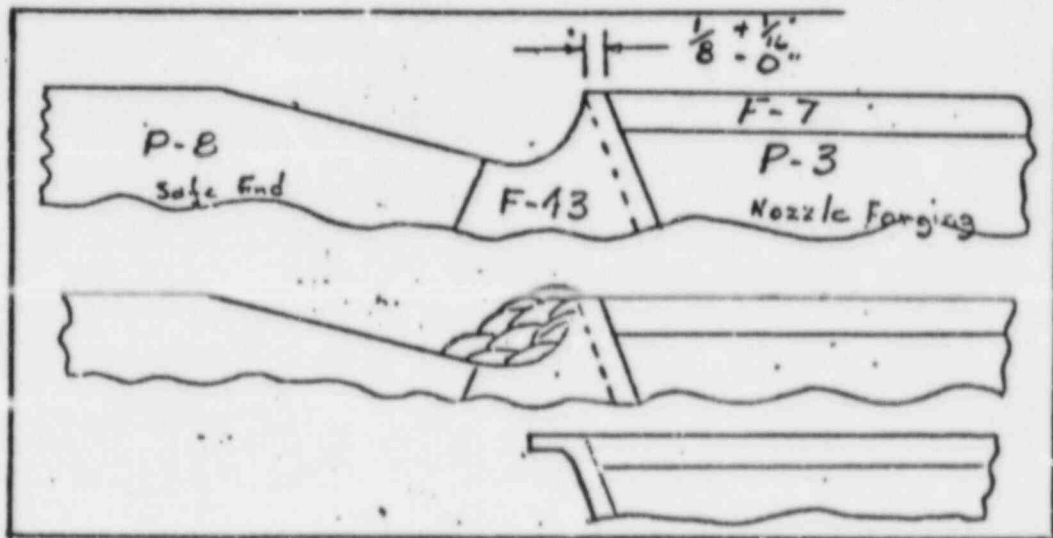
NO.: WK-21466-345-1

DATE: March 24, 1969

Weld No.: 3, 8, 22, 23 - 345

References: M&P 4.3.8.5(t), M&P 6.1.1.2(b), MA-8.43C(7), MA-8.43-2

Joint Configuration:



Welding Sequence:

1/8"Ø ENiCrFe-3(182)

Amps*

Volts*

70-100 DC-RP

24

5/32"Ø ENiCrFe-3(182)

95-125 DC-RP

24

Welding Position: Horizontal or Flat

QMA-8.43A(1)F43

Non-Destructive Testing:

Visual:

Magnetic Particle:

Liquid Penetrant: M&P 2.4.3.9(c) (FF)

Ultrasonic:

Radiographic: M&P 2.4.1.3(a) (F)

* ± 10% of value shown.

TOLERANCES: FRACTIONS: ± ; DECIMALS: + ; ANGLES: ±

NUCLEAR
 QUALITY FILE

JUN 16 1969

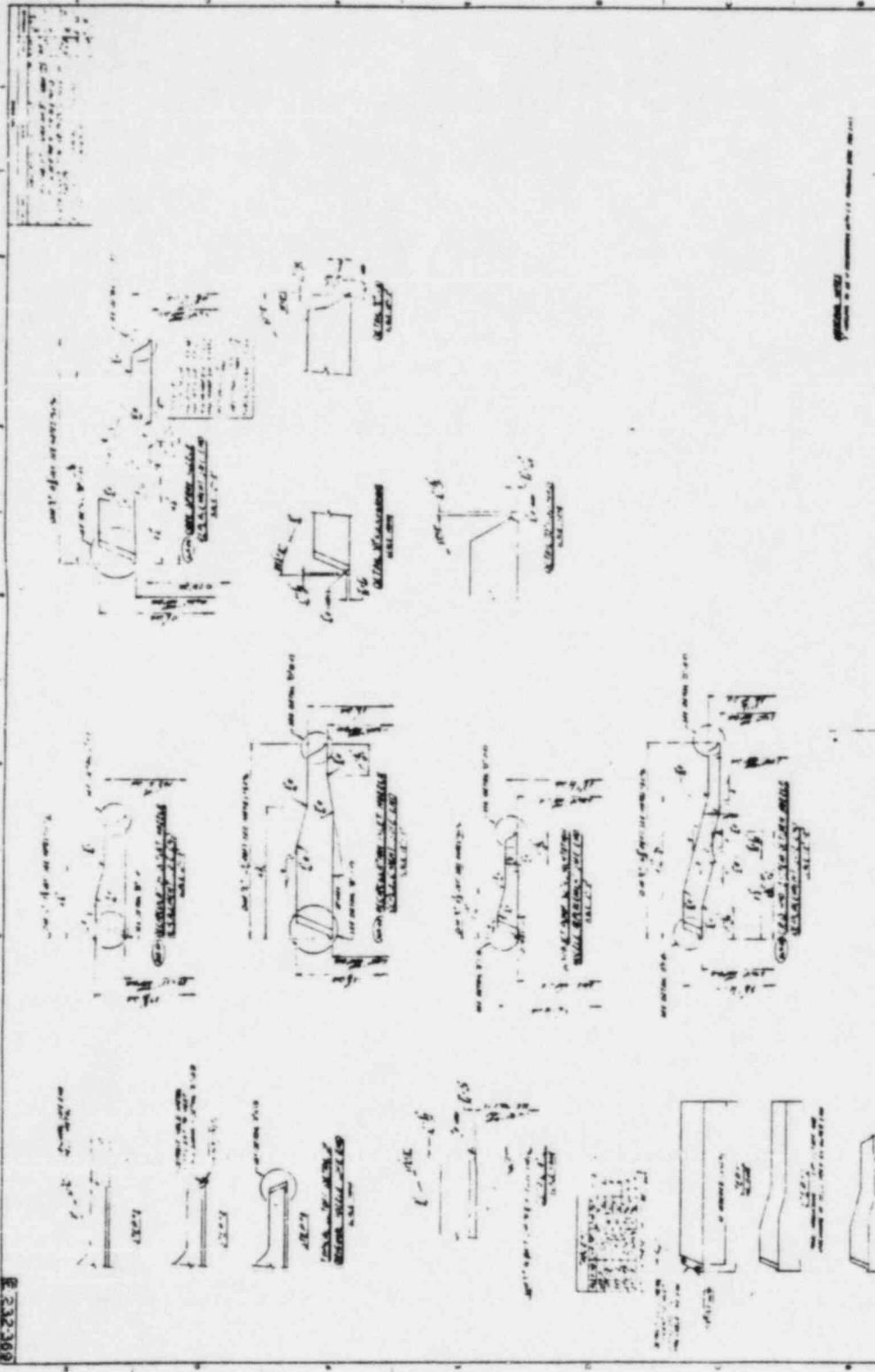
J. P. F.

NEDO-30730

APPENDIX D
COMBUSTION ENGINEERING DRAWING
E-232-369

NO. 232-380	5
DATE	
TIME	
BY	
REMARKS	
APPROVED	
CHECKED	
DESIGNED	
DRAWN	
SCALE	
SHEET NO.	
TOTAL SHEETS	

NO. 232-380	5
DATE	
TIME	
BY	
REMARKS	
APPROVED	
CHECKED	
DESIGNED	
DRAWN	
SCALE	
SHEET NO.	
TOTAL SHEETS	



232-380

APPENDIX E
COMBUSTION ENGINEERING DETAIL WELD PROCEDURE
WA-21466-369-1

COMBUSTION ENGINEERING, INC.
MATERIALS & WELDING ENGINEERING SECTION

APPROVED FOR
FABRICATION BY
V. 70195-46

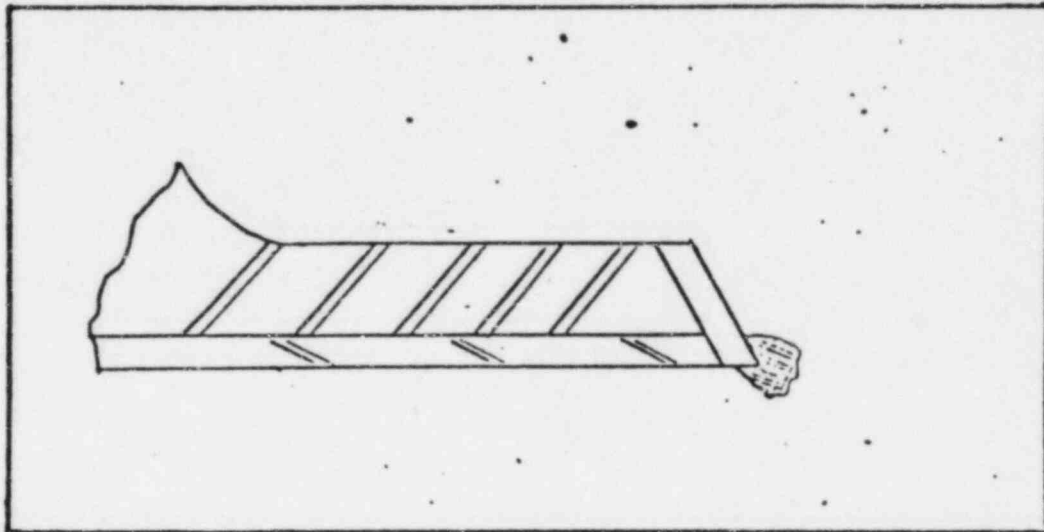
E-232-369
Weld Metal Build-up to Nozzle
Buttering

DETAIL WELDING PROCEDURE
NO.: WA-21466-369- 1
DATE: April 21, 1969

Weld No.: 1-369

References: M&P 6.1.1.2(b), MA-8.43C(5), MA-8.43-2

Joint Configuration:



Welding Sequence:

1/8"Ø Inco 182

Amps*

110

Volts*

25-27

Welding Position: Flat - Horizontal

QMA-8.43A(1)

Non-Destructive Testing:

Visual:

Magnetic Particle:

Liquid Penetrant: M&P 2.4.3.9(c) F

Ultrasonic:

Radiographic: M&P 2.4.1.3(a) F

* ± 10% of value shown.

TOLERANCES: FRACTIONS: ± ; DECIMALS: + ; ANGLES: ±

NUCLEAR
QUALITY ENG.

JUN 16 1969

J. P. F.

APPENDIX F
COMBUSTION ENGINEERING DETAIL WELD PROCEDURE
WB-21466-369-1

COMBUSTION ENGINEERING, INC.
MATERIALS & WELDING ENGINEERING SECTION

FABRICATED FOR
V-70095-47

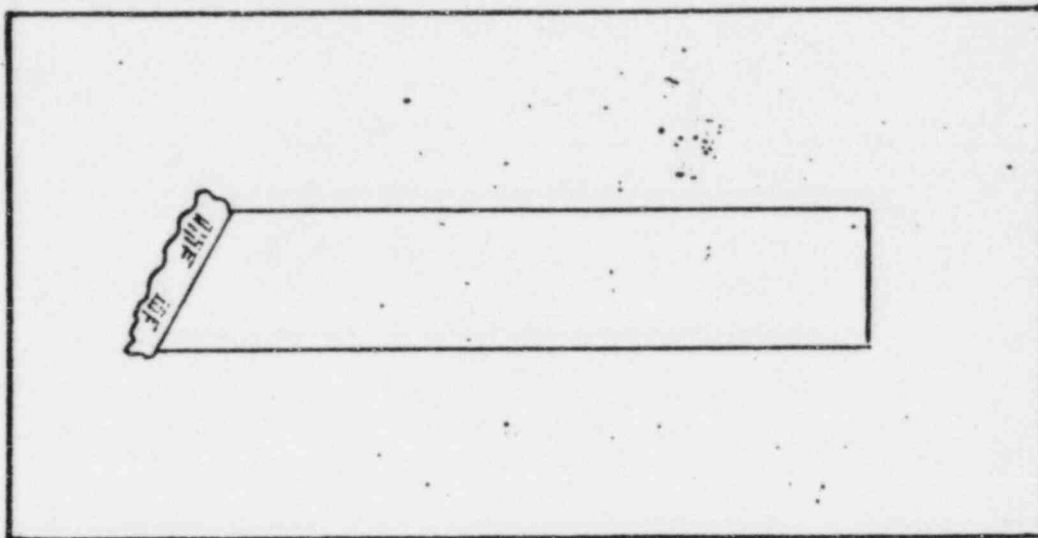
E-232-369
Safe End Weld Metal Build-up

DETAIL WELDING PROCEDURE
NO.: WB-21466-369-1
DATE: March 10, 1969

Weld No.: 2-369

References: M&P 6.1.1.2(b), MA-8.43C(5), MA-8.43-2

Joint Configuration:



Welding Sequence:

1/8"Ø Inco 182

Amps*

110

Volts*

25-27

QUALITY ENGR.

AUG 25 1969

Welding Position: Flat and Horizontal

R. A. H.
QMA-8.43A(1)

Non-Destructive Testing:

Visual:

Magnetic Particle:

Liquid Penetrant: M&P 2.4.3.9(c) F

Ultrasonic:

Radiographic: M&P 2.4.1.3(a) F

* + 10% of value shown.

TOLERANCES: FRACTIONS: ± ; DECIMALS: + ; ANGLES: ±

APPENDIX G
SPECIFICATION M&P 5.5.5.5 (a)

Specification No.: M&P 5.5.5.5(a)

Date Issued: June 26, 1969

Page 1 of 1

Issued By: Materials & Welding - NSW

PROCESS SPECIFICATION FOR THE
SOLUTION HEAT TREATING OF AUSTENITIC
STAINLESS STEEL

1.0 Scope:

- 1.1 This specification provides the requirements for solution heat treating austenitic stainless steel, Types 304, 304L, 316, and 316L.

2.0 Requirements:

- 2.1 The solution heat treatment shall be performed prior to the final machining of the material.
- 2.2 One or more thermocouples, depending on size and configuration, shall be attached to the material.
- 2.3 The material shall be placed in the furnace and the temperature shall be raised to and maintained at $1950^{\circ}\text{F} + 50^{\circ}\text{F}$ for at least 15 minutes per inch of material thickness.
- 2.4 The material shall be removed from the furnace and immediately completely immersed into ambient temperature water.
- 2.5 The material shall remain completely immersed in the water until a temperature of 600°F or lower is reached.

APPENDIX H
WELDING PROCEDURE SPECIFICATION
P12-P8-AT-Ag (F43), REVISION 1

Power & Industrial Division By _____ Manager of Engineering	BECHTEL CORPORATION WELDING STANDARD Procedure Specification PI2. P8-AT-Ag (F43) Revision 1	Metallurgical & Quality Control Services Date <u>2/2/70</u> Prepared by <u>[Signature]</u> Approved <u>[Signature]</u> G. B. Grable
--	--	---

Authorized for use on Job 6498 and only when signed by the Manager of Engineering of the Division.

1.0 SCOPE

1.1 This procedure specification is to be used for welding Inconel "battered" stainless steel safe-end piping to Inconel "battered" quenched and tempered ASTM A508 Class 2 alloy steel reactor vessel nozzles using the open-butt method with an argon internal purge. The thickness range qualified is 3/16-inch through 1-7/8-inches.

1.2 This procedure has been qualified under Section IX of the ASME Code and the ANSI Code for Pressure Piping P31.1.0 and P31.7.

2.0 PROCESS

Welding under this procedure specification shall be done using the combination Gas Tungsten-Arc and Shielded Metal process using an internal argon purge for the first two weld layers. The first three weld passes shall be made using the gas tungsten-arc process with the addition of bare filler rod (no consumable inserts). All remaining passes shall be made with the shielded metal-arc process.

3.0 BASE MATERIAL

This procedure specification shall be used only in welding ASTM A508, Class 2 to ASTM A182, Type F 304 materials whose beveled edges have been previously weld overlayed with Inconel. The overlay welding does not form a part of this procedure specification.

4.0 WELD MATERIALS

4.1 The filler metal shall conform to the F43 filler alloy number for electrodes and bare filler rod as shown in Section IX of the ASME Code.

01640 1941

- 4.2 Covered electrodes shall conform to ASTM B295 Specification for Nickel-Alloy Covered Welding Electrodes and shall be of the classification ENiCrFe-3 (Inconel IN2).
- 4.3 Bare filler rods shall conform to ASTM R304 Specification for Nickel and Nickel-Alloy Bare Welding Rods and Electrodes and shall be of the classification ERNiCr-3 (Inconel 82).
- 4.4 Electrodes that have wet or damaged coatings shall not be used.
- 4.5 All covered electrodes shall be purchased in sealed containers. Covered electrodes removed from sealed containers shall be used within four hours. Electrodes not used within four hours shall be stored in electrode storage ovens at 200° F - 350° F.
- 4.6 The bare filler rods shall be free of grease, oil or other foreign material.

5.0 WELDING

5.1 General

No welding shall be done when surfaces to be welded are wet or covered with ice. No welding shall be done when rain or snow is falling or during periods of high wind unless the work is properly protected.

5.2 Position

This procedure has been qualified for welding in all positions.

5.3 Preparation of Base Material

5.3.1 Field beveling for butt welds shall be done by machining or grinding when so required.

5.3.2 The angle of bevel, spacing and other details shall be in accordance with weld end preparation drawings included in the job specifications, and shall be essentially in accordance with Drawing No. PI2, P8-AT-Ag(F43)-1.

01648 1950



- 01648 1951
- 5.3.3 Prior to fit-up and welding, the beveled edges, root land and backside of each weld end shall be cleaned to bright, clean metal. Dirt, oil or grease shall be removed with acetone. Other foreign material shall be removed by wire brushing.
 - 5.3.4 Stainless steel brushes that have not been used on other than Inconel or stainless steel material shall be used for hand and power brushing.
 - 5.3.5 Grinding shall be done with resin bonded alumina or silicon carbide grinding wheels. No grinding shall be done with wheels previously contaminated by grinding materials other than Inconel or stainless steel.
 - 5.3.6 The weld joint shall be inspected for the presence of moisture. If moisture is present, the joint shall be dried by the use of acetone or heating with a torch to remove the moisture.
 - 5.4 Electrical Characteristics
 - 5.4.1 Gas tungsten-arc welding shall be done using a one or two percent thoriated tungsten electrode with direct current, straight-polarity (electrode negative).
 - 5.4.2 Shielded metal-arc welding shall be done using direct current, reverse-polarity (electrode negative).
 - 5.4.3 Recommended electrode sizes and values for amperage and voltage are shown on Drawing No. PI2, P8-AT-Ag(F43)-1.
 - 5.5 Gas Shielding & Purging
 - 5.5.1 The shielding gas shall be argon at 12-15 cfb through the welding torch.
 - 5.5.2 The backside of the weld joint shall be purged with a minimum of 35 cfb of argon for at least 10 minutes prior to tacking and welding.
 - 5.5.3 During tack welding and welding of the first two weld layers, the backside of the weld joint shall be purged with a minimum of 15 cfb of argon. Before the final closure of the root pass is made, the bleed hole should be opened to prevent pressure build up of the purge gas.

5.5.4 To facilitate purging the backside of the weld, purge plugs or balloons may be used as shown on Drawing No. PI2, PR-AT-Ag(F43)-2.

5.6 Technique

- 5.6.1 Clamps, welded clips, tack welds, or other appropriate means shall be used to properly align the joint for welding.
- 5.6.2 Tack welds shall be welded in full compliance with this procedure specification and, if not removed, shall be inspected visually for defects prior to starting the continuous weld.
- 5.6.3 Each weld bead shall be cleaned before depositing the next successive bead. Each weld layer shall be free of irregularities of deposit such as high spots, deep crevices, undercut, and porosity. Care must be exercised in depositing each shielded metal arc weld bead, particularly in the 4 to 8 o'clock weld area, to avoid slag entrapment. Each bead shall be ground to insure that slag has not been entrapped at the bead edge between adjacent beads or the bevel wall.
- 5.6.4 The progress of welding shall be upward for vertical welding (pipe axis horizontal). For horizontal welding (pipe axis vertical), the weld metal shall be deposited using the stringer bead technique.
- 5.6.5 Welding shall not be interrupted until at least one-third of the weld thickness is completed or 1/2-inch of weld, whichever is less.
- 5.6.6 Each weld layer shall be completed around the entire circumference of the weld groove before the succeeding weld passes are made.

5.7 Appearance of Weld

- 5.7.1 The appearance of weld beads shall be essentially as shown on Drawing No. PI2, PR-AT-Ag(F43)-1.
- 5.7.2 The width of the weld beads in vertical, flat and overhead positions should not exceed the width of six diameters of the electrode being used and the thickness of the layer should not exceed 1/8-inch.
- 5.7.3 The final weld layer shall be slightly convex and shall fuse into the surface of the base metal in such a manner as to tie in the edge of the groove on each side of the weld a minimum

01648 195



of 1/32-inch and a maximum of 1/16-inch.

5.8 Repair of Defects

5.8.1 Cracks that occur during welding shall be removed by grinding or chipping. Before welding is resumed, liquid penetrant inspection shall be used to determine that the cracks have been totally removed.

5.8.2 After welding has been completed, defects in excess of the applicable standards of acceptance detected by the inspection techniques required in the job specifications shall be removed by grinding or chipping and rewelded in full compliance with this procedure specification.

6.0 PREHEAT AND INTERPASS TEMPERATURE

6.1 A preheat temperature of 60° F minimum shall be maintained during all welding. The maximum interpass temperature shall not exceed 350° F.

6.2 Interpass temperatures shall be measured with a contact pyrometer.

7.0 POSTWELD HEAT TREATMENT

Postweld heat treatment is not required.

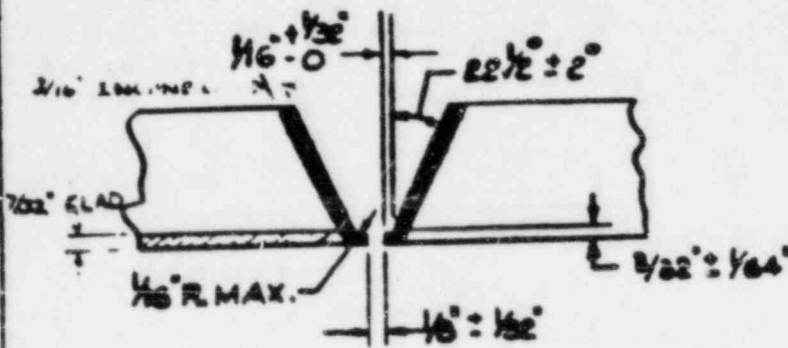
8.0 WELDER PERFORMANCE QUALIFICATION

Welders who are required to use this procedure shall be qualified in accordance with Bechtel Corporation's WELDING STANDARD WQ-NF-1, Performance Specification.

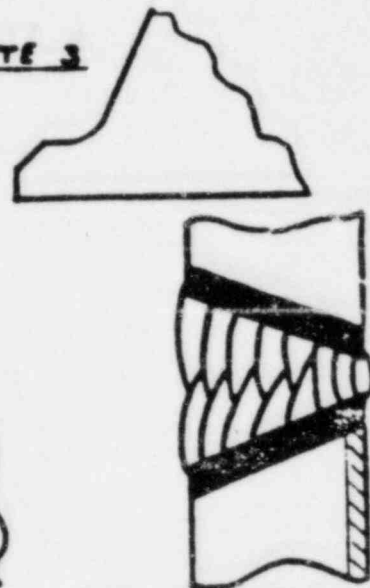
01640 - 195

No.	Date	Revision	By
1	4/1/70	Revised to include welding in all positions.	GMP
2	2/2/70	Issued for field construction	HIM

WELD BEVEL DETAILS



NOTE 3



WELD LAYER DETAILS



5G POSITION

2G POSITION

Process	Tungsten Diameter	Filler Metal Dia.	Amps (Note 4)	Volts (Note 4)
Gas Tungsten - Arc	3/32	3/32	60-110	9-14
	1/8	1/8	70-120	
Shielded Metal-Arc	----	3/32	60-100	22-25
		1/8	80-130	23-26

NOTES:

1. The first three layers shall be made by the gas tungsten-arc process. The fourth and successive layers shall be made by the shielded metal-arc process.
2. Weld layer details are illustrative only and will vary with changing wall thicknesses and size of electrodes used.
3. The top corners of the extended land shall be removed by filing for 1/2 the land thickness before fit up.
4. Actual values will be within the indicated ranges and will vary slightly with arc length.

This drawing and the design is under the property of GME. They are hereby transferred to the licensee/express agreement that they will be reproduced, copied, loaned, exhibited, or used except in the limited way and degree as provided by any written consent given by the licensor to the licensee.

4/2/70	Added 2G sketch.						GME
2/2/70	Issued for field construction						HIM
REVISIONS		BY	DATE	REV	REV	REV	REV

WELDING STANDARD
WELD BEVEL AND LAYER DETAILS

STANDARD	
FE PLAT-4-70-1	1

SIZE D 11 3 17

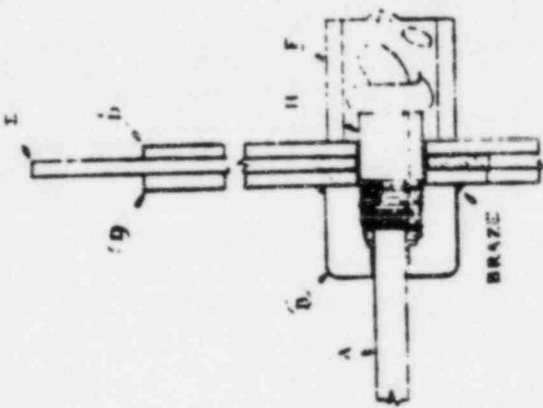
MATERIAL LIST

Item	Qty	Description
A	1	1/4 Metallic Flexible Hose - 16 long
B	2	1/4 Pipe Cap (Brass, 1/2") Steel
C	6	1/4 x 2-1/2" long Slotted Bolts Steel
D	6	Sheet Metal Discs - 1 1/2" dia. 12 ga.
E	4	1/8 Rubber Gasket Material
F	2	1/4 Pipe Coupling
G	1	1/16 4 Rod Lock (Brass 1/2") Steel
H	2	1/4 Std. Pipe - 1/2" dia. 12 ga. Steel
J	2	1 to Pulling Cable
K	2	Dust Rubber Bags - Canvas Covered
L	2	Metallic Hose Coupling
M	1	Coupling for Rubber Hose
N	1	Rubber Hose

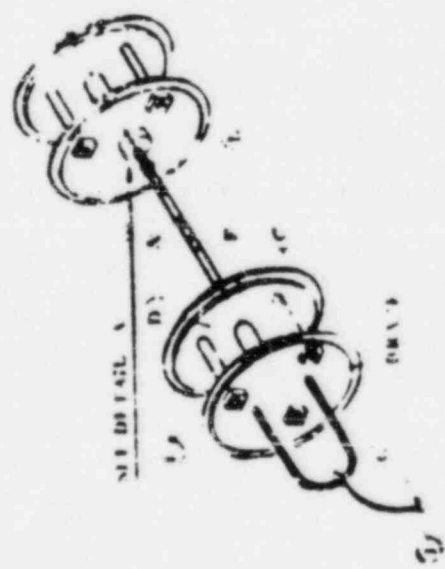
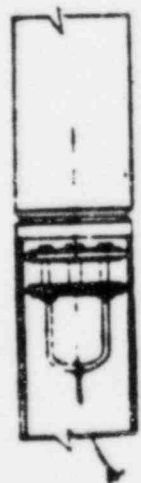
NOTES

1. Rubber discs (E) to be 1/8" larger in diameter than I.D. of pipe.
2. Metal discs (D) to be 2 smaller in diameter than O.D. of rubber disc (E).
3. Insulate bag closely with red wax, rubber pump.
4. Rubber bag to be covered with 1/2" quality canvas duck to protect from abrasive wear.
5. Disc bags to be spaced no closer than 18 inch side to side point.

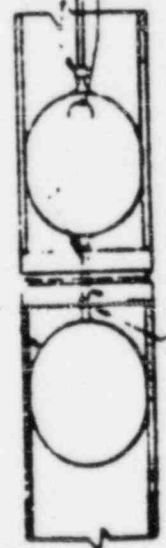
0 1 6 4 8 1 9 5 7



DETAIL A
(IF APPLICABLE)



VALVE
PRESSURE GAUGE
AIR SUPPLY



FLEXIBLE METALLIC HOSE

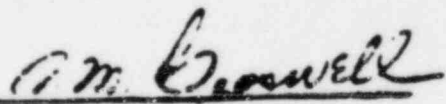
	BECHTEL CORPORATION SAN FRANCISCO, CALIF.
METALLURGY AND WELDING SECTION	
PUMP PLUG FOR MELT-ARC WELDING	
	Standard 12.18-AT-AC-132

Addendum to P12, P8-AT-Ag (F43)**Special Precautions to be Observed
During Safe End Welding**

1. Quenched and tempered ASTM A508 material shall be protected with asbestos blankets or equivalent insulation during all fit-up and welding operations. Absolutely no welding or arc strikes can be permitted on A508 material.
2. The minimum Inconel weld overlay thickness of 3/16-inch shall not be infringed by clean up operations or by grinding between safe end welding passes. Care must be taken during the deposition of the cover passes to assure that the 1/16-inch maximum base metal tie-in dimension is not exceeded.
3. Only approved tapes such as Johns Manville 357 Silver, Polyken #222, Tuck Technical Tape Style #92T Silver, or equal shall be used for holding purge dams and masking the fit up joint prior to welding.

01648 1950

February 9, 1970


A. M. Crowell
Chief Welding Engineer

BECHTEL CORPORATION
San Francisco, California

WELDING PROCEDURE QUALIFICATION RECORD

PROCEDURE SPECIFICATION NO. P12, P8-AT-Ag (F43) DATE February 16, 1970
WELDING PROCESS Gas Tungsten Arc and LOCATION San Francisco
Shielded Metal Arc California

PARENT MATERIAL QUALIFIED ON:

ASTM Spec. A508 Class II to A182 Type 304 ASME P-NO 12 to 8
Chemical Q&T Carbon Steel to 18Ni 8 Cr Stainless Steel Shape 8-inch pipe
Thickness Range Qualified 3/16-inch to 1 7/8-inches Thickness 0.938

ELECTRODE OR FILLER METAL:

ASTM Spec B 304 AWS-ASTM Class ERNiCr-3 F-No. 43 A-No None
ASTM Spec. B295 AWS-ASTM Class ENiCrFe-3 F-No. 43 A-No None
Filler Metal Chemistry (if not included in Table Q11.2) Inco 82 and Inco 182
Manufacturer, Trade Name and Wire Size Huntington Alloys Inconel 82
and Inconel 182 3/32" 0 and 1/8" 0

Flux or Shielding Gas Argon 15 cfh

JOINT DESIGN: Weld overlaid w/Inco 182

Backing Strips None
Consumable Insert None
Internal Purge Argon Flow Rate 5 cfh
Power Source DCRP (SMA) & DCSP (GTA)
1. 45° chamfer for 1/2 land thickness (i. e. 1/32-inch)

HEAT TREATMENT:

Preheat Temp. Min. 60°F Postweld Heat Treatment Temp. None
Interpass Temp. Max. 350°F P. H. T. Time - - -

TEST RESULTS		2G POSITION	2G POSITION
Reduced Section Tensile	Tensile Strength, psi	83,500	83,500
	Std. "505" bar		
Bend	Side	180° ok	180° ok
	Side	180° ok	180° ok
Other			

Mechanical Testing By Anamet Labs, Berkeley, California

Welders Name J. Miller & L. Oscarson Symbol ---

Test Conducted By H. J. Mantle

We certify that the statements in this record are correct and that the test welds were prepared, welded, and tested in accordance with the requirements of Section IX of the ASME Code.

Date 2/16/70

BECHTEL CORPORATION
By A. M. S. [Signature]
Metallurgical and Quality Control
Services Section

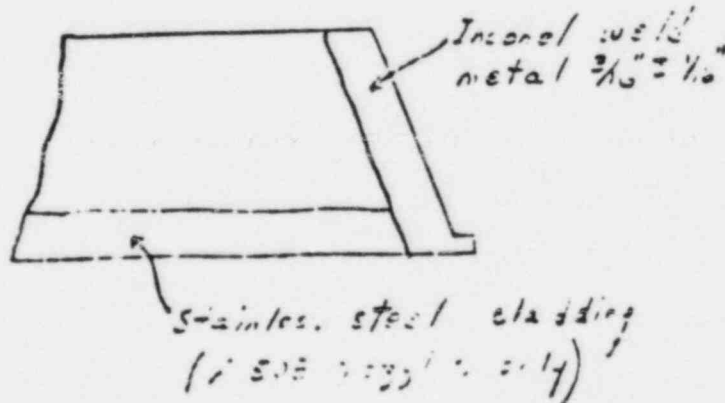
WELD-30730

ADDENDUM TO WELDING PROCEDURE

SPECIFICATION P12, P8-AT-AG-F(43)

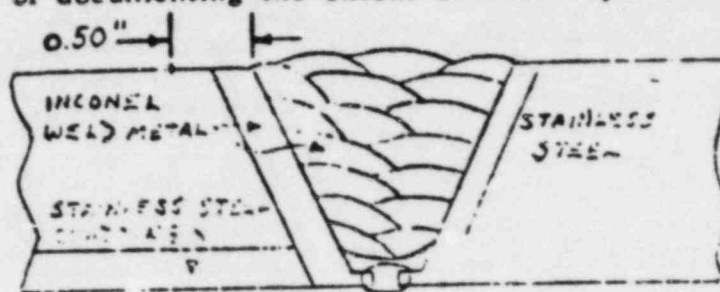
The above procedure specification as modified by this addendum shall be used for welding stainless steel safe ends to A508 nozzles on the Pilgrim Project.

1. Only approved tapes such as Johns Manville 357 Silver, Polyken #222, or equal shall be used for holding purge dams and masking the fit-up joint prior to welding.
2. Quenched and tempered ASTM A508 material shall be protected with asbestos blankets or equivalent insulation during all fit-up and welding operations. Absolutely no welding or arc strikes can be permitted on A508 material.
3. Spacer blocks made of stainless steel shall be used to properly align the joint for welding.
4. If torches are used to remove moisture, the gas used shall produce a sulfur-free flame.
5. Prior to welding, the Senior Welding Engineer shall inspect each fit-up and the filed edges of the extended land to insure that all requirements of the welding procedure have been complied with.
6. Weld joints have previously been overlayed with Inconel 600 as indicated below:



01640 1957

7. A circumferential line shall be marked with a Blunted Vibratool on the O.D. of each safe end and nozzle as indicated below for the purpose of documenting the extent of weld repairs. See paragraph 13.



8. Prior to welding, use D2 Oxygen Analyzer to insure that gas passing through the joint contains less than 1-1/2% oxygen.
9. During the welding of safe ends, the deposition of filler metal shall be closely observed at intervals by the Welding Engineer. The welding shall be performed so that the base material within 1/8 inch from the weld shall be less than 800 F, 30 seconds after the arc has passed that point.
10. The minimum Inconel weld overlay thickness of 1/8 inch shall not be reduced by clean up operations or by grinding between safe end welding passes. Care must be taken during the deposition of the cover passes to assure that the 1/16 inch maximum base metal tie-in dimension is not exceeded. The outside surface of the nozzle for the 2 inches adjacent to weld zone shall be protected from arc strikes with a stainless steel band or equivalent material and shall overlap the buttering to within a minimum of 1/16 inch of the weld groove. The open end of the safe end shall be closed to prevent fumes and other contaminants from entering the vessel.
11. For all welds except the CRD hydraulic system return and the jet pump instrument penetration seal, liquid penetrant inspection shall be conducted on exposed ID and OD surfaces after third TIG weld pass. All finished welds shall also be liquid penetrant inspected. The CRD hydraulic system return shall be radiographed after the third TIG pass, since a pre-installed thermal sleeve prevents the above liquid penetrant inspection. The jet pump instrument penetration seal weld shall be liquid penetrant inspected on the exposed OD surface after the third T. I. G. pass.
12. For the purpose of quality control, radiography may be used only as specifically directed by the Chief Welding Engineer, SFHO before completion of welding. All welds after completion shall be radiographed.
13. All repairs shall be approved and witnessed by the Senior Welding

Engineer. Prior to welding, the amount of overlay removed shall be determined using the circumferential lines marked on the OD of each component. No more than 1/16" depth of Inconel overlay shall be removed under any circumstances. A complete record of all repairs shall be maintained.

By A. M. Maxwell
Chief Welding Engineer

Date: 9/22/70

01643 1961

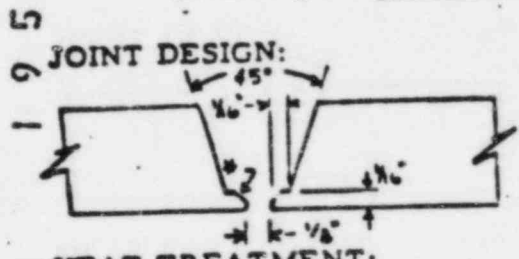
BECHTEL CORPORATION
San Francisco, California

WELDING PROCEDURE QUALIFICATION RECORD

PROCEDURE SPECIFICATION NO. P12, P8-AT-AE (F43) DATE February 16, 1970
WELDING PROCESS Gas Tungsten Arc and LOCATION San Francisco
Shielded Metal Arc California

PARENT MATERIAL QUALIFIED ON:
ASTM Spec. A508 Class II to A182 Type 304 ASME P-NO 12 to 8
Chemical Q & T Carbon Steel to 18Ni 8Cr Stainless Steel Shape 8-inch pipe
Thickness Range Qualified 3/16-inch to 1 7/8-inches Thickness 0.938

ELECTRODE OR FILLER METAL:
ASTM Spec B 304 AWS-ASTM Class ERNiCr-3 F-No. 43 A-No None
ASTM Spec B 295 AWS-ASTM Class E, NiCrFe-3 F-No. 43 A-No None
Filler Metal Chemistry (if not included in Table Q11.2) Inco 82 and Inco 182
Manufacturer, Trade Name and Wire Size Huntington Alloys Inconel 82
and Inconel 182 3/32" and 1/8" ϕ
Shielding Gas Argon 15 cfh



Backing Strips None
Consumable Insert None
Internal Purge Argon Flow Rate 5 cfh
Power Source DCRP(SMA) & DCSP (GTA)
* 45° chamfer for 1/2 land thickness (i. e. 1/32-inch)

3
4
6

HEAT TREATMENT:
Preheat Temp. Min. 60° F Postweld Heat Treatment Temp. None
Interpass Temp. Max. 350° F P. H. T. Time - - -

TEST RESULTS.		5G POSITION	5G POSITION
Reduced Section Tensile	Tensile Strength, psi	81,000	80,800
	Std. "505" bar		
Bend	Side	180° ok	180° ok
	Side	180° ok	180° ok
Other	None		

Mechanical Testing By Anamet Labs Berkeley, Lab No. 270.215
Welders Name Robert Wood Symbol - - -
Test Conducted By H. J. Mantle

We certify that the statements in this record are correct and that the test welds were prepared, welded, and tested in accordance with the requirements of Section IX of the ASME Code.

Date 2/16/70

BECHTEL CORPORATION
By A. M. Brewell
Metallurgical and Quality Control Services

APPENDIX I
HALF-BEAD HARDNESS TESTING RESULTS

I-1

NEEO-30730

Figure I-1. Hardness Test Results
(GE COMPANY PROPRIETARY)

Figure I-2. Hardness Test Results
(GE COMPANY PROPRIETARY)

Figure I-3. Hardness Test Results
(GE COMPANY PROPRIETARY)

Figure I-4. Hardness Test Results
(GE COMPANY PROPRIETARY)

Figure I-5. Hardness Test Results
(GE COMPANY PROPRIETARY)

Figure I-6. Hardness Test Results
(GE COMPANY PROPRIETARY)

I-7

NEDO-30730

Figure I-7. Hardness Test Results
(GE COMPANY PROPRIETARY)

Figure I-8. Hardness Test Results
(GE COMPANY PROPRIETARY)

Figure I-9. Hardness Test Results
(GE COMPANY PROPRIETARY)

I-10

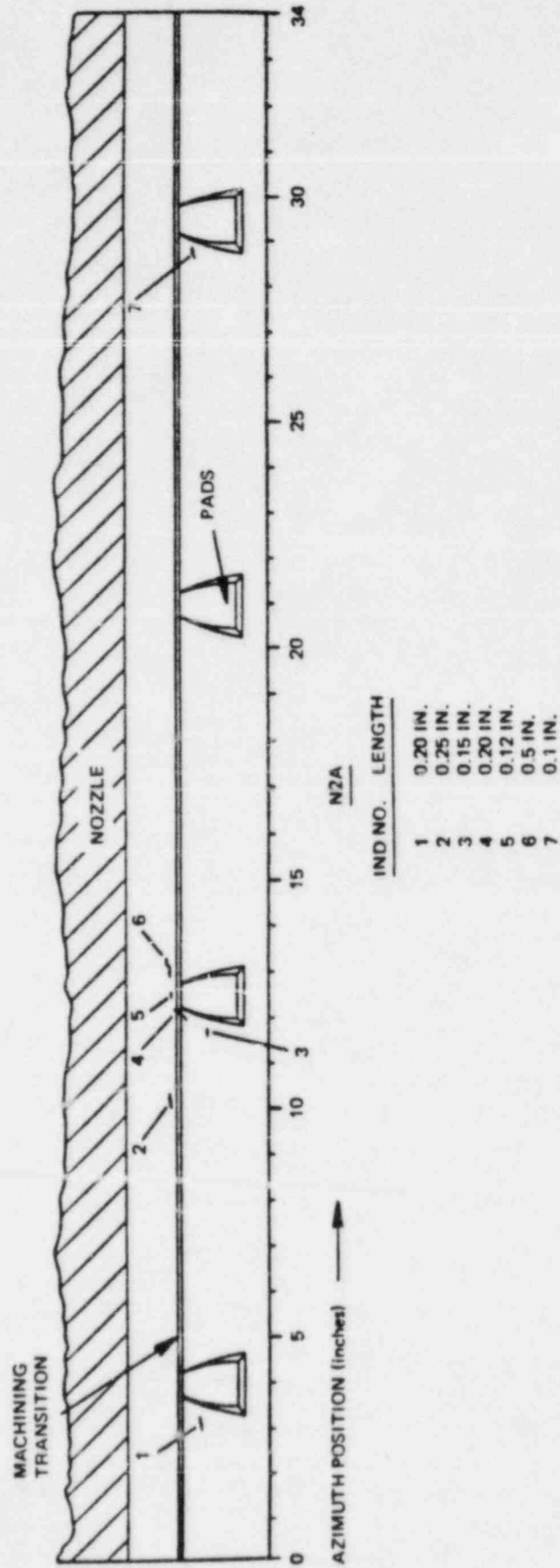
NEDO-30730

Figure I-10. Hardness Test Results
(GE COMPANY PROPRIETARY)

Figure I-11. Hardness Test Results
(GE COMPANY PROPRIETARY)

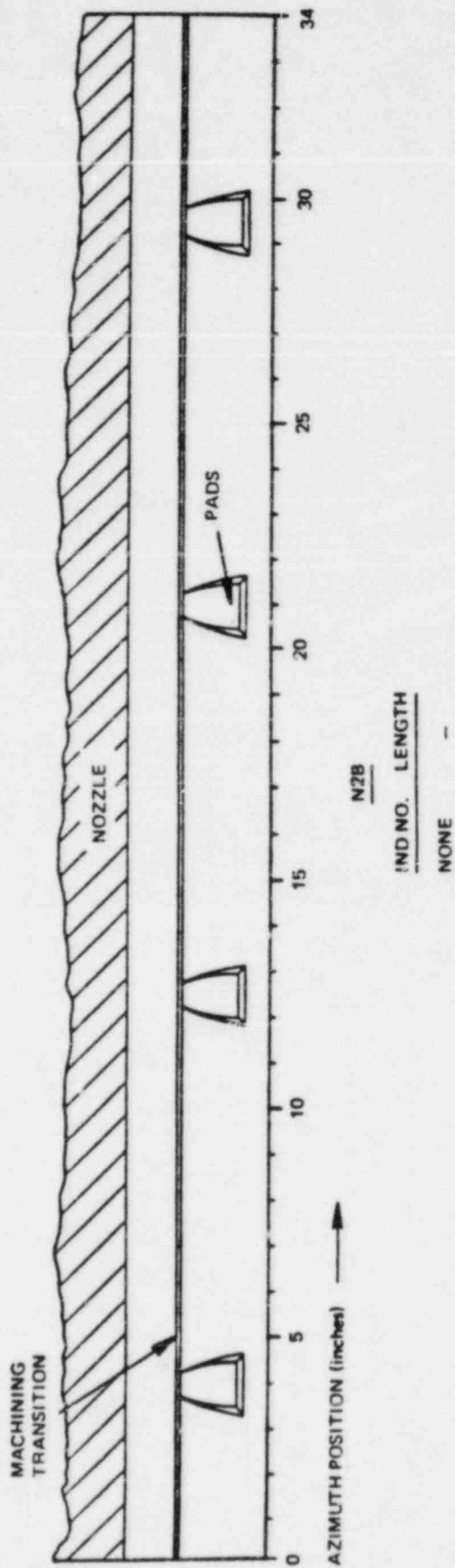
Figure I-12. Hardness Test Results
(GE COMPANY PROPRIETARY)

APPENDIX J
THERMAL SLEEVE PT AND RT CRACKING MAPS



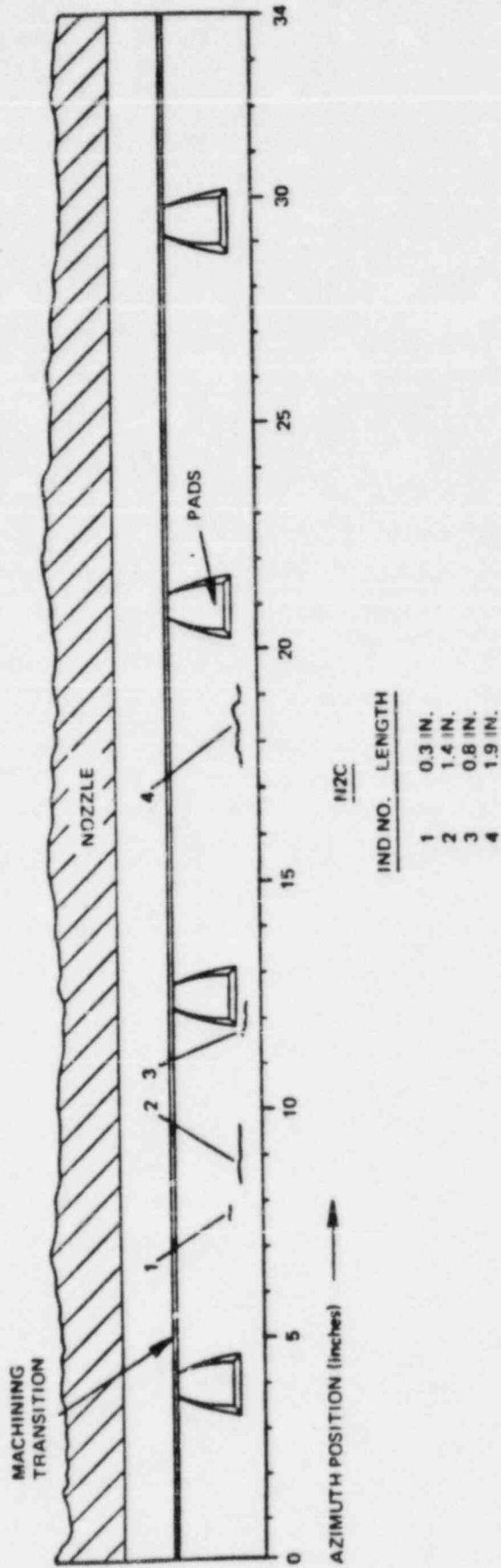
J-1

Figure J-1. Thermal Sleeve - PT Cracking Map - N2-A



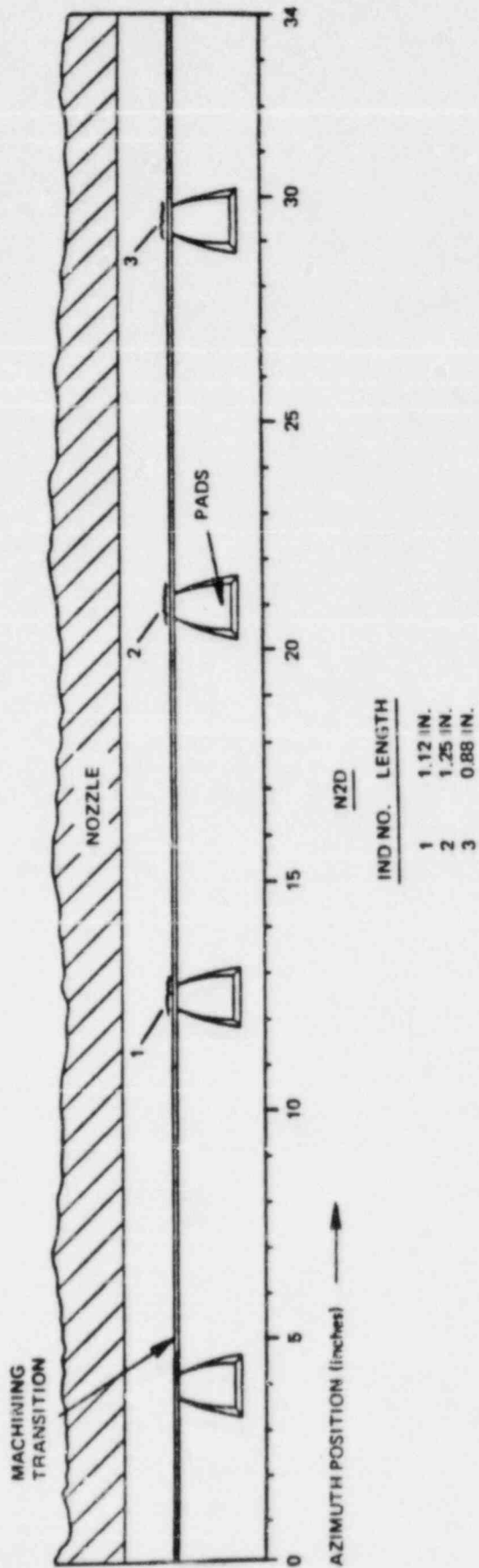
J-2

Figure J-2. Thermal Sleeve - PT Cracking Map - N2-B



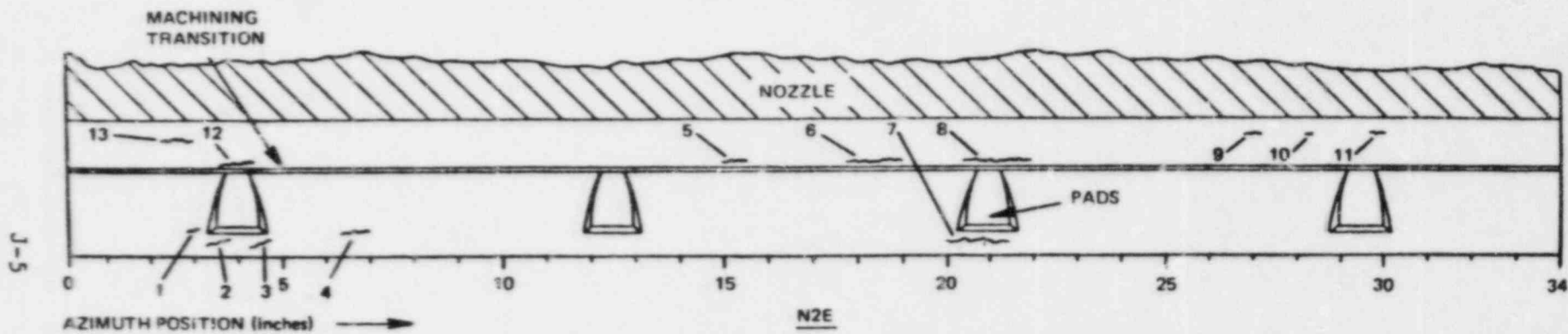
J-3

Figure J-3. Thermal Sleeve - PT Cracking Map - N2-C



J-4

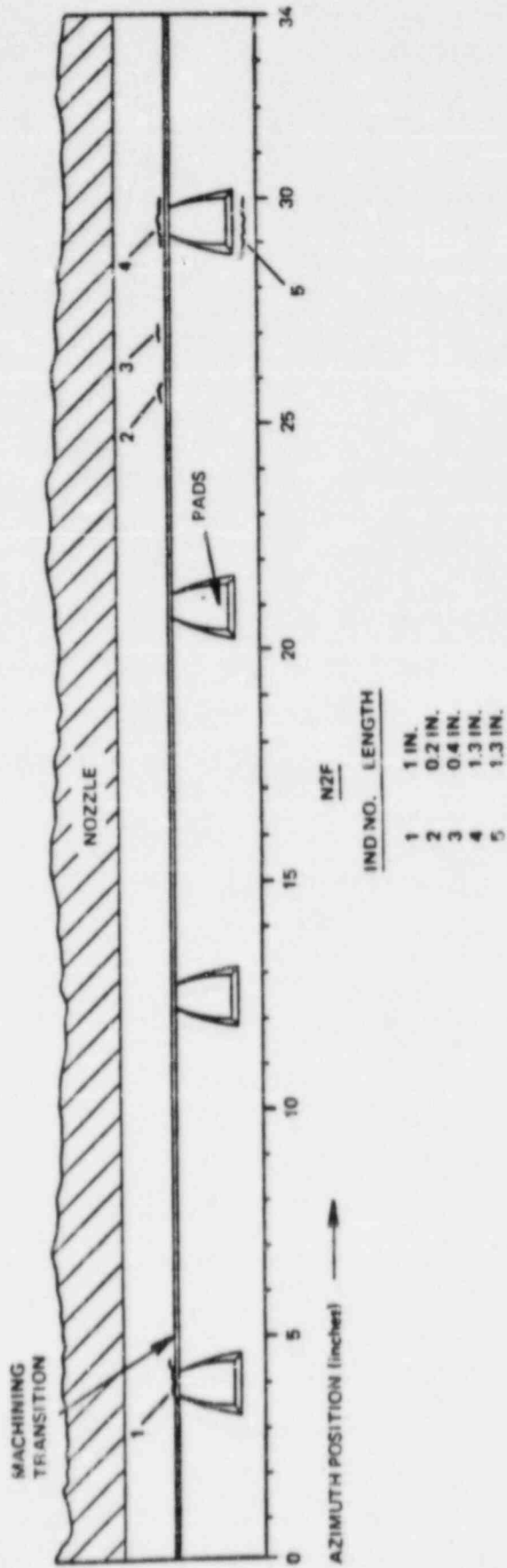
Figure J-4. Thermal Sleeve - PT Cracking Map - N2-D



IND NO.	LENGTH	IND NO.	LENGTH
1	0.4 IN.	8	1.75 IN.
2	0.7 IN.	9	0.5 IN.*
3	0.75 IN.	10	0.12 IN.*
4	0.88 IN.*	11	0.38 IN.*
5	0.75 IN.	12	0.66 IN.
6	1.38 IN.	13	0.6 IN.
7	1.5 IN.		

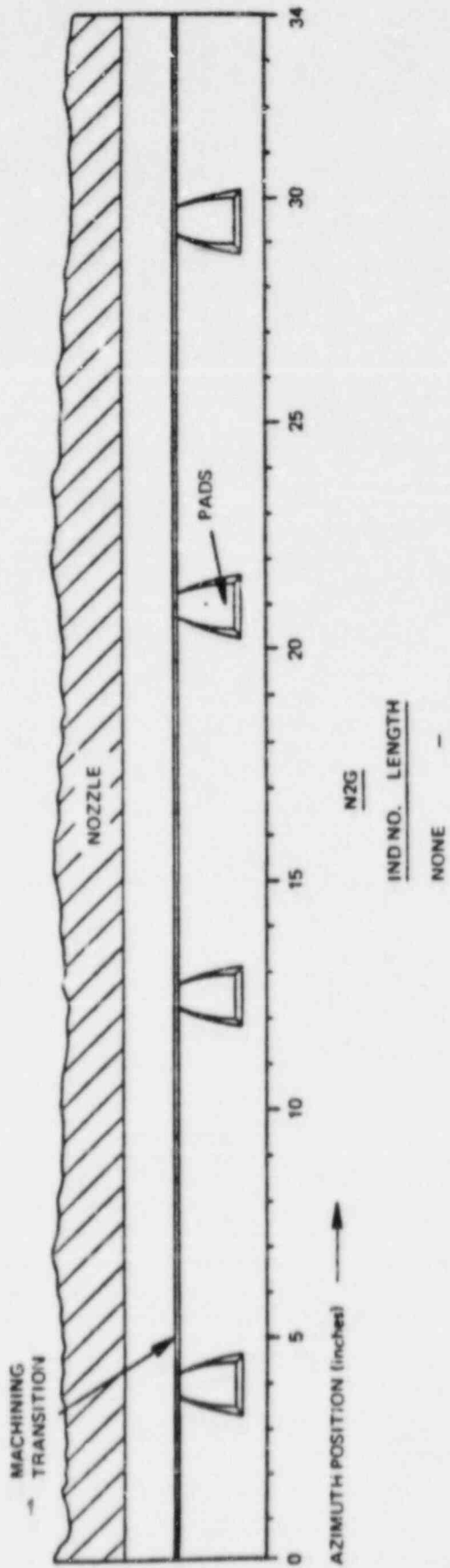
*VERY LIGHT INDICATIONS

Figure J-5. Thermal Sleeve - PT Cracking Map - N2-E



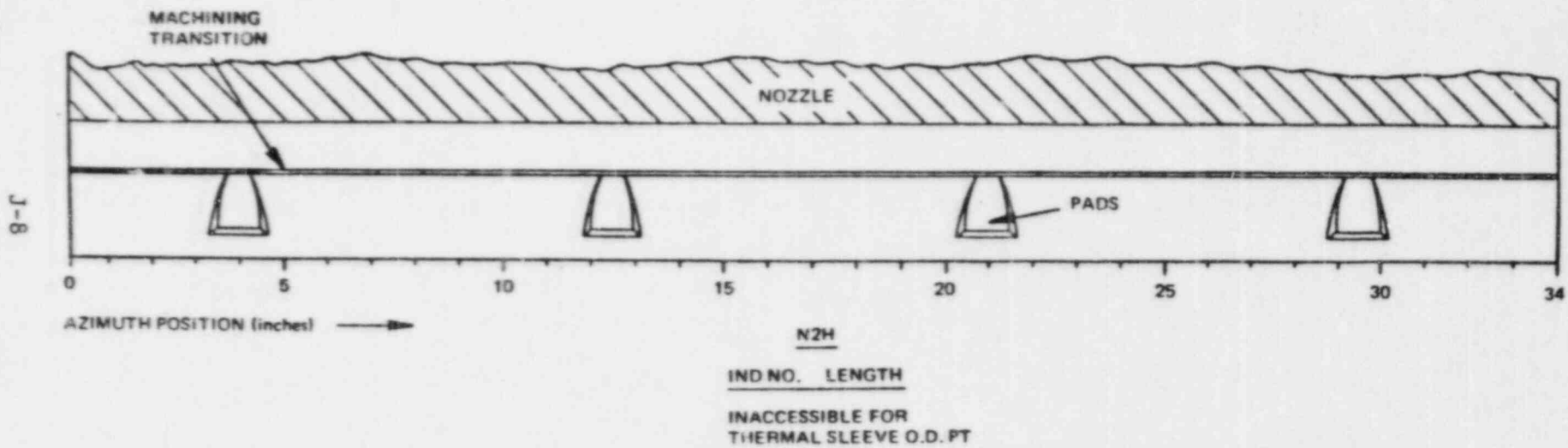
J-6

Figure J-6. Thermal Sleeve - PT Cracking Map - N2-F



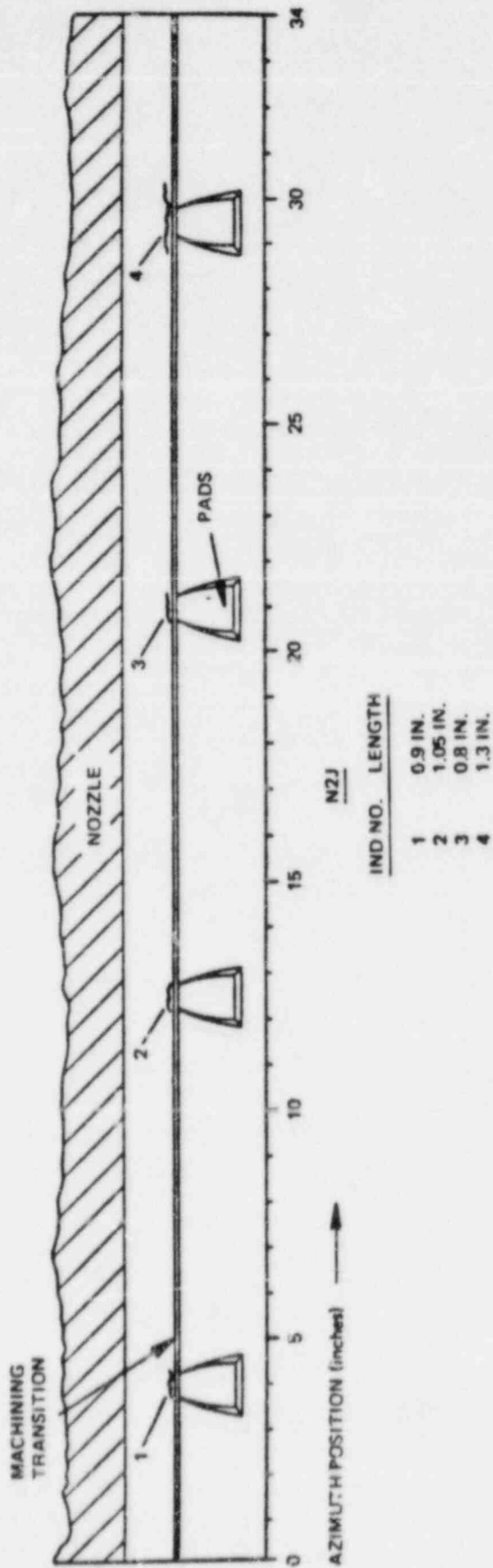
J-7

Figure J-7. Thermal Sleeve - PT Cracking Map - N2-G



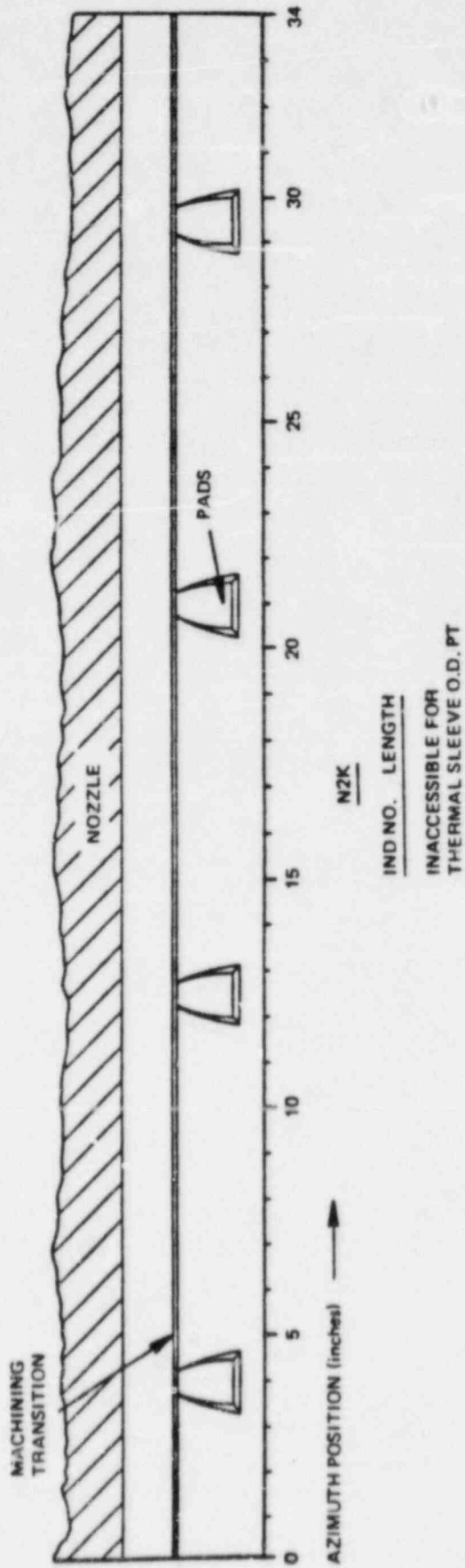
NEDO-30730

Figure J-8. Thermal Sleeve - PT Cracking Map - N2-H



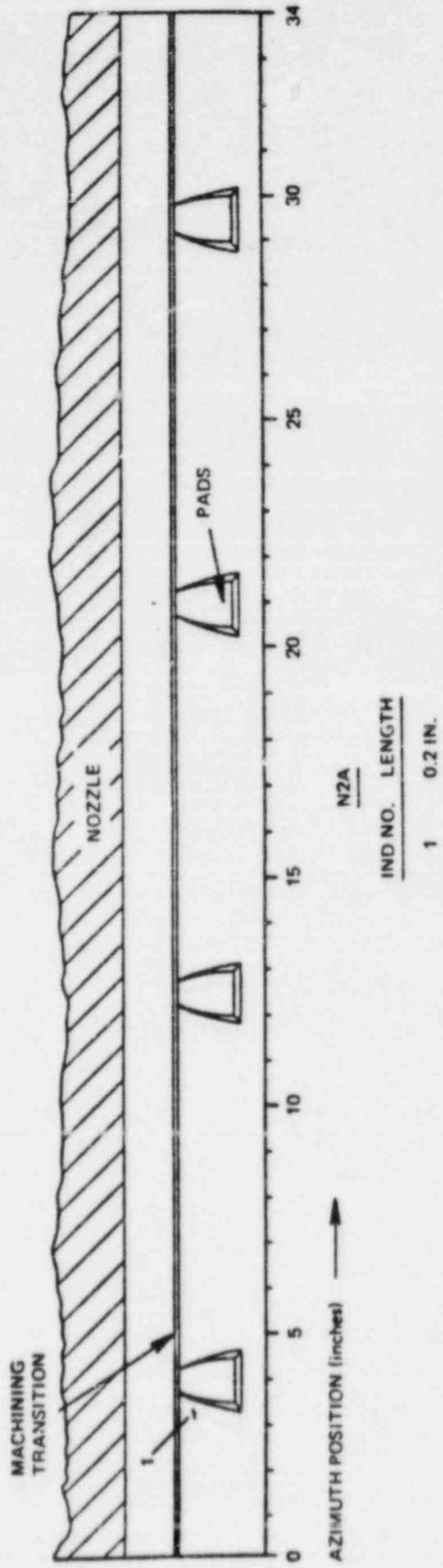
J-9

Figure J-9. Thermal Sleeve - PT Cracking Map - N2-J



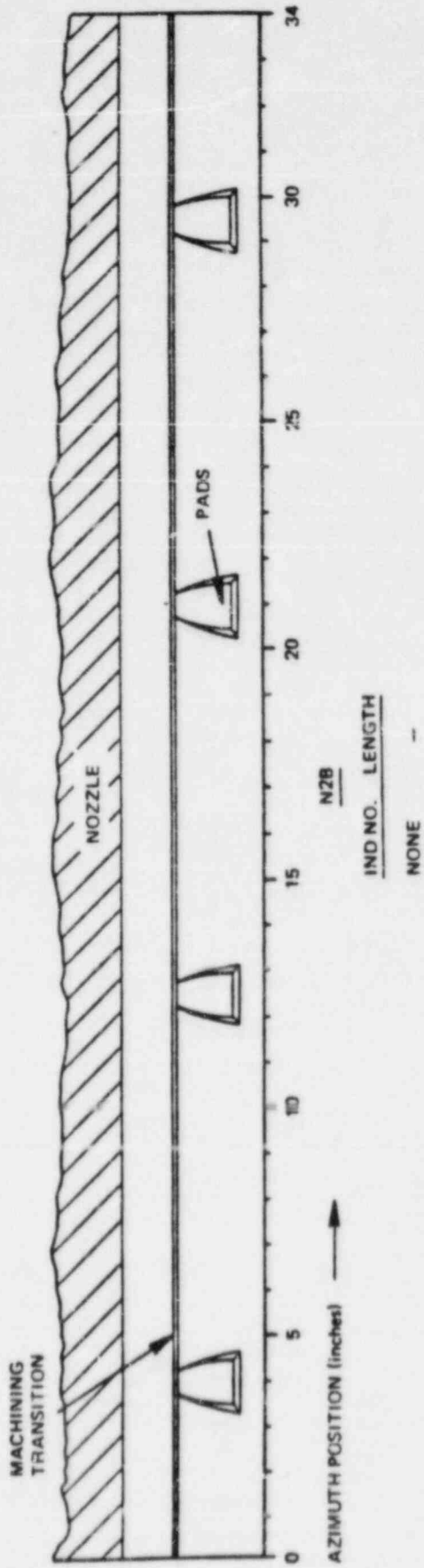
J-10

Figure J-10. Thermal Sleeve - PT Cracking Map - N2-K



J-11

Figure J-11. Thermal Sleeve - RT Cracking Map - N2-A



J-12

Figure J-12. Thermal Sleeve - RT Cracking Map - N2B

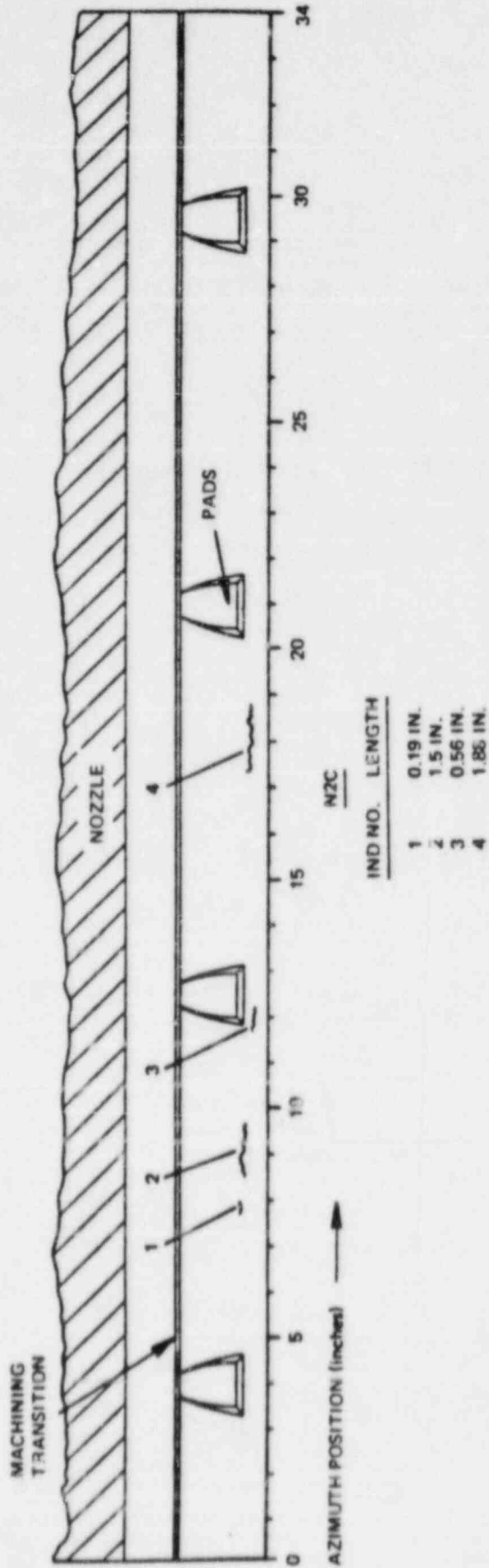


Figure J-13. Thermal Sleeve - RT Cracking Map - N2-C

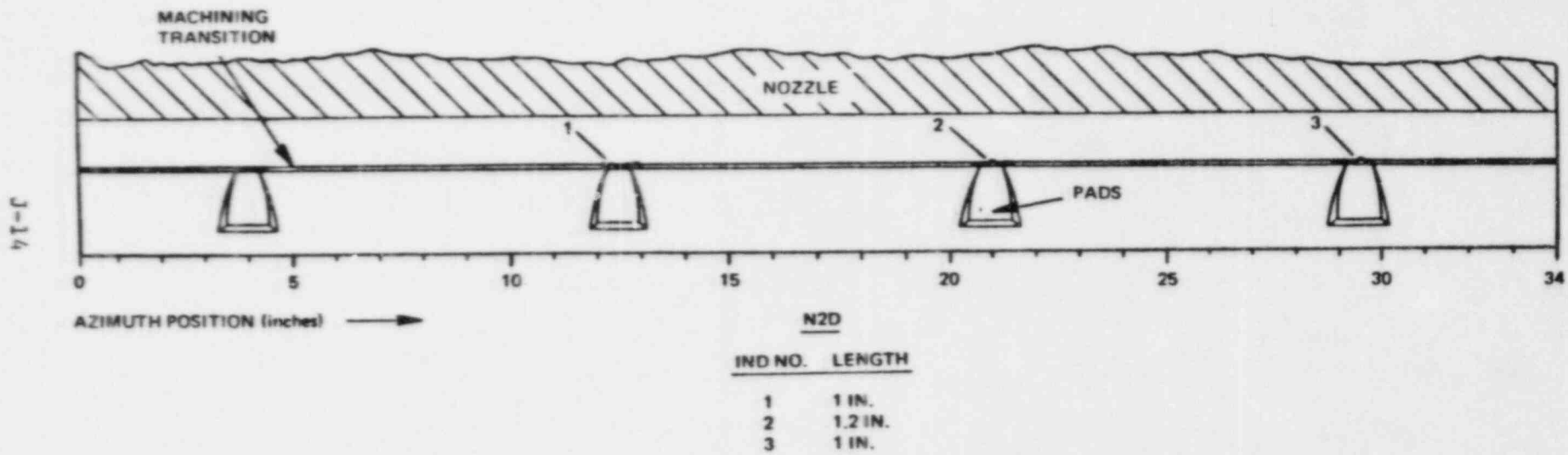
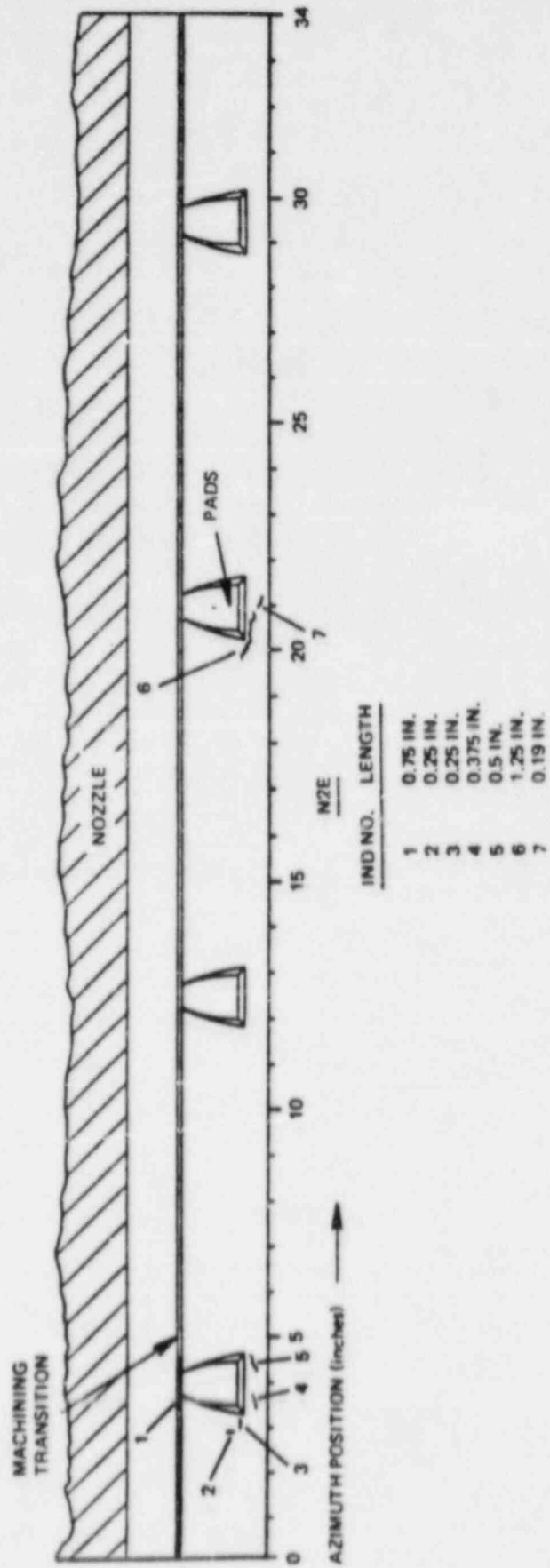
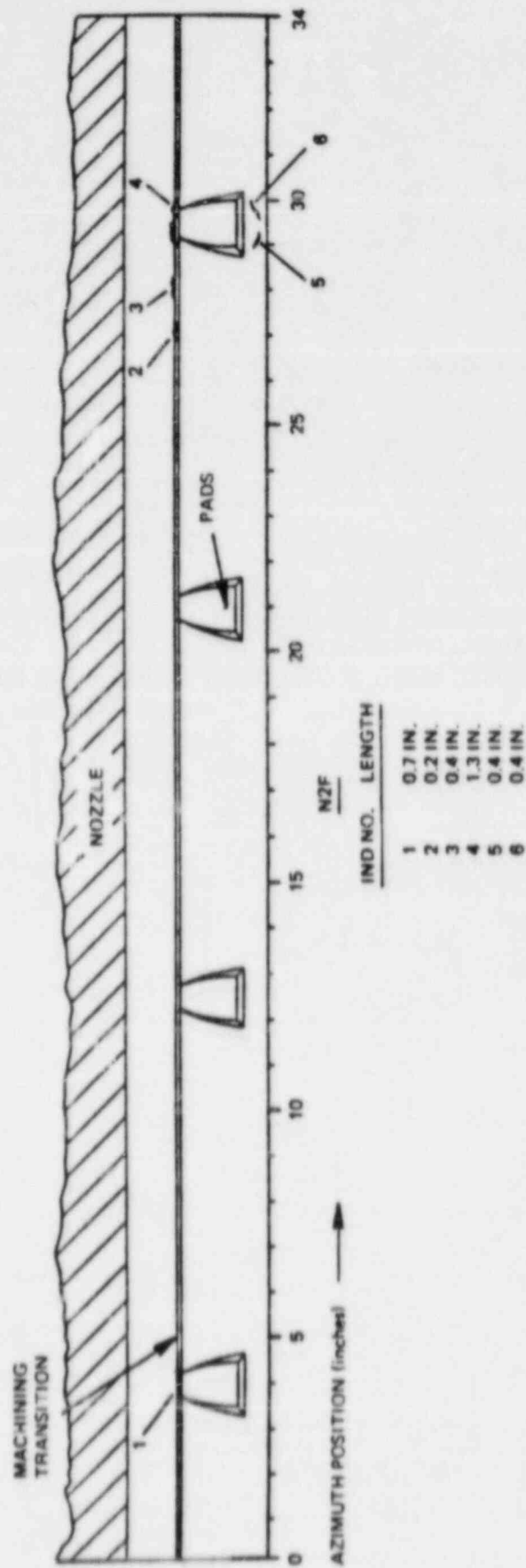


Figure J-14. Thermal Sleeve - RT Cracking Map - N2-D



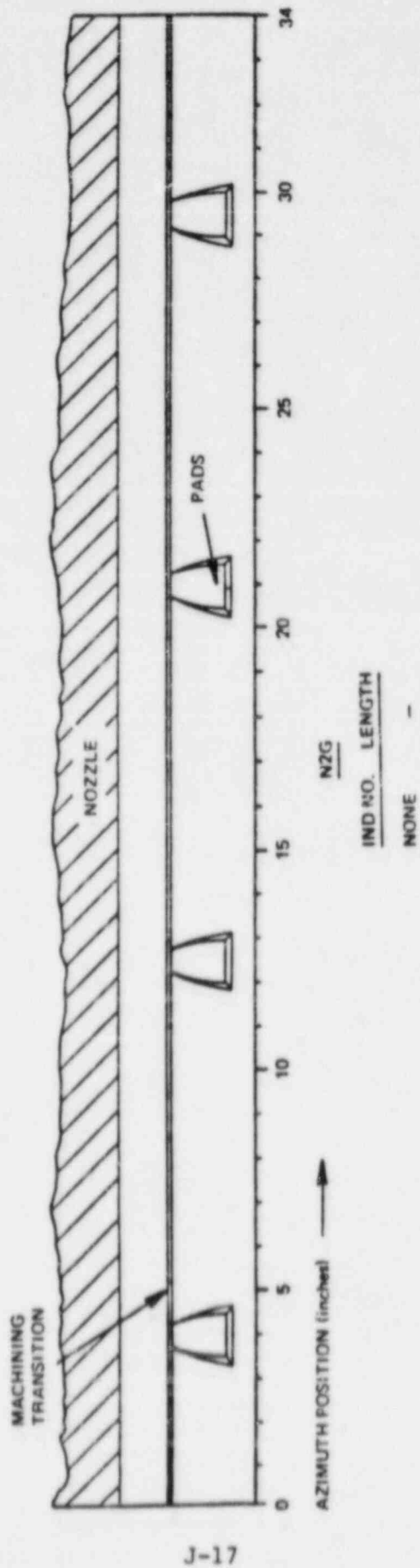
J-15

Figure J-15. Thermal Sleeve - RT Cracking Map - N2-E



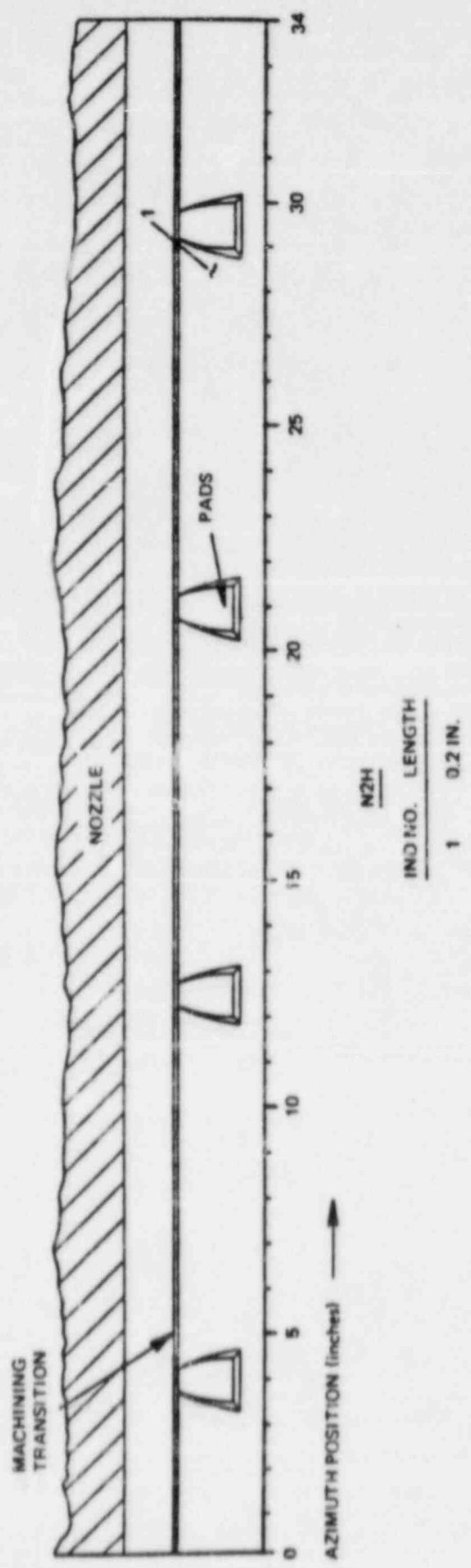
J-16

Figure J-16. Thermal Sleeve - RT Cracking Map - N2-F



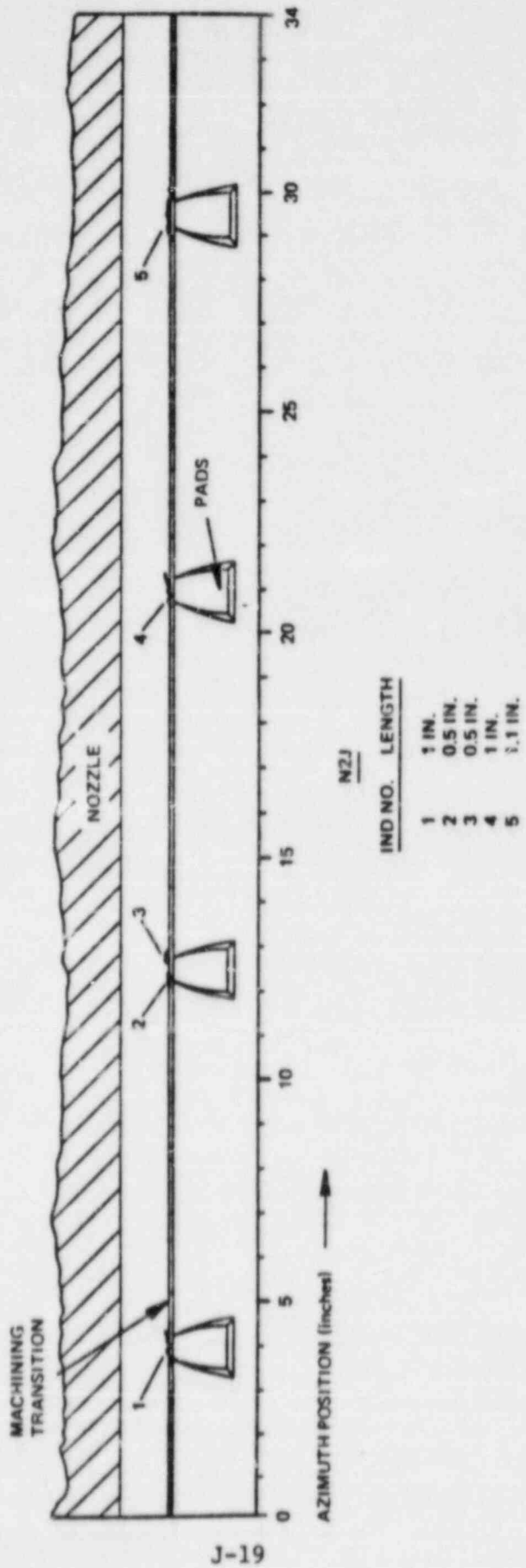
J-17

Figure J-17. Thermal Sleeve - RT Cracking Map - N2-G



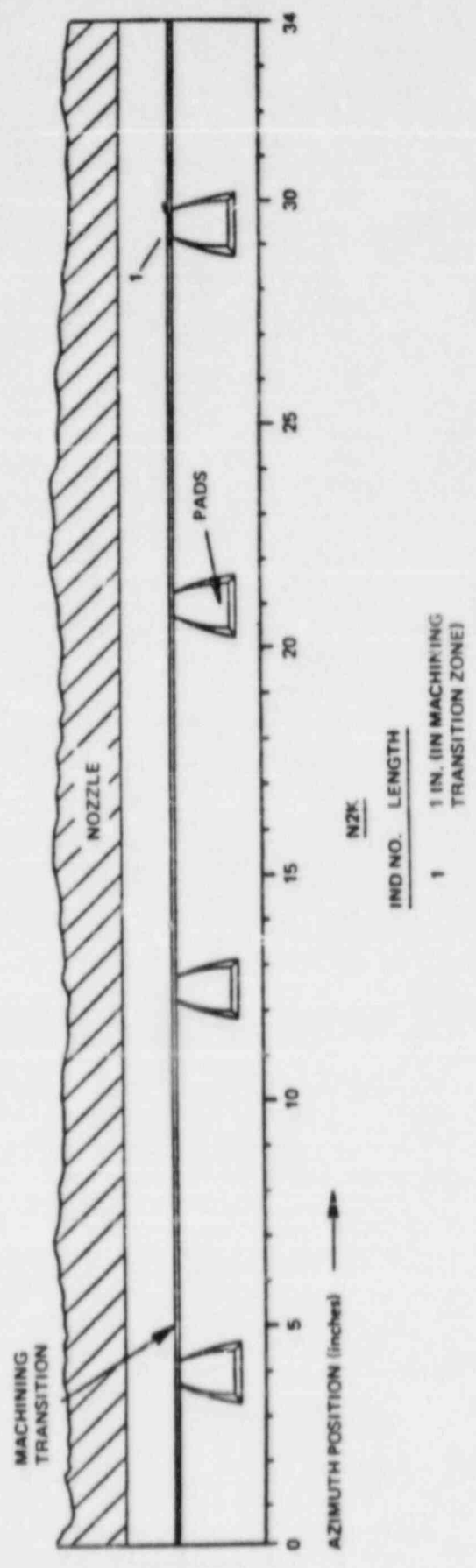
J-18

Figure J-18. Thermal Sleeve - RT Cracking Map - N2-H



J-19

Figure J-19. Thermal Sleeve - RT Cracking Map - N2-J



J-20

Figure J-20. Thermal Sleeve - RT Cracking Map - N2-K

DISTRIBUTION

EXTERNAL

Boston Edison Company
(c/o A. N. Baker, MC 883)

10 copies

INTERNAL

<u>Name</u>	<u>M/C</u>
E. Kiss	745
G. M. Gordon	785
T. L. Chapman	777
A. N. Baker	883
J. F. Klapproth (3 copies)	682
J. P. Higgins	889
R. B. Hamilton	272
K. W. Hess	277
J. P. Clark	669
S. Ranganath	777
B. M. Gordon	785
R. M. Horn	785
K. S. Ramp	785
D. E. Delwiche	785